

Fall 2021

The Development of Novel CDK8 and CDK19 Inhibitors and Degraders as Potential Anti-cancer Agents

Li Zhang

Follow this and additional works at: <https://scholarcommons.sc.edu/etd>



Part of the [Pharmacy and Pharmaceutical Sciences Commons](#)

Recommended Citation

Zhang, L.(2021). *The Development of Novel CDK8 and CDK19 Inhibitors and Degraders as Potential Anti-cancer Agents*. (Doctoral dissertation). Retrieved from <https://scholarcommons.sc.edu/etd/6558>

This Open Access Dissertation is brought to you by Scholar Commons. It has been accepted for inclusion in Theses and Dissertations by an authorized administrator of Scholar Commons. For more information, please contact digres@mailbox.sc.edu.

THE DEVELOPMENT OF NOVEL CDK8 AND CDK19 INHIBITORS AND DEGRADERS AS POTENTIAL ANTI-CANCER AGENTS

by

Li Zhang

Bachelor of Science
Shanxi University, 2011

Master of Science
University of Chinese Academy of Sciences, 2014

Submitted in Partial Fulfillment of the Requirements

For the Degree of Doctor of Philosophy in

Pharmaceutical Sciences

College of Pharmacy

University of South Carolina

2022

Accepted by:

Campbell McInnes, Major Professor

Igor Roninson, Major Professor

Michael Wyatt, Committee Member

Sajish Mathew, Committee Member

Maksymilian Chruszcz, Committee Member

Tracey L. Weldon, Interim Vice Provost and Dean of the Graduate School

© Copyright by Li Zhang, 2022
All Rights Reserved.

DEDICATION

To my dearest mother Lianping Zhang and father Fangzheng Zhang for their unconditional love and support.

ACKNOWLEDGEMENTS

I would first like to acknowledge my two mentors, Dr. Campbell McInnes and Dr. Igor Roninson, for giving me the chance to join their labs, the continuous guidance and support throughout my doctoral studies at University of South Carolina, which allows me to grow as an independent scientist. I will always appreciate their mentorship.

My appreciation also goes to my committee members, Dr. Michael Wyatt, Dr. Sajish Mathew, and Dr. Maksymilian Chruszcz for their invaluable help and suggestions. The project presented herein was improved and accomplished with every committee meeting.

I would also like to acknowledge all my colleagues, Dr. Mengqian (Max) Chen, Dr. Chen Cheng, Jing Li, Dr. Chad Beneker, Jessy Varghese, Hao Ji, Lili Wang, Xiaokai Ding, Youwen Zhang, for all the caring and support. Especially Dr. Mengqian (Max) Chen, his invaluable input greatly contributed to the project. He is also a wonderful teacher and friend, and his guidance, help, and encouragement are priceless to me.

Furthermore, I would like to acknowledge my colleagues within the department, Ms. Rachel Mckeown, Dr. Alexander Gasparian, and Dr. Thomas Hilimire, who have supported me through my PhD journey.

ABSTRACT

CDK8 and its homolog CDK19 are essential for transcription regulation and their dysregulation has been identified in numerous diseases, especially in cancers. CDK8 and CDK19 have been implicated in cancer development through their kinase activity and kinase independent functions. Despite the existing CDK8/19 inhibitors, there is still a need to develop novel CDK8/19 inhibitors with improved potency and PK profile. It is also necessary to develop CDK8/19 degraders that are able to eliminate the kinase-independent functions. Although two CDK8-degrading PROteolysis Activating Chimeras (PROTACs) have been reported, they have limited CDK8 degradation efficacy and no effect on CDK19. PROTACs with improved degradation efficacy targeting both CDK8 and CDK19 are required.

Here we present the design, synthesis, optimization, and biological evaluation of two series of CDK8/19 inhibitors and three series of CDK8/19 degrading PROTACs. The quinoline-6-carbonitrile series is derived from CDK8/19 inhibitors Senexin A and Senexin B. Among this chemical series, Senexin C (2.20a) exhibited the best inhibitory activity, being more potent and metabolically stable than its parental inhibitor. Moreover, Senexin C (2.20a) possesses unique properties compared to other CDK8/19 inhibitors including sustained target inhibition and highly tumor-enriched pharmacokinetics (PK) profile with *in vivo*

therapeutic efficacy, making it a promising lead CDK8/19 inhibitor. The thienopyridine series is derived from CDK8/19 inhibitors 15u and 15w that were initially identified as bone anabolic agents. Among this series, several compounds exhibited comparable inhibitory activity to the parental inhibitors but with unfavorable PK. Despite that, the achieved SAR will contribute to the future CDK8/19 inhibitor development of the thienopyridine series. The three series of PROTAC molecules were derived from 15u, Senexin C, and BI-1347 respectively. Among them, BI-1347-derived PROTAC 4.48 shows the best CDK8/19 degradation potency in different cell lines and species. Moreover, it offers a greater long-term benefit for leukemia treatment than its parental CDK8/19 inhibitor BI-1347.

This dissertation provides insights regarding the development of novel CDK8/19 inhibitors and degraders as potential anti-cancer agents and should contribute to the future inhibitor and degrader development targeting CDK8/19 and other kinase targets.

TABLE OF CONTENTS

Dedication.....	iii
Acknowledgements.....	iv
Abstract.....	v
List of Tables	viii
List of Figures	ix
List of Schemes	xii
List of Abbreviations.....	xiv
Chapter 1: Introduction	1
Chapter 2 Development of Quinoline-6-Carbonitrile-Based Analogues as Novel CDK8/19 Inhibitors	25
Chapter 3: Thienopyridine Scaffold as Novel Class of Selective CDK8/19 Inhibitor.....	94
Chapter 4: Development of CDK8/19 Degradable as Potential Anti-Cancer Agents.....	179
References	275

LIST OF TABLES

Table 2.1 Structure-activity relationship of Senexin A quinoline substitutions.....	83
Table 2.2 Structure-activity relationship of Senexin B naphthyl substitutions	84
Table 2.3 KINOMEscan of Senexin C at 2 μ M.....	85
Table 2.4 Binding kinetics of Senexin B and Senexin C to recombinant CDK8/cycC and CDK19/cycC proteins in KINETICfinder assay	89
Table 2.5 Pharmacokinetic Analysis of Senexin C in Balb/c mice bearing CT26 tumors	89
Table 2.6 qPCR primer sequences	90
Table 3.1 Structure-activity relationship of hybrid analogues.....	166
Table 3.2 Structure-activity relationship of 15w analogues.....	167
Table 3.3 Structure-activity relationship of 15u analogues.....	168
Table 3.4 Structure-activity relationship of 15u analogues.....	169
Table 4.1 Structures and CDK8-degradation activities of CDK8/19 PROTACs qPCR primer sequences.....	263
Table 4.2 qPCR primer sequences	268

LIST OF FIGURES

Figure 1.1 The protein structure of CDK8/CCNC (PDB code: 4F7S)	21
Figure 1.2 The regulation of RNAPII transcription via CDK8	21
Figure 1.3 The role of CDK8 in transcriptional regulation via phosphorylating TFs	22
Figure 1.4 The role of CDK8 in diseases	23
Figure 1.5 The structures of reported CDK8 inhibitors.....	24
Figure 1.6 The structures of reported PROTACs targeting CDK8	24
Figure 2.1 (A) The chemical structures of Senexin A and Senexin B. (B) The kinome profiling of Senexin B.	69
Figure 2.2 (A) The predicted binding mode of Senexin A (2.1) and 2.8a docked to CDK8/cyclin C protein (PDB code: 4F7S).....	69
Figure 2.3 The predicted binding modes of Senexin B (2.2) and 2.20a docked to CDK8/cyclin C protein (PDB code:4F7S)	70
Figure 2.4 Molecular modeling and energy minimization of compound 20b	70
Figure 2.5 Kinome profiling dendrogram (Discover X) of Senexin C at 2 μ M	71
Figure 2.6 Determination of Kds for Senexin C binding to CDK8, CDK19 (CDK11), HASPIN, MAP4K2 and MYO3B.....	72
Figure 2.7 Determination of binding kinetics of Senexin B and Senexin C to recombinant CDK8/cyclin C and CDK19/cyclin C proteins	73
Figure 2.8 Cell-based IC ₅₀ assays of Senexin C (SnxC) and Senexin B (SnxB).....	74
Figure 2.9 Effects of Senexin B and Senexin C on durability	

of the inhibition of CDK8/19-dependent gene expression in the wash-off study in 293 cells	74
Figure 2.10 Metabolic stability of Senexin B and Senexin C in human hepatocytes	75
Figure 2.11 PK/PD analysis of Senexin C in the CT26 tumor model in Balb/c mice	75
Figure 2.12 PK/PD analysis of Senexin B in the CT26 tumor model in Balb/c mice	76
Figure 2.13 <i>In vivo</i> efficacy study of Senexin C (40 mg/kg, p.o., BID) in the MV4-11 AML model in female NSG mice	76
Figure 2.14 The Lanthascreen IC ₅₀ curves of tested compounds	77
Figure 2.15 The HEK293-NFκB-Luc IC ₅₀ curves of tested compounds	79
Figure 2.16 The MV4-11-Luc IC ₅₀ curves of tested compounds	81
Figure 3.1 The chemical structures of 15u (3.1) and 15w (3.2)	159
Figure 3.2 The predicted binding model of 15u (A) and 15w (B) that docked to CDK8 protein (PDB code: 4F7S)	159
Figure 3.3 The kinome profiling of 15u (A) at 2 μM and 15w (B) at 500 nM	160
Figure 3.4 15w and 15u oral PK in female CD-1 mice (30mg/kg)	161
Figure 3.5 The HEK293-NFκB-Luc IC ₅₀ curves of tested compounds	162
Figure 4.1 The process of protein ubiquitination via UPS	248
Figure 4.2 PROTAC-mediated protein degradation	248
Figure 4.3 Chemical structure of selected CDK8/19i and their representative PROTAC derivatives	249
Figure 4.4 Effects of 24hr treatment with different PROTAC compounds on CDK8/CDK19/CCNC protein levels in 293 cells	250
Figure 4.5 Effects of co-treatment with MG132, Pomalidomide and Senexin C on HP8580-mediated CDK8 degradation in 293 cells	251

Figure 4.6 Effects of 24hr treatment with different PROTAC compounds on CDK8/CDK19/CCNC protein levels in Jurkat cells.....	252
Figure 4.7 Effects of 24-hr treatment with different PROTAC compounds on CDK8/CDK19 protein levels in different human cell lines	253
Figure 4.8 Effects of treatment with different PROTAC compounds on CDK8/CDK19 protein levels in non-human cell lines	254
Figure 4.9 Time course of CDK8/CDK19/CCNC degradation by 4.48 in 293 and CT26 cells.....	255
Figure 4.10 Effects of 24hr-treatment with different CDK8/19i and PROTACs on STAT1-S727 phosphorylation and CDK8 degradation	256
Figure 4.11 Effects of 3-day treatment with 200nM BI-1347 and 200nM 4.48 on CDK8/19-dependent gene expression in 293 parental (WT) and CDK8/19 double-knockout (dKO) cells	257
Figure 4.12 (A) Stability of transcriptional changes induced by BI1347 CDK8/19 kinase inhibitor and 4.48 PROTAC in the wash-off study in 293 cells. (B) Stability of pSTAT-S727 inhibition and CDK8/CDK19/CCNC degradation by 4.48 in 293 wash-off study.	258
Figure 4.13 Long-term effects of CDK8/19 kinase inhibitor BI1347 and CDK8/19 PROTAC 4.48 on growth of leukemia cells	259
Figure 4.14 Levels of CDK8 protein and STAT1 S727 phosphorylation (A) and mRNA expression of the CDK8/19 dependent gene CCL12 (B) in CT26 tumors from mice dosed with Vehicle, 20mg/kg 4.45 or 20mg/kg 4.48	260
Figure 4.15 Effects of 24-hr treatment with different PROTACs (JH-XI-10-02, 4.27d, 4.48) and CDK8/19 kinase inhibitors (Senexin C and BI-1347) in CCNC ^{low} Loucy cells, Jurkat cells, 293 parental (WT) or 293-CCNC-knockout (CCNC-KO) cells.....	261
Figure 4.16 The HEK293-NFκB-Luc IC ₅₀ curves of tested compounds	262

LIST OF SCHEMES

Scheme 2.1 Synthesis of 6-substituted- <i>N</i> -phenethylquinolin -4-amine derivatives.....	91
Scheme 2.2 Synthesis of 4-((2-(6-substituted-naphthalen-2 -yl)ethyl)amino)quinoline-6-carbonitrile derivatives	92
Scheme 3.1 Synthesis of 3.6	170
Scheme 3.2 Synthesis of 3.11	170
Scheme 3.3 Synthesis of 3.19	171
Scheme 3.4 Synthesis of 3.26	172
Scheme 3.5 Synthesis of 3.33	172
Scheme 3.6 Synthesis of 3.44	173
Scheme 3.7 Synthesis of 3.48	173
Scheme 3.8 Synthesis of 3.51	174
Scheme 3.9 Synthesis of 3.54	174
Scheme 3.10 Synthesis of 3.59	175
Scheme 3.11 Synthesis of 3.62	175
Scheme 3.12 Synthesis of 3.65	176
Scheme 3.13 Synthesis of 3.69	176
Scheme 3.14 Synthesis of 3.74	177
Scheme 3.15 Synthesis of 3.81	177
Scheme 3.16 Synthesis of 3.82	178
Scheme 4.1 The synthesis of PEG linker PROTACs 4.3.....	269

Scheme 4.2 The synthesis of PEG linker PROTACs 4.4	269
Scheme 4.3 The synthesis of VHL-based PROTAC 4.5	269
Scheme 4.4 The synthesis of PEG PROTACs 4.6	270
Scheme 4.5 The synthesis of inactive version of 4.3e (4.10)	270
Scheme 4.6 The synthesis of pomalidomide analogs 4.12	270
Scheme 4.7 The synthesis of pomalidomide analogs 4.14	270
Scheme 4.8 The synthesis of 2.20c analogs (4.16)	271
Scheme 4.9 The synthesis of 2.20c analogs (4.18)	271
Scheme 4.10 The synthesis of PROTAC 4.21	271
Scheme 4.11 The synthesis of pomalidomide analog 4.23	271
Scheme 4.12 The synthesis of PROTAC 4.24	271
Scheme 4.13 The synthesis of PROTAC 4.25	272
Scheme 4.14 The synthesis of PROTAC 4.26	272
Scheme 4.15 The synthesis of PROTAC 4.27	272
Scheme 4.16 The synthesis of PROTAC 4.31	272
Scheme 4.17 The synthesis of PROTAC 4.34	273
Scheme 4.18 The synthesis of PROTAC 4.38	273
Scheme 4.19 The synthesis of PROTAC 4.45	273
Scheme 4.20 The synthesis of PROTAC 4.48	274
Scheme 4.21 The synthesis of PROTAC 4.51	274
Scheme 4.22 The synthesis of PROTAC 4.52	274

LIST OF ABBREVIATIONS

ABL	V-Abl Abelson Murine Leukemia Viral Oncogene Homolog 1
ADC	Antibody-Drug Conjugate
AML	Acute Myeloid Leukemia
ASOs	Antisense Oligonucleotides
BCR	Breakpoint Cluster Region
BLI	Bioluminescence Imaging
BRAF	V-Raf Murine Sarcoma Viral Oncogene Homolog B1
CAK	CDK Activating Kinase
CAMK	Calcium/Calmodulin-Dependent Kinase
Cas9	Associated Protein 9
CDK	Cyclin-Dependent Kinase
CK1	Casein Kinase I
CLK	Cdc-Like Kinase
CRC	colorectal cancer
CRISPR	Clustered Regularly Interspaced Short Palindromic Repeats
DCAF	DDB1 and CUL4 Associated Factor
DSIF	DRB Sensitivity-Inducing Factor
DUBs	Deubiquitinases
EGFR	Epidermal Growth Factor Receptor
EMT	Epithelial-to-Mesenchymal Transition
ER	Estrogen Receptor

Eu	Europium
FRET	Fluorescence Resonance Energy Transfer
GSK3	Glycogen Synthase Kinase-3
HBA	H-Bond Acceptor
HER2	Human Epidermal Growth Factor Receptor 2
HIF1 α	Hypoxia-Inducible Factor 1-alpha
HPLC	High-Performance Liquid Chromatography
HTS.....	High-Throughput Screening
HyT	Hydrophobic Tagging
IAPs	Inhibitors of Apoptosis Proteins
IEG.....	Immediate Early Gene
IFN- γ	Interferon- γ
IL-10.....	Interleukin-10
JAK	Janus Kinase
KLF2	Krüppel Like Factor 2
LEF	Lymphotropic Factor
LPS.....	Lipopolysaccharide
MAPK.....	Mitogen-Activated Protein Kinase
MDM2	Mouse Double Minute 2 Homolog
MED12L.....	Med12-Like
MEF	Mouse Embryonic Fibroblast
mH2A1	macroH2A1
MMPs.....	Matrix Metalloproteinases
MS	Mass Spectra
NELF.....	Negative Elongation Factor

NFκB.....	Nuclear Factor Kappa B
NICD.....	NOTCH Intracellular Domain
NK Cell.....	Nature Killer Cell
NOTCH.....	Neurogenic Locus Notch Homolog Protein
PD.....	Pharmacodynamic
PDGFRα.....	Platelet-Derived Growth Factor Receptor-α
PIC.....	Pre-Initiation Complex
PK.....	Pharmacokinetic
PKA.....	Protein Kinase A
PKC.....	Protein Kinase C
PKG.....	Protein Kinase G
Pol II.....	RNA polymerase II
POI.....	Protein of Interest
PROTAC.....	PROteolysis TARgeting Chimeras
P-TEFb.....	Positive Transcription Elongation Factor
RGC.....	Receptor Guanylate Cyclases
RNF114.....	Ring Finder Protein 114
RSmads.....	Receptor-Regulated Mother Against Decapentaplegic Proteins
SBDD.....	Structure-Based Drug Design
SE.....	Super-Enhancer
SEC.....	Super-Elongation Complex
siRNAs.....	Small Interfering RNAs
SREBP-1C.....	Sterol Regulatory Element-Binding Protein
STAT.....	Signal Transducer and Activator of Transcription
STE.....	Sterile

STFs Specific Transcription Factors

TALENs Transcription Activator-Like Effector Nucleases

T-ALL T-Cell Acute Lymphoblastic Leukemia

TCF T cytokine

TFII Transcription Initiation Factor II

TFs..... Transcription Factors

TIMP3 Tissue Inhibitor of Metalloproteinase 3

TK Tyrosine Kinase

TLC Thin-Layer Chromatography

TLK Tyrosine Kinase-Like

TNBC Triple-Negative Breast Cancer

UPS Ubiquitin-Proteasome System

VEGFR2 Vascular Endothelial Growth Factor Receptor 2

ZFNs Zinc-Finger Nucleases

CHAPTER 1

INTRODUCTION

1.1 Protein Kinases: Functions and Roles in Drug Development

Protein kinases are enzymes that phosphorylate target proteins through transferring γ -phosphate of ATP to the side chain hydroxyl group of serine, threonine, or tyrosine residues on target proteins. Phosphorylation induces diverse cellular events, especially signal transduction. Despite their role in phosphorylation, protein kinases possess non-enzymatic functions as well,¹ including allosteric regulation, scaffolding, and transcription management. Human kinome analysis has identified over 500 protein kinase genes that account for ~2% of human genes.² The total of 500 protein kinases can be divided into 9 groups and some groups are further classified into subfamilies: AGC (protein kinase A (PKA), protein kinase C (PKC), and protein kinase G (PKG) families), CAMK (Calcium/Calmodulin-dependent kinase), CK1 (Casein kinase I), CMGC (cyclin-dependent kinase (CDK), mitogen-activated protein kinase (MAPK), glycogen synthase kinase-3 (GSK3) and cdc-like kinase (CLK) families), RGC (Receptor Guanylate Cyclases), STE (Sterile), TK (Tyrosine Kinase), TKL (Tyrosine Kinase-Like) and atypical protein kinases.³

Due to the key roles of protein kinases in regulating cellular events, it is not surprising that aberrant function of this class of enzymes is closely related to numerous diseases, such as inflammation,⁴ cardiovascular diseases,⁵ diabetes,⁶

and cancers.⁷ Protein kinases are the second largest group of drug targets after G-protein-coupled receptors. In addition, from 2011 to 2015, the sales of drugs that target kinases were around 240 billion dollars. Meanwhile, the majority of clinical candidates targeting protein kinases are aimed at cancer treatment.⁸

1.2 Approaches to Modulate Kinase Activities

Various drug modalities have been developed to regulate the activities and levels of protein kinases, including small molecule inhibitors, nucleic acid-based strategies, protein degraders, antibodies, and gene editing technology.

Traditional small molecule inhibitors are the most frequently used modality due to their potential for good oral bioavailability, favorable tissue distribution and lower manufacturing costs. Despite that, due to their occupancy-driven pharmacology, small molecules inhibitors have to occupy more than 90% of their targets in order to achieve therapeutic effects and thus require a high drug concentration at the active sites.⁹ The long term use of inhibitors with high concentrations not only causes off-target effects and toxicity,¹⁰ but also results in drug resistance via gene mutation, target protein accumulation and alternative compensatory pathways.¹¹⁻¹³ In addition, small molecule inhibitors can only block the catalytic activity of protein kinases and thus leave non-enzymatic functions intact. Moreover, protein kinases without appropriate binding sites are beyond the scope of small molecule inhibitors.

Nucleic acid-based strategies include small interfering RNAs (si RNAs) and antisense oligonucleotides (ASOs) that regulate protein kinases post-transcriptionally via gene silencing. Nucleic acid-based strategies can be easier to

synthesize and have a larger application scope than small molecule inhibitors. However, these agents are often associated with poor metabolic stability, bioavailability and distribution, which requires special delivery systems. In addition, they have no effects on existing or long-lived target proteins.¹⁴⁻¹⁸ Moreover, partial sequence complementarity can cause severe off-target effects.¹⁷

Protein degraders are an emerging drug modality that can be applied to regulate protein kinase activity through eliminating corresponding protein kinases, such as hydrophobic tagging (HyT) degraders,¹⁹ and PROteolysis TArgeting Chimeras (PROTAC) technology.²⁰ PROTAC technology is the most popular strategy in protein degradation which takes advantage of the ubiquitin-proteasome system (UPS).²¹⁻²⁴ It destroys both the catalytic and non-enzymatic functions of protein kinases. In addition, due to its non-stoichiometric character, only lower concentrations are required at the action site thus reducing the chance of toxicity, side effects, and the development of drug resistance. Moreover, PROTACs add an additional layer of selectivity compared to their parental small molecule inhibitors due to the requirement of ternary complex formation. Despite that, PROTAC technology is still at its early stage with no general rules for rational design and its current development is still empirical and laborious. The average molecular weight of a PROTAC molecule is currently around 1000 Daltons (beyond rule of five: <5 hydrogen bond donors, <10 hydrogen bond acceptors, molecular mass<500 Da, Log P<5) and it exhibits an increased polar surface area, which results in unfavorable bioavailability, cellular permeability, and tissue distribution.

Monoclonal antibodies recognize specific epitopes on target substrates and exhibit high selectivity.²⁵ The combination of internalizing monoclonal antibody and cellular toxic payloads results in antibody-drug conjugates (ADC) with both excellent selectivity and significant potency.^{26,27} Till now, there are 7 FDA-approved antibodies or ADC targeting protein kinases,⁸ including human epidermal growth factor receptor 2 (HER2), epidermal growth factor receptor (EGFR), vascular endothelial growth factor receptor 2 (VEGFR2) and platelet-derived growth factor receptor- α (PDGFR α). However, the monoclonal antibody and ADC are large molecules and can only be applied to kinase targets that have an extracellular domain. In addition, the manufacturing costs are much higher than for small molecule drugs and have strict storage requirements.

Gene editing strategies are used to modify DNA by adding, removing or altering the genetic material in the genome, such as transcription activator-like effector nucleases (TALENs), zinc-finger nucleases (ZFNs) and the most recently discovered clustered regularly interspaced short palindromic repeats (CRISPR)-associated protein 9 (Cas9).²⁸ The CRISPR-Cas9 technology stems from prokaryotic immune system that recognizes and eliminates the invasive nucleic acids from virus or plasmid and has been developed into a powerful gene editing tool. It can be used to knockout target genes that code for protein kinases and thus achieve therapeutic effects. Despite that, CRISPR-Cas9 technology cannot be applied to all targets due to the lethal effect after gene knockout.²⁹ In addition, the process of CRISPR-Cas9 gene editing is time consuming that allows for genetic

compensation.³⁰ Moreover, the requirement of special delivery system and the potential safety concerns largely restrict its clinical use.^{31,32}

The toolbox of drug modalities is continuously expanding and contributes to drug discovery. The choice of the right drug modality targeting specific protein kinase relies on the sufficient understanding of the target kinase as well as the parallel evaluation of different modalities.

1.3 CDK8/19: Structures and Functions

The Cyclin-dependent kinases (CDKs) belongs to the CMGC protein kinases, which are serine/threonine kinases and their activities are regulated by corresponding cyclin proteins.³ According to their functions, the 20 CDKs can be classified into two categories: one for cell cycle progression regulation, including CDK1, CDK2, CDK3, CDK4, CDK5, CDK6, CDK10, CDK11, CDK14, CDK15, CDK16, CDK17, and CDK18; the other for transcription mediation, including CDK7, CDK8, CDK9, CDK11, CDK12, CDK13, CDK19, and CDK20.^{3,33} Meanwhile, studies have shown that some CDKs that were initially implicated in transcription regulation also mediate cell cycle progression.^{34,35}

The CDK8 protein, encoded by CDK8 gene located at chromosome 13q12.13, contains 464 amino acids.³⁶ The CDK8 protein has a typical kinase fold which (**Figure 1.1**) contains two lobes (the N and C lobes) that being connected through a hinge region. The N-lobe contains 5 beta strands and an alpha helix while the C-lobe has 8 alpha helices. The ATP binding site is located at the interface between these two lobes, surrounded by the hinge region, glycine-rich region (P-loop), and activation loop (A-loop). The CDK8 protein is activated

through binding with Cyclin C protein, while the subsequent Med12 association is essential for CDK8 activation as well.³⁷ Cyclin C binds to the N-lobe of CDK8 and resulting in a movement of the alpha helix on the N-lobe which opens the catalytic cleft of CDK8 and enables the formation of conserved salt bridge between residue Glu66 and Lys52.³⁸ In addition, compared to other CDK family members, CDK8 possesses special structural features: instead of Asp-Phe-Gly (DFG) motif located at the N-terminus of the A-loop, it has a Asp-Met-Gly (DMG) motif.³⁹ Meanwhile, CDK8 exhibits an extended C-terminal domain and may contribute to substrate selectivity.⁴⁰ Moreover, unlike other CDKs, the three conserved arginine residues (Arg65, Arg150 and Arg178) in CDK8 are stabilized by interacting with the Glu99 residue in Cyclin C due to the lack of a phosphorylated residue on T-loop.^{38,39} Under the active status, the A-loop of CDK8 is in an 'open' conformation that enables the substrate binding at the C-lobe, while the DMG motif is 'in' and opens up the ATP binding site.

CDK19, a homolog of CDK8, shares 80% full sequence identity and 97% kinase domain sequence identity with CDK8. Their CCNC binding domains are also highly conserved. Despite that, compared to CDK8, CDK19 possesses an extended C-terminus with an additional 38 residues including a glutamine rich stretch that may contribute to substrate recognition, suggesting that the two homologs may participate in different cellular events. For instance, it is reported that the CDK19 kinase module negatively regulates the viral activator VP16-dependent transcription, however, CDK8 kinase module acts in a positive manner.⁴¹ In addition, CDK8 knockout leads to embryonic lethality in mice in spite

of the presence of CDK19.⁴² Moreover, upon hypoxia, CDK8 knockdown in HCT116 cells resulted in 65% gene downregulation, however, knockdown of CDK19 only affected 13% of the genes.⁴³ Furthermore, the levels of CDK8 and CDK19 are quite different in humans: while CDK8 is universally expressed, the expression of CDK19 is tissue specific.⁴⁴⁻⁴⁷ However, currently there is no CDK19 crystal structure available.

In eukaryotes, all the protein-coding genes and most non-coding RNA genes are transcribed through RNA polymerase II (Pol II) that consists of 12 subunits.⁴⁸ The transcription is triggered by the binding of specific transcription factors (STFs) to the enhancer region on chromatin that forms the STFs/enhancer complex. The STFs/enhancer complex then recruits chromatin modifier complex and reshapes the chromatin structure to facilitate the recruitment of other transcriptional co-activators such as Mediator complex and cohesin. The resulted multi-complex can then promote chromatin looping and subsequent assembly of Pre-initiation complex (PIC) at core promoter.^{49,50} PIC includes Pol II, transcription initiation factor IIA (TFIIA), TFIIB, TFIID, TFIIIE, TFIIF, and TFIIH, and modulates the activity of Pol II.^{51,52} The transient association between core mediator complex (without kinase module) and PIC activates Pol II for transcription initiation. The subsequent dissociation of core mediator complex and the escape of Pol II from PIC leads to transcription elongation. Meanwhile, RNA Pol II re-initiation is required for continuous transcription. The remaining PIC scaffold complex after RNA Pol II escaping also facilitates transcription reinitialization.⁵³ Apart from that, RNA Pol II is often paused during extension by DRB sensitivity-inducing factor (DSIF) and

negative elongation factor (NELF).⁵⁴ However, this pause can be released by pause release factors (positive transcription elongation factor (P-TEFb) or P-TEFb-containing super-elongation complex (SEC) that phosphorylate DSIF and NELF.^{55,56} The circulation of above steps makes up the Pol II-regulated transcription.

CDK8 is essential for the regulation of gene transcription in both positive and negative manners in mammals. To do so, CDK8 either forms a kinase module with cyclin C, Med12, and Med13,^{57,58} and alters the activity and stability of transcription factors (TFs) via phosphorylation.⁵⁹⁻⁶²

The human Mediator Complex is a protein assembly with 30 subunits that plays a key role in regulating RNA Pol II-mediated transcription.⁶³ It can be divided into two parts, the kinase module and the core Mediator complex. The kinase module contains four subunits (CDK8, CCNC, Med12, and Med13) and is able to reversibly associated with the core Mediator complex (consists of 26 subunits) via Med13 as shown in **Figure 1.2**.^{64,65} The ChIP-Seq data shows that kinase module is co-localized with Mediator genome-wide,⁵⁰ suggesting that kinase module is essential in regulating Mediator-mediated transcription. The transcription initiation requires RNA Pol II escape from PIC. This process is assisted by CTD phosphorylation at Ser5 of RNA Pol II by CDK7/cyclin H, a TFIIH subunit and a substrate of CDK8.⁶⁶ The kinase module suppresses transcription initiation via CDK8-mediated phosphorylation of CDK7/cyclin H.⁶⁷ In addition, when the kinase module binds to the core Mediator complex, it causes the conformation change of Mediator and excludes the binding of RNA Pol II, thus inhibiting the transcription

re-initiation.⁶⁸ Therefore, kinase module acts as a switch for transcription initiation and re-initiation. On the other hand, the kinase module containing CDK8 is able to promote transcription elongation. CDK9 is a subunit of P-TEFb, a pause release factor. While CDK8 is able to phosphorylate CDK9, it consequently enhances the recruitment and activity of P-TEFb.⁶⁹⁻⁷¹

As mentioned above, CDK8 and CDK19 are homologs. In addition, the paralogs of Med12 and Med13 have been identified as well. The Med12-like (Med12L) and Med13-like (Med13L) proteins share 59% and 53% sequence similarity with Med12 and Med13. These homologous pairs are mutually exclusive in forming the kinase module and result in a number of kinase module variants.⁷² These not only share overlapping functions,^{73,74} but also exhibit different roles in regulating transcription.^{41,72}

At the same time, CDK8 can regulate transcription in a way that may be independent of Mediator by phosphorylating TFs as shown in **Figure 1.3**. Receptor-regulated mothers against decapentaplegic proteins (R-Smads) are transcription activators that mediate BMP/TGF- β signals.⁷⁵ CDK8 phosphorylates R-Smads, which enhances the binding of R-Smads to co-activators and promotes the transcription of target genes.⁷⁶ Meanwhile, the phosphorylated R-Smads can be ubiquitinated resulting in subsequent degradation.⁷⁷ The neurogenic locus notch homolog protein (NOTCH) signaling pathway is critical for inter-cellular communication, T cell differentiation and neuronal development.⁷⁸⁻⁸⁰ The NOTCH intracellular domain (NICD) can be cleaved and enters into the nucleus after ligand binding to the extra-cellular domain of the NOTCH receptor. NICD then binds to

the NOTCH target gene and activates transcription.⁸¹ CDK8-mediated NICD phosphorylation, on the other hand, leads to NICD ubiquitination and subsequent degradation that terminates NOTCH target gene transcription.⁵⁹ Signal transducer and activator of transcription (STAT) family plays a key role in mediating cytokine responses and its deregulation is often associated with immune diseases, viral infections, and increased susceptibility to malignancies.⁸² Upon interferon- γ (IFN- γ) stimulation, STAT1 can be phosphorylated at Tyr701 by Janus kinase (JAK) and forms a dimer. The phosphorylated STAT1 dimer is then transferred into nucleus and binds to the target gene for transcription.^{83,84} Despite that, the full activation of gene expression requires the second phosphorylation at Ser727 on STAT1 which is mediated by CDK8.⁶² GCN5L-mediated acetylation of histone H3 induces the transcriptional activation of immediate early genes (IEG), which requires CDK8-mediated histone H3 phosphorylation at Ser10/Lys14.^{85,86} Sterol regulatory element-binding protein (SREBP) family is essential for adipogenesis regulation. Upon insulin stimulation, SREBP-1C is localized to the nucleus and activates the transcription of adipogenic-related genes.⁸⁷ CDK8 is able to negatively regulate SREBP-1C mediated transcription via phosphorylating SREBP-1C at Thr402. The phosphorylated SREBP-1C then undergoes ubiquitination and subsequent degradation.⁶¹ In addition, CDK8 knockdown results in lipid accumulation due to the upregulation of adipogenic genes.⁸⁸

Other than their kinase activities, both CDK8 and CDK19 exhibit kinase-independent functions as well. For instance, CDK8 is upregulated along with the loss of histone variant mH2A, which in turn increases melanoma malignancy in a

kinase-independent manner, and both wild-type (WT) and kinase-dead forms of CDK8 were reported to stimulate melanoma growth.⁸⁹ In another example, CDK8 deprivation suppresses the disease aggressiveness in B-cell leukemia mouse models but CDK8 inhibition shows only minimal effects, suggesting a kinase-independent role of CDK8 in leukemia development.⁹⁰ CDK19 knockdown reduces the proliferation of SJSA cells. Re-expression of either wild-type or kinase-dead CDK19 rescues the defects in cell proliferation, indicating a kinase-independent role of CDK19.⁹¹ It was also reported that upon IFN- γ stimulation, CDK19 activates a distinct set of genes compared to CDK8, which depends only on the scaffolding function of CDK19.⁹²

Although CDK8 is identified as a cyclin-dependent kinase involved in the regulation of transcription, its role in cell cycle regulation has been reported as well. Skp2-mediated degradation of macroH2A1 (mH2A1) enhances CDK8 expression and contributes to mouse embryonic fibroblasts (MEFs) G2/M transition, suggesting the role of CDK8 in cell cycle regulation.^{93,94} In addition, CDK8 promotes G1/S transition through the WNT/ β -catenin pathway via phosphorylating E2F1.⁹⁵ Moreover, CDK8 stimulates the transcription of p21 (a negative regulator of CDK1/2) and thus leads to G1/S process.⁹⁶ CDK7, a subunit of CDK activating kinase (CAK), is able to regulate cell cycle via phosphorylating the well-known cycle CDKs (CDK1/2/4/6). CDK8 is able to phosphorylate CDK7 and thus indirectly regulates cell cycle.⁹⁷

1.4 The Roles of CDK8/19 in Diseases

Multiple studies have identified the role of CDK8 in numerous diseases, especially in cancers, which makes it a promising drug target (**Figure 1.4**). CDK8 is identified as an oncogene in colorectal cancer (CRC) that was reported to be overexpressed in 60% CRC patients.⁹⁸⁻¹⁰⁰ The level of CDK8 is negatively correlated to the 5-year survival rate among 372 colon cancer patients.¹⁰¹ In addition, CRC patients at advanced stages exhibit much higher CDK8 level compared to early stages, indicating the role of CDK8 in promoting tumor progression.¹⁰¹ CDK8 exerts its oncogenic role in CRC mainly through the WNT/ β -catenin pathway.^{77,95,102,103} In CRC, the level of β -catenin is significantly elevated with excessive activity. When translocated into nucleus, β -catenin forms a complex with T cytokine factor (TCF) and lymphotropic factor (LEF), which recruits co-activators and induces the transcription of several oncogenes (MYC, AXIN2, and LEF1). CDK8 can indirectly promote the TCF/LEF-dependent gene transcription by phosphorylating and deactivating E2F1, a β -catenin suppressor. Studies have demonstrated that CDK8 knockdown reduced CRC proliferation in both *in vitro* cell and *in vivo* xenograft models.^{98,104} Despite that, it is reported that CDK8 deprivation increased tumor burden in APCMin intestinal tumor bearing mice.¹⁰⁵ The opposite roles of CDK8 in CRC suggests the multiple functions of CDK8 in transcription regulation under specific conditions. In order to enable the rapid proliferation, cancer cells often exhibit increased glucose consumption and glycolysis rate, this phenomenon is called the Warburg effect.¹⁰⁶⁻¹⁰⁸ A study has found that CDK8 together with hypoxia-inducible factor 1-alpha (HIF1 α) enhance the transcription

of glycolytic enzyme genes in colorectal cancer cells.⁴³ Inhibition of CDK8 interferes with glucose transporters and disrupts the glucose uptake, which hinders the cell proliferation of HCT116 cells,¹⁰⁹ indicating the role of CDK8 in glycolysis in colon cancer. In addition to promoting CRC growth, the role of CDK8 that contributes to colon cancer metastasis has been identified as well. CDK8 stimulates the transcription of miRNA-181 that inhibits the expression of tissue inhibitor of metalloproteinase 3 (TIMP3) through WNT/ β -catenin pathway and inhibition of CDK8 prevents the liver metastasis of colon cancer cells.¹¹⁰ Furthermore, CDK8 contributes to CRC invasion and metastasis via regulating matrix metalloproteinases (MMPs) through TGF- β /SMAD pathway.¹¹¹

Skp2-mediated mH2A1 degradation induces CDK8 upregulation that contributes to breast cancer cell proliferation. In addition, mH2A1 knockdown or CDK8 restoration recovers the Skp-2 loss mediated tumor suppression. Moreover, the levels of CDK8 and Skp2 is positively correlated with the tumor status among 189 human breast cancer samples.⁹⁴ Furthermore, it is reported that CDK8 is a downstream protein of estrogen receptor (ER) that promotes ER-induced transcription and deteriorates ER-positive breast cancer. Inhibition of CDK8 restrains the transcriptional elongation of ER-induced genes via suppressing estrogen-induced phosphorylation of RNAPII CTD at Ser2, which suppresses tumor growth both *in vitro* and *in vivo*.¹¹²

In melanoma, CDK8 is upregulated by the loss of histone variant mH2A that increases melanoma malignancy in a kinase-independent manner.¹¹³ Both CDK8 and CDK19 are overexpressed in advanced prostate cancers. Either CDK8/19

inhibition or knockdown reduces prostate cancer cell invasion and migration, suggesting their roles in prostate cancer progression.¹¹⁴ Study has shown that mutated K-RAS in pancreatic cancer stimulates the expression of CDK8. The elevation of CDK8 in turn triggers the epithelial-to-mesenchymal transition (EMT) through WNT pathway and contributes to the pancreatic cancer progression.¹¹⁵ Moreover, the upregulation of CDK8 in pancreatic cancer promotes angiogenesis through the CDK8- β -catenin-Krüppel like factor 2 (KLF2) pathway and thus contributes to cancer metastatic invasion.¹¹⁶ The CDK8-mediated EMT promotion has also been identified in ovarian cancer cells.^{117,118} It was reported that CDK8 and CDK19 are overexpressed in acute myeloid leukemia (AML) cell lines and negatively regulate super-enhancer (SE)-associated genes.¹¹⁹ Small molecule CDK8/19 inhibitors reduce STAT1-Ser727 phosphorylation and exhibit significant antileukemic activity both *in vitro* and *in vivo*.^{119,120} On the contrary, one study demonstrated CDK8-mediated tumor suppression in T-cell acute lymphoblastic leukemia (T-ALL). CDK8 phosphorylates intercellular NOTCH peptide and increases its degradation, which disrupts the NOTCH pathway and suppresses the progression of T-ALL,¹²¹ highlighting the context-specific and cell-type roles of CDK8.

The dysregulation of nuclear factor kappa B (NF κ B) transcription factors is closely related to cancer development due to its role in regulating inflammation.¹²² However, current NF κ B inhibitors lead to sustained NF κ B suppression and thus exhibit severe side effects. In that case, drugs that inhibit induced but not basal NF κ B activity may offer better therapeutic effects. CDK8 promotes the transcription

of NFκB target genes upon TNF-α stimulation, such as Il8, Cxcl2 and Cxcl3. Inhibition of CDK8 downregulates the transcription of tumor-promoting cytokines, however, without affecting the basal level of NFκB regulated genes.^{122,123} Moreover, upon lipopolysaccharide (LPS) stimulation, CDK8 promotes the expression of inflammatory genes.¹²⁴ CDK8 knockdown enhances the anti-inflammatory and anti-apoptotic effects of miR-297 in LPS-mediated A549 cells and mice model.

CDK8 phosphorylates STAT1 at Ser727 in resting natural killer (NK) cells and suppresses the NK cell cytotoxicity.¹²⁵ The STAT1-S727A mutant mice exhibit enhanced NK cell cytotoxicity and are resistant to different cancers.¹²⁵ In addition, the level of phosphorylated STAT1 at Ser727 does not change in CDK8-deficient NK cells, possibly due to the compensatory role of CDK8 homolog, CDK19.^{73,74} Moreover, NK cells are associated with leukemic stem cells elimination that avoids leukemia relapse.¹²⁶

The functions of CDK8/19 in transcription, metabolism, inflammation, immune regulation and metastasis, makes it a promising drug target for numerous diseases, especially cancers. Inhibiting or silencing CDK8/19 is able to reduce the invasiveness, growth, metastasis, and metabolism of cancer cells, while enhancing cancer cell differentiation, and tumor surveillance.

1.5 Development of CDK8/19 Inhibitors and Other Types of Regulators

Since CDK8 has been validated as a potential drug target due to its role in diverse diseases, especially in cancers, it has led to the development of CDK8

inhibitors.¹²⁷⁻¹²⁹ This however is still in its early stages, and most of the inhibitors were discovered in recent years. In addition, due to the homology between CDK8 and CDK19, most of the identified CDK8 inhibitors also suppress CDK19. As mentioned in the above sections, CDK19 can compensate the functions of CDK8, meanwhile, it demonstrates unique impacts in both transcription and disease progression.¹³⁰ Therefore, inhibition of both CDK8 and CDK19 may offer enhanced therapeutic effects. At the same time, developing selective CDK8 or CDK19 inhibitors is still necessary for studying the biological mechanisms of CDK8 or CDK19.

Current small molecule CDK8 inhibitors are either type I or type II inhibitors (**Figure 1.5**) although most of them are type I. Type I kinase inhibitors, also known as ATP-competitive inhibitors, are small molecules that bind to the ATP binding site.¹³¹ Type I compounds are the most common kinase inhibitor class and account for two-thirds of all FDA-approved inhibitors.¹³² Despite the clinical success of type I inhibitors, there are several concerns in developing such compounds. The first is the issue of selectivity. Since kinases are highly conserved in the ATP binding sites, many type I inhibitors exhibit poor selectivity that lead to toxicities and side effects.^{133,134} Secondly, due to the high intracellular ATP levels and a low value of ATP's Michaelis constant, a high affinity is required in order to achieve effective kinase inhibition *in vivo*.^{133,135} Thirdly, mutations often happen in the kinase ATP binding sites and disrupt the binding of inhibitors thus leading to drug resistance.^{136,137} Type II inhibitors, on the contrary, bind to inactive kinases and occupy both ATP binding site and an adjacent allosteric pocket. This may provide

better selectivity over type I inhibitors due to the uniqueness of allosteric pockets among kinases.¹³⁸ However, type II inhibitors development has several drawbacks including the lower level of inactive kinase in cells, less binding affinity and mutations, especially at the gatekeeper residue.¹³⁹ Although type II inhibitors may achieve better selectivity, this is not always the outcome.¹³⁸ Meanwhile, type I inhibitors through careful design can still achieve highly selectivity.

Some early CDK8 inhibitors were identified by testing known kinase inhibitors like the v-raf murine sarcoma viral oncogene homolog B1 (BRAF) inhibitor Sorafenib,¹⁴⁰ the breakpoint cluster region (BCR)- v-abl Abelson murine leukemia viral oncogene homolog 1 (ABL) inhibitor Ponatinib,¹⁴¹ and the VEGF inhibitor Linifanib.¹⁴² The binding affinities of these inhibitors against CDK8 are much lower than against their original targets. Moreover, X-ray crystal structure of CDK8-Sorafenib complex has been identified. Sorafenib is a type II CDK8 inhibitor and occupies both ATP binding site and the adjacent allosteric binding pocket.³⁹ However, type II CDK8 inhibitors, Sorafenib and its analogs lack cellular potency which may be due to the low levels of inactive CDK8 in cells.¹⁴³

In contrast, type I inhibitors have a good correlation of biochemical potency and cellular activity with significant selectivity, suggesting that they have more potential for CDK8 inhibitor drug development. Currently, the majority of CDK8 inhibitors are type I inhibitors and in addition, mostly target CDK19 due to the high sequence similarity between these two protein paralogs.

Cortistatin A, a steroidal alkaloid isolated from marine sponge *Corticium simplex*,¹⁴⁴ exhibits high affinity ($K_d=17$ nM) and selectivity for CDK8/19 as shown

via kinase profiling. In addition, Cortistatin A promotes SE-associated genes by inhibiting CDK8/19 that contributes to tumor suppression and exhibits anti-leukemic activity both *in vitro* and *in vivo* without any apparent toxicity. Despite that, Cortistatin A does not affect HCT116 cells and shows negligible anti-proliferative effect.¹⁴⁵ SEL120-34A,¹⁴⁶ developed by Selvita Ltd., is a selective CDK8/19 inhibitor that marginally inhibits CDK9. It inhibits the phosphorylation of STAT1-Ser727 and STAT5-Ser726 and suppresses the growth of AML both *in vitro* and *in vivo* with negligible toxicity. However, it has no effect on MOLM-14 cells. Moreover, SEL120-34A has entered into clinical trials for AML treatment (clinicaltrials.gov NCT04021368). Senexin A was discovered through a high-throughput screen for inhibitors against p21 induced transcription and later identified as a selective CDK8/19 inhibitor. It suppresses tumor-promoting paracrine activities and increases the efficacy of chemotherapy in xenograft animal models.¹⁴⁷ In addition, Senexin A partially suppresses β -catenin–dependent transcription in HCT116 colon carcinoma cells through CDK8 inhibition.¹⁴⁸ The optimization of Senexin A resulted in a more potent and selective CDK8/19 inhibitor, Senexin B. It also inhibits β -catenin related transcription in HCT116 cells.¹⁴⁹ In addition, studies have demonstrated that Senexin B inhibits tumor growth in several *in vivo* tumor models, including lung cancer, breast cancer, and AML.^{149,150} Furthermore, Senexin B has entered into clinical trials (clinicaltrials.gov NCT03065010), for advanced ER-positive breast cancer in combination with aromatase inhibitors or fulvestrant. CCT251545 and its analogue CCT251921 both target CDK8 and CDK19 with highly potent inhibition activity.^{109,151,152} They inhibit

the WNT pathway in several colorectal cancer cell lines, however, cannot suppress the proliferation of CRC cells and only slightly inhibit tumor growth in CRC xenograft model. Meanwhile, CCT compounds exhibit severe organ toxicity in different animal models.¹⁵² A later study indicates that the toxicity of these compounds is very likely due to the off-target effects.¹⁵³ BRD6989 was initially disclosed from screening of small molecular interleukin-10 (IL-10) enhancers and later identified to target both CDK8 and CDK19 via kinase profiling. In addition, it has a high selectivity for CDK19 with only moderate CDK8 inhibition (IC_{50} =500 nM). BRD6989 suppresses the phosphorylation of STAT1 at S727 and enhances IL-10 production that promoted innate immune activation.¹⁵⁴ BI-1347 is another selective CDK8/19 inhibitor with a CDK8 inhibitory IC_{50} value of 1 nM. It is able to enhance NK cell activity and promotes tumor surveillance.¹⁵⁵ In spite of the existing CDK8/19 inhibitors, further investigation is still required in order to achieve inhibitors with enhanced potency, specificity, and favorable PK profiles for both research and clinical applications.

Along with small molecule CDK8 inhibitors, other drug modalities have also been used to regulate the kinase activity of CDK8, such as small interfering RNAs, antisense oligonucleotides, CRISPR-Cas9 gene editing technology, and PROTAC technology. Compared to small molecule inhibitors, these regulators modulate the CDK8 kinase activity either through CDK8 gene knockdown/knockout or CDK8 protein degradation. Nucleic acid based compounds generally are easy to synthesize and have high specificity, however, they have poor metabolic stability and oral absorption due to the high molecular weight and a large number of

hydrogen bond donors and acceptors, which limits their clinical use.¹⁵⁻¹⁸ In addition, partial sequence complementarity can often cause severe off-target effects.¹⁷ CRISPR-Cas9 technology is a novel gene editing tool and was applied in gene therapy for treatment of numerous diseases.¹⁵⁶⁻¹⁵⁸ However, the poor stability, delivery issues and potential safety concerns largely hamper its clinical application.^{31,32} Moreover, both nucleic-acid based strategies and CRISPR-Cas9 technology have no effects on existing or long-lived target proteins.¹⁴ PROTAC technology, on the other hand, is able to block kinase activities post-translationally through degradation. In addition, through protein degradation, PROTAC molecules can eliminate both the catalytic and non-enzymatic functions of kinase at the same time. Two PROTAC molecules (**Figure 1.6**), JH-XI-10-02 and YKL-06-101, have been developed through conjugation of Cortistatin A analog or THZ4-55 with Cereblon E3 ligase binder pomalidomide or thalidomide through a PEG linker. They promote the ubiquitination and degradation of CDK8 in Jurkat and BV173 cells, without affecting its paralog CDK19.^{159,160}

This dissertation focuses on the design, synthesis, optimization, and biological evaluation of novel small molecule CDK8/19 inhibitors and PROTACs as potential anti-cancer agents.

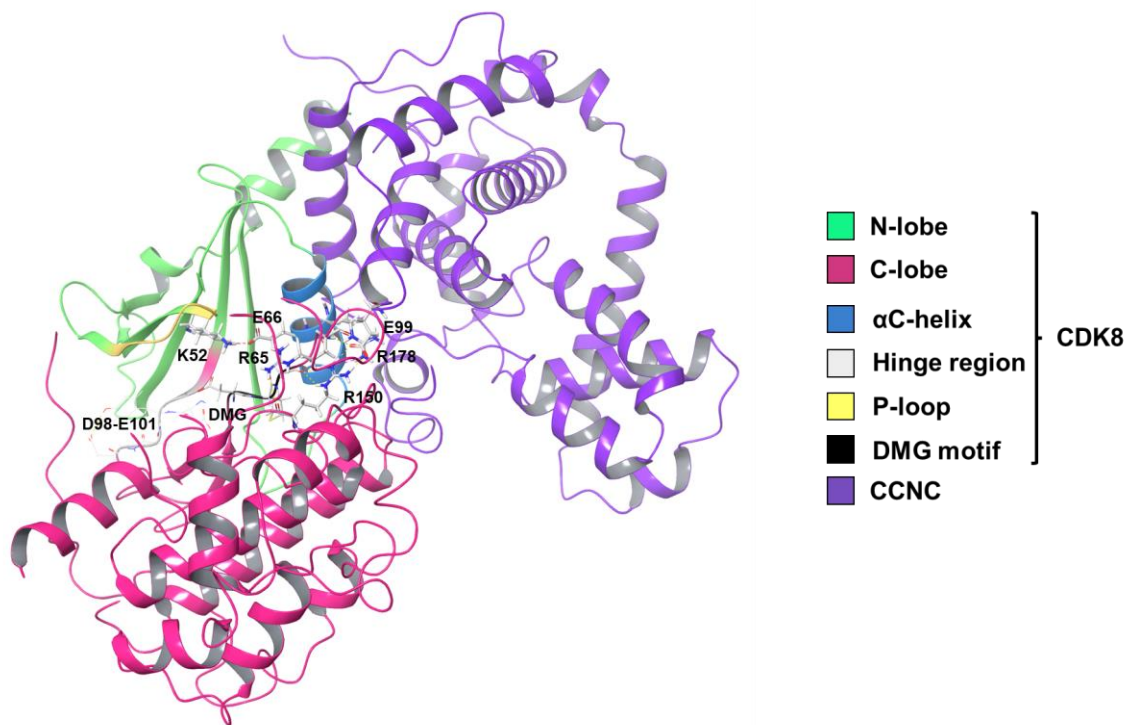


Figure 1.1 The protein structure of CDK8/CCNC (PDB code: 4F7S). CDK8 is a bi-lobe protein and activated by binding with its partner CCNC. The ATP binding site is between the N-lobe and C-lobe. The key motifs are identified in colors.

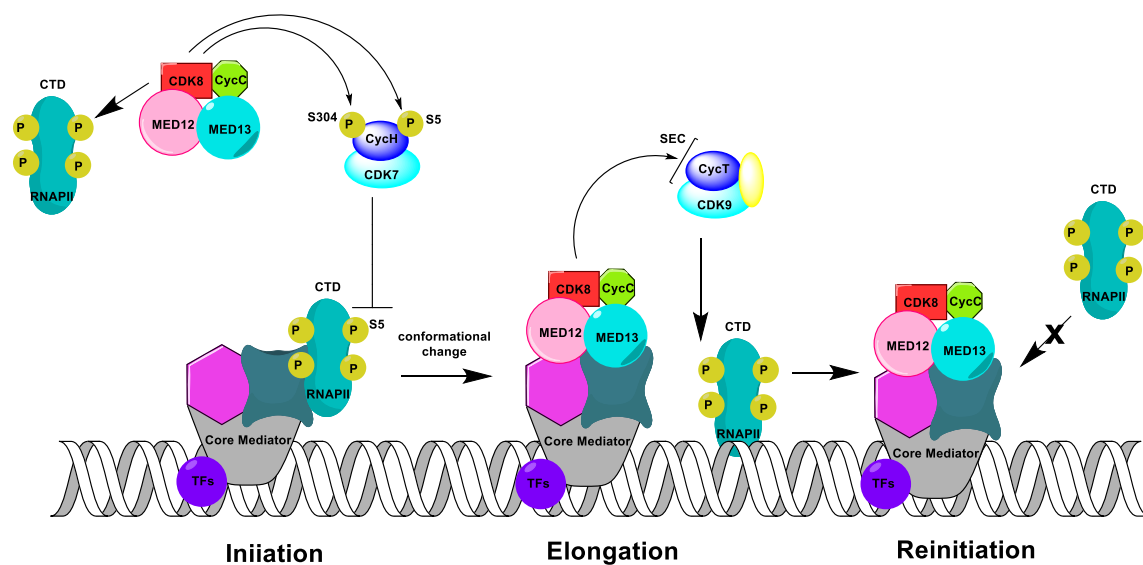


Figure 1.2 The regulation of RNAPII transcription via CDK8. CDK8 participates in initiation, elongation, and re-initiation in either a positive or negative manner.

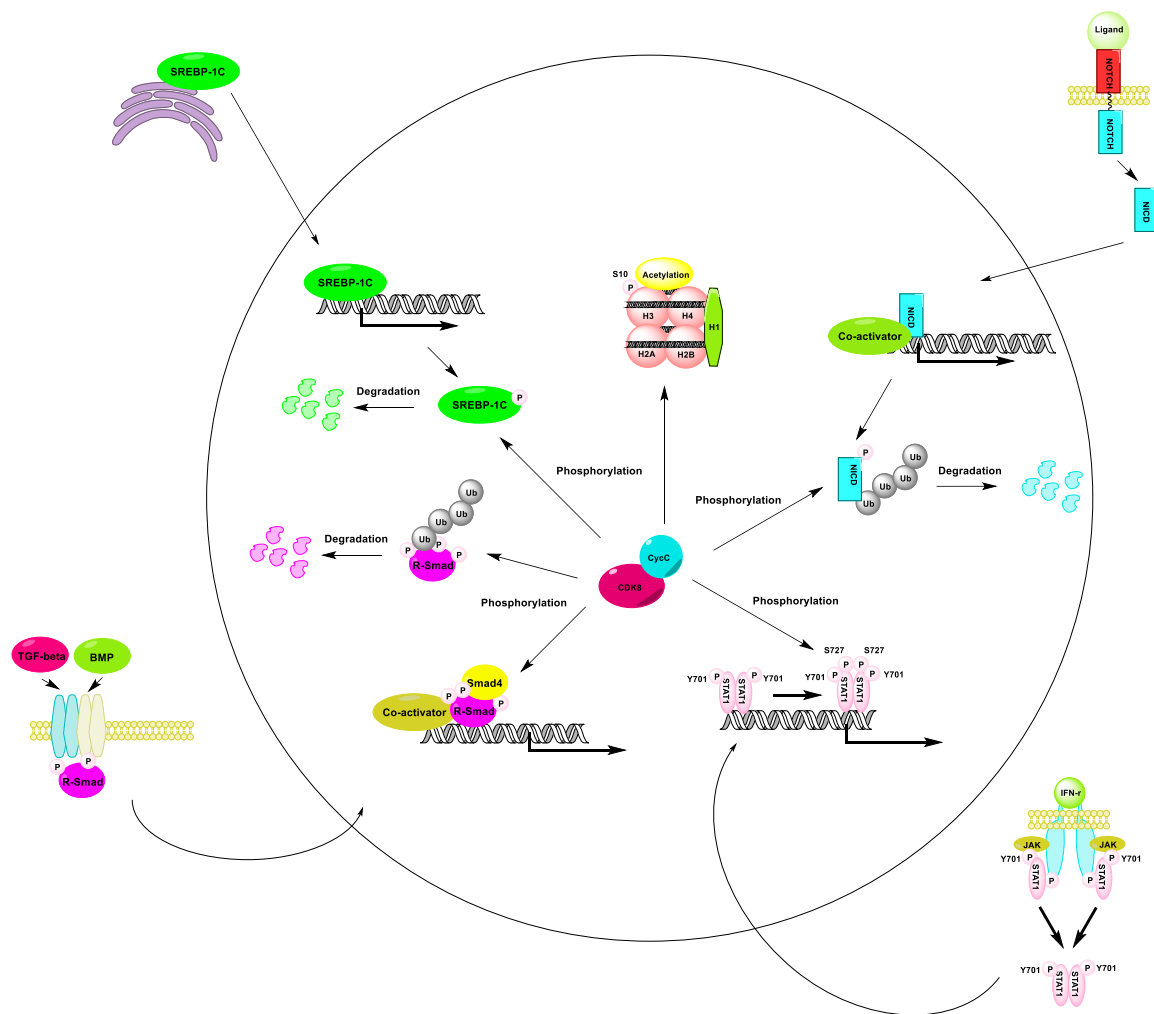


Figure 1.3 The role of CDK8 in transcriptional regulation via phosphorylating TFs.

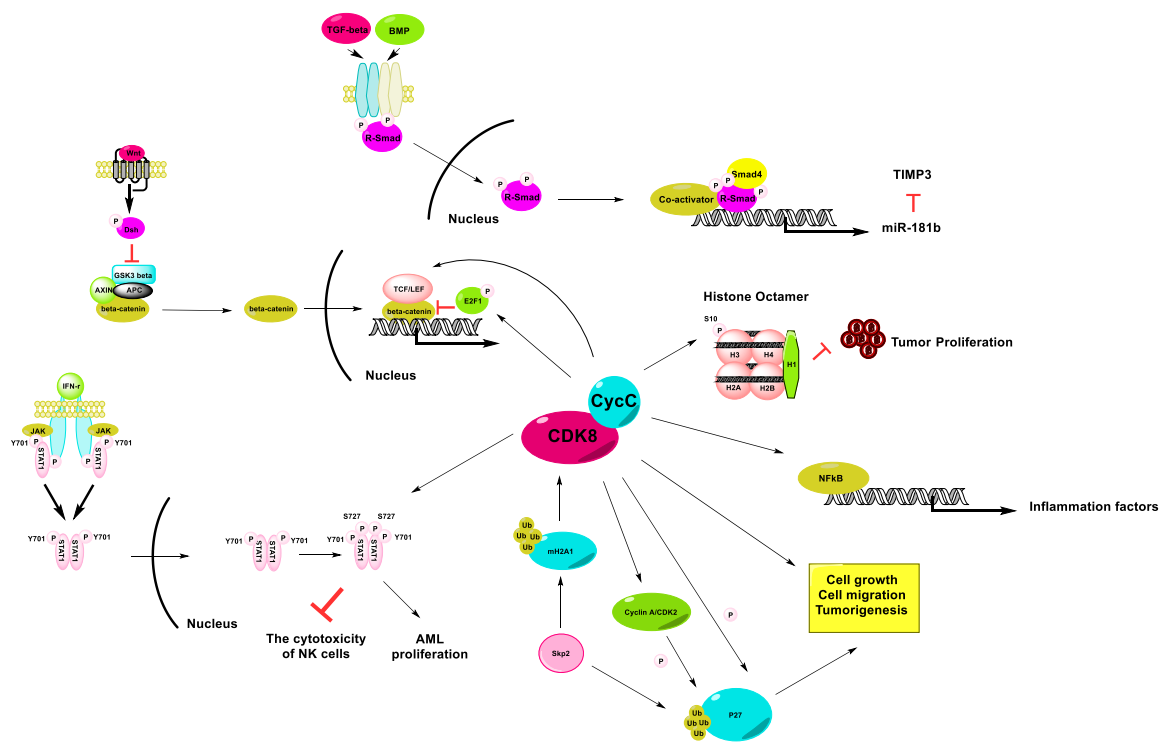
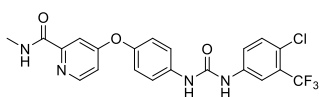
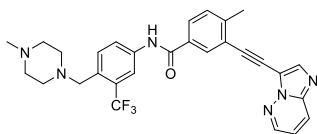


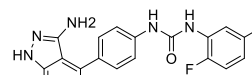
Figure 1.4 The role of CDK8 in diseases.



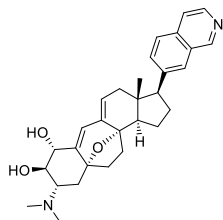
Sorafenib
CDK8 IC₅₀=199nM



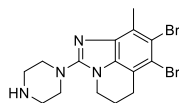
Ponatinib
CDK8 IC₅₀=14nM



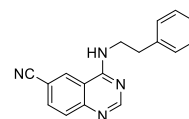
Linifanib
CDK8 IC₅₀=14nM



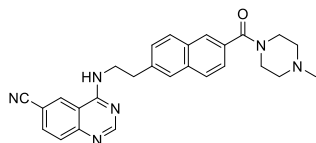
Cortistatin A
CDK8 IC₅₀=5nM



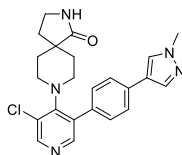
SEL120-34A
CDK8 IC₅₀=4nM



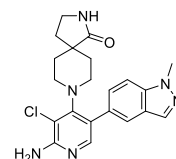
Senexin A
CDK8 IC₅₀=280nM



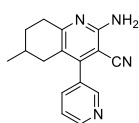
Senexin B
CDK8 IC₅₀=40nM



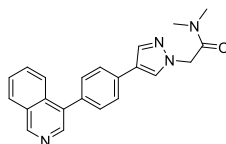
CCT251545
CDK8 IC₅₀=5nM



CCT251921
CDK8 IC₅₀=2.3nM

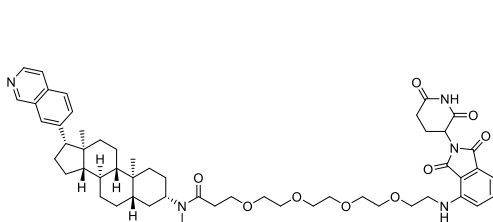


BRD6989
CDK8 IC₅₀=500nM

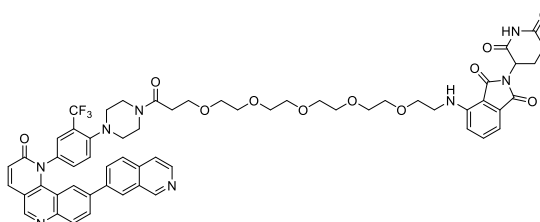


BI-1347
CDK8 IC₅₀=1nM

Figure 1.5 The structures of reported CDK8 inhibitors.



JH-XI-10-02
CDK8 IC₅₀=159nM



YKL-06-101
CDK8 IC₅₀=31nM

Figure 1.6 The structures of reported PROTACs targeting CDK8.

CHAPTER 2

DEVELOPMENT OF QUINOLINE-6-CARBONITRILE-BASED ANALOGS AS NOVEL CDK8/19 INHIBITORS

2.1 Introduction

Senexin A (**2.1**) and Senexin B (**2.2**) are quinazoline-based selective CDK8/19 inhibitors (**Figure 2.1A**) developed by Senex Biotechnology, Inc.^{161,162} Senexin A was initially derived from high throughput screening for molecules that inhibit p21- and DNA damage-activated transcription, and later was identified as a selective inhibitor of CDK8/19. It exhibits significant CDK8 and CDK19 binding affinity with K_d values of 830 nM and 310 nM.¹⁴⁷ Senexin A inhibits damage-induced paracrine activities in tumor cells and increases the efficacy of chemotherapy in xenograft animal models.¹⁴⁷ Further optimization of Senexin A resulted in Senexin B which has better potency and selectivity. It inhibits CDK8 activity with a IC_{50} value of 40 nM at kinase level. According to KINOME scan results (DiscoverX), Senexin B shows high CDK8/19 selectivity among 451 kinases with only a few off-targets as shown in **Figure 2.1B**. Senexin B suppresses the tumor growth and enhances the anti-cancer effect of doxorubicin in triple-negative breast cancer (TNBC) xenografts.¹⁶³ Meanwhile, Senexin B-mediated CDK8 inhibition not only reduces the tumor burden in estrogen positive breast cancer xenografts, but also exhibits a synergistic effect with ER antagonist

fulvestrant.¹¹² The synergistic effect of Senexin B is also seen when combined with an anti-HER2 monoclonal antibody or the EGFR inhibitor lapatinib for the treatment of HER2 positive breast and colon cancer cell lines.¹⁶⁴ Although Senexin B has no effect on tumor growth in mouse CT26 tumor xenograft model, it suppresses tumor metastasis to the liver.¹⁶³ In addition, CDK8/19 inhibition via Senexin B suppresses the induced NFκB-driven transcription without affecting the basal expression of NFκB-regulated genes, suggesting the function of CDK8/19 in mediating transcriptional reprogramming.¹⁶⁵ Senexin B (a.k.a. BCD-115) is the first selective CDK8/19 inhibitor to enter clinical trials (clinicaltrials.gov NCT03065010) for advanced ER-positive breast cancer in combination with aromatase inhibitors or fulvestrant. However, Senexin B showed an unfavorable PK profile in humans and its main metabolite has no CDK8 inhibitory activity (Data not shown).

Despite the significant selectivity and anti-cancer therapeutic effects of Senexin B, there is still room to improve its potency and PK profile. Thanks to the abundance of three-dimensional structures of biological molecules via either X-ray crystallography or nuclear magnetic resonance, structure-based drug design (SBDD) strategy is now widely applied in the drug discovery and design.¹⁶⁶⁻¹⁶⁹ SBDD strategy allow the prediction of ligand binding sites in the target protein and estimates the binding affinity of ligands with considerable accuracy.¹⁶⁹⁻¹⁷¹ This information can then be used for design and optimization of new ligands with enhanced affinity and selectivity. Meanwhile, for target proteins without determined structures, computational methods such as homology modeling^{172,173} can be applied to predict the three-dimensional structures based on similar proteins. In

addition, when compared to combinatorial chemistry¹⁷⁴ and high-throughput screening (HTS),^{175,176} SBDD is both time- and cost-efficient, and can eliminate failures at an earlier stage, thus speeding up drug discovery progress and achieving great success.

In this chapter, Senexin A and Senexin B are chosen as the starting scaffolds. SBDD is carried out for the following design and structural modification to achieve CDK8/19 inhibitor candidates with increased potency and favorable PK profile.

2.2 Results and Discussion

2.2.1 Structure-Based Design of Quinoline Senexin Analogues

A molecular docking study of Senexin A (**2.1**) was carried out by using the reported crystal structure of CDK8/cyclin C in complex with an analog of Senexin A (PDB ID: 4F7S).¹⁷⁷ In the most plausible binding mode, shown in **Figure 2.2**, the 1-*N* atom on the quinazoline ring of Senexin A forms a hydrogen bond with NH of Ala100 at the hinge region of CDK8. Hinge interactions are conserved in most ATP competitive kinase inhibitors. The nitrogen lone pair of the 6-cyano group accepts a hydrogen bond from the strong H-bond donor of the positively charged NH₃ of Lys52. In addition, the phenethyl aromatic ring was predicted to form aromatic hydrogen bonds with the carbonyl oxygen of Gly33. Interestingly, the *N*-3 atom on the quinazoline ring was not observed to make significant interactions with CDK8 in docked structures, suggesting that it does not contribute to the binding affinity and is not required for drug-target interaction.

Based on this prediction, a docking study of the quinoline version of Senexin A showed that **2.8a** possessed the same interactions as its parent quinazoline compound at the head part (**Figure 2.2**), and its phenethyl aromatic ring formed aromatic hydrogen bonds with the carbonyl oxygens of Ala155 and Val27. Synthesis and testing of **2.8a** along with Senexin A demonstrated that **2.8a** is more potent than Senexin A in both *in vitro* and cell-based assays, with a Lanthascreen kinase IC₅₀ value of 17 nM (**Table 2.1**). This can be attributed to the increased basicity of the *N*-1 atom in the quinoline context and thus leading to a stronger H-bond interaction with Ala100. Due to the increased activity of **2.8a** compared to Senexin A and furthermore the good pharmacokinetic properties of quinolines in general, research efforts focused on modifications of **2.8a** to improve its *in vitro* potency while further optimizing its drug-like properties.

To further investigate the contributions of functional groups at the 6-position of the quinoline ring system, a series of analogs (**2.8b-j**) were synthesized with varying groups replacing the nitrile functional group as shown in **Scheme 2.1**. According to the results from Lanthascreen and cell-based assays (**Table 2.1**), the H-bond acceptor role of the 6-cyano group with Lys52 mentioned above is key to inhibitory activity. In the first instance, removal of this group to generate the unsubstituted quinoline (**2.8b**) led to a roughly 60-fold decrease in CDK8 activity (Lanthascreen) thus giving a direct measure of its contribution. Further replacement of this group with halogens or a trifluoromethyl group (**2.8c-f**) significantly decreased CDK8 inhibition potency with the chloro-substitution being the most effective of the series. The interchange of the nitrile for a nitro group

(**2.8g**) generated an analogue of similar potency suggesting that an H-bond acceptor (HBA) group leads to the most favorable interaction with Lys52. Substitution with an aromatic amino group (**2.8i**) led to a dramatic potency loss further suggesting the requirement of a HBA to facilitate interaction with the lysine sidechain. Two additional compounds bearing larger functional groups (**2.8h**-amide and **2.8j**-acetamide) again confirm the need for an appropriate HBA group and also point to the detrimental effect of steric hindrance in binding to CDK8. The results obtained for compounds tested in the cell-based reporter assays for the most parts were in line with the Lanthascreen data but yielded higher IC₅₀ values, perhaps reflective of the differences in cellular penetration of these analogs. The quinoline-6-carbonitrile scaffold was chosen for further drug discovery and optimization studies due to its optimal binding to CDK8 and the desire to exclude an aromatic nitro group of **2.8g** as a known toxicophore.

2.2.2 Lead Optimization of Quinoline Senexin B Derivatives

After determining the optimal substitution of the quinoline ring, the next step was to investigate the impact of this scaffold on the inhibitory effect of Senexin B (**2.2**). The quinoline version of Senexin B (**2.20a**) was synthesized (**Scheme 2.2**). Consistent with the results for Senexin A and **2.8a**, **2.20a** exhibited improved CDK8 inhibitory activity compared to its quinazoline counterpart (**2.2**) in both Lanthascreen and cell-based assays (**Table 2.2**). In addition to the quinoline, a number of other alternate core structures were synthesized and evaluated. These included 1,7-naphthyridine, 1,8-naphthyridine and cinnoline versions of Senexin B however all were significantly less potent thereby confirming that the quinoline was

the optimal core structure (data not shown). In each of these alternate cores, the equivalent of *N*-1 is absent or considerably less basic than the quinoline confirming the structure hypothesis.

The docking studies of Senexin B (**2.2**) and **2.20a** were carried out using the same CDK8 crystal structure (PDB ID: 4F7S) and the predicted binding modes are shown in **Figure 2.3**. The key interactions of Senexin B (**2.2**) and **2.20a** were shown to be similar where the *N*-1 of the quinazoline/quinoline ring forms the conserved H-bond with NH of Ala100 in the hinge region. As with Senexin A (**2.1**) and its quinoline counterpart **2.8a**, the 6-cyano nitrogen is involved in a H-bond with the side chain ammonium of Lys52. In addition, for **2.20a**, the naphthyl ring is predicted to form a Pi-Cation interaction with the guanidinium group of Arg356 and a Pi-Pi stacking interaction with the imidazole ring of His106. The amide oxygen in the bridge between the naphthyl and methylpiperazine rings interact through a H-bond with Lys109. Both compounds also make hydrophobic interactions in the ATP binding cleft.

Since consistent improvements in activity were observed for both **2.8a** and **2.20a** relative to the corresponding parent quinazoline compounds, a further series of 4-((2-(6-substituted-naphthalen-2-yl)ethyl)amino)quinoline-6-carbonitrile derivatives were designed, synthesized, and evaluated as shown in **Scheme 2.2 and Table 2.2**. To explore the SAR of the tail group, replacement of the naphthyl ring with a second quinoline group was undertaken thus generating **2.20b**. The rationale for this modification was to provide additional interactions with nearby residues while increasing hydrophilicity and aqueous solubility of **2.20a**. **2.20b**,

however, was found to be inactive in the Lanthascreen assay and loses cellular potency compared to **2.20a**. The docking results for **2.20b** indicate a similar binding mode to that of **2.20a**, suggesting that it may not be the interactions of the second quinoline ring that interfere with target binding. One possibility is that the additional nitrogen in **2.20b** may result in a stabilized intramolecular conformation that entropically disfavors binding of this analog to CDK8. Indeed, molecular modeling simulation predicts that the second quinoline nitrogen may interact with the amino group through hydrogen bond to form a six membered ring-like intramolecular structure and that this conformation is further stabilized by other favorable interactions (**Figure 2.4**), providing a potential explanation for its dramatically reduced potency.

Further modifications were made by varying the substitutions of the piperazine ring of **2.20a** (**2.20c-2.20n**, **Table 2.2**). According to the predicted binding mode of **2.20a**, the methylpiperazine group is located near the front pocket of CDK8 ATP binding site and is somewhat solvent exposed. To expand the SAR of the tail group while potentially increasing the inhibitory potency and drug-likeness, the methylpiperazine group was modified in several ways including isosteric replacement and alkylation. First, removal of the methyl group to generate the unsubstituted piperazine of **2.20c** shown slightly decreased potency in Lanthascreen assay, however, significantly reduced the inhibitory activity by almost 6-fold with respect to the 293 cellular reporter assay. Acetylation of the free piperazine (**2.20d**) led to a decrease in Lanthascreen activity but a substantial recovery of 293 cellular activity. The Boc-protected piperazine analog **2.20e**

exhibited similar trends and had an improved cellular potency relative to the acetylated analog (**2.20d**). Isosteric replacement of the piperazine group with thiomorpholine (**2.20f**) led to a roughly 3-fold reduction in both enzymatic and 293 cellular activities. The thiomorpholine sulfoxide (**2.20g**) was found to have similar activity as **2.20f**, and a 1-imino-1λ6-thiomorpholine 1-oxide replacement (**2.20h**) for the piperazine caused a decrease in cellular potency. A variety of alkylated piperazine Senexin derivatives were generated including propan-1-ol (**2.20i**), propan-1-amine (**2.20j**), and the Boc protected version of **2.20j** (**2.20k**). Of these, **2.20i** is the most potent in terms of Lanthascreen inhibitory activity. A marked drop-off in the cellular reporter activity was observed with **2.20j**, however, this was recovered in the Boc protected analogue **2.20k** that has the second-best cellular reporter activity compared to **2.20a**. Further substitution of the naphthyl ring with a *N,N*-dimethylformamide (**2.20l**), the *N*-(3-aminopropyl)-*N*-methylacetamide (**2.20m**) and the Boc protected version of **2.20m** (**2.20n**). **2.20l** has similarly good activity in the Lanthascreen assay but 2-fold less active in the 293 cell-based assay when compared to **2.20a**, whereas the other two derivatives (**2.20m** and **2.20n**) were less potent in both assay formats. Replacement of 4-NH bridging atoms (through which the quinoline is substituted), with oxygen, sulfur or amide group markedly decreased inhibitory potency (data not shown), suggesting the importance of 4-NH in the pharmacophore model.

2.2.3 Characterization of the Lead Quinoline Inhibitor (Senexin C) in Cell-Free and Cell-Based Assays

Based on its most potent CDK8/19 inhibitory activity in the cell-based assay, compound **2.20a**, designated Senexin C was chosen as the lead compound and therefore subjected to a series of assays to determine its drug-like properties. To evaluate the kinase selectivity, the KINOMEscan screening assay (DiscoverX) was conducted for Senexin C, tested at 2 μ M, against a comprehensive panel of 468 human kinases. The profiling revealed a high level of selectivity for Senexin C against CDK8 and CDK19 (>85% inhibition) and only three off-target kinases (HASPIN, MAP4K2 and MYO3B) were identified as inhibited at this concentration over 35% (**Figure 2.5, Table 2.3**). Notably, no other members of the CDK family were significantly inhibited. A detailed dose-response analysis (11-point 3-fold serial dilutions) was then performed to determine the binding constants (K_d s) for all the inhibited kinases (**Figure 2.6**). Senexin C competes for ATP analog binding to CDK8 and CDK19 with similar K_d s, 55 nM and 44 nM respectively, and to the other three off-target kinases with much higher K_d values (HASPIN: 1000 nM; MAP4K2: 940 nM; MYO3B: > 30,000 nM). Furthermore, the KINETICfinder TR-FRET based kinetic assay (Enzymlogica) was carried out to characterize the binding kinetics parameters of Senexin B and Senexin C and used recombinant CDK8 and CDK19 proteins coupled with their cyclin partner Cyclin C (cycC) (**Table 2.4, Figure 2.7**). Results revealed that Senexin C has a slightly lower CDK8 K_d than Senexin B (1.4 nM vs 2.0M) and similar CDK19 K_d to Senexin B (2.9 nM vs 3.0 nM). The residence time (τ) of Senexin C binding to CDK8/cycC or CDK19/cycC

is 2-3 fold longer than that of Senexin B, suggesting another potential mechanism for the better potency of Senexin C over Senexin B in different kinase assays. Significant differences were observed between IC_{50}/K_d values determined using different functional and binding assays. The DiscoverX active-site dependent competition binding assay gave more than an order of magnitude difference in CDK8 K_d relative to the value determined using the KINETICfinder TR-FRET based kinetic assay or to the IC_{50} value determined by the Lanthascreen kinase binding assay. One possible explanation is that the Discover X assay uses recombinant CDK8 protein without its cyclin partner cycC while the other two assays use cycC-coupled CDK8 recombinant proteins. Binding to cyclin C changes the conformation of CDK8 according to X-ray studies and this interaction likely affects the target binding affinities of compounds.

Besides the well-established CDK8/19-dependent NF κ B activity and MV4-11 growth-inhibition assays used for determining cellular SAR, the activities of Senexin B and Senexin C were determined in other CDK8/19 dependent biological assays. First, the effects of different concentrations of Senexin C were compared on TNF- α induced NF κ B reporter activity in parental (WT) and CDK8/19 double-knockout (dKO) 293 cells (**Figure 2.8A**). Senexin C had no effect on reporter induction in dKO cells but suppressed such induction in WT cells, confirming its target selectivity. Next, the effects of Senexin B and Senexin C on mRNA expression of CDK8/19 dependent genes in HEK293 cells, including basal expression of MYC (**Figure 2.8B**) and NF κ B-inducible expression of CXCL8

(**Figure 2.8C**) were examined. Senexin C was more potent than Senexin B in both assays.

Further experiments examined the durability of CDK8/19 inhibition by Senexin C and Senexin B in a cell-based drug wash-off assay.¹⁷⁸ 293 cells were first treated with vehicle (0.1% DMSO), 1 μ M Senexin B, or 1 μ M Senexin C for 3 hours to allow maximal inhibition of mRNA levels of CDK8/19 dependent genes MYC and KCTD12. Then the drug-containing media were removed, cells were washed twice with drug-free media and further incubated in drug-free media for different periods. Subsequently, cells were lysed for RNA extraction and qPCR analysis to determine the recovery kinetics. **Figure 2.9** shows that the inhibition of these genes in Senexin B-treated cells was completely reversed at 3 hours post wash-off whereas the Senexin C treated cells were observed to recover target gene expression at a much slower rate, maintaining ~30% of maximal inhibition even at 24 hours post wash-off time point. These results indicate that CDK8/19 inhibition is far more durable after treatment with Senexin C relative to Senexin B, in agreement with the longer residence time of Senexin C.

To compare the metabolic stability of Senexin B and Senexin C, human hepatocytes were incubated with 2 μ M of each compound at 37°C after which drug concentrations were quantified at different time points by LC-MS/MS. As shown in **Figure 2.10**, the metabolic clearance rate of Senexin C in cultured hepatocytes was greatly decreased relative to Senexin B. The intrinsic clearance (Cl_{int}) for Senexin C decreases to 0.00639 mL/min/ 10^6 when compared to the Cl_{int} for Senexin B (0.0198 mL/min/ 10^6).

2.2.4 *In Vivo* Characterization of Senexin C in Novel

Pharmacokinetic (PK)/ Pharmacodynamic (PD)/ Toxicity Assays for CDK8/19 Inhibition

A PK/PD analysis of Senexin C in a novel assay based on the murine CT26 colon carcinoma tumor model was conducted in Balb/c mice. CT26 cells were injected s.c. in syngeneic Balb/c mice and allowed to grow to 200~300 mm³. Tumor-bearing mice then received Senexin C administered either i.v. at 2.5 mg/kg or orally at 100 mg/kg, and the compound concentrations in blood and tumor were measured by LC-MS/MS. Strikingly, the amount of Senexin C in tumor tissue was ~20 times higher than the amount in blood after i.v. administration and ~40 times higher after oral administration, with a much slower clearance rate in the tumor (**Figure 2.11A, B; Table 2.5**). To measure PD effects of CDK8/19 inhibition in treated tumor tissue, we have used RNA-Seq to identify genes that are affected by different CDK8/19 inhibitors in CT26 cells *in vivo* (unpublished data). Two of the CDK8/19-dependent genes that produced the most rapid response to CDK8/19 inhibitors in CT26 tumors were murine CCL12 and KLF2. Orally administered Senexin C inhibited KLF2 and CCL12 expression in CT26 tumors *in vivo*, starting 2 hours after oral gavage and reaching maximal inhibition at 12-hour time point (**Figure 2.11C**).

A 7-day toxicity study of Senexin C in the same animal model was then carried out. Mice received Senexin C at 100 mg/kg daily by oral gavage for 7 days. There were no adverse cage side observations and no change in body weights (**Figure 2.11D**). PK/PD analysis of the endpoint tissue samples (12 hours post last

dose) confirmed sustained inhibition of PD marker genes in the tumor (**Figure 2.11E**) as well as enriched tumor tissue PK values (**Figure 2.11F**). The amount of Senexin C in liver and lung tissues was also quantified at the endpoint. These tissues, like the tumor, also accumulated high drug concentrations, suggesting a high volume of distribution of Senexin C (**Figure 2.11F**). In contrast to Senexin C, Senexin B, administered to the same CT26 tumor-bearing model at the same dose, showed greater accumulation in blood than in the tumor (**Figure 2.12A**) and was less efficient than Senexin C in suppressing tumor PD marker gene CCL12 (**Figure 2.12B**).

Given the favorable tumor PK profile and low toxicity of Senexin C, its therapeutic efficacy in an additional *in vivo* model was further explored in a CDK8/19-dependent MV4-11 human acute myeloid leukemia growing systemically in NSG mice.^{119,179} To enable bioluminescence imaging (BLI), MV4-11 cells were modified by transduction with a lentiviral vector pHIV-Luc-ZsGreen expressing firefly luciferase. The resulting MV4-11-luc cells (also used for a cellular CDK8 inhibition assay in **Table 2.1 and 2.2**), were inoculated into the tail vein of NSG mice. Following BLI imaging one week after inoculation, animals were randomized into two groups and then treated with vehicle or Senexin C by oral gavage. Tumor growth was monitored weekly by BLI. As shown in **Figure 2.13**, treatment with Senexin C at 40 mg/kg BID for 4 weeks strongly suppressed the systemic growth of MV4-11 AML with good tolerability.

2.3 Conclusion

A series of quinoline-6-carbonitrile-based novel CDK8/19 Mediator kinase inhibitors have been developed through a structure-based design strategy. Among this chemical series, Senexin C (**2.20a**) exhibited the best inhibitory activity against CDK8/19 in both target binding affinity and various cell-based assays. When compared with its prototype Senexin B, Senexin C is not only a more potent CDK8/19 inhibitor but also more metabolically stable. Moreover, as described Senexin C possesses unique properties compared to other CDK8/19 inhibitors including sustained target inhibition and highly tumor-enriched PK profile. In light of these properties, its potent and selective profile coupled with its *in vivo* efficacy, Senexin C is a promising lead Mediator kinase inhibitor with therapeutic potential.

2.4 Experimental Section

2.4.1 Chemistry

All chemical reagents and solvents were purchased from commercial sources and used without further purification. The reactions were monitored by thin-layer chromatography (TLC), visualized by UV light (254 or 365 nm). The microwave oven reactions were conducted via Biotage microwave reactor. The purification of the products was finished by Biotage flash chromatography using silica gel columns. All NMR spectra were recorded with a Bruker spectrometer at 300 or 400 MHz in deuterated solvents. High-performance liquid chromatography (HPLC) and Mass spectra (MS) were used to confirm the purity and molecular weight of each compound. All compounds are >95% pure by HPLC analysis (data included in the Supporting Information).

5-(ethoxymethylene)-2,2-dimethyl-1,3-dioxane-4,6-dione (2.4)

To a 100 mL flask was added 2,2-dimethyl-1,3-dioxane-4,6-dione (34.7 mmol, 5 g), and 5-(ethoxymethylene)-2,2-dimethyl-1,3-dioxane-4,6-dione (35 mmol, 7 g). The mixture was stirred at 100°C for 1.5h. Upon completion, the mixture was condensed via rotavap. The resulting light-yellow solid residue was 5-(ethoxymethylene)-2,2-dimethyl-1,3-dioxane-4,6-dione (6.5 g, 94% yield) and used for the next step without further purification. ESI-MS *m/z*: 201 [M+H]⁺.

General procedure for preparation of 2,2-dimethyl-5-((phenylamino)methylene)-1,3-dioxane-4,6-dione derivatives (2.5a-2.5f)

To a 100 mL round bottom flask was charged with a solution of 4-substituted benzonitrile (1 eq) in DCM (80 mL). This was followed by adding 5-(ethoxymethylene)-2,2-dimethyl-1,3-dioxane-4,6-dione **2.4** (2 eq) in DCM (20 mL). The resulting solution was at room temperature for 30 min. Upon completion, the resulting solid was filtered off and washed with hexane to give the target compounds **2.5a-2.5f**.

4-[(2,2-dimethyl-4,6-dioxo-1,3-dioxan-5-ylidene)methylamino]benzonitrile (2.5a)

A white solid (3.7 g, 40% yield) and used without further purification. ESI-MS *m/z*: 273 ([M+H]⁺).

2,2-dimethyl-5-((phenylamino)methylene)-1,3-dioxane-4,6-dione (2.5b)

A white solid (1g, 55% yield) and used without further purification. ESI-MS *m/z*: 248 ([M+H]⁺).

5-[(4-chloroanilino)methylene]-2,2-dimethyl-1,3-dioxane-4,6-dione (2.5c)

A white solid (1.72 g, 31% yield) and used without further purification. ESI-MS m/z: 282 ($[M+H]^+$).

5-[(4-bromoanilino)methylene]-2,2-dimethyl-1,3-dioxane-4,6-dione (2.5d)

A yellow solid (2.5 g, 38% yield) and used without further purification. ESI-MS m/z: 327 ($[M+H]^+$).

5-[(4-iodoanilino)methylene]-2,2-dimethyl-1,3-dioxane-4,6-dione (2.5e)

A yellow solid (1.5 g, 20% yield) and used without further purification. ESI-MS m/z: 374 ($[M+H]^+$).

2,2-dimethyl-5-[[4-(trifluoromethyl)anilino]methylene]-1,3-dioxane-4,6-dione (2.5f)

A white solid (4 g, 64% yield) and used without further purification. ESI-MS m/z: 316 ($[M+H]^+$).

General procedure for preparation of 6-substituted quinolin-4-ol derivatives (2.6a-2.6f)

To a 250 mL round bottom flask was added with **2.5a-2.5f** (1 eq) in phenoxybenzene. The resulting solution was at 220°C for 40 min. Upon completion, the resulting solution was cooled to room temperature and hexane was added. The precipitate was collected by filtration and washed with hexane, the crude compound was purified via flash column chromatography using a gradient of 0-5% MeOH/DCM to give target compounds **2.6a-2.6f**.

4-hydroxyquinoline-6-carbonitrile (2.6a)

A brown solid (1.5 g, 65% yield) and used without further purification. ESI-MS m/z: 171 ($[M+H]^+$).

quinolin-4-ol (2.6b)

A white solid (1.0 g, 67% yield) and used without further purification. ESI-MS m/z: 146 ($[M+H]^+$).

6-chloroquinolin-4-ol (**2.6c**)

A brown solid (1 g, 91% yield). ESI-MS m/z: 180 ($[M+H]^+$).

6-bromoquinolin-4-ol (**2.6d**)

A brown solid (1.2 g, 70% yield). ESI-MS m/z: 225 ($[M+H]^+$).

6-iodoquinolin-4-ol (**2.6e**)

A brown solid (0.8 g, 73% yield). ESI-MS m/z: 272 ($[M+H]^+$).

6-(trifluoromethyl)quinolin-4-ol (**2.6f**)

A brown solid (0.8 g, 30% yield). ESI-MS m/z: 214 ($[M+H]^+$).

6-nitroquinolin-4-ol (**2.6g**)

A mixture of concentrated nitric acid (13.8 mmol, 0.6 mL) and concentrated sulfuric acid (24.1 mmol, 1.29 mL) was added slowly to a solution of quinolin-4-ol **2.6b** (3.45 mmol, 0.5 g) in concentrated sulfuric acid (0.6 mL). The temperature of the reaction mixture was kept at -15 to 0°C. The mixture was stirred for 2 h at the same temperature, added to ice-water (1:1) and the precipitation was collected by filtration and dried under vacuum to give 6-nitroquinolin-4-ol **2.6g** as a white solid (0.43 g, 65% yield). ESI-MS m/z: 191 ($[M+H]^+$).

General procedure for preparation of *4-chloro-6-substituted quinoline derivatives* (**2.7a-2.7g**)

To a 100 mL round-bottom flask was placed a solution of **2.6a-g** (1 eq) in dioxane (0.5 mmol/mL), and POCl₃ (5 eq) was added. Reaction was stirred for 1.5 h at 90°C. Upon completion, solvent was removed under reduced pressure. The

pH value of the solution was adjusted to 8 with saturated sodium carbonate solution. The resulting solution was extracted with three times of ethyl acetate, organic layers were combined and dried over anhydrous sodium sulfate and concentrated in vacuum. The crude was purified using flash column chromatography using a gradient of 0-2% MeOH/DCM to give **2.7a-2.7g**.

4-chloroquinoline-6-carbonitrile (2.7a)

A white solid (480 mg, 44% yield). ESI-MS m/z: 189 ($[M+H]^+$). 1H -NMR (300MHz, CD_3OD): δ 8.94 (d, $J=4.8$ Hz, 1H), 8.76 (d, $J=1.5$ Hz, 1H), 8.24 (d, $J=8.8$ Hz, 2H), 8.07 (dd, $J=1.8, 8.9$ Hz, 1H), 7.82 (d, $J=5.0$ Hz, 1H).

4-chloroquinoline (2.7b)

A white solid (193 mg, 86% yield). ESI-MS m/z: 164 ($[M+H]^+$).

4,6-dichloroquinoline (2.7c)

A white solid (1.32 g, 47% yield). ESI-MS m/z: 199 ($[M+H]^+$).

6-bromo-4-chloro-quinoline (2.7d)

A yellow solid (0.35 g, 27% yield). ESI-MS m/z: 243 ($[M+H]^+$).

4-chloro-6-iodo-quinoline (2.7e)

A brown solid (0.36 g, 42% yield). ESI-MS m/z: 290 ($[M+H]^+$).

4-chloro-6-(trifluoromethyl)quinoline (2.7f)

A brown solid (0.27 g, 31% yield). ESI-MS m/z: 232 ($[M+H]^+$).

4-chloro-6-nitro-quinoline (2.7g)

A white solid (250 mg, 91% yield). ESI-MS m/z: 209 ($[M+H]^+$).

General preparation of *6-substituted -N-phenethylquinolin-4-amine derivatives*
(2.8a-2.8g)

To a 10 mL round-bottom flask was added a solution of benzylamine (1 eq) and 4-substituted-quinoline-6-carbonitrile **2.7a-2.7g** (1 eq) in DMSO (0.5 mmol/mL), and TEA (3 eq) was added. Reaction was stirred for 4h at 100°C. Upon completion, the mixture was cooled to room temperature and water was added, the mixture was extracted with DCM for three times, and the organic layers were collected and washed with brine and dried by Na₂SO₄. Condensed and purified by flash column chromatography to give **2.8a-2.8g**.

4-(phenethylamino)quinoline-6-carbonitrile (2.8a)

A white solid (5 mg, 17% yield). ESI-MS m/z: 274 ([M+H]⁺). HRMS (ESI, ([M + H]⁺)): calculated for C₁₈H₁₅N₃, 274.13; found, 274.1339. ¹H-NMR (300MHz, CD₃OD): δ 8.58 (d, J=1.4 Hz, 1H), 8.43 (d, J=5.8 Hz, 1H), 7.83 (qd, J=1.6, 9.0 Hz, 2H), 7.24 (m, 5H), 6.6 (d, J=5.9 Hz, 1H), 3.62 (d, J=7.2 Hz, 2H), 3.03 (d, J=7.2 Hz, 2H). ¹³C-NMR (300MHz, DMSO-d₆): δ 153.50, 150.12, 149.87, 139.25, 130.42, 129.58, 128.97, 128.79, 128.79, 128.41, 128.41, 126.26, 119.35, 118.42, 105.77, 99.81, 44.08, 33.84.

N-(2-phenylethyl)quinolin-4-amine (2.8b)

A yellow solid (32 mg, 23% yield). ESI-MS m/z: 249 ([M+H]⁺). ¹H-NMR (300MHz, CDCl₃): δ 8.57 (d, J=5.3 Hz, 1H), 7.98 (d, J=8.9 Hz, 1H), 7.63 (d, J=7.6 Hz, 1H), 7.59 (d, J=7.6 Hz, 1H), 7.42-7.28 (m, 6H), 6.49 (d, J=5.3 Hz, 1H), 5.10 (s, 1H), 3.62 (q, J=6.7 Hz, 2H), 3.07 (t, J=6.7 Hz, 2H).

6-chloro-N-(2-phenylethyl)quinolin-4-amine (2.8c)

A yellow solid (6 mg, 6% yield). ESI-MS m/z: 283 ([M+H]⁺). ¹H-NMR (300MHz, CDCl₃): δ 8.55 (d, J=5.2 Hz, 1H), 7.94 (d, J=9.0 Hz, 1H), 7.56 (dd, J=9.0,

2.0 Hz, 2H), 7.39-7.28 (m, 5H), 6.43 (d, $J=5.2$ Hz, 1H), 3.61 (q, $J=5.7$ Hz, 2H), 3.07 (t, $J=6.9$ Hz, 2H).

6-bromo-*N*-(2-phenylethyl)quinolin-4-amine (2.8d)

A brown solid (20 mg, 21% yield). ESI-MS m/z : 328 ($[M+H]^+$). $^1\text{H-NMR}$ (300MHz, CDCl_3): δ 8.55 (d, $J=5.3$ Hz, 1H), 7.84 (d, $J=9.0$ Hz, 1H), 7.7 (d, $J=2.0$ Hz, 1H), 7.67 (dd, $J=9.0, 2.0$ Hz, 1H), 7.39-7.12 (m, 5H), 6.49 (d, $J=5.3$ Hz, 1H), 3.59 (q, $J=5.5$ Hz, 2H), 3.06 (t, $J=6.8$ Hz, 2H).

6-iodo-*N*-phenethylquinolin-4-amine (2.8e)

A brown solid (12 mg, 13% yield). ESI-MS m/z : 374 ($[M+H]^+$). $^1\text{H-NMR}$ (300MHz, CDCl_3): δ 8.53 (d, $J=5.9$ Hz, 1H), 7.99 (d, $J=2.0$ Hz, 1H), 7.83 (dd, $J=9.0, 2.0$ Hz, 1H), 7.69 (d, $J=9$ Hz, 1H), 7.31 (m, 5H), 6.43 (d, $J=5.9$ Hz, 1H), 3.59 (q, $J=5.4$ Hz, 2H), 3.05 (t, $J=7.1$ Hz, 2H).

***N*-phenethyl-6-(trifluoromethyl)quinolin-4-amine (2.8f)**

A yellow solid (26 mg, 32% yield). ESI-MS m/z : 317 ($[M+H]^+$). $^1\text{H-NMR}$ (300MHz, CDCl_3): δ 8.63 (d, $J=5.8$ Hz, 1H), 8.06 (d, $J=8.5$ Hz, 1H), 7.90 (s, 1H), 7.78 (dd, $J=8.5, 1.7$ Hz, 1H), 7.39-7.28 (m, 5H), 6.55 (d, $J=5.8$ Hz, 1H), 5.21 (m, 1H), 3.63 (q, $J=7.2$ Hz, 2H), 3.08 (t, $J=7.2$ Hz, 2H).

6-nitro-*N*-(2-phenylethyl)quinolin-4-amine (2.8g)

A yellow solid (30 mg, 40% yield). ESI-MS m/z : 294 ($[M+H]^+$). $^1\text{H-NMR}$ (300MHz, CDCl_3): δ 8.67 (d, $J=5.6$ Hz, 1H), 8.65 (d, $J=2.5$ Hz, 1H), 8.37 (d, $J=9.3, 2.5$ Hz, 1H), 8.04 (d, $J=9.3$ Hz, 1H), 7.41-7.29 (m, 5H), 6.58 (d, $J=5.6$ Hz, 1H), 3.66 (q, $J=7.0$ Hz, 2H), 3.06 (t, $J=7.0$ Hz, 2H).

4-(2-phenylethylamino)quinoline-6-carboxamide (2.8h)

To a 10 mL round-bottom flask was added a solution of 4-(2-phenylethylamino)quinoline-6-carbonitrile **2.8a** (0.2 mmol, 55 mg) in t-BuOH (3 mL). Then KOH (0.2 mmol, 12 mg) was added and the mixture was refluxed for 2h. Upon completion, the mixture was cooled to room temperature, diluted with water, extracted with DCM. The organic layers were combined, washed with brine, dried by Na₂SO₄, condensed, and purified by flash column chromatography using a gradient of 0-5% MeOH/DCM to give 4-(2-phenylethylamino)quinoline-6-carboxamide (55 mg, yield 94%). ESI-MS m/z: 292 ([M+H]⁺). ¹H-NMR (300MHz, CD₃OD): δ 8.71 (d, *J*=1.8 Hz, 1H), 8.39 (d, *J*=5.9 Hz, 1H), 8.10 (dd, *J*=8.8, 1.9 Hz, 1H), 7.84 (d, *J*=8.9 Hz, 1H), 7.30 (s, 2H), 7.28 (s, 2H), 7.21 (m, 1H), 6.63 (d, *J*=5.9 Hz, 1H), 3.67 (t, *J*=7.2 Hz, 2H), 3.06 (t, *J*=7.2 Hz, 2H).

*N*⁴-(2-phenylethyl)quinoline-4,6-diamine (**2.8i**)

To a 10 mL round-bottom flask was added a solution of 6-nitro-N-(2-phenylethyl)quinolin-4-amine **2.8g** (0.27 mmol, 80 mg) in EtOH (2 mL) and water (1 mL). Then NH₄Cl (2.2 mmol, 118 mg) and Fe (2.73 mmol, 152 mg) was added. Reaction was stirred for 2h at reflux. Upon completion, the mixture was cooled to room temperature, then filtered and the solution was condensed. The residue was added with water and extracted with DCM for three times, and the organic layers were collected and washed with brine and dried by Na₂SO₄. Condensed and purified by flash column chromatography using a gradient of 0-8% MeOH/DCM to give *N*⁴-(2-phenylethyl)quinoline-4,6-diamine as a white solid (60 mg, 84% yield). ESI-MS m/z: 264 ([M+H]⁺). ¹H-NMR (300MHz, CDCl₃): δ 8.37 (d, *J*=5.3 Hz, 1H), 7.80 (d, *J*=8.9 Hz, 1H), 7.38-7.24 (m, 5H), 7.06 (dd, *J*=8.9, 2.4 Hz, 1H),

6.68 (d, $J=2.4$ Hz, 1H), 6.41 (d, $J=5.3$ Hz, 1H), 4.74 (s, 1H), 3.86 (s, 2H), 3.58 (q, $J=6.9$ Hz, 2H), 3.04 (t, $J=7.4$ Hz, 2H).

N-[4-(2-phenylethylamino)-6-quinolyl]acetamide (**2.8j**)

To a 10 mL round-bottom flask was added a solution of *N*⁴-(2-phenylethyl)quinoline-4,6-diamine **2.8i** (0.1 mmol, 27 mg) in pyridine (2 mL). Then acetic anhydride (0.1 mmol, 11 mg) was added and the mixture was stirred at room temperature for 2h. Upon completion, the mixture was condensed and purified by flash column chromatography using a gradient of 0-5% MeOH/DCM to give *N*-[4-(2-phenylethylamino)-6-quinolyl]acetamide (12 mg, yield 39%). ESI-MS m/z : 306 ($[M+H]^+$). ¹H-NMR (300MHz, CDCl₃): δ 10.07 (s, 1H), 8.47 (s, 1H), 8.11 (d, $J=6.3$ Hz, 1H), 8.06 (d, $J=8.8$ Hz, 1H), 7.92 (d, $J=8.8$ Hz, 1H), 7.52 (s, 1H), 7.33-7.22 (m, 5H), 6.35 (d, $J=6.3$ Hz, 1H), 3.67 (t, $J=7.2$ Hz, 2H), 3.06 (t, $J=7.2$ Hz, 2H), 2.29 (s, 3H).

methyl 6-methylnaphthalene-2-carboxylate (**2.10**)

To a 250 mL round-bottom flask was added a solution of methyl 6-bromonaphthalene-2-carboxylate **2.9** (6.79 mmol, 1.8 g) and methylboronic acid (10.2 mmol, 610 mg) in acetonitrile (30 mL) and water (10 mL). Then tetrakis(triphenylphosphine)palladium(0) (0.68 mmol, 785 mg) and potassium carbonate (20.4 mmol, 2.82 g) was added. Reaction was protected with nitrogen and stirred for overnight at 80°C. Upon completion, the mixture was cooled to room temperature and water was added, the mixture was extracted with ethyl acetate for three times, and the organic layers were collected and washed with brine and dried by Na₂SO₄. Condensed and purified by flash column chromatography using

a gradient of 0-2% MeOH/DCM to give methyl 6-methylnaphthalene-2-carboxylate as a white solid (1.15 g, 85% yield). ESI-MS m/z : 201 ($[M+H]^+$). 1H NMR (300MHz, $CDCl_3$): δ 8.57 (s, 1H), 8.03 (dd, $J=8.6, 1.6$ Hz, 1H), 7.85 (d, $J=8.4$ Hz, 1H), 7.78 (d, $J=8.4$ Hz, 1H), 7.65 (s, 1H), 7.38 (dd, $J=8.6, 1.6$ Hz, 1H), 3.97 (s, 3H), 2.54 (s, 3H).

methyl 6-(bromomethyl)naphthalene-2-carboxylate (2.12)

To a 250 mL round-bottom flask was added a solution of methyl 6-methylnaphthalene-2-carboxylate **2.10** (5.59 mmol, 1.12 g) in CCl_4 (20 mL). Then NBS (5.87 mmol, 1.05 g) and AIBN (0.28 mmol, 46 mg) were added and the mixture was protected with nitrogen and reflux for 4h. Upon completion, the mixture was cooled to room temperature and hexane (25 mL) was added, the mixture was stirred at room temperature for 2h. Filter the mixture and wash the residue with hexane. The filtrate were collected and condensed and purified by flash column chromatography using a gradient of 0-30% ethyl acetate/hexane to give methyl 6-(bromomethyl)naphthalene-2-carboxylate as a white solid (1.3 g, 83% yield). ESI-MS m/z : 280 ($[M+H]^+$). 1H -NMR (300MHz, $CDCl_3$): δ 8.58 (d, $J=1.8$ Hz, 1H), 8.30 (dd, $J=8.9, 1.8$ Hz, 1H), 8.27 (d, $J=8.6$ Hz, 1H), 8.10 (d, $J=8.9$ Hz, 1H), 7.64 (d, $J=8.6$ Hz, 1H), 4.71 (s, 2H), 4.00 (s, 3H).

methyl 2-(chloromethyl)quinoline-6-carboxylate (2.13)

To a 10 mL round-bottom flask was added a mixture of methyl 2-methylquinoline-6-carboxylate **2.11** (0.5 mmol, 100 mg), AIBN (0.005 mmol, 8 mg), and NCS (0.5 mmol, 66 mg) in $ClCH_2CH_2Cl$ (4 mL) was stirred at 80 °C for overnight. Then, the reaction mixture was cooled to room temperature,

condensed, and purified flash column chromatography by using a gradient of 0-3% MeOH/DCM to give methyl 2-(chloromethyl)quinoline-6-carboxylate (27 mg, yield 23%). ESI-MS m/z : 236 ($[M+H]^+$). 1H -NMR (300MHz, $CDCl_3$): δ 8.59 (d, $J=1.6$ Hz, 1H), 8.32 (dd, $J=8.8, 1.8$ Hz, 1H), 8.30 (d, $J=8.4$ Hz, 1H), 8.10 (d, $J=8.8$ Hz, 1H), 7.68 (d, $J=8.4$ Hz, 1H), 4.85 (s, 2H), 4.00 (s, 3H).

methyl 6-(cyanomethyl)naphthalene-2-carboxylate (2.14)

To a 250 mL round-bottom flask was added a solution of methyl 6-(bromomethyl)naphthalene-2-carboxylate **2.12** (1.79 mmol, 500 mg) in methanol (15 mL). Then KCN (5.37 mmol, 350 mg) was added and the mixture was protected with nitrogen and reflux for 8 h. Upon completion, the mixture was cooled to room temperature and condensed, the residue was dissolved in DCM and water, then extracted with DCM three times, the organic layers were combined and washed with sat NaCl aq, dried by Na_2SO_4 . After that, condensed and purified by flash column chromatography using a gradient of 0-5% MeOH/DCM to give methyl 6-(cyanomethyl)naphthalene-2-carboxylate as a white solid (160 mg, 40% yield). ESI-MS m/z : 226 ($[M+H]^+$). 1H -NMR (300MHz, $CDCl_3$): δ 8.61 (s, 1H), 8.11 (dd, $J=8.6, 1.9$ Hz, 1H), 8.30 (dd, $J=8.9, 1.8$ Hz, 1H), 7.98 (d, $J=8.6$ Hz, 1H), 7.89 (d, $J=5.5$ Hz, 1H), 7.87 (s, 1H), 7.46 (dd, $J=8.6, 1.9$ Hz, 1H), 3.99 (s, 3H), 3.95 (s, 2H).

2-(chloromethyl)quinoline-6-carboxylic acid (2.15)

To a 10 mL round-bottom flask was added a mixture of methyl 2-(chloromethyl)quinoline-6-carboxylate **2.13** (0.74 mmol, 200 mg), and LiOH-H₂O (0.13 mmol, 6 mg) in THF (4 mL) and water (2 mL). The mixture was stirred at room

temperature for 4h. Then, the reaction mixture was condensed and diluted with water, then acidified by 1N HCl to pH=5. The precipitate was collected and washed with water until the pH=7. The precipitate was dried to give 2-(chloromethyl)quinoline-6-carboxylic acid (11 mg, yield 59%) and used without further purification. ESI-MS m/z: 222 ($[M+H]^+$).

6-(cyanomethyl)naphthalene-2-carboxylic acid (2.16)

To a 10 mL round-bottom flask was added a solution of methyl 6-(cyanomethyl)naphthalene-2-carboxylate **2.14** (1.99 mmol, 448 mg) in THF (3 mL) and water (3 mL). Then LiOH-H₂O (2.2 mmol, 92 mg) was added and the mixture was stirred at room temperature for 4h. Upon completion, the mixture was condensed and dissolved in 2 mL water and acidified by 2N HCl to pH 2-3. The precipitation was collected and washed with water until pH=7 and dried to give 6-(cyanomethyl)naphthalene-2-carboxylic acid (396 mg, 94%) that used for the next step without further purification. ESI-MS m/z: 212 ($[M+H]^+$).

[2-(chloromethyl)-6-quinolyl]-(4-methylpiperazin-1-yl)methanone (2.17)

To a 10 mL round-bottom flask was added a solution of 2-(chloromethyl)quinoline-6-carboxylic acid **2.15** (0.09 mmol, 200 mg) in DCM (20 mL), then SOCl₂ (1.1 mmol, 80 μ L) was added and the mixture was stirred at room temperature for 4h, condensed and dissolved in DCM (20 mL) again. Then, 1-methylpiperazine (1.1 mmol, 120 μ L) was added and stirred at room temperature for 1h. Upon completion, ice water was added and the mixture was extracted with DCM. The organic layers were combined, washed with brine, dried by Na₂SO₄, condensed, and purified by flash column chromatography using a gradient of 0-

5% MeOH/DCM to give [2-(chloromethyl)-6-quinolyl]-(4-methylpiperazin-1-yl)methanone (110 mg, yield 42%). ESI-MS m/z : 304 ($[M + H]^+$). 1H -NMR (300MHz, $CDCl_3$): δ 8.23 (d, $J=8.6$ Hz, 1H), 8.10 (d, $J=8.6$ Hz, 1H), 7.91 (d, $J=1.7$ Hz, 1H), 7.73 (dd, $J=8.6, 1.7$ Hz, 1H), 7.66 (d, $J=8.6$ Hz, 1H), 4.84 (s, 2H), 3.85 (s, 2H), 3.47 (s, 2H), 2.51 (s, 2H), 2.39 (s, 2H), 2.33 (s, 3H).

The general preparation of **2.18a**, **2.18c-2.18h**

To a 10 mL round-bottom flask was added a solution of 6-(cyanomethyl)naphthalene-2-carboxylic acid **2.16** (1 eq) in DCM (0.5 mmol/mL), then HATU (1.5 eq) and DIEA (3 eq) were added and the mixture was stirred at room temperature for 30 min. After that, amine derivatives (1 eq) in DCM were added and stirred at room temperature for 4h. Upon completion, water was added, the mixture was extracted with DCM for three times, the organic layers were combined, washed with sat $NaHCO_3$ aq and brine, dried by Na_2SO_4 , condensed and purified by flash column chromatography using a gradient of 0-5% MeOH/DCM to give products **2.18a**, **2.18c-2.18g**.

2-[6-(4-methylpiperazine-1-carbonyl)-2-naphthyl]acetonitrile (2.18a)

A light yellow solid (500 mg, yield 91%). ESI-MS m/z : 294 ($[M + H]^+$). 1H -NMR (300MHz, $CDCl_3$): δ 7.89-7.84 (m, 4H), 7.52 (dd, $J=8.5, 1.8$ Hz, 2H), 7.43 (dd, $J=8.5, 1.8$ Hz, 1H), 3.93 (s, 2H), 3.85 (s, 2H), 3.49 (s, 2H), 2.51 (s, 2H), 2.39 (s, 2H), 2.33 (s, 3H).

tert-butyl-4-[6-(cyanomethyl)naphthalene-2-carbonyl]piperazine-1-carboxylate (2.18c)

A white solid (343 mg, 61%). ESI-MS m/z : 380 ($[M + H]^+$). $^1\text{H-NMR}$ (300MHz, CDCl_3): δ 7.90 (s, 2H), 7.87 (d, $J=4.5$ Hz, 2H), 7.52 (d, $J=8.6$ Hz, 1H), 7.45 (d, $J=8.6$ Hz, 1H), 3.94 (s, 2H), 3.69 (m, 2H), 3.47 (m, 4H), 3.17 (q, $J=7.5$ Hz, 2H), 1.46 (s, 9H).

2-[6-(thiomorpholine-4-carbonyl)-2-naphthyl]acetonitrile (2.18d)

A light yellow solid (932 mg, 76%). ESI-MS m/z : 297 ($[M + H]^+$). $^1\text{H-NMR}$ (300MHz, CDCl_3): δ 7.88 (m, 4H), 7.50 (dd, $J=8.5, 1.5$ Hz, 1H), 7.45 (dd, $J=8.5, 1.5$ Hz, 1H), 4.05 (s, 2H), 3.94 (s, 2H), 3.74 (s, 2H), 2.72 (s, 2H), 2.63 (s, 2H).

3-[4-[6-(cyanomethyl)naphthalene-2-carbonyl]piperazin-1-yl]propyl acetate (2.18e)

A yellow solid (295 mg, yield 44%). ESI-MS m/z : 380 ($[M + H]^+$). $^1\text{H-NMR}$ (300MHz, CDCl_3): δ 7.90-7.85 (m, 4H), 7.53 (d, $J=8.2$ Hz, 1H), 7.43 (d, $J=8.2$ Hz, 1H), 4.13 (t, $J=6.5$ Hz, 2H), 3.93 (s, 2H), 3.84 (m, 2H), 3.48 (m, 2H), 2.53 (m, 2H), 2.46 (t, $J=6.9$ Hz, 2H), 2.41 (m, 2H), 2.04 (s, 3H), 1.82 (m, 2H).

tert-butyl-(3-(4-(6-(cyanomethyl)-2-naphthoyl)piperazin-1-yl)propyl)carbamate (2.18f)

A white solid (300 mg, 66%). ESI-MS m/z : 437 ($[M + H]^+$).

6-(cyanomethyl)-N,N-dimethyl-naphthalene-2-carboxamide (2.18g)

A white solid (175 mg, yield 78%). ESI-MS m/z : 239 ($[M + H]^+$). $^1\text{H-NMR}$ (300MHz, CDCl_3): δ 7.91-7.85 (m, 4H), 7.55 (dd, $J=8.4, 1.5$ Hz, 1H), 7.43 (dd, $J=8.5, 1.6$ Hz, 1H), 3.93 (s, 2H), 3.16 (s, 3H), 3.03 (s, 3H).

tert-butyl-(3-(6-(cyanomethyl)-N-methyl-2-naphthamido)propyl)carbamate (2.18h)

A white solid (166 mg, yield 67%). ESI-MS m/z : 382 ($[M + H]^+$).

2-[6-(4-methylpiperazine-1-carbonyl)-2-quinolyl]acetonitrile (2.18b)

To a 10 mL round-bottom flask was added a solution of 2-(cyanomethyl)quinoline-6-carboxylic acid **2.17** (0.54 mmol, 115 mg) in DCM (3 mL), then SOCl₂ (1.63 mmol, 0.12 mL) was added and the mixture was reflux for 4 h. The mixture was then cooled to room temperature and condensed and dissolved in DCM again, then a solution of 1-methylpiperazine (0.6 mmol, 60 mg) and TEA (0.65 mmol, 66 mg) in DCM (3 mL) was added to the previous solution and stirred at room temperature for 2h. Upon completion, the mixture was added with water and extracted with DCM for three times, the organic layers were combined, washed with sat NaCl aq, dried by Na₂SO₄, condensed and purified by flash column chromatography using a gradient of 0-5% MeOH/DCM to give 2-[6-(4-methylpiperazine-1-carbonyl)-2-quinolyl]acetonitrile (76 mg, 48%). ESI-MS m/z: 295 ([M+H]⁺). ¹H-NMR (300MHz, CDCl₃): δ 8.25 (d, *J*=8.5 Hz, 1H), 8.09 (d, *J*=8.7 Hz, 1H), 7.92 (d, *J*=1.7 Hz, 1H), 7.75 (dd, *J*= 8.7, 1.7 Hz, 1H), 7.58 (d, *J*=8.5 Hz, 1H), 4.13 (s, 2H), 3.85 (s, 2H), 3.48 (s, 2H), 2.52 (s, 2H), 2.39 (s, 2H), 2.34 (s, 3H). The general preparation of **2.19a-2.19h**

To a 10 mL round-bottom flask was added a solution of **2.18a-2.18h** (1 eq) and raney Ni (1 eq) in MeOH (1 mmol/mL) and NH₄OH (1 mmol/mL). Then the mixture was saturated with H₂, and stirred at room temperature for overnight. After that, the solution was diluted with hexane, filtered, the residue was washed with hexane, the filtrate was condensed to give target products **2.19a-h** respectively and used without further purification.

[6-(2-aminoethyl)-2-naphthyl]-(4-methylpiperazin-1-yl)methanone (2.19a)

A light yellow solid (99 mg, yield 98%) and used for the next step without further purification. ESI-MS m/z: 298 ($[M+H]^+$).

[2-(2-aminoethyl)-6-quinolyl]-(4-methylpiperazin-1-yl)methanone **(2.19b)**

A yellow solid (150 mg, yield 98%), and used without further purification. ESI-MS m/z: 299 ($[M+H]^+$).

tert-butyl-4-[6-(2-aminoethyl)naphthalene-2-carbonyl]piperazine-1-carboxylate
(2.19c)

A white solid (290 mg, yield 96%) and used for the next step without further purification. ESI-MS m/z: 384 ($[M+H]^+$).

[6-(2-aminoethyl)-2-naphthyl]-thiomorpholino-methanone **(2.19d)**

A yellow solid (399 mg, 42%). ESI-MS m/z: 301 ($[M+H]^+$). $^1\text{H-NMR}$ (300MHz, DMSO- d_6): δ 7.97 (d, $J=7.8$ Hz, 2H), 7.96 (s, 1H), 7.93 (d, $J=8.7$ Hz, 1H), 7.84 (s, 1H), 7.49 (d, $J=8.2$, 2H), 3.89 (m, 2H), 3.51 (m, 2H), 3.11 (m, 4H), 2.66 (m, 4H).

[6-(2-aminoethyl)-2-naphthyl]-[4-(3-hydroxypropyl)piperazin-1-yl]methanone
(2.19e)

A light yellow solid (234 mg, yield 88%) and used for the next step without further purification. ESI-MS m/z: 342 ($[M+H]^+$).

tert-butyl-(3-(4-(6-(2-aminoethyl)-2-naphthoyl)piperazin-1-yl)propyl)carbamate
(2.19f)

A brown solid (215 mg, yield 88%) and used for the next step without further purification. ESI-MS m/z: 441 ($[M+H]^+$).

6-(2-aminoethyl)-N,N-dimethyl-naphthalene-2-carboxamide **(2.19g)**

A yellow solid (122 mg, yield 71%) and used for the next step without further purification. ESI-MS m/z : 243 ($[M+H]^+$).

tert-butyl-(3-(6-(2-aminoethyl)-N-methyl-2-naphthamido)propyl)carbamate
(2.19h)

A white solid (219 mg, yield 77%) and used for the next step without further purification. ESI-MS m/z : 386 ($[M+H]^+$).

The general preparation of **2.20a-2.20h**

To a 10 mL round bottom flask was charged with a solution of 4-chloroquinoline-6-carbonitrile (1 eq) and **2.19a-2.19h** (1 eq) in DMSO (1 mmol/mL). Then TEA (3 eq) was added and the mixture was stirred at 110°C for overnight. Upon completion, the reaction was cooled to room temperature and water was added, the mixture was then extracted with DCM for three times, the organic layers were combined and dried by Na_2SO_4 , condensed, and purified through flash column chromatography using a gradient of 0-7% MeOH/DCM to give target products **2.20a**, **2.20b**, **2.20e**, **2.20f**, **2.20i**, **2.20k**, **2.20l**, **2.20n**. Boc deprotection of **2.20e**, **2.20k**, and **2.20n** by TFA achieved **2.20c**, **2.20j**, and **2.20m**. Acetylation of **2.20c** afforded **2.20d**. Oxidation of **2.20f** with sodium periodate led to **2.20g**. The sulfanimine intermediate that resulted from reaction of **2.20g** with trifluoroacetamide, was hydrolyzed to **2.20h**.

4-[2-[6-(4-methylpiperazine-1-carbonyl)-2-naphthyl]ethylamino]quinoline-6-carbonitrile (**2.20a**)

A grey solid (28 mg, 17% yield). ESI-MS m/z : 450 ($[M+H]^+$). HRMS (ESI, ($[M+H]^+$)): calculated for $C_{28}H_{27}N_5O$, 450.22; found, 450.2288. 1H -NMR

(300MHz, CDCl₃): δ 8.36 (d, J =5.6 Hz, 1H), 8.11 (s, 1H), 8.03 (d, J =8.4 Hz, 1H), 7.90 (s, 1H), 7.85 (d, J =8.7 Hz, 1H), 7.81 (d, J =8.7 Hz, 1H), 7.75 (dd, J =8.4, 1.9 Hz, 1H), 7.66 (s, 1H), 7.51 (dd, J =8.4, 1.5 Hz, 1H), 7.40 (dd, J =8.4, 1.5 Hz, 1H), 6.59 (d, J =5.6 Hz, 1H), 3.88 (s, 2H), 3.68 (m, 2H), 3.53 (s, 2H), 3.21 (t, J =6.9 Hz, 2H), 2.54 (s, 2H), 2.41 (s, 2H), 2.35 (s, 3H). ¹³C-NMR (300MHz, DMSO-d₆): δ 169.22, 155.30, 143.51, 139.84, 137.64, 134.46, 133.45, 131.59, 130.96, 130.32, 128.59, 128.42, 127.76, 127.04, 126.72, 124.66, 121.51, 117.94, 116.46, 108.56, 99.79, 51.93, 51.93, 44.38, 42.02, 39.50, 39.50, 33.69..

4-[2-[6-(4-methylpiperazine-1-carbonyl)-2-quinolyl]ethylamino]quinoline-6-carbonitrile (2.20b)

A brown solid (50 mg, yield 23%). ESI-MS m/z : 451 ([$M+H$]⁺). ¹H-NMR (300MHz, DMSO-d₆): δ 8.60 (d, J =5.5 Hz, 1H), 8.39 (d, J =1.5 Hz, 1H), 8.26 (d, J =8.5 Hz, 1H), 8.20 (d, J =8.5 Hz, 1H), 7.99 (d, J =8.7 Hz, 1H), 7.94 (d, J =1.6 Hz, 1H), 7.84 (dd, J =8.6, 1.8 Hz, 1H), 7.74 (dd, J =8.6, 1.8 Hz, 1H), 7.55 (s, 1H), 7.42 (d, J =8.5 Hz, 1H), 6.50 (d, J =5.5 Hz, 1H), 3.86 (s, 2H), 3.76 (q, J =5.5 Hz, 2H), 3.49 (s, 2H), 3.44 (t, J =6.0 Hz, 2H), 2.53 (s, 2H), 2.39 (s, 2H), 2.34 (s, 3H). ¹³C-NMR (300MHz, CDCl₃): δ 169.60, 161.27, 153.46, 150.46, 149.71, 147.76, 138.02, 134.23, 130.92, 130.08, 129.11, 129.08, 127.35, 127.30, 126.75, 122.71, 119.34, 118.98, 107.79, 99.89, 54.93, 54.93, 47.88, 47.88, 46.20, 42.15, 36.14.

4-[2-[6-(piperazine-1-carbonyl)-2-naphthyl]ethylamino]quinoline-6-carbonitrile (2.20c)

To a 10 mL round-bottom flask was added a solution of **2.20e** (0.19 mmol, 100 mg) in DCM (3 mL), then TFA (0.6 mL) was added. The mixture was stirred at

room temperature for 4h. Upon completion, the mixture was condensed to give **2.20c** (50 mg, 62%). ESI-MS m/z : 436 ($[M+H]^+$). 1H -NMR (300MHz, DMSO- d_6): δ 9.62(s, 1H), 8.62 (d, $J=7.3$ Hz, 1H), 8.27 (dd, $J=8.7, 1.3$ Hz, 1H), 8.04-7.90 (m, 5H), 7.61 (dd, $J=8.4, 1.3$ Hz, 1H), 7.55 (dd, $J=8.4, 1.3$ Hz, 1H), 7.09 (d, $J=7.3$ Hz, 1H), 3.94(q, $J=6.6$ Hz, 2H), 3.73 (m, 4H), 3.21 (m, 6H). ^{13}C -NMR (300MHz, DMSO- d_6): δ 169.27, 155.35, 144.06, 139.91, 137.56, 134.54, 133.44, 131.75, 131.01, 129.81, 128.64, 128.38, 127.72, 127.06, 126.75, 124.76, 121.83, 117.94, 116.44, 108.72, 99.93, 44.53, 42.67, 42.67, 39.52, 39.52, 33.62.

*4-[2-[6-(4-acetyl)piperazine-1-carbonyl]-2-naphthyl]ethylamino]quinoline-6-carbonitrile (**2.20d**)*

To a 100 mL round-bottom flask was added a solution of **2.20c** (0.15 mmol, 65 mg) and DIEA (0.3 mmol, 39 mg) in DCM (3 mL) and cooled to 0°C, then acetyl chloride (0.22 mmol, 18 mg) was added and the reaction was stirred at room temperature for 2h. Then water was added, extracted with DCM, the organic layers were combined, dried by Na_2SO_4 , condensed, and purified by flash column chromatography using a gradient of 0-5% MeOH/DCM to give **2.20d** (65 mg, 91% yield). ESI-MS m/z : 478 ($[M+H]^+$). 1H -NMR (300MHz, CD_3OD): δ 8.68 (s, 1H), 8.40 (d, $J=5.9$ Hz, 1H), 7.94 (s, 1H), 7.96-7.85 (m, 4H), 7.80 (s, 1H), 7.54 (dd, $J=8.4, 1.6$ Hz, 1H), 7.49 (dd, $J=8.4, 1.6$ Hz, 1H), 6.80 (d, $J=5.9$ Hz, 1H), 3.86 (t, $J=7.0$ Hz, 2H), 3.72 (m, 4H), 3.26 (t, $J=7.0$ Hz, 2H), 3.22 (m, 4H), 2.13 (s, 3H). ^{13}C -NMR (300MHz, Methanol- d_4): δ 172.77, 171.99, 154.93, 149.59, 139.41, 135.46, 133.42, 133.38, 132.93, 129.95, 129.91, 129.56, 129.26, 128.47, 127.89, 126.88,

125.41, 119.69, 119.24, 119.08, 109.89, 100.92, 55.77, 55.77, 45.58, 43.75, 43.75, 35.44, 21.21.

tert-butyl-4-[6-[2-[(6-cyano-4-quinolyl)amino]ethyl]naphthalene-2-carbonyl]piperazine-1-carboxylate (2.20e)

A grey solid (179 mg, yield 43%). ESI-MS m/z : 536 ($[M+H]^+$). 1H -NMR (300MHz, DMSO- d_6): δ 8.90 (s, 1H), 8.53 (d, $J=5.9$ Hz, 1H), 8.05 (m, 1H), 7.97-7.88 (m, 6H), 7.58 (dd, $J=8.4, 1.3$ Hz, 1H), 7.49 (dd, $J=8.4, 1.3$ Hz, 1H), 6.79 (d, $J=5.9$ Hz, 1H), 3.71 (m, 2H), 3.58 (m, 4H), 3.47 (m, 2H), 3.40 (m, 2H), 3.19 (m, 2H), 1.41 (s, 9H). ^{13}C -NMR (300MHz, DMSO- d_6): δ 169.23, 153.82, 151.62, 151.16, 138.14, 133.29, 132.49, 130.97, 130.56, 129.10, 128.71, 128.47, 128.36, 127.61, 126.84, 126.41, 126.41, 124.64, 119.03, 118.02, 106.36, 99.87, 79.20, 53.57, 53.57, 43.97, 39.50, 39.50, 33.90, 28.01, 28.01, 28.01.

4-[2-[6-(thiomorpholine-4-carbonyl)-2-naphthyl]ethylamino]quinoline-6-carbonitrile (2.20f)

A light yellow solid (297 mg, 41%). ESI-MS m/z : 453 ($[M+H]^+$). 1H -NMR (300MHz, DMSO- d_6): δ 8.86 (s, 1H), 8.52 (d, $J=5.8$ Hz, 1H), 7.96 (d, $J=7.8$ Hz, 1H), 7.94 (s, 1H), 7.90 (d, $J=7.8$ Hz, 1H), 7.88 (s, 2H), 7.69 (t, $J=5.0$ Hz, 1H), 7.57 (dd, $J=8.6, 1.4$ Hz, 1H), 7.47 (dd, $J=8.2, 1.2$ Hz, 1H), 3.88 (m, 2H), 3.67 (m, 2H), 3.65 (q, $J=6.8$ Hz, 2H), 3.17 (t, $J=6.8$ Hz, 2H), 2.66 (m, 4H). ^{13}C -NMR (300MHz, DMSO- d_6): δ 165.50, 153.53, 150.17, 149.87, 138.29, 133.22, 132.87, 131.05, 130.44, 129.65, 128.98, 128.43, 128.43, 127.71, 126.85, 125.98, 124.38, 119.35, 118.45, 105.83, 99.91, 43.89, 43.89, 40.43, 39.52, 33.97, 33.97.

4-[2-[6-(1-oxo-1,4-thiazinane-4-carbonyl)-2-naphthyl]ethylamino]quinoline-6-carbonitrile (2.20g)

To a 50 mL round-bottom flask was added a solution of **2.20f** (0.57 mmol, 258 mg) in MeOH (8 mL) and cooled to -40°C. Then NaIO₄ (0.63 mmol, 134 mg) in water (2 mL) was added to the above solution slowly. The mixture was stirred at -40°C for 30 min, then stirred at 0°C for another 2h, and stirred at room temperature for overnight. Upon completion, water was added, extracted with DCM, the organic layers were combined and dried by Na₂SO₄, condensed, and purified by flash column chromatography via a gradient of 0-7% MeOH/DCM to give **2.20g** (194 mg, 73%). ESI-MS m/z: 469 ([M+H]⁺). ¹H-NMR (300MHz, CDCl₃): δ 8.62 (d, *J*=5.3 Hz, 1H), 8.18 (s, 1H), 7.98 (d, *J*=8.8 Hz, 1H), 7.91 (s, 1H), 7.82 (t, *J*=7.9 Hz, 2H), 7.71 (d, *J*=8.8 Hz, 1H), 7.65 (s, 1H), 7.49 (d, *J*=8.8 Hz, 1H), 7.41 (d, *J*=8.8 Hz, 1H), 6.55 (d, *J*=5.3 Hz, 1H), 5.77 (m, 1H), 4.08 (m, 4H), 3.67 (q, *J*=6.1 Hz, 2H), 3.20 (t, *J*=6.9 Hz, 2H), 2.79 (m, 4H).

4-[2-[6-(1-imino-1-oxo-1,4-thiazinane-4-carbonyl)-2-naphthyl]ethylamino]quinoline-6-carbonitrile (2.20h)

To a 25 mL round-bottom flask was added a solution of **2.20g** (0.36 mmol, 166 mg) in DCM (10 mL). Then iodobenzene diacetate (0.53 mmol, 171 mg), 2,2,2-trifluoroacetamide (0.71 mmol, 80 mg), rhodium(II) acetate dimer (0.0018 mmol, 8 mg), and MgO (1.42 mmol, 57 mg) were added, the mixture was stirred at room temperature for overnight. Upon completion, the mixture was filtered through celite, and washed the celite with DCM, the filtration was condensed and purified by flash column chromatography using a gradient of 0-7% MeOH/DCM to give N-[4-[6-[2-

[(6-cyano-4-quinolyl)amino]ethyl]naphthalene-2-carbonyl]-1-oxo-1,4-thiazinan-1-ylidene]-2,2,2-trifluoro-acetamide (108 mg, 53%). To a 100 mL round-bottom flask was added a solution of N-[4-[6-[2-[(6-cyano-4-quinolyl)amino]ethyl]naphthalene-2-carbonyl]-1-oxo-1,4-thiazinan-1-ylidene]-2,2,2-trifluoro-acetamide (0.17 mmol, 100 mg) and K₂CO₃ (0.86 mmol, 119 mg) in MeOH (7 mL). Then the mixture was stirred at room temperature for overnight. Upon completion, the mixture was filtered, and washed the residue with MeOH, the filtration was condensed and purified by flash column using a gradient of 0-7% MeOH/DCM to give **2.20h** (50 mg, 60%). ESI-MS m/z: 484 ([M+H]⁺). ¹H-NMR (300MHz, DMSO-d₆): δ 8.86 (s, 1H), 8.52 (d, *J*=5.6 Hz, 1H), 8.05 (s, 1H), 7.96 (d, *J*=8.8 Hz, 1H), 7.91 (d, *J*=8.8 Hz, 1H), 7.88 (m, 3H), 7.70 (m, 1H), 7.57 (t, *J*=7.2 Hz, 2H), 6.71 (d, *J*=5.6 Hz, 1H), 3.90 (m, 2H), 3.73 (m, 2H), 3.65 (q, *J*=6.9 Hz, 2H), 3.17 (t, *J*=7.6 Hz, 2H), 3.14 (m, 4H). ¹³C-NMR (300MHz, DMSO-d₆): δ 169.60, 153.49, 150.17, 149.83, 138.43, 133.37, 132.09, 130.97, 130.40, 129.65, 128.97, 128.49, 128.46, 127.70, 126.85, 126.32, 124.49, 119.33, 118.44, 105.82, 99.89, 52.67, 52.67, 43.88, 39.61, 39.61, 33.97.

4-[2-[6-[4-(3-hydroxypropyl)piperazine-1-carbonyl]-2-naphthyl]ethylamino]quinoline-6-carbonitrile (2.20i)

A light yellow solid (28 mg, yield 20%). ESI-MS m/z: 494 ([M+H]⁺). ¹H-NMR (300MHz, CDCl₃): δ 8.61 (d, *J*=5.3 Hz, 1H), 8.20 (s, 1H), 8.01 (d, *J*=8.6 Hz, 1H), 7.88-7.71 (m, 4H), 7.63 (s, 1H), 7.48 (d, *J*=8.1 Hz, 1H), 7.38 (d, *J*=8.1 Hz, 1H), 6.57 (d, *J*=5.9 Hz, 1H), 5.89 (m, 1H), 3.81 (t, *J*=5.0 Hz, 2H), 3.66 (m, 2H), 3.48 (s, 4H), 3.19 (t, *J*=7.3 Hz, 2H), 2.66 (t, *J*=5.6 Hz, 2H), 2.50 (m, 4H), 1.75 (m, 2H). ¹³C-

NMR (300MHz, DMSO-d6): δ 168.94, 153.35, 150.21, 149.72, 138.25, 133.23, 132.71, 130.98, 130.27, 129.66, 128.99, 128.41, 128.35, 127.58, 126.79, 126.21, 124.58, 119.28, 118.41, 105.82, 99.86, 59.14, 54.82, 52.79, 52.79, 43.85, 39.50, 39.50, 33.94, 29.46.

4-[2-[6-[4-(3-aminopropyl)piperazine-1-carbonyl]-2-naphthyl]ethylamino]quinoline-6-carbonitrile (2.20j)

To a 10 mL round-bottom flask was added a solution of **2.20k** (0.32 mmol, 191 mg) in DCM (5 mL). Then TFA (1 mL) was added and the mixture was stirred at room temperature for 4h. Upon completion, the mixture was condensed and purified by flash column in a gradient of 0-10% MeOH/DCM to give **2.20j** (185 mg, 95% yield). ESI-MS m/z : 493 ($[M+H]^+$). 1H -NMR (300MHz, DMSO-d6): δ 9.66 (s, 1H), 9.11 (s, 1H), 8.63 (d, $J=7.4$ Hz, 1H), 8.28 (d, $J=8.7$ Hz, 1H), 8.04 (s, 1H), 8.03 (d, $J=7.4$ Hz, 1H), 7.94 (m, 4H), 7.62 (d, $J=8.7$ Hz, 2H), 7.56 (d, $J=8.7$ Hz, 1H), 7.11 (d, $J=7.4$ Hz, 1H), 3.94 (q, $J=6.7$ Hz, 2H), 3.45 (m, 2H), 3.21 (m, 8H), 2.88 (m, 2H), 1.96 (m, 2H), 1.24 (m, 2H). ^{13}C -NMR (300MHz, DMSO-d6): δ 169.18, 155.43, 144.02, 139.83, 137.66, 134.62, 133.53, 131.58, 131.02, 129.86, 128.66, 128.47, 127.80, 127.11, 126.88, 124.79, 121.77, 117.97, 117.77, 108.77, 99.97, 53.55, 52.90, 52.90, 50.82, 50.82, 44.55, 36.23, 33.70, 21.65.

tert-butyl-N-[3-[4-[6-[2-[(6-cyano-4-quinolyl)amino]ethyl]naphthalene-2-carbonyl]piperazin-1-yl]propyl]carbamate (2.20k)

A yellow solid (191 mg, 46% yield). ESI-MS m/z : 593 ($[M+H]^+$). 1H -NMR (300MHz, DMSO-d6): δ 9.66 (s, 1H), 9.10 (s, 1H), 8.61 (d, $J=7.3$ Hz, 1H), 8.27 (dd, $J=8.8$, 1.3 Hz, 1H), 8.03 (d, $J=8.8$ Hz, 1H), 7.95 (d, $J=8.5$ Hz, 2H), 7.89 (s, 1H),

7.85 (d, $J=8.5$ Hz, 2H), 7.59 (dd, $J=8.8, 1.3$ Hz, 1H), 7.50 (m, 1H), 7.10 (d, $J=7.3$ Hz, 1H), 3.94 (q, $J=6.9$ Hz, 2H), 3.57 (m, 2H), 3.22 (t, $J=7.3$ Hz, 2H), 2.95 (s, 3H), 2.92 (m, 2H), 1.91 (m, 2H). ^{13}C -NMR (300MHz, DMSO- d_6): δ 168.95, 155.60, 152.97, 150.46, 149.28, 138.24, 133.26, 132.69, 131.01, 129.93, 129.93, 129.02, 128.46, 128.39, 127.61, 126.84, 126.28, 124.64, 119.27, 118.33, 105.98, 99.89, 77.42, 55.16, 55.16, 54.95, 54.95, 52.47, 43.92, 38.18, 33.95, 28.28, 28.28, 28.28, 26.55.

6-[2-[(6-cyano-4-quinolyl)amino]ethyl]-N,N-dimethyl-naphthalene-2-carboxamide
(2.20l)

A grey solid (152 mg, yield 77%). ESI-MS m/z : 395 ($[\text{M}+\text{H}]^+$). ^1H -NMR (300MHz, CD_3OD): δ 8.60 (d, $J=1.4$ Hz, 1H), 8.45 (d, $J=5.9$ Hz, 1H), 7.91-7.80 (m, 6H), 7.53 (dd, $J=8.2, 1.8$ Hz, 1H), 7.48 (dd, $J=8.2, 1.8$ Hz, 1H), 7.74 (dd, $J=8.6, 1.8$ Hz, 1H), 6.71 (d, $J=5.9$ Hz, 1H), 3.76 (t, $J=7.1$ Hz, 2H), 3.24 (t, $J=7.1$ Hz, 2H), 3.15 (s, 3H), 3.05 (s, 3H). ^{13}C -NMR (300MHz, DMSO- d_6): δ 170.13, 153.37, 150.18, 149.73, 138.15, 133.25, 133.15, 130.92, 130.30, 129.63, 128.95, 128.38, 128.28, 127.40, 126.77, 126.19, 124.70, 119.28, 118.40, 105.82, 99.86, 43.86, 43.86, 34.83, 33.94.

N-(3-aminopropyl)-6-[2-[(6-cyano-4-quinolyl)amino]ethyl]-N-methyl-naphthalene-2-carboxamide
(2.20m)

To a 100 mL round-bottom flask was added a solution of **2.20n** (6.7 mmol, 763 mg) in DCM (5 mL). Then TFA (1 mL) was added and the mixture was stirred at room temperature for 4h. Upon completion, the mixture was condensed and purified by flash column in a gradient of 0-10% MeOH/DCM to give **2.20m** (280

mg, 96% yield). ESI-MS m/z : 438 ($[M+H]^+$). 1H -NMR (300MHz, DMSO- d_6): δ 9.66 (s, 1H), 9.10 (s, 1H), 8.61 (d, $J=7.3$ Hz, 1H), 8.27 (dd, $J=8.8, 1.3$ Hz, 1H), 8.03 (d, $J=8.8$ Hz, 1H), 7.95 (d, $J=8.5$ Hz, 2H), 7.89 (s, 1H), 7.85 (d, $J=8.5$ Hz, 2H), 7.59 (dd, $J=8.8, 1.3$ Hz, 1H), 7.50 (m, 1H), 7.10 (d, $J=7.3$ Hz, 1H), 3.94 (q, $J=6.9$ Hz, 2H), 3.57 (m, 2H), 3.22 (t, $J=7.3$ Hz, 2H), 2.95 (s, 3H), 2.92 (m, 2H), 1.91 (m, 2H). ^{13}C -NMR (300MHz, DMSO- d_6): δ 170.65, 158.56, 158.22, 155.43, 143.99, 139.84, 137.31, 134.61, 133.18, 131.07, 129.87, 128.54, 128.34, 127.57, 127.09, 126.22, 124.75, 121.76, 117.97, 116.45, 108.77, 99.97, 44.59, 36.79, 33.71, 30.73, 24.80. *tert-butyl-N-[3-[[6-[2-[(6-cyano-4-quinolyl)amino]ethyl]naphthalene-2-carbonyl]-methyl-amino]propyl]carbamate (2.20n)*

A white solid (360 mg, 59% yield). ESI-MS m/z : 538 ($[M+H]^+$). 1H -NMR (300MHz, CD_2Cl_2): δ 8.55 (d, $J=5.1$ Hz, 1H), 8.22 (s, 1H), 7.94 (d, $J=8.6$ Hz, 1H), 7.83 (d, $J=8.6$ Hz, 2H), 7.79 (s, 1H), 7.72 (dd, $J=8.6, 2.0$ Hz, 1H), 7.67 (s, 1H), 7.47 (d, $J=8.5$ Hz, 1H), 7.41 (d, $J=8.5$ Hz, 1H), 6.59 (d, $J=5.1$ Hz, 1H), 5.83 (m, 1H), 5.47 (m, 1H), 3.66 (m, 4H), 3.20 (m, 4H), 2.94 (s, 3H), 1.82 (m, 2H), 1.43 (s, 9H).

2.4.2 Docking studies

Molecular docking was performed on a previously reported CDK8 crystal structure (PDB ID: 4F7S) using the Induced Fit module within the Maestro Interface. The 2020 version of the Small Molecule Drug Discovery Suite containing these components was used (Schrodinger, Inc.)

2.4.3 Pharmacology

2.4.3.1 Lanthascreen Eu kinase binding assay for CDK8/Cyclin C

This assay is a binding competition assay. The Alexa Fluor 647 labeled tracer can bind to the ATP pocket of tagged CDK8 protein, whereas the europium (Eu)-labeled anti-tag antibody can also recognize the tagged CDK8. Simultaneous binding of both tracer and antibody to CDK8 causes a high degree of FRET (fluorescence resonance energy transfer) from the Eu donor fluorophore to the Alexa Fluor 647 acceptor fluorophore on the tracer. Introduction of CDK8 inhibitors will compete with the tracer and result in loss of FRET signals. Materials and reagents that were used in this assay include His-tagged CDK8/Cyclin C recombinant protein (Invitrogen, PV4402), kinase buffer A (Invitrogen, PV3189), kinase tracer 236 (Invitrogen, PV5592), biotin anti-His tag antibody (Invitrogen, PV6089), Eu-streptavidin (Invitrogen, PV5899), 384-well plate (Greiner, white, No. 781207). Kinase/antibody solution, tracer solution, and inhibitor dilutions were prepared according to the manufacturer's protocol. 5 μ L of CDK8/biotin-anti-His Ab/SA-Eu mix in 1x kinase buffer A and 5 μ L of tracer solution in 1x kinase buffer A were added to the wells, after that, 5 μ L inhibitor dilutions in 1x kinase buffer A were added. The plate was shaken for 30 seconds and incubated for 60 minutes at room temperature in the dark. The plate was read on the Molecular Devices SpectraMax iD5 Microplate Reader (FRET model, excitation 350 nm, emissions at 615 and 665 nm). The emission ratios of the acceptor/tracer emission (665nm) to the antibody/donor emission (615 nm) were plotted versus log concentration of inhibitors to fit the sigmoidal dose-dependent curves for IC₅₀ calculation using

GraphPad Prism 7.0 (GraphPad Software, San Diego, CA). The IC₅₀ curves of compounds are shown in **Figure 2.14**.

2.4.3.2 293-NFκB-luc cell-based assay

The detailed procedure for this NFκB-dependent cell-based CDK8/19i activity assay was previously described.¹⁸⁰ Briefly, 293-WT-NFKB-LUC#8 (293-WT) and 293-dKO-NFKB-LUC#2 (293-KO) cells were seeded in 96-well plates, cultured for 24 hours and then treated with tested compounds at different concentrations with 10 ng/mL TNF-α added for 3 hours. 4 μL potassium luciferin solution (15 mg/mL, GoldBio) was then added to each well to determine the luciferase reporter activity, represented by the luminescence intensities measured by the SpectraMax iD5 Microplate Reader. Reporter activities of inhibitor-treated cells were normalized by the reporter activities of cells without the inhibitor and further processed with GraphPad Prism 7.0 for curve-fitting and IC₅₀ calculation. The IC₅₀ curves of compounds are shown in **Figure 2.15**.

2.4.3.3 MV4-11-luc cell-based assay

A luciferase-expressing derivative of CDK8/19-dependent MV4-11 leukemia cell line, named MV4-11-luc, was generated using the lentiviral vector pHIV-Luc-ZsGreen (Addgene #39196). MV4-11-luc cells were maintained in RPMI1640 media supplemented with 10% FBS and 1% Penicillin-Streptomycin. For the 7-day growth inhibition assay to evaluate CDK8/19i activity, MV4-11-luc cells were seeded at 2,000 cells per well in 200 μL media in 96-well white plates (Corning 3917, USA) and then treated with vehicle control (0.1% DMSO) or tested compound at concentrations from 1 nM to 5 μM (by adding 22.2 μL 10X compound

solutions directly to the culture). The treated cells were cultured at 37 °C/5% CO₂ for 7 days before measuring the luciferase activities and determining IC₅₀ values of inhibitor-induced growth inhibition by SpectraMax iD5 Microplate Reader and GraphPad software as described in the previous section. The IC₅₀ curves of compounds are shown in **Figure 2.16**.

2.4.3.4 DiscoverX K_d determination

Dissociation constants for Senexin C was determined at DiscoverX (**Figure 2.6**).

2.4.3.5 KINOMEScan selectivity profiling

Kinome profiling for Senexin C was performed by KINOMEScan (DiscoverX, Fremont, CA). The compound was profiled at a concentration of 2 µM (**Table 2.3**).

2.4.3.6 RNA extraction and qPCR

Procedures for RNA-qPCR analysis of cells treated with CDK8/19i under different culture conditions, including basal and TNFα-stimulated conditions and drug wash-off conditions, were previously described in detail.¹⁷⁸ To evaluate effects on basal MYC mRNA expression, 293 cells were treated with tested compounds (in 0.1% DMSO) under regular culture conditions for 3 hours. To evaluate effects on TNFα-induced CXCL8 mRNA expression, 293 cells were pretreated with tested compounds (in 0.1% DMSO) for 1 hour and then treated with 10 ng/mL TNFα for 2 hours. For the wash-off study, 293 cells were pretreated with tested compounds (in 0.1% DMSO) for 3 hours before removal of the drug-containing media and washed with drug-free media twice, followed by incubation

with drug-free media for indicated time periods. RNA was extracted with RNeasy Mini Kit (Qiagen) and cDNAs were prepared using iScript cDNA SuperMix (QuantaBio). Gene expression was quantified with iTaq Universal SYBR Green Supermix reagent (QuantaBio) using CFX384 Real-Time System (Bio-Rad). Relative mRNA expression was calculated with the formula of $2^{-(C_{t_{\text{housekeeping_gene}}} - C_{t_{\text{test_gene}}})}$ and percentage of inhibition was calculated by normalization to the expression levels in vehicle (0.1% DMSO) control. The sequences of the primers used for qPCR are listed in Supporting Information **Table 2.6**.

2.4.3.7 Quantification of compounds in biological samples by LC-MS/MS

For liquid biological samples (conditioned media, cell suspension or serum/plasma samples, etc.), undiluted or diluted samples were directly used as starting materials for sample preparation. For solid tissue samples (tumors or organs), about 100 mg tissue mass was cut into small pieces and homogenized in 5x volume of ice-cold PBS before being used as 6x diluted starting materials. To prepare for LC-MS/MS analysis, 40 μL sample was mixed with 160 μL ice-cold methanol containing 200 nM internal standard (deuterated Senexin B, SnxB-D8) by vortexing 15 seconds and then incubated on ice for 30 minutes before being centrifuged at 20,000 g for 10 minutes. 100 μL of supernatant (in 80% methanol) was transferred to 9 mm Autosampler Inserts and diluted with 100 μL water to make samples (in 40% methanol) for LC-MS/MS analysis performed by the Mass Spectrometry Center at the University of South Carolina (UofSC). The Multiple

Reaction Monitoring (MRM) ion transitions used for SnxB-D8 (IS), Senexin B and Senexin C are 459 → 181, 451 → 181 and 450 → 350 respectively.

2.4.3.8 Human hepatocyte metabolic stability assay

Cryopreserved female human hepatocytes (H1500.H15B) were obtained from Sekisui XenoTech, Kansas City, KS. Frozen hepatocytes were thawed in the XenoTech Hepatocyte Incubation Media (K2500, XenoTech) and incubated with vehicle control (0.1% DMSO) or tested compound at 2 µM at 37°C. Hepatocyte suspension aliquots (30 µL) were collected at different time points and the concentrations of tested compound were measured by LC-MS/MS.

2.4.3.9 *In vivo* studies

Animal studies were approved by the Institutional Animal Care and Use Committee (IACUC) of UofSC and performed at the Department of Laboratory Animal Research (DLAR) at UofSC. For PK/PD analysis of Senexin C, one million of murine CT26 colon carcinoma cells were injected subcutaneously in the right flank of 8-week-old female Balb/c mice and allowed to grow to 200~300 mm³. The tumor bearing animals then received Senexin C at 2.5 mg/kg by intravenous injection (10 mL/kg of 2.5 mg/mL Senexin C solution in 5% Dextrose) or 100 mg/kg by oral gavage (10 mL/kg of 10 mg/mL Senexin C solution in 30% propylene glycol / 70% PEG-400 vehicle). At different time points post administration, blood samples were collected in BD microtainers with K₂EDTA for plasma preparation and animals were euthanized for tumor collection. For the tumor specimens dissected from each animal, a piece of 50~100 mg tumor sample was stabilized in RNA-later reagent (Qiagen) and several 100 mg tumor pieces were snap-frozen on

dry ice and stored at -80°C for later protein and tumor PK analysis. The compound concentrations in blood and tumor samples were measured by LC-MS/MS. RNA-later stabilized tumor samples were processed for RNA extraction using Direct-zol RNA Miniprep Kit (Zymo Research, Irvine, CA), followed by qPCR quantification for gene expression. For the 7-day toxicity study of Senexin C, the same animal model was used and tumor-bearing mice were dosed with Senexin C at 100 mg/kg daily by oral gavage for 7 days. Animals were monitored twice daily and body weights were measured every two days. The endpoint tissue samples were collected at 12 hours post last dose and analyzed for PK/PD.

For the efficacy study in an *in vivo* AML model, one million MV4-11-luc cells were inoculated in 8-week-old female NSG mice via tail-vein injection. One week post inoculation, animals were randomly assigned to two groups and treated with either vehicle solution (30% propylene glycol / 70% PEG-400) or Senexin C at 40 mg/kg twice daily (p.o., BID) for 4 weeks. Tumor growth was monitored through weekly bioluminescence imaging (BLI) using IVIS Lumina III system.

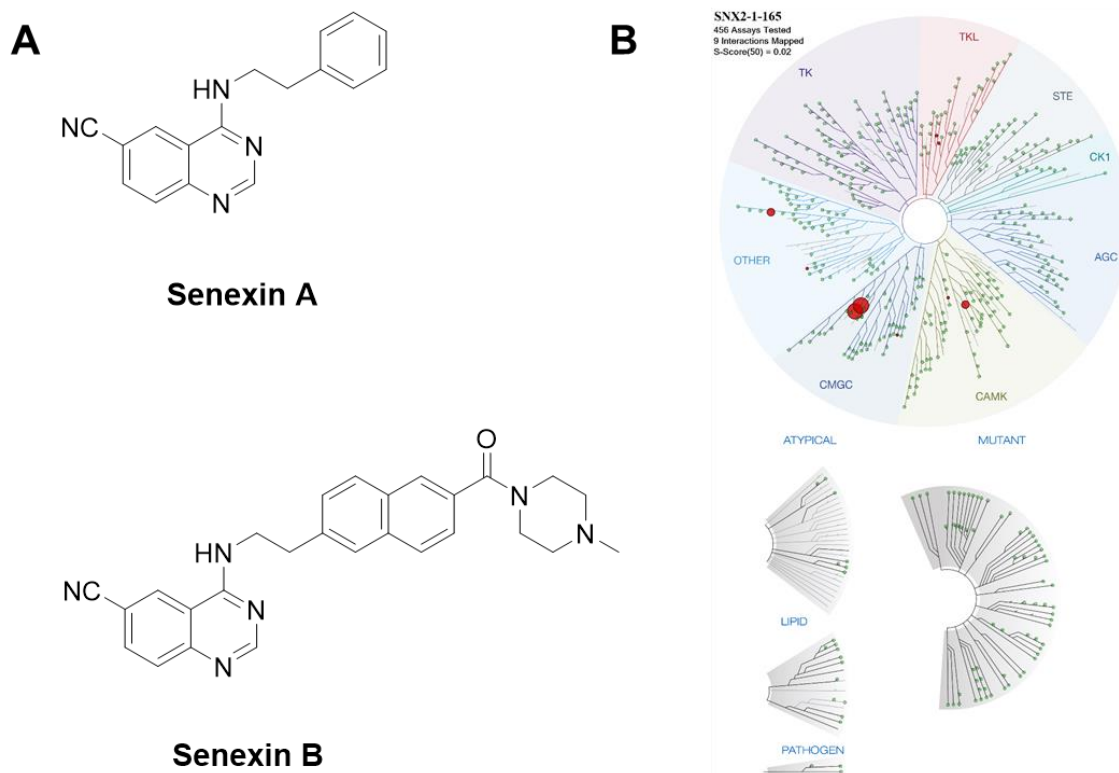


Figure 2.1 (A) The chemical structures of Senexin A and Senexin B. (B) The kinome profiling of Senexin B.

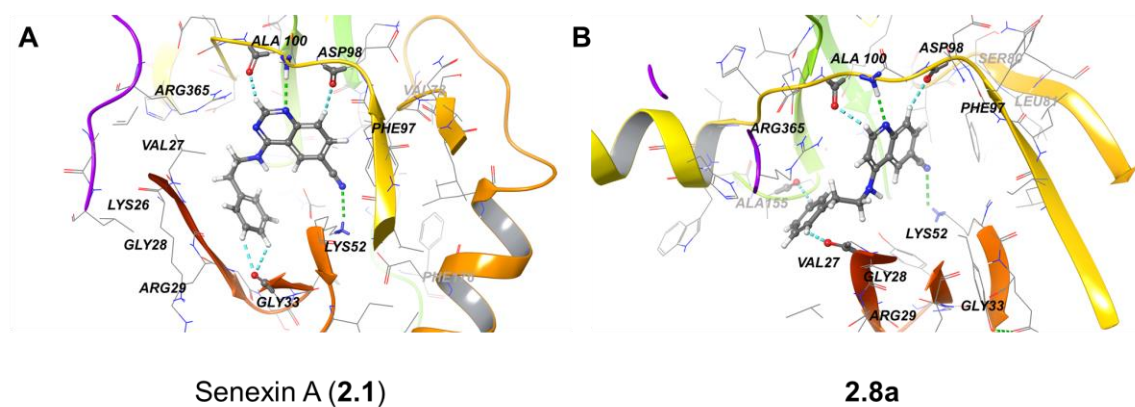


Figure 2.2 The predicted binding mode of Senexin A (**2.1**) and **2.8a** docked to CDK8/cyclin C protein (PDB code: 4F7S).

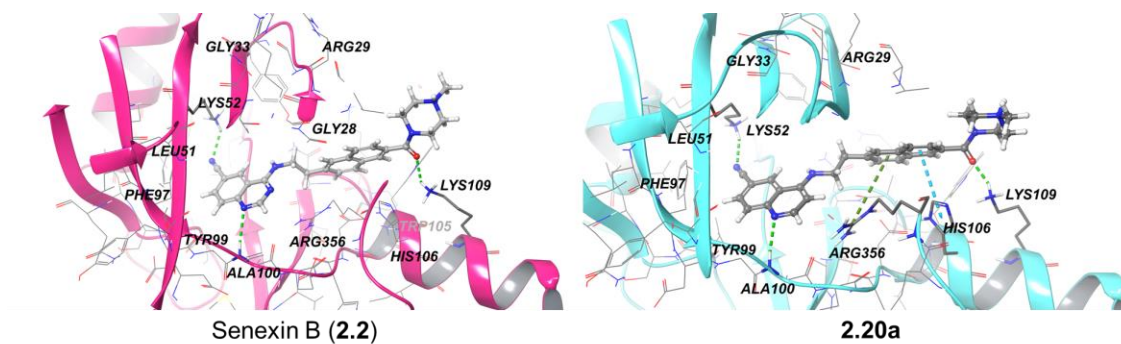


Figure 2.3 The predicted binding modes of Senexin B (**2.2**) and **2.20a** docked to CDK8/cyclin C protein (PDB code: 4F7S).

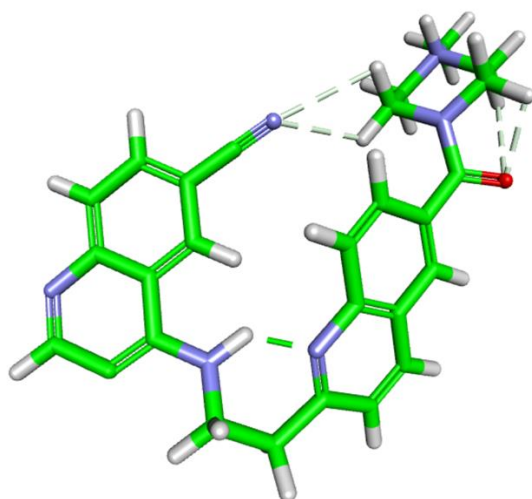


Figure 2.4 Molecular modeling and energy minimization of compound **20b**.

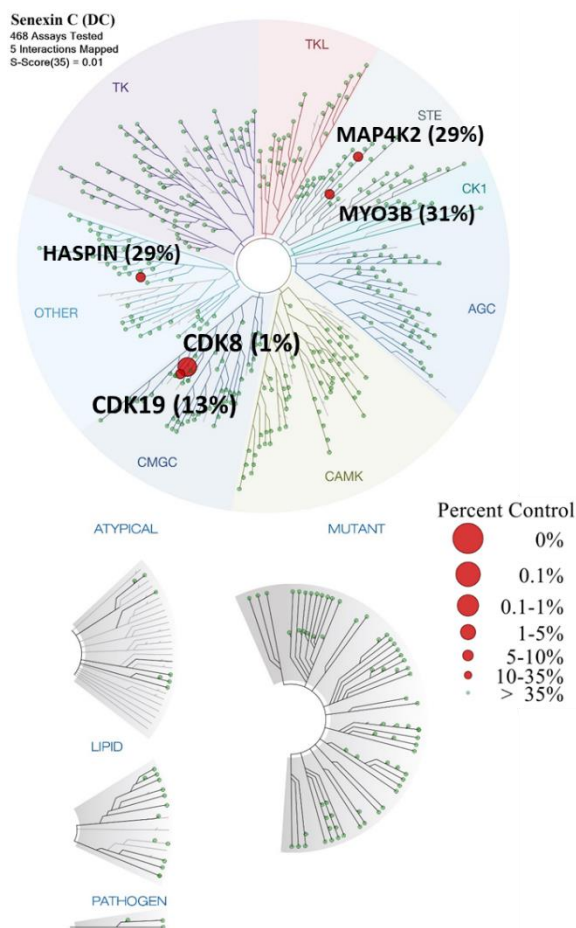


Figure 2.5 Kinome profiling dendrogram (Discover X) of Senexin C at 2 μ M.

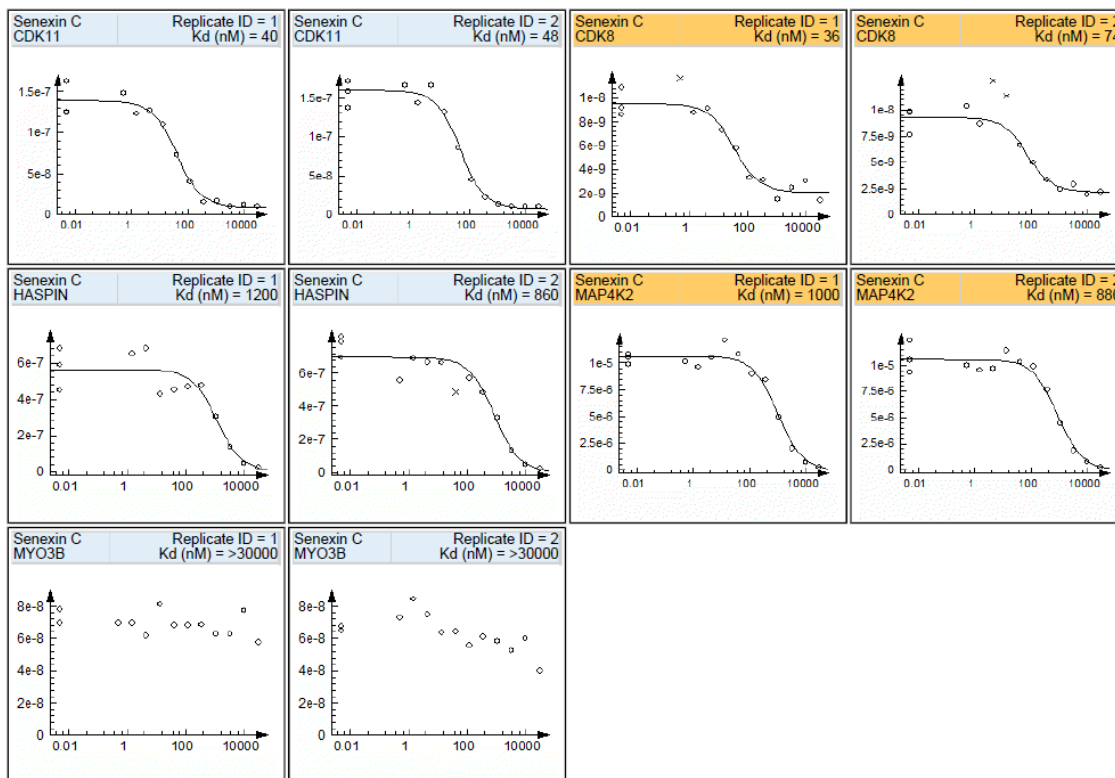


Figure 2.6 Determination of K_d s for Senexin C binding to CDK8, CDK19 (CDK11), HASPIN, MAP4K2 and MYO3B.

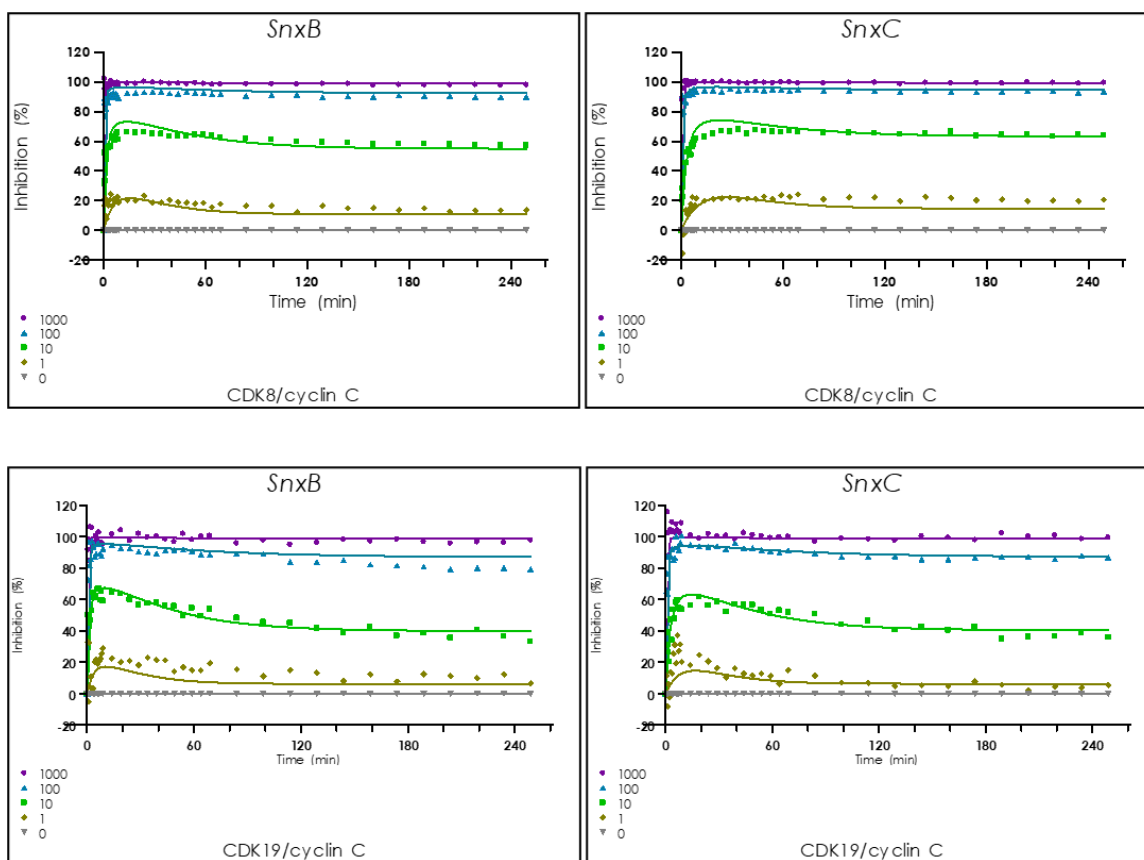


Figure 2.7 Determination of binding kinetics of Senexin B and Senexin C to recombinant CDK8/cyclin C and CDK19/cyclin C proteins.

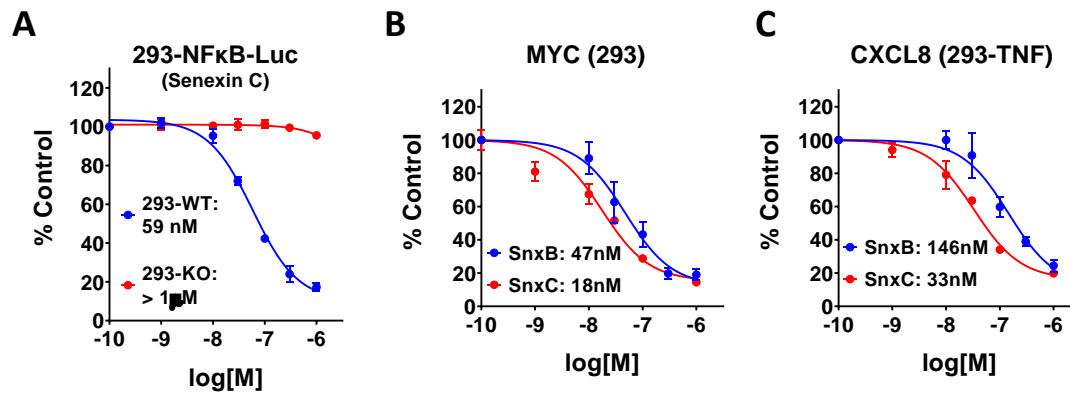


Figure 2.8 Cell-based IC₅₀ assays of Senexin C (SnxC) and Senexin B (SnxB). **(A)** 293-WT and dKO cells expressing Luciferase reporter under CDK8/19-dependent NFκB promoter treated with 10 ng/mL TNF-α and SnxC at different concentrations for 3 hours. **(B)** Effects of SnxB and SnxC (3 hours treatment) on MYC mRNA expression in 293 cells. **(C)** Effects of SnxB and SnxC on CXCL8 mRNA expression in 293 cells treated with 10 ng/mL TNF-α.

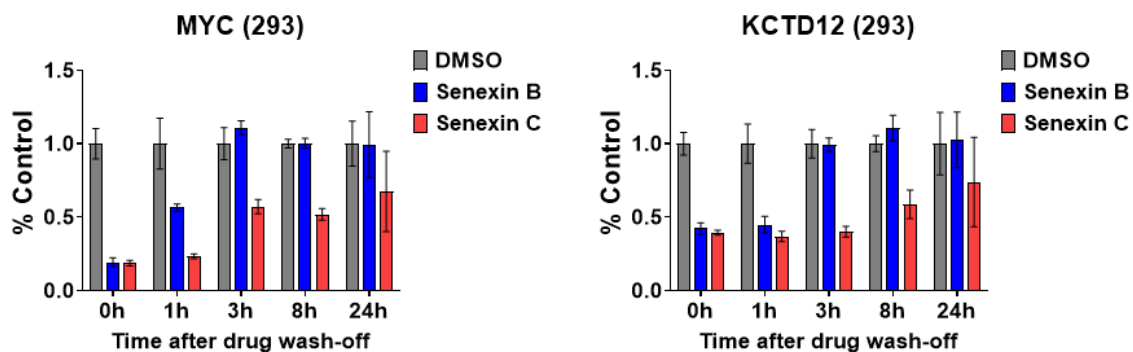


Figure 2.9 Effects of Senexin B and Senexin C on durability of the inhibition of CDK8/19-dependent gene expression in the wash-off study in 293 cells.

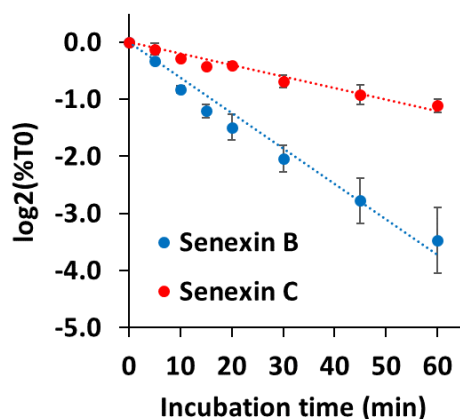


Figure 2.10 Metabolic stability of Senexin B and Senexin C in human hepatocytes.

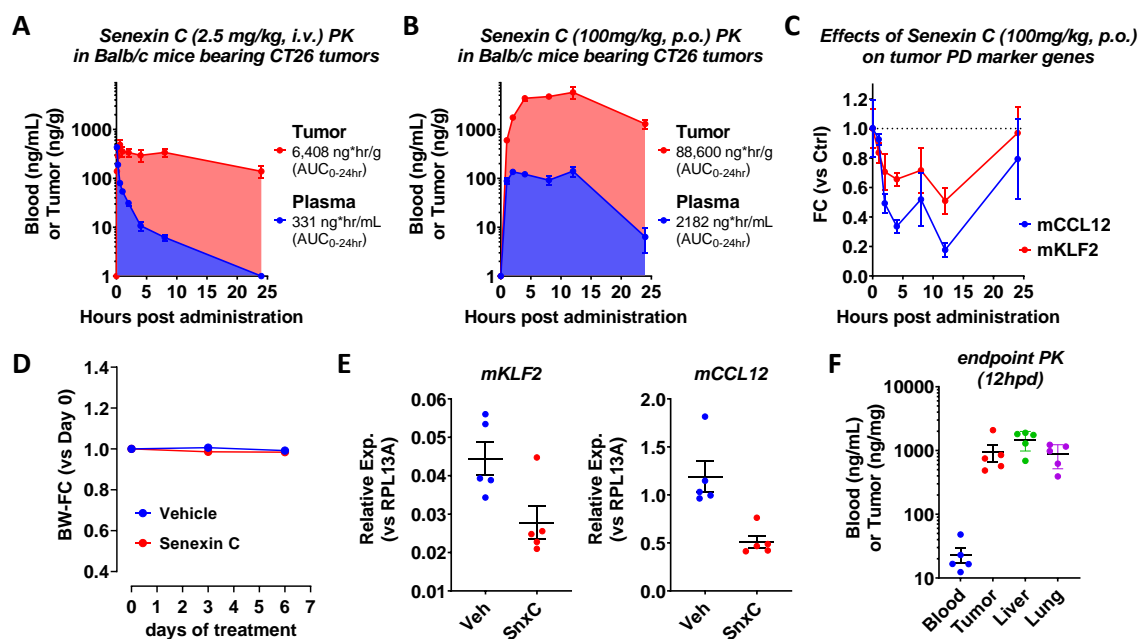


Figure 2.11 PK/PD analysis of Senexin C in the CT26 tumor model in Balb/c mice. **A.** Senexin C accumulation in the plasma and tumor tissues 0.5, 1, 2, 4, 8, 12 and 24 hrs after receiving a single i.v. dose at 2.5 mg/kg. **B.** The same after a single oral dose at 100 mg/kg. **C.** Expression of CDK8/19 dependent genes in CT26 tumors from the mice in **(B)**. **D.** Changes in body weights of animals orally dosed by Senexin C for 7 days (100 mg/kg, q.d.). **E.** Expression of PD marker genes in endpoint CT26 tumors collected at 12 hours post oral dosing on day 7. **F.** Endpoint PK of Senexin C in blood and tissues from the mice in **(E)**.

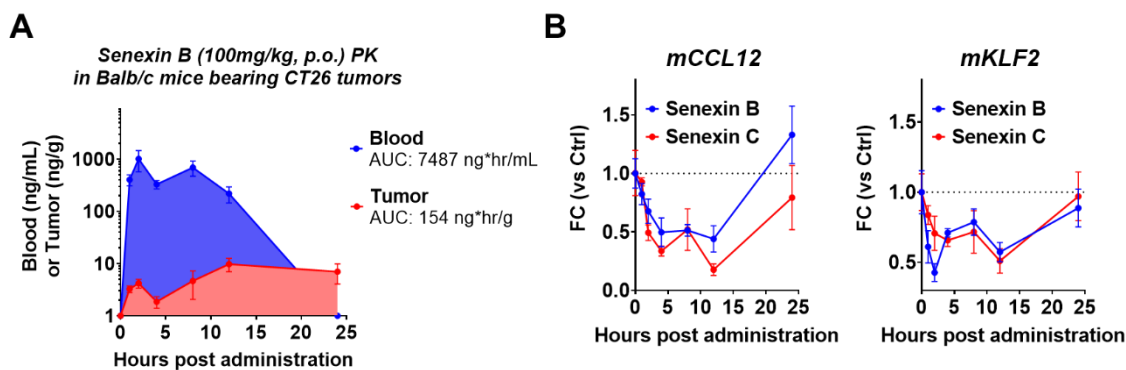


Figure 2.12. PK/PD analysis of Senexin B in the CT26 tumor model in Balb/c mice. **A.** Senexin B accumulation in the serum and tumor tissues, 0.5, 1, 2, 4, 8, 12 and 24 hrs after receiving one oral dose at 100 mg/kg. **B.** Expression of the CDK8/19-dependent genes in CT26 tumors in mice orally dosed with 100 mg/kg Senexin B or Senexin C.

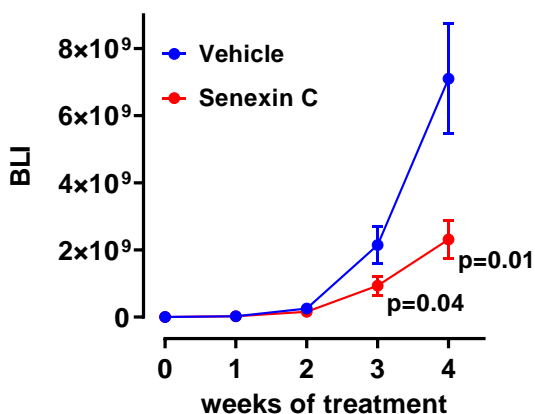
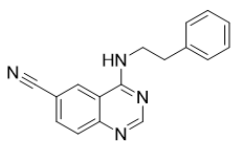
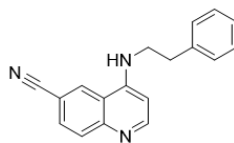
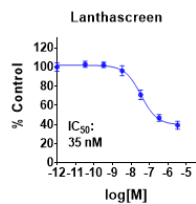


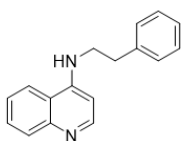
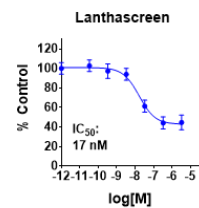
Figure 2.13. *In vivo* efficacy study of Senexin C (40mg/kg, p.o., BID) in the MV4-11 AML model in female NSG mice. Treatment started 7 days post inoculation (1×10^6 MV4-11-luc cells via tail vein) and tumor growth was monitored through weekly bioluminescence imaging (BLI).



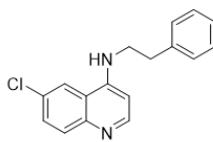
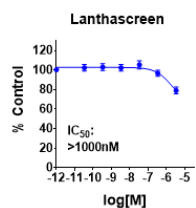
Senxin A (2.1)



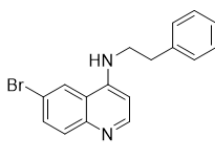
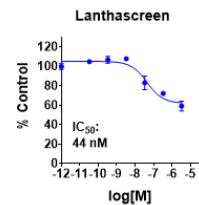
2.8a



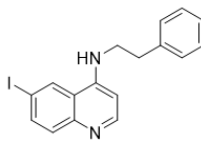
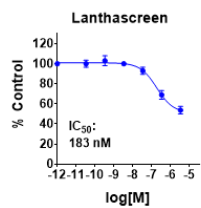
2.8b



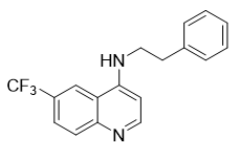
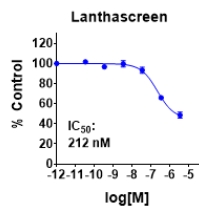
2.8c



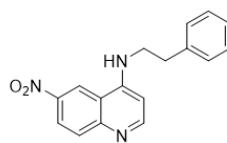
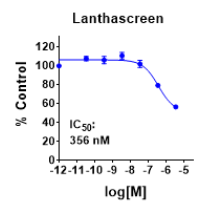
2.8d



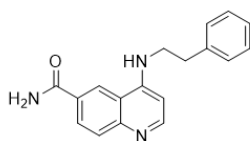
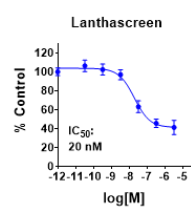
2.8e



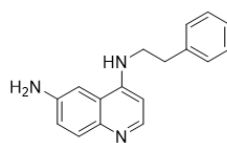
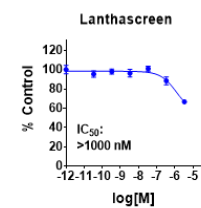
2.8f



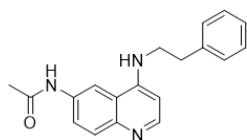
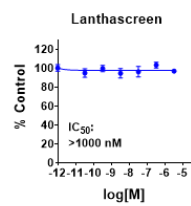
2.8g



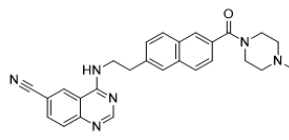
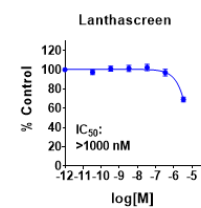
2.8h



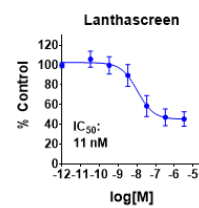
2.8i



2.8j



Senxin B (2.2)



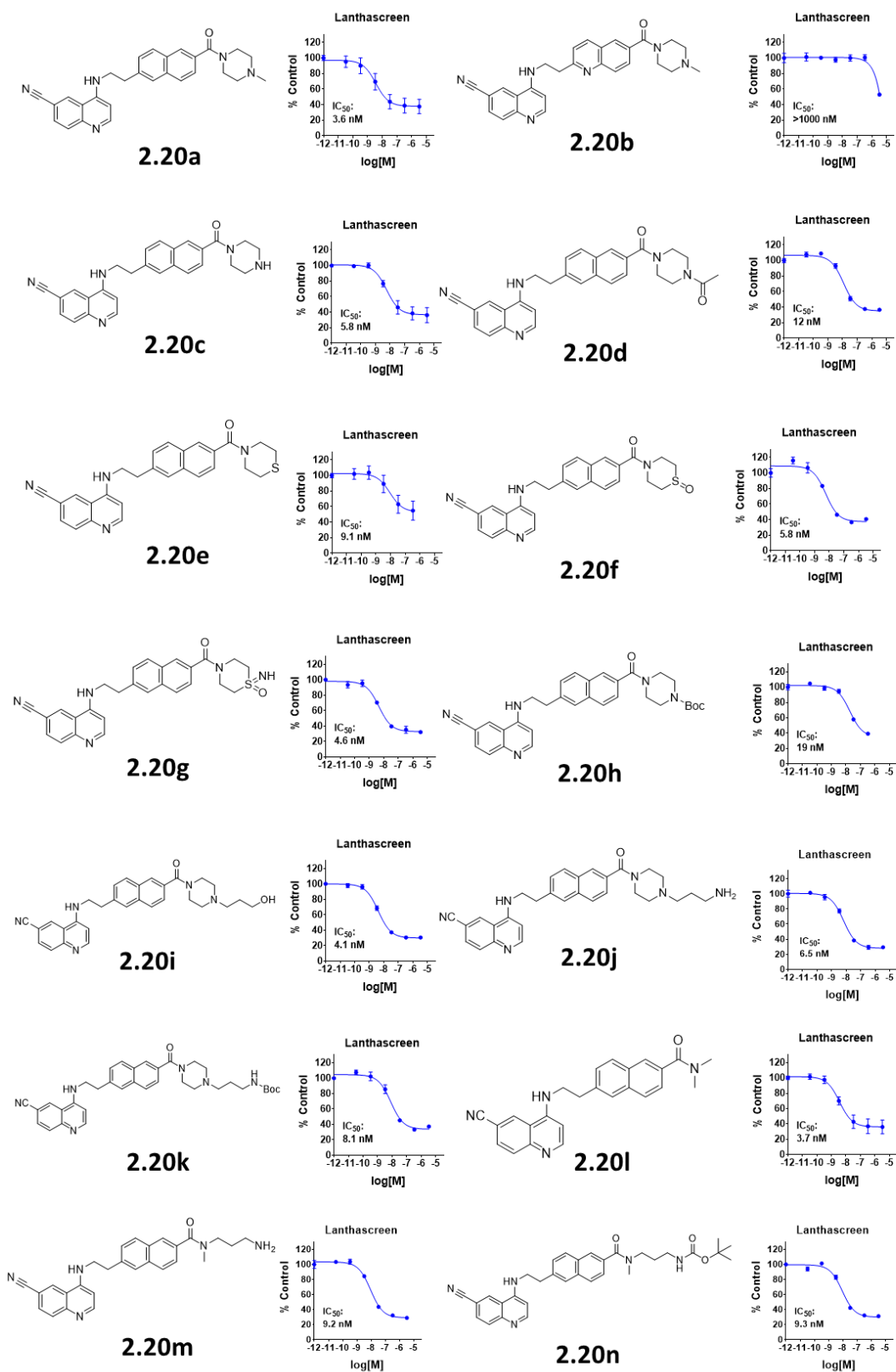
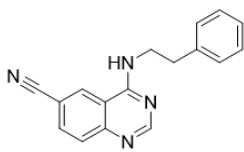
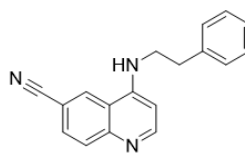
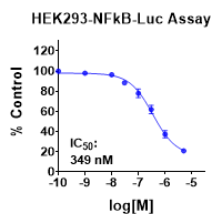


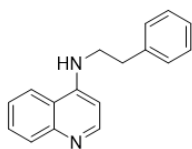
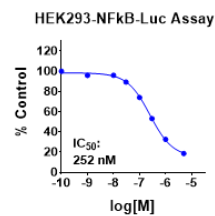
Figure 2.14 The Lanthascreen IC_{50} curves of tested compounds.



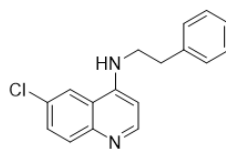
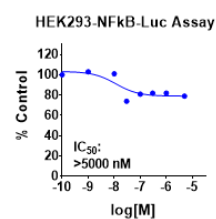
Senxin A (2.1)



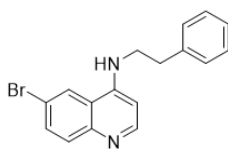
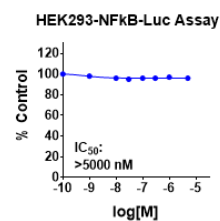
2.8a



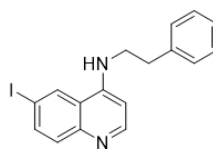
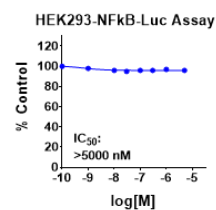
2.8b



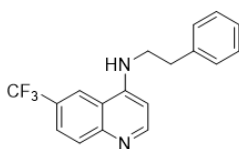
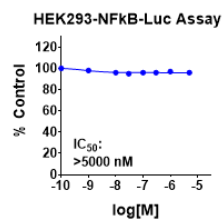
2.8c



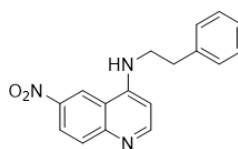
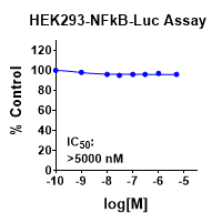
2.8d



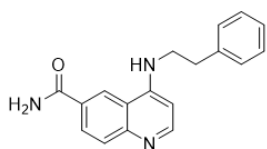
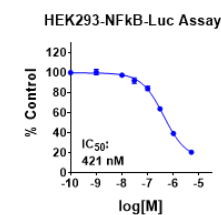
2.8e



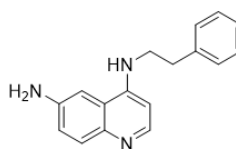
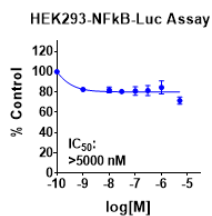
2.8f



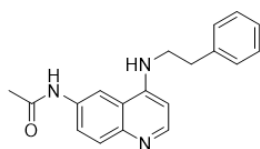
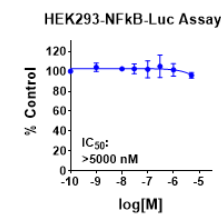
2.8g



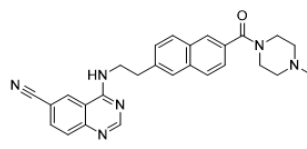
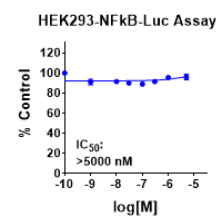
2.8h



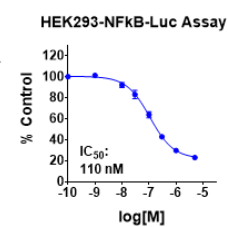
2.8i



2.8j



Senxin B (2.2)



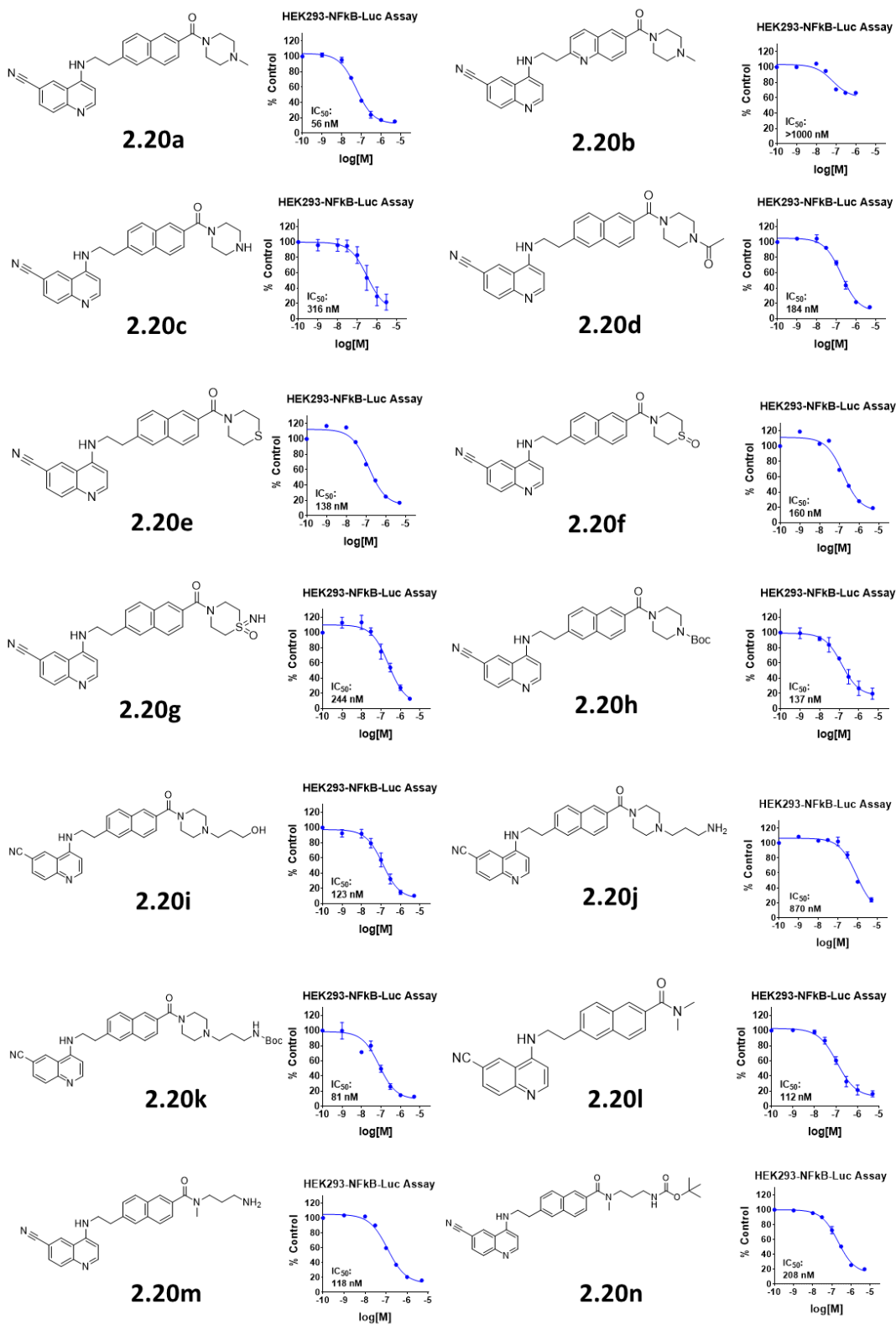
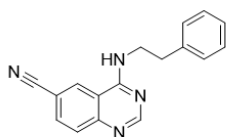
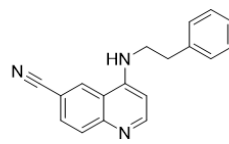
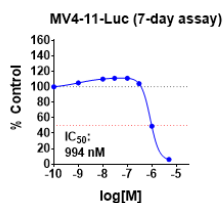


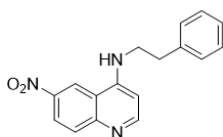
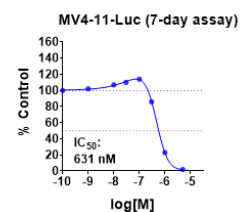
Figure 2.15 The HEK293-NFκB-Luc IC_{50} curves of tested compounds.



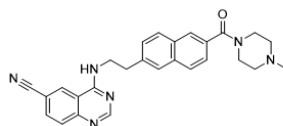
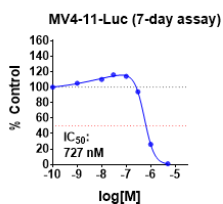
Senxin A (2.1)



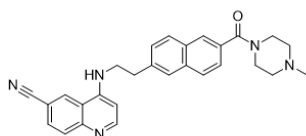
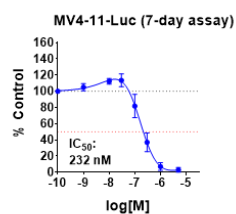
2.8a



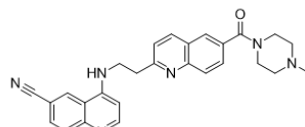
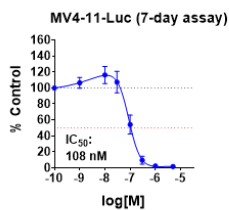
2.8g



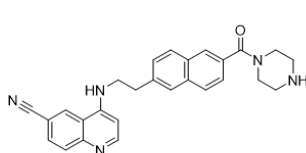
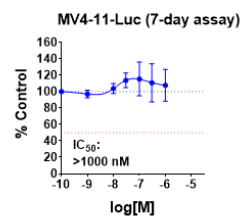
Senxin B (2.2)



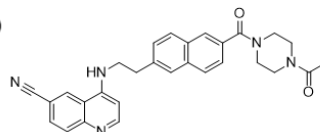
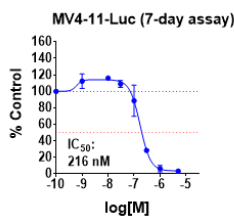
2.20a



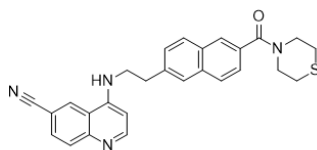
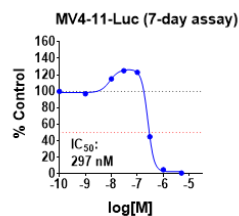
2.20b



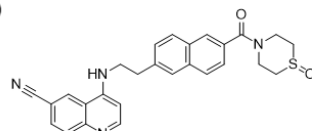
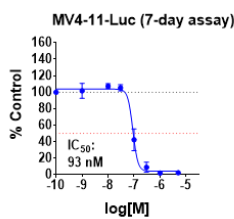
2.20c



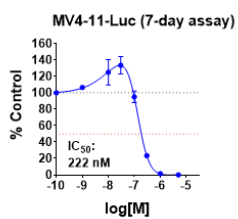
2.20d



2.20e



2.20f



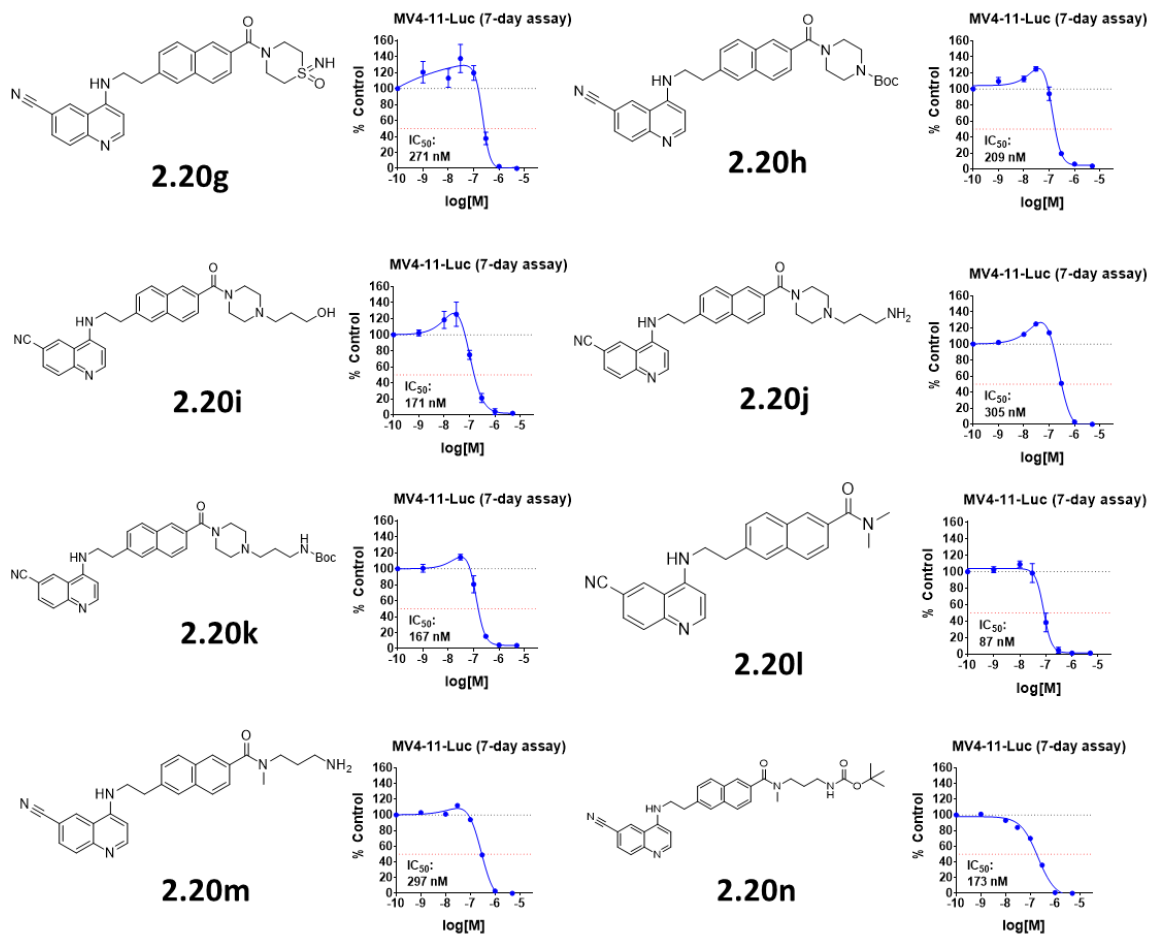
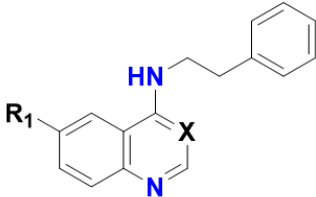


Figure 2.16 The MV4-11-Luc IC_{50} curves of tested compounds.

Table 2.1 Structure-activity relationship of Senexin A quinoline substitutions



Compound	R ₁	X	Lanthascreen IC ₅₀ (nM)	HEK293-Luc IC ₅₀ (nM)	MV4-11-Luc IC ₅₀ (nM)
Senexin A (2.1)	CN	N	35±4	349±14	994±42
2.8a	CN	C	17±4	252±13	631±21
2.8b	H	C	>1000	> 5000	-
2.8c	Cl	C	44±15	> 5000	-
2.8d	Br	C	183±26	> 5000	-
2.8e	I	C	212±47	> 5000	-
2.8f	CF ₃	C	356±43	> 5000	-
2.8g	NO ₂	C	20±2	421±19	727±45
2.8h	C(O)NH ₂	C	>1000	> 5000	-
2.8i	NH ₂	C	>1000	> 5000	-
2.8j	NHC(O)CH ₃	C	>1000	> 5000	-

Table 2.2 Structure-activity relationship of Senexin B naphthyl substitutions

Compound	R ₁	X	Y	Lanthascreen IC ₅₀ (nM)	HEK293-Luc IC ₅₀ (nM)	MV4-11-Luc GI ₅₀ (nM)
Senexin B (2.2)		N	C	11±3	110±15	232±42
2.20a		C	C	3.6±1	56±10	108±12
2.20b		N	C	>1000	>1000	>1000
2.20c		C	C	5.8±1	316±27	216±27
2.20d		C	C	12±1	184±11	297±14
2.20e		C	C	19±3	137±15	209±24
2.20f		C	C	9.1±2	138±12	93±16
2.20g		C	C	5.8±1	160±8	222±20
2.20h		C	C	4.6±1	244±26	271±28
2.20i		C	C	4.1±1	123±22	171±26
2.20j		C	C	6.5±2	870±100	305±3
2.20k		C	C	8.1±2	81±16	167±26
2.20l		C	C	3.7±1	112±15	87±20
2.20m		C	C	9.2±1	118±28	297±45
2.20n		C	C	9.3±2	208±34	173±19

Table 2.3 KINOMEScan of Senexin C at 2 μ M

DiscoverX Gene Symbol	Entrez Gene Symbol	Percent Control	DiscoverX Gene Symbol	Entrez Gene Symbol	Percent Control
AAK1	AAK1	84	MAK	MAK	100
ABL1(E255K)-phosphorylated	ABL1	93	MAP3K1	MAP3K1	78
ABL1(F317I)-nonphosphorylated	ABL1	88	MAP3K15	MAP3K15	83
ABL1(F317I)-phosphorylated	ABL1	89	MAP3K2	MAP3K2	68
ABL1(F317L)-nonphosphorylated	ABL1	93	MAP3K3	MAP3K3	83
ABL1(F317L)-phosphorylated	ABL1	74	MAP3K4	MAP3K4	81
ABL1(H396P)-nonphosphorylated	ABL1	73	MAP4K2	MAP4K2	29
ABL1(H396P)-phosphorylated	ABL1	81	MAP4K3	MAP4K3	100
ABL1(M351T)-phosphorylated	ABL1	80	MAP4K4	MAP4K4	93
ABL1(Q252H)-nonphosphorylated	ABL1	73	MAP4K5	MAP4K5	95
ABL1(Q252H)-phosphorylated	ABL1	89	MAPKAPK2	MAPKAPK2	91
ABL1(T315I)-nonphosphorylated	ABL1	90	MAPKAPK5	MAPKAPK5	62
ABL1(T315I)-phosphorylated	ABL1	76	MARK1	MARK1	81
ABL1(Y253F)-phosphorylated	ABL1	74	MARK2	MARK2	100
ABL1-nonphosphorylated	ABL1	71	MARK3	MARK3	94
ABL1-phosphorylated	ABL1	67	MARK4	MARK4	78
ABL2	ABL2	93	MAST1	MAST1	96
ACVR1	ACVR1	92	MEK1	MAP2K1	59
ACVR1B	ACVR1B	92	MEK2	MAP2K2	64
ACVR2A	ACVR2A	89	MEK3	MAP2K3	87
ACVR2B	ACVR2B	90	MEK4	MAP2K4	58
ACVRL1	ACVRL1	93	MEK5	MAP2K5	63
ADCK3	CABC1	100	MEK6	MAP2K6	80
ADCK4	ADCK4	97	MELK	MELK	97
AKT1	AKT1	89	MERTK	MERTK	89
AKT2	AKT2	100	MET	MET	90
AKT3	AKT3	100	MET(M1250T)	MET	88
ALK	ALK	89	MET(Y1235D)	MET	78
ALK(C1156Y)	ALK	83	MINK	MINK1	56
ALK(L1196M)	ALK	92	MKK7	MAP2K7	75
AMPK-alpha1	PRKAA1	94	MKNK1	MKNK1	72
AMPK-alpha2	PRKAA2	42	MKNK2	MKNK2	71
ANKK1	ANKK1	69	MLCK	MYLK3	100
ARK5	NUAK1	89	MLK1	MAP3K9	87
ASK1	MAP3K5	91	MLK2	MAP3K10	79
ASK2	MAP3K6	79	MLK3	MAP3K11	99
AURKA	AURKA	88	MRCKA	CDC42BPA	98
AURKB	AURKB	75	MRCKB	CDC42BPB	100
AURKC	AURKC	100	MST1	STK4	95
AXL	AXL	95	MST1R	MST1R	100
BIKE	BMP2K	97	MST2	STK3	100
BLK	BLK	100	MST3	STK24	100
BMPR1A	BMPR1A	95	MST4	MST4	68
BMPR1B	BMPR1B	70	MTOR	MTOR	79
BMPR2	BMPR2	66	MUSK	MUSK	90
BMX	BMX	100	MYLK	MYLK	83
BRAF	BRAF	84	MYLK2	MYLK2	91
BRAF(V600E)	BRAF	89	MYLK4	MYLK4	98
BRK	PTK6	97	MYO3A	MYO3A	100
BRSK1	BRSK1	100	MYO3B	MYO3B	31
BRSK2	BRSK2	96	NDR1	STK38	79
BTK	BTK	78	NDR2	STK38L	96

BUB1	BUB1	68	NEK1	NEK1	84
CAMK1	CAMK1	84	NEK10	NEK10	41
CAMK1B	PNCK	92	NEK11	NEK11	60
CAMK1D	CAMK1D	80	NEK2	NEK2	100
CAMK1G	CAMK1G	92	NEK3	NEK3	60
CAMK2A	CAMK2A	100	NEK4	NEK4	60
CAMK2B	CAMK2B	97	NEK5	NEK5	97
CAMK2D	CAMK2D	94	NEK6	NEK6	93
CAMK2G	CAMK2G	100	NEK7	NEK7	94
CAMK4	CAMK4	95	NEK9	NEK9	97
CAMKK1	CAMKK1	100	NIK	MAP3K14	88
CAMKK2	CAMKK2	82	NIM1	MGC42105	67
CASK	CASK	84	NLK	NLK	90
CDC2L1	CDK11B	96	OSR1	OXSR1	51
CDC2L2	CDC2L2	97	p38-alpha	MAPK14	84
CDC2L5	CDK13	64	p38-beta	MAPK11	80
CDK11	CDK19	13	p38-delta	MAPK13	97
CDK2	CDK2	95	p38-gamma	MAPK12	100
CDK3	CDK3	86	PAK1	PAK1	92
CDK4	CDK4	67	PAK2	PAK2	84
CDK4-cyclinD1	CDK4	83	PAK3	PAK3	98
CDK4-cyclinD3	CDK4	80	PAK4	PAK4	97
CDK5	CDK5	100	PAK6	PAK6	90
CDK7	CDK7	69	PAK7	PAK7	100
CDK8	CDK8	1.3	PCTK1	CDK16	68
CDK9	CDK9	97	PCTK2	CDK17	98
CDKL1	CDKL1	94	PCTK3	CDK18	97
CDKL2	CDKL2	75	PDGFRA	PDGFRA	97
CDKL3	CDKL3	87	PDGFRB	PDGFRB	94
CDKL5	CDKL5	70	PDPK1	PDPK1	86
CHEK1	CHEK1	100	PFCDPK1(P.falciparum)	CDPK1	83
CHEK2	CHEK2	98	PFPK5(P.falciparum)	MAL13P1.279	70
CIT	CIT	48	PFTAIRE2	CDK15	100
CLK1	CLK1	60	PFTK1	CDK14	98
CLK2	CLK2	93	PHKG1	PHKG1	95
CLK3	CLK3	65	PHKG2	PHKG2	100
CLK4	CLK4	69	PIK3C2B	PIK3C2B	80
CSF1R	CSF1R	85	PIK3C2G	PIK3C2G	57
CSF1R-autoinhibited	CSF1R	91	PIK3CA	PIK3CA	90
CSK	CSK	85	PIK3CA(C420R)	PIK3CA	73
CSNK1A1	CSNK1A1	76	PIK3CA(E542K)	PIK3CA	55
CSNK1A1L	CSNK1A1L	88	PIK3CA(E545A)	PIK3CA	73
CSNK1D	CSNK1D	87	PIK3CA(E545K)	PIK3CA	55
CSNK1E	CSNK1E	81	PIK3CA(H1047L)	PIK3CA	84
CSNK1G1	CSNK1G1	100	PIK3CA(H1047Y)	PIK3CA	91
CSNK1G2	CSNK1G2	89	PIK3CA(I800L)	PIK3CA	72
CSNK1G3	CSNK1G3	76	PIK3CA(M1043I)	PIK3CA	80
CSNK2A1	CSNK2A1	56	PIK3CA(Q546K)	PIK3CA	70
CSNK2A2	CSNK2A2	64	PIK3CB	PIK3CB	64
CTK	MATK	56	PIK3CD	PIK3CD	61
DAPK1	DAPK1	100	PIK3CG	PIK3CG	76
DAPK2	DAPK2	100	PIK4CB	PI4KB	51
DAPK3	DAPK3	95	PIKFYVE	PIKFYVE	86
DCAMKL1	DCLK1	63	PIM1	PIM1	62
DCAMKL2	DCLK2	94	PIM2	PIM2	81
DCAMKL3	DCLK3	96	PIM3	PIM3	96
DDR1	DDR1	100	PIP5K1A	PIP5K1A	84
DDR2	DDR2	64	PIP5K1C	PIP5K1C	87
DLK	MAP3K12	68	PIP5K2B	PIP4K2B	85
DMPK	DMPK	98	PIP5K2C	PIP4K2C	84
DMPK2	CDC42BPG	83	PKAC-alpha	PRKACA	93
DRAK1	STK17A	100	PKAC-beta	PRKACB	100
DRAK2	STK17B	87	PKMYT1	PKMYT1	100
DYRK1A	DYRK1A	63	PKN1	PKN1	100
DYRK1B	DYRK1B	83	PKN2	PKN2	89
DYRK2	DYRK2	68	PKNB(M.tuberculosis)	pknB	93
EGFR	EGFR	91	PLK1	PLK1	63
EGFR(E746-A750del)	EGFR	100	PLK2	PLK2	80
EGFR(G719C)	EGFR	93	PLK3	PLK3	80
EGFR(G719S)	EGFR	100	PLK4	PLK4	90

EGFR(L747-E749del, A750P)	EGFR	77	PRKCD	PRKCD	83
EGFR(L747-S752del, P753S)	EGFR	98	PRKCE	PRKCE	98
EGFR(L747-T751del,Sins)	EGFR	74	PRKCH	PRKCH	91
EGFR(L858R)	EGFR	93	PRKCI	PRKCI	89
EGFR(L858R,T790M)	EGFR	82	PRKCQ	PRKCQ	100
EGFR(L861Q)	EGFR	64	PRKD1	PRKD1	90
EGFR(S752-I759del)	EGFR	99	PRKD2	PRKD2	88
EGFR(T790M)	EGFR	93	PRKD3	PRKD3	100
EIF2AK1	EIF2AK1	84	PRKG1	PRKG1	100
EPHA1	EPHA1	93	PRKG2	PRKG2	84
EPHA2	EPHA2	100	PRKR	EIF2AK2	88
EPHA3	EPHA3	100	PRKX	PRKX	100
EPHA4	EPHA4	93	PRP4	PRPF4B	71
EPHA5	EPHA5	97	PYK2	PTK2B	92
EPHA6	EPHA6	79	QSK	KIAA0999	55
EPHA7	EPHA7	91	RAF1	RAF1	98
EPHA8	EPHA8	91	RET	RET	100
EPHB1	EPHB1	92	RET(M918T)	RET	85
EPHB2	EPHB2	86	RET(V804L)	RET	88
EPHB3	EPHB3	81	RET(V804M)	RET	91
EPHB4	EPHB4	89	RIOK1	RIOK1	94
EPHB6	EPHB6	86	RIOK2	RIOK2	64
ERBB2	ERBB2	73	RIOK3	RIOK3	85
ERBB3	ERBB3	76	RIPK1	RIPK1	100
ERBB4	ERBB4	95	RIPK2	RIPK2	100
ERK1	MAPK3	95	RIPK4	RIPK4	57
ERK2	MAPK1	93	RIPK5	DSTYK	69
ERK3	MAPK6	89	ROCK1	ROCK1	52
ERK4	MAPK4	87	ROCK2	ROCK2	71
ERK5	MAPK7	94	ROS1	ROS1	91
ERK8	MAPK15	76	RPS6KA4(Kin.Dom.1-N-terminal)	RPS6KA4	100
ERN1	ERN1	58	RPS6KA4(Kin.Dom.2-C-terminal)	RPS6KA4	62
FAK	PTK2	89	RPS6KA5(Kin.Dom.1-N-terminal)	RPS6KA5	86
FER	FER	91	RPS6KA5(Kin.Dom.2-C-terminal)	RPS6KA5	100
FES	FES	81	RSK1(Kin.Dom.1-N-terminal)	RPS6KA1	91
FGFR1	FGFR1	85	RSK1(Kin.Dom.2-C-terminal)	RPS6KA1	97
FGFR2	FGFR2	98	RSK2(Kin.Dom.1-N-terminal)	RPS6KA3	62
FGFR3	FGFR3	100	RSK2(Kin.Dom.2-C-terminal)	RPS6KA3	65
FGFR3(G697C)	FGFR3	93	RSK3(Kin.Dom.1-N-terminal)	RPS6KA2	100
FGFR4	FGFR4	96	RSK3(Kin.Dom.2-C-terminal)	RPS6KA2	91
FGR	FGR	90	RSK4(Kin.Dom.1-N-terminal)	RPS6KA6	60
FLT1	FLT1	99	RSK4(Kin.Dom.2-C-terminal)	RPS6KA6	96
FLT3	FLT3	89	S6K1	RPS6KB1	78
FLT3(D835H)	FLT3	88	SBK1	SBK1	57
FLT3(D835V)	FLT3	67	SGK	SGK1	50
FLT3(D835Y)	FLT3	73	SgK110	SgK110	91
FLT3(ITD)	FLT3	97	SGK2	SGK2	61
FLT3(ITD,D835V)	FLT3	55	SGK3	SGK3	75
FLT3(ITD,F691L)	FLT3	59	SIK	SIK1	91
FLT3(K663Q)	FLT3	87	SIK2	SIK2	100
FLT3(N841I)	FLT3	100	SLK	SLK	92
FLT3(R834Q)	FLT3	70	SNARK	NUAK2	75
FLT3-autoinhibited	FLT3	88	SNRK	SNRK	75
FLT4	FLT4	97	SRC	SRC	92
FRK	FRK	92	SRMS	SRMS	75
FYN	FYN	89	SRPK1	SRPK1	91

GAK	GAK	100	SRPK2	SRPK2	94
GCN2(Kin.Dom.2,S808G)	EIF2AK4	93	SRPK3	SRPK3	96
GRK1	GRK1	63	STK16	STK16	71
GRK2	ADRBK1	63	STK33	STK33	93
GRK3	ADRBK2	73	STK35	STK35	100
GRK4	GRK4	100	STK36	STK36	88
GRK7	GRK7	87	STK39	STK39	44
GSK3A	GSK3A	94	SYK	SYK	97
GSK3B	GSK3B	67	TAK1	MAP3K7	63
HASPIN	GSG2	29	TAOK1	TAOK1	76
HCK	HCK	96	TAOK2	TAOK2	77
HIPK1	HIPK1	73	TAOK3	TAOK3	79
HIPK2	HIPK2	67	TBK1	TBK1	88
HIPK3	HIPK3	52	TEC	TEC	100
HIPK4	HIPK4	75	TESK1	TESK1	96
HPK1	MAP4K1	94	TGFBF1	TGFBF1	100
HUNK	HUNK	74	TGFBF2	TGFBF2	96
ICK	ICK	54	TIE1	TIE1	85
IGF1R	IGF1R	94	TIE2	TEK	89
IKK-alpha	CHUK	76	TLK1	TLK1	94
IKK-beta	IKKBK	76	TLK2	TLK2	88
IKK-epsilon	IKBKE	91	TNIK	TNIK	89
INSR	INSR	93	TNK1	TNK1	95
INSRR	INSRR	88	TNK2	TNK2	94
IRAK1	IRAK1	45	TNNI3K	TNNI3K	100
IRAK3	IRAK3	94	TRKA	NTRK1	53
IRAK4	IRAK4	67	TRKB	NTRK2	57
ITK	ITK	93	TRKC	NTRK3	69
JAK1(JH1domain-catalytic)	JAK1	94	TRPM6	TRPM6	88
JAK1(JH2domain-pseudokinase)	JAK1	58	TSSK1B	TSSK1B	100
JAK2(JH1domain-catalytic)	JAK2	56	TSSK3	TSSK3	81
JAK3(JH1domain-catalytic)	JAK3	65	TTK	TTK	72
JNK1	MAPK8	54	TXK	TXK	94
JNK2	MAPK9	67	TYK2(JH1domain-catalytic)	TYK2	62
JNK3	MAPK10	61	TYK2(JH2domain-pseudokinase)	TYK2	63
KIT	KIT	95	TYRO3	TYRO3	77
KIT(A829P)	KIT	82	ULK1	ULK1	66
KIT(D816H)	KIT	57	ULK2	ULK2	71
KIT(D816V)	KIT	100	ULK3	ULK3	70
KIT(L576P)	KIT	100	VEGFR2	KDR	82
KIT(V559D)	KIT	95	VPS34	PIK3C3	68
KIT(V559D,T670I)	KIT	90	VRK2	VRK2	58
KIT(V559D,V654A)	KIT	89	WEE1	WEE1	88
KIT-autoinhibited	KIT	88	WEE2	WEE2	95
LATS1	LATS1	76	WNK1	WNK1	72
LATS2	LATS2	88	WNK2	WNK2	59
LCK	LCK	92	WNK3	WNK3	75
LIMK1	LIMK1	95	WNK4	WNK4	69
LIMK2	LIMK2	93	YANK1	STK32A	76
LKB1	STK11	87	YANK2	STK32B	89
LOK	STK10	94	YANK3	STK32C	100
LRRK2	LRRK2	85	YES	YES1	100
LRRK2(G2019S)	LRRK2	56	YSK1	STK25	83
LTK	LTK	93	YSK4	MAP3K19	50
LYN	LYN	88	ZAK	ZAK	94
LZK	MAP3K13	46	ZAP70	ZAP70	81

Table 2.4 Binding kinetics of Senexin B and Senexin C to recombinant CDK8/cycC and CDK19/cycC proteins in KINETICfinder assay

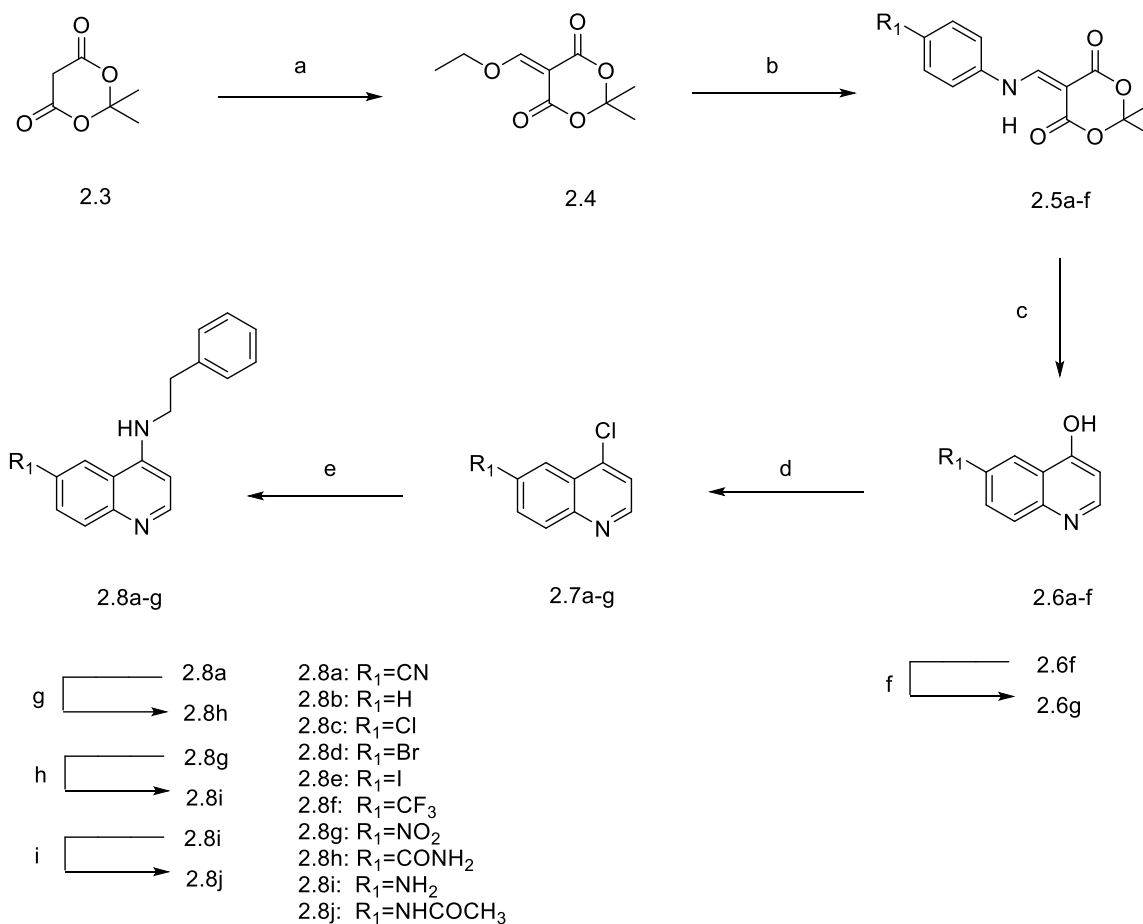
Target	Compound	k_{on} ($M^{-1}s^{-1}$)	k_{off} (s^{-1})	τ (min)	$T_{1/2}$ (min)	K_d (M)
CDK8/cyclin C	Senexin B	1.65E+06	0.00325	5.13	3.55	1.97E-09
	Senexin C	8.78E+05	0.00122	13.63	9.45	1.39E-09
CDK19/cyclin C	Senexin B	2.13E+06	0.00628	2.65	1.84	2.95E-09
	Senexin C	9.39E+05	0.00272	6.13	4.25	2.90E-09

Table 2.5 Pharmacokinetic Analysis of Senexin C in Balb/c mice bearing CT26 tumors

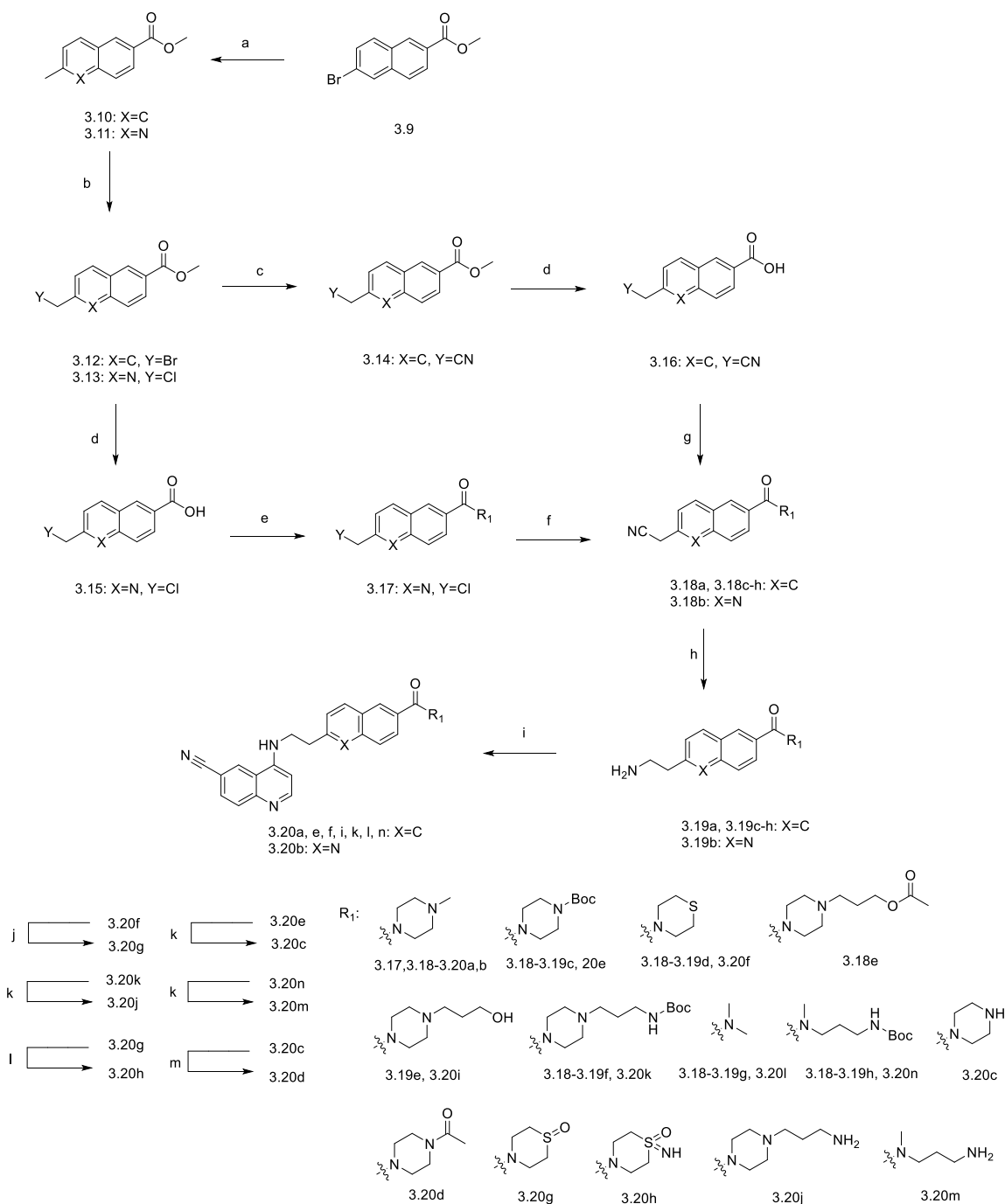
Parameters	iv (2.5mg/kg)		po (100mg/kg)	
	Plasma	Tumor	Plasma	Tumor
C_0 (ng/mL)	503			
K_{el} (hr^{-1})	0.93	0.06	0.2	0.1
$T_{1/2}$ (hr)	0.75	12.1	3.53	7.27
T_{max} (hr)		0.58	12	12
C_{max} (ng/mL or ng/g)		488	144	5728
AUC_{0-24hr} (ng*hr/mL or ng*hr/g)	331	6408	2182	88600
F%			16.5%	34.6%

Table 2.6 qPCR primer sequences

Primer Name	Species	Sequence
GAPDH-F	Human	CCATCACCATCTTCCAGGAGCG
GAPDH-R	Human	AGAGATGATGACCCTTTTGGC
MYC-F	Human	CCAACAGGAACTATGACCTCGACTAC
MYC-R	Human	CTCGAATTTCTTCCAGATATCCT
CXCL8-F	Human	TCCTGATTTCTGCAGCTCTGT
CXCL8-R	Human	AAATTTGGGGTGGAAAGGTT
KCTD12-F	Human	TTTATCACTGTGCTATCAATCAAAA
KCTD12-R	Human	TGCTGTAGAAAATATTCCTTGAAGA
mRPL13A-F	Mouse	GGGCAGGTTCTGGTATTGGAT
mRPL13A-R	Mouse	GGCTCGGAAATGGTAGGGG
mKLF2-F	Mouse	CCTAAAGGCGCATCTGCGTA
mKLF2-R	Mouse	CTGTGTGCTTTCGGTAGTGG
mCCL12-F	Mouse	CAGTCCTCAGGTATTGGCTGG
mCCL12-R	Mouse	GCTTCCGGACGTGAATCTTCT



Scheme 2.1 Synthesis of 6-substituted-*N*-phenethylquinolin-4-amine derivatives. Reagents and conditions: (a) triethoxymethane, 100°C; (b) *p*-substituted aniline, DCM, r.t.; (c) phenoxybenzene, 220°C; (d) POCl₃, 1,4-dioxane, 90°C; (e) 2-phenylethan-1-amine, DIEA, DMSO, 100°C; (f) HNO₃, H₂SO₄, 0°C to r.t.; (g) KOH, *t*-BuOH, 90°C; (h) NH₄Cl, Fe, EtOH, H₂O, reflux; (i) acetic anhydride, pyridine, r.t..



Scheme 2.2. Synthesis of 4-((2-(6-substituted-naphthalen-2-yl)ethyl)amino)quinoline-6-carbonitrile derivatives. Reagents and conditions: (a) Pd(PPh₃)₄, K₂CO₃, toluene, water, 80°C; (b) NBS, AIBN, CCl₄, reflux for **12**; NCS, AIBN, DCE, 80°C for **13**; (c) KCN, MeOH, reflux; (d) LiOH, THF, water; (e) SOCl₂, 1-methylpiperazine, DCM, 60°C to r.t.; (f) KCN, ethanol, water, 60°C; (g) HATU, DIEA, DCM/DMF, r.t.; (h) raney Ni, MeOH/H₂O/NH₄OH, H₂, r.t.; (i) 4-chloroquinoline-6-carbonitrile, DIEA, DMSO, 120°C; (j) NaIO₄, MeOH, H₂O, r.t.;

(k) TFA, DCM, r.t.; (l) rhodium acetate dimer, iodobenzene diacetate, 2,2,2-trifluoroacetamide, MgO, DCM, r.t.; (m) acetyl chloride, DIEA, DCM, 0°C to r.t..

CHAPTER 3

THIENOPYRIDINE SCAFFOLD AS NOVEL CLASS OF SELECTIVE CDK8/19 INHIBITORS

3.1 Introduction

The thienopyridine analogues developed by Daiichi Sankyo as bone anabolic agents¹⁸¹ and later identified as potential CDK8 inhibitors with high potency,¹⁸² offer a new scaffold for CDK8 inhibitor development. Among the thienopyridine analogues, two compounds 15u (**3.1**) and 15w (**3.2**) (**Figure 3.1**) show most potent CDK8 inhibitory activity at nano molar range with negligible toxicity.^{178,180}

A docking study of 15u and 15w was then carried out to analyze their possible binding modes with CDK8 as shown in **Figure 3.2**. According to the result, the pyridine nitrogen of the thienopyridine ring forms a H-bond with Ala100 of CDK8 that anchors the molecule into the hinge region. The carbonyl oxygen of the amide group attached to the thiophene ring forms two H-bonds, one to the NH of Asp173 and the other to the positive charged ammonium of Lys52. The phenyl ring of the tail section of the inhibitor forms a π -cation interaction with Arg356. The carbonyl oxygen of the benzamide of both 15u and 15w forms a H-bond with

Arg29. Moreover, both molecules form hydrophobic interaction with surrounding residues including Val27, Gly28, Val35, Trp105, and His106.

The kinase selectivity of 15u and 15w are evaluated via kinome profiling (Discover X) as shown in **Figure 3.3**. 15w was tested at 500 nM and selectively targets CDK8 and CDK19 with only one off-target (RIOK2). 15u was evaluated at 2 μ M and exhibits high CDK8/19 selectivity as well, however, with increased off-targets due to higher concentration used in the assay. RIOK2 is also an off-target for 15u. The complete kinome profiling results are shown in the experimental section.

The thienopyridine compounds 15u and 15w exhibit significant selectivity and inhibitory potency against CDK8/19, thus offering a novel chemical scaffold for the development of CDK8/19 inhibitors. In this chapter, SBDD-based drug design, modification, and optimization were carried out on both 15u and 15w in order to achieve novel CDK8/19 inhibitor candidates with significant potency and PK profile.

3.2 Results and Discussion

According to docking results, the predicted binding model of 15u and 15w are similar to Senexin C, suggesting that the SAR of Senexin analogues may be applicable to the thienopyridine series. Therefore, a hybrid strategy was carried out for inhibitor design and modification. A series of compounds were designed and synthesized via exchanging the structural motifs in 15u and 15w with the motifs in Senexin C as shown in **Scheme 3.1** and **Scheme 3.2**. The CDK8 inhibitory activity of resulting hybrid compounds were evaluated via the cell-based

NFkB IC₅₀ assay as shown in **Table 3.1**. The compounds **3.6a** and **3.6b** (Senexin C head combined with 15u or 15w tail) are less active than 15u and 15w. Compounds **3.11a** and **3.11b** (15u/15w head combined with Senexin A or Senexin B tail) are also less potent than their parental compounds Senexin A and Senexin B (**Table 3.1**). In addition, the two intermediates of **3.11a** and **3.11b** (**3.9a** and **3.9b**) were evaluated and found to have no inhibitory activity, indicating the importance of amide group on the thiophene ring to the binding affinity. Although the hybrid strategy did not result in compounds with significant inhibitory activity, it did however provide SAR information for further studies.

15w was found to be 2.5-fold more potent than 15u, thus giving it priority for further modification. The difference between the structures of 15w and 15u is the additional -CH₂- group at the tail section as shown in **Figure 3.1**. The initial modification of 15w was undertaken by moving the -CH₂- group to the other side of the ring, thus offering more flexibility to the tail section. The synthesis of this analog (**3.19**) is shown in **Scheme 3.3**. Compound **3.19** loses activity according to the IC₅₀ assay (**Table 3.2**) possibly due to both the increase of entropy and the change of tail orientation that diminishes binding affinity, suggesting that the original location of -CH₂- group is essential for good binding affinity. Another modification of 15w was undertaken by replacing the dimethylamide with a piperazine group as shown in **Scheme 3.4**. This leads to a novel structural motif at the tail section, where the resulting compound **3.26a** shows comparable inhibitory activity to 15w. Based on this result, four more analogs of **3.26a** were designed and synthesized as shown in **Scheme 3.4** and **Scheme 3.5**. The

rationale is to replace the methyl group with larger functional groups and enhance the hydrophobic interaction at the front pocket. As shown in **Table 3.2**, the removal of the methyl group resulted in compound **3.33** with inhibitory activity reduced by nearly 16 times. Meanwhile, protection of the free NH with a Boc group resulted in compound **3.32** and rescued the inhibitory activity, but with lower potency than **3.26a**. Compounds **3.26b** and **3.26c** with ethyl and cyclopropyl are slightly less potent than **3.26a** as well. Taking together, demethylation or the replacement of methyl group with larger functional groups dampens the binding affinity of **3.26a**.

Despite the potent CDK8 inhibitory activity, further modification of 15w and **3.26a** was not attempted due to the unfavorable PK profile obtained as shown in **Figure 3.4**. On the contrary, 15u possesses good PK properties and thus was used for additional studies. The modification of 15u was initially undertaken at the tail part. The N,N-dimethyl group was further substituted with a number of functional groups as shown in **Scheme 3.6**. The IC₅₀ values of the resulting compounds based on cell-based NFκB assay are shown in **Table 3.3**. Compound **3.43a** with a methylpiperazine group is three-times less potent than 15u. The demethylation of **3.43a** (**3.44a**) further dampened the inhibitory activity, while Boc protection of the piperazine (**3.43b**) rescued the activity and showed comparable inhibitory activity to 15u. Despite that, the acetylpiperazine analog **3.43c** is only nearly 2-fold more potent than **3.44a**. The substitution of the piperazine group of **3.44a** with cycloalkyl groups resulted in compounds **3.43d-f**. Compounds **3.43d** and **3.43e** showed the same inhibitory activity as **3.43b** and which is comparable to 15u. Compound **3.43f** with a cyclohexyl group, on the other hand, shows a slight decrease in inhibitory

activity likely due to its larger volume. The N,N-dimethyl group was also replaced with short flexible carbon chain groups that resulted in compounds **3.43g-i** and **3.44b**. **3.43g** and **3.43h** are both active compounds, although they are less potent than 15u; **3.43h** is more potent than **3.43g** due to the removal of the free NH at the tail. **3.43i** and **3.44b** are also both active compounds. Where **3.44b** shows comparable activity to 15u and is 15-fold more potent than **3.43i**. In this context, the free NH₂ group contributes to the binding affinity. In general, the above tail part modifications generally sustained the inhibitory activity, but didn't increase the potency.

Further modification focused on the head part of 15u. The head section of the inhibitor molecule binds at the CDK8 hinge region where there are a number of residues that it can form interactions with and contribute to binding affinity. A series of analogs have been designed and synthesized as shown in **Schemes 3.7-3.16**. The CDK8 inhibitory activity of resulting compounds is shown in **Table 3.4**. The compounds **3.48** and **3.51** along with 15u demonstrate the importance of nitrogen atom of the pyridine ring at the head part. The thienopyrimidine analog **3.48** has no inhibitory activity, which may be due to the reduced basicity of position 1 nitrogen that forms a H-bond with Ala100. When the position 1 nitrogen of 15u moves to position 2, the resulting compound **3.51**, however, shows an 8-fold decrease in inhibitory activity. These two analogs suggest that the location and basicity of the nitrogen atom on the pyridine ring are essential to the inhibitory activity. In addition, the NH₂ group on the thiophene ring is key to the binding affinity and its removal caused activity loss as shown in compounds **3.54** and **3.59**.

Meanwhile, the amide carbonyl oxygen acts as a H-bond acceptor according to docking results, and the replacement of the amide with a cyano group should achieve a stronger H-bond with Lys52. However, the resulting compound **3.62** exhibits much lower potency which may be due to the orientation of cyano group that forms a weaker H-bond with Lys52. Surprisingly, when the thiophene ring is changed to furan, the resulting compound **3.65** totally loses inhibitory activity. Another scaffold hopping attempt was the replacement of the thiophene ring with pyrrole ring, the rationale being to provide an extra interaction with the hinge region contributing to the binding affinity. However, this modification (compound **3.74**) also leads to an activity loss. The reason is very likely due to the intramolecular H-bond. The pyrrole NH can compete with the NH₂ group and forms an intramolecular H-bond with the adjacent amide oxygen, which changes its orientation and consequently disrupts the H-bond with Lys52. This hypothesis is further confirmed by compounds **3.69** and **3.59**. The lack of NH₂ at the head part leads to the increasing flexibility of the amide group and thus cannot form an effective H-bond with Lys52. Meanwhile, the NH₂ group itself may also contribute to binding affinity. Based on these results, a further modification was carried out to form a third ring joined to the thiophene. The rationale was to fix the position of H-bond acceptor and thus decrease the entropy, while the third ring itself may form additional interactions with the hinge region. The resulting compound **3.82**, however, shows no inhibitory activity. Compound **3.83**, on the other hand, shows good inhibitory activity, although less potent than 15u.

3.3 Conclusion

A series of thienopyridine novel CDK8/19 kinase inhibitors have been developed through a structure-based design strategy. The inhibitory activity of resulting compounds was evaluated via cell-based NFkB IC₅₀ assay. The structural modifications were carried out at different sections of parental inhibitors 15u and 15w. Compound **3.26a** exhibits comparable inhibitory activity to the most potent parental inhibitor 15w, however, it doesn't improve its unfavorable PK profile. Despite that, a variety of SAR information was achieved, which can be used for the further development of CDK8/19 inhibitors of this series.

3.4 Experimental Section

3.4.1 Chemistry

All chemical reagents and solvents were purchased from commercial sources and used without further purification. The reactions were monitored by thin-layer chromatography (TLC), visualized by UV light (254 or 365 nm). The microwave oven reactions were conducted via Biotage microwave reactor. The purification of the products was finished by Biotage flash chromatography using silica gel columns. All NMR spectra were recorded with a Bruker spectrometer at 300 or 400 MHz in deuterated solvents. High-performance liquid chromatography (HPLC) and Mass spectra (MS) were used to confirm the purity and molecular weight of each compound. All compounds are >95% pure by HPLC analysis (data included in the Supporting Information).

tert-butyl 4-[4-[2-(dimethylamino)-2-oxo-ethyl]phenyl]-1,4-diazepane-1-carboxylate (3.4a)

To a 100 mL round-bottom flask was added a solution of 2-(4-bromophenyl)-N,N-dimethyl-acetamide (4.13 mmol, 1 g), and tert-butyl 1,4-diazepane-1-carboxylate (5 mmol, 1 g) in t-BuOH (5 mL) and dioxane (10 mL). Then, 2-Dicyclohexylphosphino-2'-(N,N-dimethylamino)biphenyl (0.62 mmol, 244 mg), t-BuONa (5.78 mmol, 556 mg), and tris(dibenzylideneacetone)dipalladium (0.21 mmol, 189 mg) were added. The reaction was protected with nitrogen and heated to reflux for 2h. Upon completion, the mixture was cooled to room temperature and water was added, the mixture was extracted with ethyl acetate for three times, and the organic layers were collected and washed with brine and dried by Na₂SO₄. Condensed and purified by flash column chromatography using a gradient of 0-5% MeOH/DCM to give tert-butyl 4-[4-[2-(dimethylamino)-2-oxo-ethyl]phenyl]-1,4-diazepane-1-carboxylate as a light-yellow solid (1.42 g, 95% yield). ESI-MS m/z: 362 ([M+H]⁺).

tert-butyl 4-[4-(dimethylcarbamoyl)phenyl]-1,4-diazepane-1-carboxylate (3.4b)

To a 100 mL round-bottom flask was added a solution of 4-bromo-N,N-dimethyl-benzamide (2.19 mmol, 500 mg), and tert-butyl 1,4-diazepane-1-carboxylate (2.63 mmol, 527 mg) in t-BuOH (5 mL) and dioxane (10 mL). Then, 2-dicyclohexylphosphino-2'-(N,N-dimethylamino)biphenyl (0.33 mmol, 129 mg), t-BuONa (3.1 mmol, 295 mg), and tris(dibenzylideneacetone)dipalladium (0.11 mmol, 100 mg) were added. The reaction was protected with nitrogen and heated to reflux for 2h. Upon completion, the mixture was cooled to room temperature and water was added, the mixture was extracted with ethyl acetate for three times, and the organic layers were collected and washed with brine and dried by Na₂SO₄.

Condensed and purified by flash column chromatography using a gradient of 0-5% MeOH/DCM to give tert-butyl 4-[4-(dimethylcarbamoyl)phenyl]-1,4-diazepane-1-carboxylate as a light-yellow solid (320 mg, 42% yield). ESI-MS m/z: 348 ($[M+H]^+$).

2-[4-(1,4-diazepan-1-yl)phenyl]-N,N-dimethyl-acetamide (3.5a)

To a 100 mL round-bottom flask was added a solution of tert-butyl 4-[4-(dimethylamino)-2-oxo-ethyl]phenyl]-1,4-diazepane-1-carboxylate (1.11 mmol, 400 mg) in DCM (5 mL) and TFA (1 mL) was added and the mixture was stirred at room temperature for 2h. Upon completion, the mixture was condensed to give 2-[4-(1,4-diazepan-1-yl)phenyl]-N,N-dimethyl-acetamide as a light-brown oil (163 mg, 56% yield). ESI-MS m/z: 262 ($[M+H]^+$).

4-(1,4-diazepan-1-yl)-N,N-dimethyl-benzamide (3.5b)

To a 100 mL round-bottom flask was added a solution of tert-butyl 4-[4-(dimethylcarbamoyl)phenyl]-1,4-diazepane-1-carboxylate (0.92 mmol, 320 mg) in DCM (5 mL) and TFA (1 mL) was added and the mixture was stirred at room temperature for 2h. Upon completion, the mixture was condensed to give 4-(1,4-diazepan-1-yl)-N,N-dimethyl-benzamide as a light-brown oil (137 mg, 60% yield). ESI-MS m/z: 248 ($[M+H]^+$).

2-[4-[4-(6-cyano-4-quinolyl)-1,4-diazepan-1-yl]phenyl]-N,N-dimethyl-acetamide (3.6a)

To a 10 mL round-bottom flask was added a solution of 2-[4-(1,4-diazepan-1-yl)phenyl]-N,N-dimethyl-acetamide (0.23 mmol, 60 mg) and 4-chloro-6-(trifluoromethyl)quinoline (0.23 mmol, 43 mg) in DMSO (3 mL), and TEA (1.2

mmol, 116 mg) was added. Reaction was stirred for 4h at 110°C. Upon completion, the mixture was cooled to room temperature and water was added, the mixture was extracted with DCM for three times, and the organic layers were collected and washed with brine and dried by Na₂SO₄. Condensed and purified by flash column chromatography using a gradient of 0-5% MeOH/DCM to give 2-[4-[4-(6-cyano-4-quinolyl)-1,4-diazepan-1-yl]phenyl]-N,N-dimethyl-acetamide as a white solid (46 mg, 49% yield). ESI-MS m/z: 414 ([M+H]⁺). ¹H-NMR (300MHz, CDCl₃): δ 8.73 (d, J=5.2 Hz, 1H), 8.40 (d, J=1.4 Hz, 1H), 8.08 (d, J=8.7 Hz, 1H), 7.77 (dd, J=8.7, 1.4 Hz, 1H), 7.14 (d, J=8.6 Hz, 2H), 6.92 (d, J=5.2 Hz, 1H), 6.74 (d, J=8.6 Hz, 2H), 3.82 (t, J=5.2 Hz, 2H), 3.70 (t, J=6.5 Hz, 2H), 3.62 (s, 2H), 3.60 (t, J=4.8 Hz, 2H), 3.44 (t, J=5.6 Hz, 2H), 3.01 (s, 3H), 2.96 (s, 3H), 2.29 (m, 2H).

4-[4-(6-cyano-4-quinolyl)-1,4-diazepan-1-yl]-N,N-dimethyl-benzamide (3.6b)

To a 10 mL round-bottom flask was added a solution of 4-(1,4-diazepan-1-yl)-N,N-dimethyl-benzamide (0.24 mmol, 60 mg) and 4-chloroquinoline-6-carbonitrile (0.29 mmol, 55 mg) in DMSO (3 mL), and TEA (1.2 mmol, 120 mg) was added. Reaction was stirred for 4h at 110°C. Upon completion, the mixture was cooled to room temperature and water was added, the mixture was extracted with DCM for three times, and the organic layers were collected and washed with brine and dried by Na₂SO₄. Condensed and purified by flash column chromatography using a gradient of 0-5% MeOH/DCM to give 4-[4-(6-cyano-4-quinolyl)-1,4-diazepan-1-yl]-N,N-dimethyl-benzamide as a white solid (42 mg, 43% yield). ESI-MS m/z: 400 ([M+H]⁺). ¹H-NMR (300MHz, CDCl₃): δ 8.74 (d, J=5.3 Hz, 1H), 8.41 (d, J=1.6 Hz, 1H), 8.11 (d, J=8.7 Hz, 1H), 7.79 (dd, J=8.7, 1.6 Hz,

1H), 7.40 (d, J=8.7 Hz, 2H), 6.94 (d, J=5.3 Hz, 1H), 6.75 (d, J=8.7 Hz, 2H), 3.87 (t, J=4.8 Hz, 2H), 3.77 (t, J=6.1 Hz, 2H), 3.62 (t, J=5.0 Hz, 2H), 3.44 (t, J=5.0 Hz, 2H), 3.07 (s, 6H), 2.31 (m, 2H).

2-chloro-4-(2-phenylethylamino)pyridine-3-carbonitrile (3.8a)

To a 10 mL round-bottom flask was added a solution of 2,4-dichloropyridine-3-carbonitrile (4.13 mmol, 714 mg) in acetonitrile (10 mL), then cooled to 0°C, then a solution of 2-phenylethanamine (4.13 mmol, 500 mg) was added. The reaction was stirred at 0°C for 4h, then allowed to room temperature for another 4h. Upon completion, the mixture was condensed and purified by flash chromatography by using a gradient of 0-5% MeOH/DCM to give 2-chloro-4-(2-phenylethylamino)pyridine-3-carbonitrile (91 mg, yield 86%). ESI-MS m/z: 259 ([M + H]⁺). ¹H-NMR (300MHz, CDCl₃): 8.05 (d, J=6.1 Hz, 1H), 7.37-7.20 (m, 5H), 6.46 (d, J=6.1 Hz, 1H), 5.33 (s, 1H), 3.53 (q, J=6.9 Hz, 2H), 2.96 (t, J=7.2 Hz, 2H).

2-chloro-4-[2-[6-(4-methylpiperazine-1-carbonyl)-2-naphthyl]ethylamino]pyridine-3-carbonitrile (3.8b)

To a 10 mL round-bottom flask was added a solution of [6-(2-aminoethyl)-2-naphthyl]-(4-methylpiperazin-1-yl)methanone (0.67 mmol, 200 mg), 2,4-dichloropyridine-3-carbonitrile (0.67 mmol, 116 mg), and TEA (0.67 mmol, 68 mg) in CH₃CN (5 mL), then stirred at 60°C for overnight. Then the mixture was cooled to room temperature, condensed and purified by flash chromatography by using a gradient of 0-5% MeOH/DCM to give 2-chloro-4-[2-[6-(4-methylpiperazine-1-carbonyl)-2-naphthyl]ethylamino]pyridine-3-carbonitrile (197 mg, yield 68%). ESI-MS m/z: 435 ([M + H]⁺). ¹H-NMR (300MHz, CDCl₃): 8.06 (d, J=5.9 Hz, 1H), 7.88

(s, 1H), 7.84 (t, J=7.8 Hz, 2H), 7.67 (s, 1H), 7.50 (dd, J=8.5, 1.5 Hz, 1H), 7.37 (dd, J=8.5, 1.5 Hz, 1H), 6.5 (d, J=6.3 Hz, 1H), 3.84 (m, 2H), 3.61 (q, J=6.5 Hz, 2H), 3.52 (m, 2H), 3.12 (t, J=6.3 Hz, 2H), 2.50 (m, 2H), 2.41 (m, 2H), 2.34 (s, 3H).

methyl 3-amino-4-(2-phenylethylamino)thieno[2,3-b]pyridine-2-carboxylate (3.9a)

To a 10 mL round-bottom flask was added a solution of 2-chloro-4-(2-phenylethylamino)pyridine-3-carbonitrile (0.78 mmol, 200 mg), Na₂CO₃ (1.55 mmol, 165mg), and methyl 2-sulfanylacacetate (1.55 mmol, 165 mg) in DMF (3 mL), then stirred at 60°C for 1.5h. Then the mixture was cooled to room temperature and crushed NaOH (1.55 mmol, 62 mg) was added and stirred at room temperature for 6h, then water was added, the precipitation was collected and washed with water, then dried and purified by flash chromatography by using a gradient of 0-5% MeOH/DCM to give methyl 3-amino-4-(2-phenylethylamino)thieno[2,3-b]pyridine-2-carboxylate (146 mg, yield 58%). ESI-MS m/z: 328 ([M+H]⁺). ¹H-NMR (300MHz, CDCl₃): 8.24 (d, J=5.7 Hz, 1H), 7.38-7.24 (m, 5H), 6.38 (d, J=5.7 Hz, 1H), 5.58 (s, 1H), 5.36 (s, 2H), 3.86 (s, 3H), 3.51 (q, J=6.7 Hz, 2H), 3.02 (t, J=6.7 Hz, 2H).

methyl 3-amino-4-[2-[6-(4-methylpiperazine-1-carbonyl)-2-naphthyl]ethylamino]thieno[2,3-b]pyridine-2-carboxylate (3.9b)

A mixture of 2-chloro-4-[2-[6-(4-methylpiperazine-1-carbonyl)-2-naphthyl]ethylamino]pyridine-3-carbonitrile (0.45 mmol, 197 mg), methyl 2-sulfanylacacetate (0.91 mmol, 97 mg), sodium carbonate (0.91 mmol, 96 mg) in DMF (4 mL) was stirred at 60°C for 1.5 h. Then, the reaction mixture was cooled to room temperature and crushed NaOH (0.91 mmol, 37 mg) was added. The mixture was

stirred at room temperature for additional 6h and poured into water (10 ml). The filtrate was collected and washed with water, dried under vacuum to give methyl 3-amino-4-[2-[6-(4-methylpiperazine-1-carbonyl)-2-naphthyl]ethylamino]thieno[2,3-b]pyridine-2-carboxylate (126 mg, yield 55%). ESI-MS m/z : 504 ($[M + H]^+$). 1H -NMR (300MHz, DMSO- d_6): 8.83 (s, 1H), 8.67 (t, $J=5.5$ Hz, 1H), 8.54 (s, 1H), 8.18 (dd, $J=8.6, 1.8$ Hz, 1H), 8.00 (s, 1H), 7.93 (d, $J=8.6$ Hz, 1H), 7.92 (s, 2H), 7.83 (s, 1H), 7.70 (d, $J=8.8$ Hz, 1H), 7.55 (s, 1H), 7.52 (dd, $J=8.4, 1.5$ Hz, 1H), 7.45 (dd, $J=8.4, 1.5$ Hz, 1H), 3.89 (q, $J=5.9$ Hz, 2H), 3.64 (s, 2H), 3.17 (t, $J=6.2$ Hz, 2H), 3.15 (s, 2H), 2.33 (s, 4H), 2.20 (s, 3H).

3-amino-4-(2-phenylethylamino)thieno[2,3-b]pyridine-2-carboxylic acid (3.10a)

To a 10 mL round-bottom flask was added a solution of methyl 3-amino-4-(2-phenylethylamino)thieno[2,3-b]pyridine-2-carboxylate (0.61 mmol, 200 mg) in methanol (2 mL) and water (2 mL), then LiOH- H_2O (1.83 mmol, 77 mg) was added and the mixture was stirred at 70°C. Upon completion, the mixture condensed, water was added, and the mixture was acidified with acetic acid and stirred for 5 min, the precipitate was collected, washed with water, dry under vacuum as a white solid (152 mg, yield 79%). ESI-MS m/z : 314 ($[M + H]^+$). 1H -NMR (300MHz, CD_3OD): 8.05 (d, $J=6.1$ Hz, 1H), 7.33-7.22 (m, 5H), 6.47 (d, $J=6.1$ Hz, 1H), 3.57 (t, $J=6.9$ Hz, 2H), 3.00 (t, $J=6.9$ Hz, 2H).

3-amino-4-((2-(6-(4-methylpiperazine-1-carbonyl)naphthalen-2-yl)ethyl)amino)thieno[2,3-b]pyridine-2-carboxylic acid (3.10b)

To a 10 mL round-bottom flask was added a solution of methyl 3-amino-4-[2-[6-(4-methylpiperazine-1-carbonyl)-2-naphthyl]ethylamino]thieno[2,3-

b]pyridine-2-carboxylate (0.61 mmol, 307 mg) in methanol (2 mL) and water (2 mL), then LiOH-H₂O (1.83 mmol, 77 mg) was added and the mixture was stirred at 70°C. Upon completion, the mixture condensed, water was added, and the mixture was acidified with acetic acid and stirred for 5 min, the precipitate was collected, washed with water, dry under vacuum as a white solid (152 mg, yield 70%). ESI-MS m/z: 490 ([M+H]⁺).

3-amino-4-(2-phenylethylamino)thieno[2,3-b]pyridine-2-carboxamide (3.11a)

To a 10 mL round-bottom flask was added a solution of 3-amino-4-(2-phenylethylamino)thieno[2,3-b]pyridine-2-carboxylic acid (0.16 mmol, 50 mg) DMF (3 mL). Then HATU (0.24 mmol, 91 mg) and TEA (0.4 mmol, 40 mg) were added and the mixture was stirred at room temperature for 15 min, then NH₄OH (0.48 mmol, 17 mg) was added, and the mixture was stirred at room temperature for 2h. Upon completion, water was added and extracted with DCM, the organic layers were combined and washed with sat NaCl aq and dried by Na₂SO₄, condensed and purified by flash chromatography by using a gradient of 0-5% MeOH/DCM to give 3-amino-4-(2-phenylethylamino)thieno[2,3-b]pyridine-2-carboxamide (35 mg, yield 70%). ESI-MS m/z: 328 ([M+H]⁺). ¹H-NMR (300MHz, CDCl₃): 8.23 (d, J=5.7 Hz, 1H), 7.38-7.24 (m, 5H), 6.40 (d, J=5.7 Hz, 1H), 5.75 (s, 1H), 5.54 (s, 2H), 5.39 (s, 2H), 3.52 (q, J=6.6 Hz, 2H), 3.02 (t, J=6.6 Hz, 2H).

3-amino-4-[2-[6-(4-methylpiperazine-1-carbonyl)-2-naphthyl]ethylamino]thieno[2,3-b]pyridine-2-carboxamide (3.11b)

To a 10 mL round-bottom flask was added a solution of methyl 3-amino-4-[2-[6-(4-methylpiperazine-1-carbonyl)-2-naphthyl]ethylamino]thieno[2,3-

b]pyridine-2-carboxylate (0.007 mmol, 36 mg) in MeOH (1 ml), THF (1 mL), and water (1 mL). Then LiOH-H₂O (0.36 mmol, 15 mg) was added, and the mixture was stirred at 60°C for overnight. Upon completion, the mixture was cooled to room temperature, condensed and dissolved in DMF again, HATU (0.11 mmol, 41 mg), and TEA (0.22 mmol, 28 mg) were added and stirred at room temperature for 15 min, then NH₄OH (0.21 mmol, 7.5 mg) was added and the mixture was stirred at room temperature for 3h. Upon completion, the mixture was added with water and extracted with DCM, the organic layers were combined, dried by Na₂SO₄, condensed and purified by flash column chromatography using a gradient of 0-8% MeOH/DCM to give 3-amino-4-[2-[6-(4-methylpiperazine-1-carbonyl)-2-naphthyl]ethylamino]thieno[2,3-b]pyridine-2-carboxamide (5 mg, yield 14%). ESI-MS m/z: 489 ([M+H]⁺). ¹H-NMR (300MHz, CDCl₃): 8.24 (d, J=5.7 Hz, 1H), 7.89-7.81 (m, 3H), 7.71 (s, 1H), 7.51 (dd, J=8.3, 1.3 Hz, 1H), 7.42 (dd, J=8.3, 1.3 Hz, 1H), 6.43 (d, J=5.7 Hz, 1H), 5.82 (t, J=5.7 Hz, 1H), 5.55 (s, 2H), 5.40 (s, 2H), 3.85 (s, 2H), 3.60 (q, J=6.4 Hz, 2H), 3.51 (s, 2H), 3.19 (t, J=6.4 Hz, 2H), 2.50 (s, 2H), 2.40 (s, 2H), 2.34 (s, 3H).

benzyl 4-[(4-methoxycarbonylphenyl)methyl]-1,4-diazepane-1-carboxylate (3.13)

To a 100 mL round-bottom flask was added a solution of methyl 4-(bromomethyl)benzoate (6.6 mmol, 1.5 g) and benzyl 1,4-diazepane-1-carboxylate (6.6 mmol, 1.53g) in THF (10 mL), then then DIEA (13.1 mmol, 1.69 g) was added and the mixture was reflux for 3h. After that, the mixture was cooled to room temperature, and added with water, extracted with DCM, the organic layers were combined, washed with brine, dried by Na₂SO₄, condensed to give benzyl 4-[(4-

methoxycarbonylphenyl)methyl]-1,4-diazepane-1-carboxylate (2.4 g, 96%). ESI-MS m/z : 383 ($[M+H]^+$).

4-[(4-benzyloxycarbonyl-1,4-diazepan-1-yl)methyl]benzoic acid (3.14)

To a 100 mL round-bottom flask was added a solution of benzyl 4-[(4-methoxycarbonylphenyl)methyl]-1,4-diazepane-1-carboxylate (7.53 mmol, 2.88 g) in EtOH (10 mL) and water (10 mL). Then NaOH (15.1 mmol, 602 mg) was added and the mixture was refluxed for 4h. Upon completion, the mixture was cooled to room temperature, condensed, diluted with water, acidified by 2N HCl to pH=4, extracted with DCM, the organic layers were combined, dried by Na₂SO₄, condensed to give 4-[(4-benzyloxycarbonyl-1,4-diazepan-1-yl)methyl]benzoic acid (2.77 g, yield 99%). ESI-MS m/z : 369 ($[M+H]^+$).

benzyl 4-[[4-(dimethylcarbamoyl)phenyl]methyl]-1,4-diazepane-1-carboxylate (3.15)

To a 100 mL round-bottom flask was added a solution of 4-[(4-benzyloxycarbonyl-1,4-diazepan-1-yl)methyl]benzoic acid (1.63 mmol, 600 mg) in DCM (10 mL), then DIEA (4.9 mmol, 631 mg) and HATU (2.44 mmol, 928 mg) were added and the mixture was stirred at room temperature for 15 min, then dimethylamine (4.9 mmol, 220 mg) was added and the mixture was stirred for 2h. Upon completion, the mixture was added with water, extracted with DCM, the organic layers were combined, washed with brine, dried by Na₂SO₄, condensed and purified by flash column chromatography using a gradient of 0-5% MeOH/DCM to give benzyl 4-[[4-(dimethylcarbamoyl)phenyl]methyl]-1,4-diazepane-1-carboxylate (505 mg, 78%). ESI-MS m/z : 396 ($[M+H]^+$).

4-(1,4-diazepan-1-ylmethyl)-N,N-dimethyl-benzamide (3.16)

To a 25 mL round-bottom flask was added a solution of benzyl 4-[[4-(dimethylcarbamoyl)phenyl]methyl]-1,4-diazepane-1-carboxylate (1.8 mmol, 711 mg) in EtOH (4 mL) and ethyl acetate (4 mL). Then Pd/C (0.63 mmol, 67 mg) was added, the mixture was saturated with H₂, and stirred at room temperature for overnight. After that, the mixture was diluted with hexane, filtered, and the residue was washed with hexane, the filtration was condensed to give 4-(1,4-diazepan-1-ylmethyl)-N,N-dimethyl-benzamide (430 mg, 92%) and used without further purification. ESI-MS m/z: 262 ([M+H]⁺).

4-[[4-(2-chloro-3-cyano-4-pyridyl)-1,4-diazepan-1-yl]methyl]-N,N-dimethyl-benzamide (3.17)

To a 100 mL round-bottom flask was added a solution of 4-(1,4-diazepan-1-ylmethyl)-N,N-dimethyl-benzamide (1.91 mmol, 500 mg) in acetonitrile (10 mL), then 2,4-dichloropyridine-3-carbonitrile (1.91 mmol, 331 mg) and DIPEA (3.82 mmol, 494 mg) were added. The mixture was stirred at 80°C for overnight. Upon completion, the mixture was cooled to room temperature, condensed, diluted with water, extracted with DCM, the organic layers were combined, dried by Na₂SO₄, condensed, and purified by flash column chromatography using a gradient of 0-7% MeOH/DCM to give 4-[[4-(2-chloro-3-cyano-4-pyridyl)-1,4-diazepan-1-yl]methyl]-N,N-dimethyl-benzamide (387 mg, 51%). ESI-MS m/z: 440 ([M+H]⁺).

methyl 3-amino-4-[4-[[4-(dimethylcarbamoyl)phenyl]methyl]-1,4-diazepan-1-yl]thieno[2,3-b]pyridine-2-carboxylate (3.18)

To a 50 mL round-bottom flask was added a solution of 4-[[4-(2-chloro-3-cyano-4-pyridyl)-1,4-diazepan-1-yl]methyl]-N,N-dimethyl-benzamide (0.93 mmol, 371 mg) in MeOH (5 mL), then methyl 2-sulfanylacacetate (2.8 mmol, 297 mg) and MeONa (1.86 mmol, 101 mg) were added. The mixture was stirred at 100°C for overnight. Upon completion, the mixture was condensed and purified by flash column chromatography using a gradient of 0-7% MeOH/DCM to give methyl 3-amino-4-[4-[[4-(dimethylcarbamoyl)phenyl]methyl]-1,4-diazepan-1-yl]thieno[2,3-b]pyridine-2-carboxylate (391 mg, 90%). ESI-MS m/z : 468 ($[M+H]^+$). 1H -NMR (300MHz, DMSO- d_6): 8.40 (d, $J=5.5$ Hz, 1H), 7.38 (m, 4H), 7.12 (m, 2H), 7.08 (d, $J=5.5$ Hz, 1H), 3.77 (s, 3H), 3.70 (s, 2H), 3.67 (m, 2H), 2.96 (m, 4H), 2.76 (m, 2H), 2.08 (s, 6H), 1.87 (m, 2H).

3-amino-4-[4-[[4-(dimethylcarbamoyl)phenyl]methyl]-1,4-diazepan-1-yl]thieno[2,3-b]pyridine-2-carboxamide (3.19)

To a 25 mL round-bottom flask was added a solution of methyl 3-amino-4-[4-[[4-(dimethylcarbamoyl)phenyl]methyl]-1,4-diazepan-1-yl]thieno[2,3-b]pyridine-2-carboxylate (0.53 mmol, 246 mg) in THF (3 mL) and water (3 mL), then LiOH- H_2O (1.58 mmol, 66 mg) was added. The mixture was stirred at 50°C for overnight. Upon completion, the mixture was condensed and dissolved in DMF (5 mL). Then HATU (0.79 mmol, 300 mg), DIPEA (1.1 mmol, 136 mg) were added and stirred for 15 min. After that, NH_4OH (2.1 mmol, 74 mg) was added and the mixture was stirred for 2h. Upon completion, the mixture was diluted with water, extracted with DCM, the organic layers were combined, dried by Na_2SO_4 , condensed and purified by flash column chromatography using a gradient of 0-7% MeOH/DCM to give 3-

amino-4-[4-[[4-(dimethylcarbamoyl)phenyl]methyl]-1,4-diazepan-1-yl]thieno[2,3-b]pyridine-2-carboxamide (200 mg, 84%). ESI-MS m/z : 483 ($[M+H]^+$). $^1\text{H-NMR}$ (300MHz, CDCl_3): 8.44 (d, $J=5.4$ Hz, 1H), 7.39 (s, 4H), 7.29 (s, 2H), 6.92 (d, $J=5.4$ Hz, 1H), 5.35 (s, 2H), 3.71 (s, 2H), 3.39 (s, 2H), 3.31 (s, 2H), 3.11 (s, 3H), 3.00 (s, 3H), 2.84 (t, $J=6.0$ Hz, 2H), 2.76 (s, $J=6.0$ Hz, 2H), 1.92 (m, 2H).

benzyl 4-(4-formylphenyl)-1,4-diazepane-1-carboxylate (3.21)

To a 100 mL round-bottom flask was added a solution of 4-fluorobenzaldehyde (8.1 mmol, 1 g) and benzyl 1,4-diazepane-1-carboxylate (8.9 mmol, 2.1 g) in DMF (20 mL). Then K_2CO_3 (24.2 mmol, 3.34 g) was added, and stirred at 90°C for overnight. Upon completion, the mixture was cooled to room temperature, water was added, extracted with DCM, the organic layers were combined, dried by Na_2SO_4 , condensed, and purified by flash column using a gradient of 0-7% MeOH/DCM to give benzyl 4-(4-formylphenyl)-1,4-diazepane-1-carboxylate (860 mg, 32%). ESI-MS m/z : 339 ($[M+H]^+$). $^1\text{H-NMR}$ (300MHz, CDCl_3): 9.73 (s, 1H), 7.72 (m, 2H), 7.31 (m, 5H), 6.72 (m, 2H), 5.09 (d, $J=17$ Hz, 2H), 3.65 (m, 6H), 3.37 (m, 2H), 1.99 (m, 2H).

The general preparation of **3.22**

To a 100 mL round-bottom flask was added a solution of benzyl 4-(4-formylphenyl)-1,4-diazepane-1-carboxylate (1eq) and 1-substituted-piperazine (2eq) in DCM. Then pH of the above solution was adjusted to 4-5 using acetic acid, then NaBH_3CN (1.5eq) was added, and the reaction was stirred at room temperature for overnight. Upon completion, sat NaHCO_3 aq was added and the mixture was extracted with DCM, the organic layers were combined, dried by

Na₂SO₄, condensed, and purified by flash column using a gradient of 0-7% MeOH/DCM to give **3.22**.

benzyl 4-[4-[(4-methylpiperazin-1-yl)methyl]phenyl]-1,4-diazepane-1-carboxylate
(3.22a)

700 mg, 65%. ESI-MS m/z: 423 ([M+H]⁺). ¹H-NMR (300MHz, CDCl₃): 7.33 (s, 5H), 7.14 (d, J=8.6 Hz, 2H), 6.63 (d, J=8.6 Hz, 2H), 5.10 (d, J=15.7 Hz, 2H), 3.64 (m, 2H), 3.54 (m, 4H), 3.40 (s, 2H), 3.34 (m, 2H), 2.44 (m, 8H), 2.27 (s, 3H), 1.99 (m, 2H).

benzyl 4-[4-[(4-ethylpiperazin-1-yl)methyl]phenyl]-1,4-diazepane-1-carboxylate
(3.22b)

942 mg, 88% yield. ESI-MS m/z: 437 ([M+H]⁺). ¹H-NMR (300MHz, CDCl₃): 7.34 (s, 5H), 8.14 (d, J=7.1 Hz, 2H), 6.63 (d, J=7.1 Hz, 2H), 5.11 (d, J=15 Hz, 2H), 3.64 (m, 2H), 3.55 (m, 4H), 3.43 (s, 2H), 3.37 (t, J=6.0 Hz, 1H), 3.30 (t, J=6.0 Hz, 1H), 2.50 (m, 8H), 2.44 (q, J=7.0 Hz, 2H), 1.98 (m, 2H), 1.09 (t, J=7.0 Hz, 2H).

benzyl 4-[4-[(4-cyclopropylpiperazin-1-yl)methyl]phenyl]-1,4-diazepane-1-carboxylate **(3.22c)**

702 mg, 64% yield. ESI-MS m/z: 415 ([M+H]⁺). ¹H-NMR (300MHz, CD₂Cl₂): 7.11 (d, J=8.3 Hz, 2H), 6.65 (d, J=8.3 Hz, 2H), 3.55 (m, 6H), 3.40 (s, 2H), 3.24 (m, 2H), 2.61 (m, 4H), 2.43 (m, 4H), 1.93 (m, 2H), 1.60 (m, 1H), 1.39 (s, 6H), 1.33 (s, 3H), 0.41 (m, 2H), 0.32 (m, 2H).

The general preparation of **3.23**.

To a 100 mL round-bottom flask was added a solution of **3.22** (1eq) in conc. HCl. The mixture was stirred at room temperature for 2h, condensed to give **3.23** and used without further purification.

1-[4-[(4-methylpiperazin-1-yl)methyl]phenyl]-1,4-diazepane (3.23a)

350 mg, 92% yield. ESI-MS m/z: 289 ($[M+H]^+$).

1-[4-[(4-ethylpiperazin-1-yl)methyl]phenyl]-1,4-diazepane (3.23b)

600 mg, 92% yield. ESI-MS m/z: 303 ($[M+H]^+$).

1-[4-[(4-cyclopropylpiperazin-1-yl)methyl]phenyl]-1,4-diazepane (3.23c)

522 mg, 98% yield. ESI-MS m/z: 315 ($[M+H]^+$).

The general preparation of **3.24**.

To a 100 mL round-bottom flask was added a solution of **3.23** (1eq) in acetonitrile. Then 2,4-dichloropyridine-3-carbonitrile (1eq) and DIPEA (3eq) were added, and the mixture was stirred at 80°C for overnight. Upon completion, water was added and the mixture was extracted with DCM, the organic layers were combined, dried by Na₂SO₄, condensed, and purified by flash column using a gradient of 0-7% MeOH/DCM to give **3.24**.

3-chloro-4-[4-[4-[(4-methylpiperazin-1-yl)methyl]phenyl]-1,4-diazepan-1-yl]pyridine-2-carbonitrile (3.24a)

228 mg, 28% yield. ESI-MS m/z: 425 ($[M+H]^+$). ¹H-NMR (300MHz, CDCl₃): 7.98 (d, J=6.7 Hz, 1H), 7.17 (d, J=8.6 Hz, 2H), 6.67 (d, J=8.6 Hz, 2H), 6.57 (d, J=6.7 Hz, 1H), 4.00 (t, J=4.7 Hz, 2H), 3.78 (t, J=4.7 Hz, 2H), 3.72 (t, J=6.0 Hz, 2H), 3.56 (t, J=6.0 Hz, 2H), 3.47 (s, 2H), 2.60 (s, 8H), 2.38 (s, 3H), 2.13 (m, 2H).

2-chloro-4-[4-[4-[(4-ethylpiperazin-1-yl)methyl]phenyl]-1,4-diazepan-1-yl]pyridine-3-carbonitrile (3.24b)

328 mg, 41% yield. ESI-MS m/z : 440 ($[M + H]^+$). 1H -NMR (300MHz, CD_2Cl_2): 7.95 (d, $J=6.7$ Hz, 1H), 7.16 (d, $J=8.7$ Hz, 2H), 6.69 (d, $J=8.7$ Hz, 2H), 6.60 (d, $J=6.7$ Hz, 1H), 3.99 (m, 2H), 3.77 (m, 2H), 3.71 (m, 2H), 3.56 (m, 2H), 3.47 (s, 2H), 2.69 (m, 8H), 2.65 (q, $J=7.1$ Hz, 2H), 2.11 (m, 2H), 1.19 (t, $J=7.1$ Hz, 3H).

2-chloro-4-[4-[4-[(4-cyclopropylpiperazin-1-yl)methyl]phenyl]-1,4-diazepan-1-yl]pyridine-3-carbonitrile (3.24c)

610 mg, 82% yield. ESI-MS m/z : 452 ($[M + H]^+$).

The general preparation of **3.25**.

To a 100 mL round-bottom flask was added a solution of **3.24** (1eq) and methyl 2-sulfanylacacetate (3eq) in MeOH. Then MeONa (3eq) was added and the mixture was stirred at 90 °C for overnight. Upon completion, condensed, and purified by flash column using a gradient of 0-7% MeOH/DCM to give **3.25**.

methyl 3-amino-4-[4-[4-[(4-methylpiperazin-1-yl)methyl]phenyl]-1,4-diazepan-1-yl]thieno[2,3-b]pyridine-2-carboxylate (3.25a)

209 mg, 79%. ESI-MS m/z : 495 ($[M + H]^+$). 1H -NMR (300MHz, $CDCl_3$): 8.47 (d, $J=5.3$ Hz, 1H), 7.19 (d, $J=8.7$ Hz, 2H), 6.91 (d, $J=5.3$ Hz, 1H), 6.78 (s, 2H), 6.70 (d, $J=8.7$ Hz, 2H), 3.86 (s, 3H), 3.75 (m, 2H), 3.61 (m, 2H), 3.51 (s, 2H), 3.36 (m, 2H), 3.29 (m, 2H), 2.64 (s, 8H), 2.40 (s, 3H), 2.19 (m, 2H).

methyl 3-amino-4-[4-[4-[(4-ethylpiperazin-1-yl)methyl]phenyl]-1,4-diazepan-1-yl]thieno[2,3-b]pyridine-2-carboxylate (3.25b)

169 mg, 45% yield. ESI-MS m/z : 509 ($[M + H]^+$). 1H -NMR (300MHz, CD_2Cl_2): 8.45 (d, $J=5.7$ Hz, 1H), 7.16 (d, $J=8.6$ Hz, 2H), 6.95 (d, $J=5.7$ Hz, 1H), 6.79 (s, 2H), 6.71 (d, $J=8.6$ Hz, 2H), 6.60 (d, $J=6.7$ Hz, 1H), 3.83 (s, 3H), 3.76 (t, $J=4.7$ Hz, 2H), 3.60 (t, $J=6.4$ Hz, 2H), 3.38 (s, 2H), 3.35 (m, 2H), 3.27 (m, 2H), 2.43 (m, 8H), 2.37 (q, $J=7.1$ Hz, 2H), 2.17 (m, 2H), 1.04 (t, $J=7.1$ Hz, 3H).

methyl 3-amino-4-[4-[4-[(4-cyclopropylpiperazin-1-yl)methyl]phenyl]-1,4-diazepan-1-yl]thieno[2,3-*b*]pyridine-2-carboxylate (**3.25c**)

314 mg, 45% yield. ESI-MS m/z : 521 ($[M + H]^+$). 1H -NMR (300MHz, CD_2Cl_2): 8.45 (d, $J=5.5$ Hz, 1H), 7.16 (d, $J=7.9$ Hz, 2H), 6.95 (d, $J=5.5$ Hz, 1H), 6.80 (s, 2H), 6.71 (d, $J=7.9$ Hz, 2H), 3.83 (s, 3H), 3.76 (t, $J=4.4$ Hz, 2H), 3.60 (t, $J=4.4$ Hz, 2H), 3.38 (s, 2H), 3.35 (m, 2H), 3.27 (m, 2H), 2.60 (m, 4H), 2.39 (m, 4H), 2.17 (t, $J=6.5$ Hz, 2H), 1.59 (m, 1H), 0.40 (m, 2H), 0.32 (m, 2H).

The general preparation of **3.26**.

To a 100 mL round-bottom flask was added a solution of **3.25** (1eq) and LiOH-H₂O (2eq) in THF and water. Then the mixture was stirred at 60 °C for overnight. After that, the mixture was condensed and dissolved in DMF, then HATU (1.5eq) and DIEA (3eq) were added and stirred for 15 min. Then NH₄OH (3eq) was added and stirred at room temperature for 2h. Upon completion, water was added, extracted with DCM, the organic layers were combined, dried by Na₂SO₄, condensed, and purified by flash column using a gradient of 0-7% MeOH/DCM to give **3.26**.

3-amino-4-[4-[4-[(4-methylpiperazin-1-yl)methyl]phenyl]-1,4-diazepan-1-yl]thieno[2,3-*b*]pyridine-2-carboxamide (**3.26a**)

60 mg, 30% yield. ESI-MS m/z : 480 ($[M+H]^+$). 1H -NMR (300MHz, DMSO- d_6): 8.39 (d, $J=5.2$ Hz, 1H), 7.08 (d, $J=9.6$ Hz, 3H), 7.07 (s, 2H), 6.97 (s, 2H), 6.71 (d, $J=8.4$ Hz, 2H), 3.75 (m, 2H), 3.52 (t, $J=6.1$ Hz, 2H), 3.32 (s, 2H), 3.29 (m, 2H), 2.33 (m, 8H), 2.16 (s, 3H), 2.13 (m, 2H).

*3-amino-4-[4-[4-[(4-ethylpiperazin-1-yl)methyl]phenyl]-1,4-diazepan-1-yl]thieno[2,3-*b*]pyridine-2-carboxamide (3.26b)*

81 mg, 49% yield. ESI-MS m/z : 494 ($[M+H]^+$). 1H -NMR (300MHz, DMSO- d_6): 8.39 (d, $J=5.4$ Hz, 1H), 7.10 (s, 2H), 7.08 (d, $J=8.5$ Hz, 2H), 7.06 (d, $J=5.4$ Hz, 1H), 6.97 (s, 2H), 6.71 (d, $J=8.5$ Hz, 2H), 3.76 (t, $J=4.8$ Hz, 2H), 3.52 (t, $J=6.0$ Hz, 2H), 3.31 (s, 2H), 3.29 (m, 2H), 3.19 (m, 2H), 2.35 (m, 10H), 2.13 (m, 2H), 0.98 (t, $J=7.0$ Hz, 3H).

*3-amino-4-[4-[4-[(4-cyclopropylpiperazin-1-yl)methyl]phenyl]-1,4-diazepan-1-yl]thieno[2,3-*b*]pyridine-2-carboxamide (3.26c)*

118 mg, 61% yield. ESI-MS m/z : 506 ($[M+H]^+$). 1H -NMR (300MHz, DMSO- d_6): 8.38 (d, $J=5.4$ Hz, 1H), 7.08-7.05 (m, 5H), 6.98 (s, 2H), 6.71 (d, $J=8.3$ Hz, 2H), 3.75 (m, 2H), 3.52 (t, $J=6.5$ Hz, 2H), 3.33 (s, 2H), 3.28 (m, 2H), 3.19 (m, 2H), 2.48 (m, 4H), 2.31 (m, 4H), 2.13 (m, 2H), 1.57 (m, 1H), 0.37 (m, 2H), 0.25 (m, 2H).

tert-butyl 4-(4-formylphenyl)-1,4-diazepane-1-carboxylate (3.27)

To a 100 mL round-bottom flask was added a solution of 4-fluorobenzaldehyde (10 mmol, 1.24 g) and *tert*-butyl 1,4-diazepane-1-carboxylate (10 mmol, 2 g) in DMSO (20 mL). Then K_2CO_3 (20 mmol, 2.76 g) was added and the mixture was stirred at 110 °C for overnight. After that, the mixture was cooled to room temperature, water was added, extracted with DCM, the organic layers

were combined, dried by Na_2SO_4 , condensed to give tert-butyl 4-(4-formylphenyl)-1,4-diazepane-1-carboxylate (2.57 g, 85%). ESI-MS m/z : 305 ($[\text{M}+\text{H}]^+$).

4-(1,4-diazepan-1-yl)benzaldehyde (3.28)

To a 100 mL round-bottle flask was added a solution of tert-butyl 4-(4-formylphenyl)-1,4-diazepane-1-carboxylate (3.04 mmol, 924 mg) in DCM (6 mL). Then TFA (2 mL) was added and the mixture was stirred at room temperature for 4h. Upon completion, the mixture was condensed to give 4-(1,4-diazepan-1-yl)benzaldehyde (620 mg, 100% yield) and used without further purification. ESI-MS m/z : 205 ($[\text{M}+\text{H}]^+$).

2-chloro-4-[4-(4-formylphenyl)-1,4-diazepan-1-yl]pyridine-3-carbonitrile (3.29)

To a 100 mL round-bottle flask was added a solution of 4-(1,4-diazepan-1-yl)benzaldehyde (3.04 mmol, 620 mg) and 2,4-dichloropyridine-3-carbonitrile (3.04 mmol, 525 mg) in acetonitrile (10 mL). Then DIEA (6.1 mmol, 1.04 mL) was added and the mixture was stirred at 80°C for overnight. Upon completion, the mixture was cooled to room temperature, water was added, and the mixture was extracted with DCM, the organic layers were combined, washed with brine and dried by Na_2SO_4 and concentrated and purified by flash column chromatography using a gradient of 0-8% MeOH/DCM to give 2-chloro-4-[4-(4-formylphenyl)-1,4-diazepan-1-yl]pyridine-3-carbonitrile (910 mg, 88% yield). ESI-MS m/z : 341 ($[\text{M}+\text{H}]^+$). $^1\text{H-NMR}$ (300MHz, CD_2Cl_2): 9.72 (s, 1H), 7.99 (d, $J=6.4$ Hz, 1H), 7.72 (d, $J=8.9$ Hz, 2H), 6.81 (d, $J=8.9$ Hz, 2H), 6.62 (d, $J=6.4$ Hz, 1H), 4.00 (m, 2H), 3.88 (m, 2H), 3.74 (t, $J=6.2$ Hz, 2H), 3.66 (t, $J=6.2$ Hz, 2H), 2.14 (m, 2H).

tert-butyl 4-[[4-[4-(2-chloro-3-cyano-4-pyridyl)-1,4-diazepan-1-yl]phenyl]methyl]piperazine-1-carboxylate (**3.30**)

To a 100 mL round-bottle flask was added a solution of 2-chloro-4-[4-(4-formylphenyl)-1,4-diazepan-1-yl]pyridine-3-carbonitrile (0.91 mmol, 310 mg) and *tert-butyl* piperazine-1-carboxylate (1.36 mmol, 254 mg) in DCM (10 mL). The pH of the solution was adjusted by acetic acid to 4. Then NaBH₃CN (2.46 mmol, 154 mg) was added and the mixture was stirred at room temperature for overnight. Upon completion, sat NaHCO₃ aq was added and the mixture was extracted DCM, the organic layers were combined and washed with brine and washed with brine and dried by Na₂SO₄ and concentrated and purified by flash column chromatography using a gradient of 0-8% MeOH/DCM to give *tert-butyl* 4-[[4-[4-(2-chloro-3-cyano-4-pyridyl)-1,4-diazepan-1-yl]phenyl]methyl]piperazine-1-carboxylate (425 mg, 91% yield). ESI-MS *m/z*: 512 ([M+H]⁺). ¹H-NMR (300MHz, CD₂Cl₂): 7.96 (d, J=6.7 Hz, 1H), 7.14 (d, J=8.6 Hz, 2H), 6.69 (d, J=8.6 Hz, 2H), 6.60 (d, J=6.7 Hz, 1H), 3.99 (t, J=4.7 Hz, 2H), 3.77 (t, J=4.7 Hz, 2H), 3.71 (t, J=6.0 Hz, 2H), 3.55 (t, J=6.0 Hz, 2H), 3.36 (m, 4H), 3.35 (s, 2H), 2.31 (m, 4H), 2.11 (m, 2H), 1.42(s, 9H).

methyl 3-amino-4-[4-[4-[(4-*tert*-butoxycarbonylpiperazin-1-yl)methyl]phenyl]-1,4-diazepan-1-yl]thieno[2,3-*b*]pyridine-2-carboxylate (**3.31**)

To a 10 mL round-bottle flask was added a solution of *tert-butyl* 4-[[4-[4-(2-chloro-3-cyano-4-pyridyl)-1,4-diazepan-1-yl]phenyl]methyl]piperazine-1-carboxylate (0.83 mmol, 425 mg) and methyl 2-sulfanylacacetate (1.66 mmol, 177 mg) in MeOH (4 mL). Then NaOMe (1.66 mmol, 90 mg) was added and the mixture

was stirred at 100°C for overnight. Upon completion, the mixture was condensed and purified by flash column chromatography using a gradient of 0-8% MeOH/DCM to give methyl 3-amino-4-[4-[4-[(4-tert-butoxycarbonylpiperazin-1-yl)methyl]phenyl]-1,4-diazepan-1-yl]thieno[2,3-b]pyridine-2-carboxylate (294 mg, 61% yield). ESI-MS m/z : 581 ($[M+H]^+$). 1H -NMR (300MHz, CD_2Cl_2): 8.46 (d, $J=5.4$ Hz, 1H), 7.16 (d, $J=8.6$ Hz, 2H), 6.69 (d, $J=8.6$ Hz, 2H), 6.95 (d, $J=5.4$ Hz, 1H), 6.79 (s, 2H), 6.72 (d, $J=8.6$ Hz, 2H), 3.83 (s, 3H), 3.77 (t, $J=5.5$ Hz, 2H), 3.61 (t, $J=5.9$ Hz, 2H), 3.40 (s, 2H), 3.38 (t, $J=4.5$ Hz, 4H), 3.35 (m, 2H), 3.28 (m, 2H), 2.35 (t, $J=4.5$ Hz, 4H), 2.18 (m, 2H), 1.43(s, 9H).

tert-butyl 4-[[4-[4-(3-amino-2-carbamoyl-thieno[2,3-b]pyridin-4-yl)-1,4-diazepan-1-yl]phenyl]methyl]piperazine-1-carboxylate (3.32)

To a 10 mL round-bottle flask was added a solution of methyl 3-amino-4-[4-[4-[(4-tert-butoxycarbonylpiperazin-1-yl)methyl]phenyl]-1,4-diazepan-1-yl]thieno[2,3-b]pyridine-2-carboxylate (0.49 mmol, 284 mg) and LiOH-H₂O (0.98 mmol, 41 mg) in THF (4 mL) and water (2 mL). Then the mixture was stirred at 60°C for overnight. Upon completion, the mixture was condensed and dissolved in DMF. Then HATU (0.73 mmol, 279 mg), DIEA (0.98 mmol, 126 mg) were added and the mixture was stirred at room temperature for 15 min, then NH₄OH (4 mmol, 140 mg) was added and the mixture was stirred for 2h. Upon completion, water was added, the mixture was extracted with DCM, the organic layers were combined, dried by Na₂SO₄, condensed and purified by flash column chromatography using a gradient of 0-8% MeOH/DCM to give *tert-butyl 4-[[4-[4-(3-amino-2-carbamoyl-thieno[2,3-b]pyridin-4-yl)-1,4-diazepan-1-*

yl]phenyl]methyl]piperazine-1-carboxylate (182 mg, 66% yield). ESI-MS m/z : 566 ($[M+H]^+$). 1H -NMR (300MHz, CD_2Cl_2): 8.44 (d, $J=5.5$ Hz, 1H), 7.16 (d, $J=8.3$ Hz, 2H), 6.99 (s, 2H), 6.96 (d, $J=5.5$ Hz, 1H), 6.71 (d, $J=8.3$ Hz, 2H), 5.41 (s, 2H), 3.76 (t, $J=4.7$ Hz, 2H), 3.60 (t, $J=6.0$ Hz, 2H), 3.43 (s, 2H), 3.39 (t, $J=4.7$ Hz, 4H), 3.36 (m, 2H), 3.27 (m, 2H), 2.38 (t, $J=4.7$ Hz, 4H), 2.18 (m, 2H), 1.43 (s, 9H).

3-amino-4-[4-[4-(piperazin-1-ylmethyl)phenyl]-1,4-diazepan-1-yl]thieno[2,3-b]pyridine-2-carboxamide (3.33)

To a 10 mL round-bottle flask was added a solution of tert-butyl 4-[[4-[4-(3-amino-2-carbamoyl-thieno[2,3-b]pyridin-4-yl)-1,4-diazepan-1-yl]phenyl]methyl]piperazine-1-carboxylate (0.27 mmol, 150 mg) in DCM (3 mL). Then TFA (1 mL) was added and the mixture was stirred at room temperature for 4h. Upon completion, the mixture was condensed and purified by flash column chromatography using a gradient of 0-9% MeOH/DCM to give 3-amino-4-[4-[4-(piperazin-1-ylmethyl)phenyl]-1,4-diazepan-1-yl]thieno[2,3-b]pyridine-2-carboxamide (73 mg, 59% yield). ESI-MS m/z : 466 ($[M+H]^+$). 1H -NMR (300MHz, DMSO- d_6): 8.80 (s, 1H), 8.42 (d, $J=5.4$ Hz, 1H), 7.15 (s, 2H), 7.14 (d, $J=8.4$ Hz, 2H), 7.09 (d, $J=5.4$ Hz, 1H), 6.89 (s, 2H), 6.77 (d, $J=8.4$ Hz, 2H), 3.79 (m, 2H), 3.64 (m, 2H), 3.55 (t, $J=5.0$ Hz, 2H), 3.25 (m, 4H), 3.17 (m, 4H), 2.73 (m, 4H), 2.11 (m, 2H).

ethyl 4-fluorobenzoate (3.35)

To a 100 mL round-bottom flask was added a solution of 4-fluorobenzoic acid (35.7 mmol, 5 g) in ethanol, then conc. H_2SO_4 was added and the mixture was refluxed for overnight. Upon completion, the reaction was cooled to room

temperature and condensed. Then ice water was added and neutralized by sat Na_2CO_3 aq solution, extracted with DCM, the organic layers were combined and dried by Na_2SO_4 , condensed to give ethyl 4-fluorobenzoate (5.1 g, yield 85%) and used without further purification. ESI-MS m/z : 169 ($[\text{M}+\text{H}]^+$). $^1\text{H-NMR}$ (300MHz, CDCl_3): 8.06-8.01 (m, 2H), 7.08 (t, $J=8.5$ Hz, 2H), 4.35 (q, $J=7.1$ Hz, 2H), 1.37 (t, $J=7.14$, 3H).

ethyl 4-(1,4-diazepan-1-yl)benzoate (3.36)

To a 10 mL round-bottom flask was added a solution of 4-ethyl 4-fluorobenzoate (0.6 mmol, 100 mg) and 1,4-diazepane (1.2 mmol, 119 mg) in DMSO (3 mL), the mixture was stirred at 120°C for overnight. After that, the mixture was cooled to room temperature and water was added, the mixture was extracted with DCM, the organic layers were combined, dried by Na_2SO_4 , condensed, and purified by flash column chromatography using a gradient of 0-7% MeOH/DCM to give ethyl 4-(1,4-diazepan-1-yl)benzoate (100 mg, yield 68%). ESI-MS m/z : 249 ($[\text{M}+\text{H}]^+$). $^1\text{H-NMR}$ (300MHz, CDCl_3): 7.88 (d, $J=8.7$ Hz, 2H), 6.65 (d, $J=8.7$ Hz, 2H), 4.31 (q, $J=7.1$ Hz, 2H), 3.63 (t, $J=6.3$ Hz, 2H), 3.58 (t, $J=5.4$ Hz, 2H), 3.02 (d, $J=5.7$ Hz, 2H), 2.81 (d, $J=5.7$ Hz, 2H), 1.91-1.87 (m, 2H), 1.35 (t, $J=7.1$ Hz, 3H).

benzyl 4-(4-ethoxycarbonylphenyl)-1,4-diazepane-1-carboxylate (3.37)

To a 100 mL round-bottom flask was added a solution of ethyl 4-(1,4-diazepan-1-yl)benzoate (11.6 mmol, 2.89 g) and DIPEA (23.3 mmol, 3 g) in DCM (35 mL), and cooled to 0°C. Then benzyl carbonochloridate (11.6 mmol, 2 g) was added and the mixture was stirred at room temperature for overnight. After that, the mixture was added with water and extracted with DCM, the organic layers were

combined and washed with brine, dried by Na₂SO₄, condensed to give benzyl 4-(4-ethoxycarbonylphenyl)-1,4-diazepane-1-carboxylate (4 g, yield 90%). ESI-MS m/z: 383 ([M+H]⁺). ¹H-NMR (300MHz, CDCl₃): 7.90 (d, J=8.8 Hz, 2H), 7.38-7.29 (m, 5H), 6.65 (d, J=8.8 Hz, 2H), 5.12 (s, 1H), 5.07 (s, 1H), 4.32 (q, J=7.0 Hz, 2H), 3.63 (s, 2H), 3.60 (q, J=7.9 Hz, 4H), 3.34 (dt, J=22.8, 6.1 Hz, 2H), 1.98 (m, 2H), 1.36 (t, J=7.9 Hz, 3H).

4-(4-benzyloxycarbonyl-1,4-diazepan-1-yl)benzoic acid (3.38)

To a 100 mL round-bottom flask was added a solution of benzyl 4-(4-ethoxycarbonylphenyl)-1,4-diazepane-1-carboxylate (7.84 mmol, 3 g) in MeOH (15 mL) and water (15 mL). Then NaOH (19.6 mmol, 784 mg) was added and the mixture was reflux for 2 h. Upon completion, the mixture was cooled to room temperature, condensed, and diluted with water, then acidified by 2N HCl to pH=3. The precipitate was collected via filtration, the residue was washed with water, dried under vacuum to get 4-(4-benzyloxycarbonyl-1,4-diazepan-1-yl)benzoic acid (2 g, yield 72%) and used for the next step without further purification. ESI-MS m/z: 355 ([M+H]⁺).

The general preparation of **3.39**.

To a 100 mL round-bottom flask was added a solution of 4-(4-benzyloxycarbonyl-1,4-diazepan-1-yl)benzoic acid (1eq) in DCM (10 mL), then DIEA (2eq) and HATU (1.5eq) were added and the mixture was stirred at room temperature for 15 min, then amines (2eq) was added and the mixture was stirred for 2h. Upon completion, the mixture was added with water, extracted with DCM, the organic layers were combined, washed with brine, dried by Na₂SO₄,

condensed and purified by flash column chromatography using a gradient of 0-5% MeOH/DCM to give **3.39**.

benzyl 4-[4-(4-methylpiperazine-1-carbonyl)phenyl]-1,4-diazepane-1-carboxylate
(3.39a)

620 mg, 84% yield. ESI-MS m/z : 437 ($[M+H]^+$).

benzyl 4-[4-(4-tert-butoxycarbonylpiperazine-1-carbonyl)phenyl]-1,4-diazepane-1-carboxylate **(3.39b)**

620 mg, 84% yield. ESI-MS m/z : 437 ($[M+H]^+$).

benzyl 4-[4-(4-acetylpiperazine-1-carbonyl)phenyl]-1,4-diazepane-1-carboxylate
(3.39c)

936 mg, 71% yield. ESI-MS m/z : 465 ($[M+H]^+$). $^1\text{H-NMR}$ (300MHz, CD_2Cl_2): 7.32 (m, 7H), 6.69 (d, $J=8.3$ Hz, 2H), 5.10 (s, 1H), 5.05 (s, 1H), 3.64-3.57 (m, 12H), 3.46 (m, 2H), 3.35 (m, 2H), 2.07 (s, 3H), 1.96 (m, 2H).

benzyl 4-[4-(4-cyclopropylpiperazine-1-carbonyl)phenyl]-1,4-diazepane-1-carboxylate **(3.39d)**

1.1 g, 84% yield. ESI-MS m/z : 463 ($[M+H]^+$). $^1\text{H-NMR}$ (300MHz, CD_2Cl_2): 7.33-7.29 (m, 7H), 6.68 (d, $J=8.3$ Hz, 2H), 5.10 (s, 1H), 5.05 (s, 1H), 3.64-3.53 (m, 10H), 3.34 (m, 2H), 2.58 (m, 4H), 1.96 (m, 2H), 1.63 (m, 1H), 0.41 (m, 4H).

benzyl 4-[4-(4-cyclopentylpiperazine-1-carbonyl)phenyl]-1,4-diazepane-1-carboxylate **(3.39e)**

1.2 g, 87% yield. ESI-MS m/z : 491 ($[M+H]^+$). $^1\text{H-NMR}$ (300MHz, CD_2Cl_2): 7.37-7.29 (m, 7H), 6.68 (d, $J=8.3$ Hz, 2H), 5.10 (s, 1H), 5.04 (s, 1H), 3.64-3.56 (m,

10H), 3.35 (m, 2H), 2.50 (m, 1H), 2.46 (m, 4H), 1.96 (m, 2H), 1.83 (m, 1H), 1.66 (m, 2H), 1.54 (m, 2H), 1.37 (m, 2H).

benzyl 4-[4-(4-cyclohexylpiperazine-1-carbonyl)phenyl]-1,4-diazepane-1-carboxylate (**3.39f**)

1.3 g, 91% yield. ESI-MS m/z : 505 ($[M+H]^+$). 1H -NMR (300MHz, CD_2Cl_2): 7.34-7.28 (m, 7H), 6.68 (d, $J=8.3$ Hz, 2H), 5.09 (s, 1H), 5.04 (s, 1H), 3.63-3.56 (m, 10H), 3.35 (m, 2H), 2.63 (m, 4H), 2.39 (m, 1H), 1.96 (m, 2H), 1.81 (m, 4H), 1.23 (m, 6H).

benzyl 4-[4-(3-hydroxypropylcarbamoyl)phenyl]-1,4-diazepane-1-carboxylate (**3.39g**)

660 mg, yield 96%. ESI-MS m/z : 412 ($[M+H]^+$). 1H -NMR (300MHz, $CDCl_3$): 7.65 (d, $J=8.4$ Hz, 2H), 7.33-7.28 (m, 5H), 6.68 (m, 1H), 6.65 (d, $J=8.4$ Hz, 2H), 5.11 (s, 1H), 5.06 (s, 1H), 3.70-3.55 (m, 10H), 3.33 (m, 2H), 1.95 (m, 2H), 1.74 (m, 2H).

benzyl 4-[4-[3-hydroxypropyl(methyl)carbamoyl]phenyl]-1,4-diazepane-1-carboxylate (**3.39h**)

660 mg, 93% yield. ESI-MS m/z : 426 ($[M+H]^+$). 1H -NMR (300MHz, $CDCl_3$): 7.32 (m, 7H), 6.66 (d, $J=9.7$ Hz, 2H), 5.12 (s, 1H), 5.08 (s, 1H), 3.69-3.56 (m, 10H), 3.34 (m, 2H), 3.04 (s, 3H), 1.97 (m, 2H), 1.80 (m, 2H).

benzyl 4-[4-[3-(*tert*-butoxycarbonylamino)propyl-methyl-carbamoyl]phenyl]-1,4-diazepane-1-carboxylate (**3.39i**)

1.01 g, 68% yield. ESI-MS m/z : 525 ($[M+H]^+$). 1H -NMR (300MHz, $CDCl_3$): 7.33 (d, $J=13.6$ Hz, 2H), 7.32 (m, 5H), 6.65 (m, 2H), 5.11 (d, $J=13.6$ Hz, 2H), 3.63

(m, 2H), 3.56 (m, 2H), 3.34 (m, 2H), 3.14 (m, 2H), 3.03 (s, 6H), 1.98 (m, 2H), 1.77 (m, 2H), 1.42 (s, 9H).

The general preparation of **3.40**.

To a 25 mL round-bottom flask was added a solution of **3.39** (1eq) in EtOH and ethyl acetate. Then Pd/C (1eq) was added, the mixture was saturated with H₂, and stirred at room temperature for overnight. After that, the mixture was diluted with hexane, filtered, and the residue was washed with hexane, the filtration was condensed to give **3.40** and used without further purification.

[4-(1,4-diazepan-1-yl)phenyl]-(4-methylpiperazin-1-yl)methanone (**3.40a**)

395 mg, 92% yield. ESI-MS m/z: 303 ([M+H]⁺).

tert-butyl 4-[4-(1,4-diazepan-1-yl)benzoyl]piperazine-1-carboxylate (**3.40b**)

430 mg, 89% yield. ESI-MS m/z: 389 ([M+H]⁺). ¹H-NMR (300MHz, CDCl₃): 7.33 (d, J=8.8 Hz, 2H), 6.66 (d, J=8.8 Hz, 2H), 3.60 (m, 8H), 3.44 (m, 4H), 3.05 (m, 2H), 2.85 (m, 2H), 1.94 (m, 2H), 1.46 (s, 9H).

1-[4-[4-(1,4-diazepan-1-yl)benzoyl]piperazin-1-yl]ethanone (**3.40c**)

400 mg, 98% yield. ESI-MS m/z: 331 ([M+H]⁺).

(4-cyclopropylpiperazin-1-yl)-[4-(1,4-diazepan-1-yl)phenyl]methanone (**3.40d**):

1.07 g, 95% yield. ESI-MS m/z: 329 ([M+H]⁺).

(4-cyclopentylpiperazin-1-yl)-[4-(1,4-diazepan-1-yl)phenyl]methanone (**3.40e**):

1.01 g, 96% yield. ESI-MS m/z: 357 ([M+H]⁺).

(4-cyclohexylpiperazin-1-yl)-[4-(1,4-diazepan-1-yl)phenyl]methanone (**3.40f**): 1.1

g, 96% yield. ESI-MS m/z: 371 ([M+H]⁺).

4-(1,4-diazepan-1-yl)-N-(3-hydroxypropyl)benzamide (3.40g): 450 mg, 89% yield. ESI-MS m/z : 278 ($[M+H]^+$). 1H -NMR (300MHz, CD_3OD): 7.71 (d, $J=9.1$ Hz, 2H), 6.79 (d, $J=9.1$ Hz, 2H), 3.72-3.60 (m, 6H), 3.45 (t, $J=7.1$ Hz, 2H), 3.12 (m, 2H), 2.94 (m, 2H), 2.02 (m, 2H), 1.81 (m, 2H).

4-(1,4-diazepan-1-yl)-N-(3-hydroxypropyl)-N-methyl-benzamide (3.40h): 500 mg, 90% yield. ESI-MS m/z : 292 ($[M+H]^+$). 1H -NMR (300MHz, CD_3OD): 7.34 (d, $J=9.0$ Hz, 2H), 6.81 (d, $J=9.0$ Hz, 2H), 3.74-3.53 (m, 6H), 3.16 (m, 2H), 3.07 (s, 3H), 2.97 (m, 2H), 2.05 (m, 2H), 1.86 (m, 2H).

tert-butyl N-[3-[[4-(1,4-diazepan-1-yl)benzoyl]-methyl-amino]propyl]carbamate (3.40i): 634 mg, 84% yield. ESI-MS m/z : 391 ($[M+H]^+$).

The general preparation of **3.41**.

To a 100 mL round-bottom flask was added a solution of **3.40** (1eq) in acetonitrile, then 2,4-dichloropyridine-3-carbonitrile (1eq) and DIPEA (2eq) were added. The mixture was stirred at 80°C for overnight. Upon completion, the mixture was cooled to room temperature, condensed, diluted with water, extracted with DCM, the organic layers were combined, dried by Na_2SO_4 , condensed, and purified by flash column chromatography using a gradient of 0-7% MeOH/DCM to give **3.41**.

2-chloro-4-[4-[4-(4-methylpiperazine-1-carbonyl)phenyl]-1,4-diazepan-1-yl]pyridine-3-carbonitrile (3.41a)

444 mg, 77%. ESI-MS m/z : 440 ($[M+H]^+$).

tert-butyl 4-[4-[4-(2-chloro-3-cyano-4-pyridyl)-1,4-diazepan-1-yl]benzoyl]piperazine-1-carboxylate (**3.41b**)

318 mg, 55%. ESI-MS m/z : 526 ($[M+H]^+$).

4-[4-[4-(4-acetylpiperazine-1-carbonyl)phenyl]-1,4-diazepan-1-yl]-2-chloro-pyridine-3-carbonitrile (**3.41c**)

136 mg, 19% yield. ESI-MS m/z : 468 ($[M+H]^+$). $^1\text{H-NMR}$ (300MHz, CD_2Cl_2): 7.97 (d, $J=6.4$ Hz, 1H), 7.33 (d, $J=8.8$ Hz, 2H), 6.73 (d, $J=8.8$ Hz, 2H), 6.61 (d, $J=6.5$ Hz, 1H), 4.00 (t, $J=4.9$ Hz, 2H), 3.83 (t, $J=4.9$ Hz, 2H), 3.72 (t, $J=6.0$ Hz, 2H), 3.61 (t, $J=5.7$ Hz, 4H), 3.56 (m, 4H), 3.47 (m, 2H), 2.13 (m, 2H), 2.07 (s, 3H).

2-chloro-4-[4-[4-(4-cyclopropylpiperazine-1-carbonyl)phenyl]-1,4-diazepan-1-yl]pyridine-3-carbonitrile (**3.41d**)

410 mg, 50% yield. ESI-MS m/z : 466 ($[M+H]^+$). $^1\text{H-NMR}$ (300MHz, CD_2Cl_2): 7.97 (d, $J=6.5$ Hz, 1H), 7.30 (d, $J=8.9$ Hz, 2H), 6.72 (d, $J=8.9$ Hz, 2H), 6.62 (d, $J=6.5$ Hz, 1H), 4.00 (t, $J=4.9$ Hz, 2H), 3.82 (t, $J=4.9$ Hz, 2H), 3.72 (t, $J=5.8$ Hz, 2H), 3.60 (t, $J=5.8$ Hz, 2H), 3.51 (m, 4H), 2.58 (t, $J=5.0$ Hz, 4H), 2.12 (m, 2H), 1.64 (m, 1H), 0.45 (m, 2H), 0.39 (m, 2H).

2-chloro-4-[4-[4-(4-cyclopentylpiperazine-1-carbonyl)phenyl]-1,4-diazepan-1-yl]pyridine-3-carbonitrile (**3.41e**)

421 mg, 61% yield. ESI-MS m/z : 494 ($[M+H]^+$). $^1\text{H-NMR}$ (300MHz, CD_2Cl_2): 7.96 (d, $J=6.5$ Hz, 1H), 7.30 (d, $J=8.9$ Hz, 2H), 6.72 (d, $J=8.9$ Hz, 2H), 6.62 (d, $J=6.5$ Hz, 1H), 4.00 (t, $J=4.9$ Hz, 2H), 3.82 (t, $J=4.9$ Hz, 2H), 3.72 (t, $J=5.8$

Hz, 2H), 3.60 (t, J=5.8 Hz, 2H), 3.58 (m, 4H), 2.55 (m, 1H), 2.50 (t, J=5.2 Hz, 4H), 2.12 (m, 2H), 1.84 (m, 2H), 1.65 (m, 2H), 1.55 (m, 2H), 1.38 (m, 2H).

benzyl 4-[4-(4-cyclohexylpiperazine-1-carbonyl)phenyl]-1,4-diazepane-1-carboxylate (**3.41f**)

1.3 g, 91% yield. ESI-MS m/z: 505 ($[M+H]^+$). 1H -NMR (300MHz, CD_2Cl_2): 7.34-7.28 (m, 7H), 6.68 (d, J=8.3 Hz, 2H), 5.09 (s, 1H), 5.04 (s, 1H), 3.63-3.56 (m, 10H), 3.35 (m, 2H), 2.63 (m, 4H), 2.39 (m, 1H), 1.96 (m, 2H), 1.81 (m, 4H), 1.23 (m, 6H).

4-[4-(2-chloro-3-cyano-4-pyridyl)-1,4-diazepan-1-yl]-N-(3-hydroxypropyl)benzamide (**3.41g**)

420 mg, 51% yield. ESI-MS m/z: 414 ($[M+H]^+$). 1H -NMR (300MHz, $CDCl_3$): 8.00 (d, J=6.4 Hz, 1H), 7.68 (d, J=8.6 Hz, 2H), 6.71 (d, J=8.6 Hz, 2H), 6.58 (d, J=6.4 Hz, 1H), 6.47 (m, 1H), 4.01 (t, J=4.2 Hz, 2H), 3.85 (t, J=4.2 Hz, 2H), 3.73-3.58 (m, 8H), 2.15 (m, 2H), 1.78 (m, 1H).

4-[4-(2-chloro-3-cyano-4-pyridyl)-1,4-diazepan-1-yl]-N-(3-hydroxypropyl)-N-methyl-benzamide (**3.41h**)

430 mg, 47% yield. ESI-MS m/z: 429 ($[M+H]^+$). 1H -NMR (300MHz, $CDCl_3$): 8.00 (d, J=6.4 Hz, 1H), 7.38 (d, J=9.1 Hz, 2H), 6.71 (d, J=9.1 Hz, 2H), 6.58 (d, J=6.4 Hz, 1H), 4.02 (t, J=5.2 Hz, 2H), 3.84 (t, J=5.2 Hz, 2H), 3.73-3.55 (m, 8H), 3.04 (s, 3H), 2.14 (m, 2H), 1.81 (m, 2H).

tert-butyl N-[3-[[4-[4-(3-chloro-2-cyano-4-pyridyl)-1,4-diazepan-1-yl]benzoyl]-methyl-amino]propyl]carbamate (**3.41i**)

567 mg, 66% yield. ESI-MS m/z : 528 ($[M+H]^+$). 1H -NMR (300MHz, $CDCl_3$): 8.00 (d, $J=6.8$ Hz, 1H), 7.33 (d, $J=8.5$ Hz, 2H), 6.70 (d, $J=8.8$ Hz, 2H), 6.60 (d, $J=6.4$ Hz, 1H), 4.01 (m, 2H), 3.83 (m, 2H), 3.71 (m, 2H), 3.61 (m, 2H), 3.54 (m, 2H), 3.13 (m, 2H), 3.02 (s, 6H), 2.14 (m, 2H), 1.78 (m, 2H), 1.42 (s, 9H).

The general preparation of **3.42**.

To a 10 mL round-bottom flask was added a solution of 2-chloro-4-[4-[4-(4-methylpiperazine-1-carbonyl)phenyl]-1,4-diazepan-1-yl]pyridine-3-carbonitrile (1eq) in MeOH, then methyl 2-sulfanylacetate (2eq) and MeONa (2 eq) were added. The mixture was stirred at 100°C for overnight. Upon completion, the mixture was condensed and purified by flash column chromatography using a gradient of 0-7% MeOH/DCM to give **3.42**.

methyl 3-amino-4-[4-[4-(4-methylpiperazine-1-carbonyl)phenyl]-1,4-diazepan-1-yl]thieno[2,3-b]pyridine-2-carboxylate (3.42a)

379 mg, 75% yield. ESI-MS m/z : 509 ($[M+H]^+$). 1H -NMR (300MHz, $CDCl_3$): 8.48 (d, $J=5.2$ Hz, 1H), 7.38 (d, $J=8.6$ Hz, 2H), 6.91 (d, $J=5.2$ Hz, 1H), 6.78 (m, 2H), 6.72 (d, $J=8.6$ Hz, 2H), 3.86 (s, 3H), 3.80 (t, $J=4.9$ Hz, 2H), 3.66 (m, 6H), 3.37 (m, 2H), 3.26 (m, 2H), 2.43 (m, 4H), 3.32 (s, 3H), 2.20 (m, 2H).

methyl 3-amino-4-[4-[4-(4-tert-butoxycarbonylpiperazine-1-carbonyl)phenyl]-1,4-diazepan-1-yl]thieno[2,3-b]pyridine-2-carboxylate (3.42b)

288 mg, 85%. ESI-MS m/z : 595 ($[M+H]^+$). 1H -NMR (300MHz, $CDCl_3$): 8.48 (d, $J=5.2$ Hz, 1H), 7.37 (d, $J=8.9$ Hz, 2H), 6.91 (d, $J=5.2$ Hz, 1H), 6.77 (m, 2H), 6.72 (d, $J=8.9$ Hz, 2H), 3.86 (s, 3H), 3.80 (t, $J=6.1$ Hz, 2H), 3.64 (m, 6H), 3.47 (m, 4H), 3.70 (m, 2H), 3.27 (m, 2H), 2.20 (m, 2H), 1.47 (s, 9H).

methyl 4-[4-[4-(4-acetylpiperazine-1-carbonyl)phenyl]-1,4-diazepan-1-yl]-3-amino-thieno[2,3-b]pyridine-2-carboxylate (3.42c)

100 mg, 69% yield. ESI-MS m/z : 537 ($[M+H]^+$).

methyl 3-amino-4-[4-[4-(4-cyclopropylpiperazine-1-carbonyl)phenyl]-1,4-diazepan-1-yl]thieno[2,3-b]pyridine-2-carboxylate (3.42d)

214 mg, 45% yield. ESI-MS m/z : 535 ($[M+H]^+$). 1H -NMR (300MHz, CD_2Cl_2): 8.46 (d, $J=5.3$ Hz, 1H), 7.34 (d, $J=8.9$ Hz, 2H), 6.95 (d, $J=5.3$ Hz, 1H), 6.79 (s, 2H), 6.74 (d, $J=8.9$ Hz, 2H), 3.84 (s, 3H), 3.80 (t, $J=5.2$ Hz, 2H), 3.66 (t, $J=5.2$ Hz, 2H), 3.56 (m, 4H), 3.37 (m, 2H), 3.28 (m, 2H), 2.61 (t, $J=5.0$ Hz, 4H), 2.20 (m, 2H), 1.65 (m, 1H), 0.45 (m, 2H), 0.39 (m, 2H).

methyl 3-amino-4-[4-[4-(4-cyclopentylpiperazine-1-carbonyl)phenyl]-1,4-diazepan-1-yl]thieno[2,3-b]pyridine-2-carboxylate (3.42e)

376 mg, 78% yield. ESI-MS m/z : 563 ($[M+H]^+$).

methyl 3-amino-4-[4-[4-(4-cyclohexylpiperazine-1-carbonyl)phenyl]-1,4-diazepan-1-yl]thieno[2,3-b]pyridine-2-carboxylate (3.42f)

86 mg, 47% yield. ESI-MS m/z : 577 ($[M+H]^+$).

methyl 3-amino-4-[4-[4-(3-hydroxypropylcarbamoyl)phenyl]-1,4-diazepan-1-yl]thieno[2,3-b]pyridine-2-carboxylate (3.42g)

323 mg, 71%. ESI-MS m/z : 484 ($[M+H]^+$). 1H -NMR (300MHz, $CDCl_3$): 8.49 (d, $J=5.2$ Hz, 1H), 7.71 (d, $J=9.1$ Hz, 2H), 6.91 (d, $J=5.2$ Hz, 1H), 6.74 (d, $J=9.1$ Hz, 2H), 6.72 (s, 2H), 6.47 (m, 2H), 3.86 (s, 3H), 3.82 (t, $J=4.6$ Hz, 2H), 3.72-3.61 (m, 8H), 3.39 (m, 2H), 3.29 (m, 2H), 2.21 (m, 2H), 1.78 (m, 2H).

methyl 3-amino-4-[4-[4-[3-hydroxypropyl(methyl)carbamoyl]phenyl]-1,4-diazepan-1-yl]thieno[2,3-b]pyridine-2-carboxylate (3.42h)

388 mg, 78%. ESI-MS m/z : 498 ($[M+H]^+$). 1H -NMR (300MHz, $CDCl_3$): 8.49 (d, $J=5.2$ Hz, 1H), 7.41 (d, $J=8.8$ Hz, 2H), 6.92 (d, $J=5.2$ Hz, 1H), 6.78 (m, 2H), 6.73 (d, $J=8.8$ Hz, 2H), 3.86 (s, 3H), 3.80 (t, $J=5.8$ Hz, 2H), 3.67 (m, 4H), 3.59 (q, $J=6.4$ Hz, 2H), 3.38 (m, 2H), 3.28 (m, 2H), 3.08 (s, 3H), 2.21 (m, 2H), 1.82 (m, 2H).

methyl 3-amino-4-[4-[4-[3-(tert-butoxycarbonylamino)propyl-methyl-carbamoyl]phenyl]-1,4-diazepan-1-yl]thieno[2,3-b]pyridine-2-carboxylate (3.42i)

250 mg, 40%. ESI-MS m/z : 528 ($[M+H]^+$). 1H -NMR (300MHz, $CDCl_3$): 8.48 (d, $J=5.0$ Hz, 1H), 7.37 (d, $J=8.8$ Hz, 2H), 6.92 (d, $J=5.0$ Hz, 1H), 6.79 (s, 2H), 6.72 (d, $J=8.8$ Hz, 2H), 3.86 (s, 3H), 3.80 (t, $J=4.7$ Hz, 2H), 3.66 (t, $J=6.3$ Hz, 2H), 3.56 (m, 2H), 3.38 (m, 2H), 3.27 (m, 2H), 3.14 (m, 2H), 3.06 (s, 3H), 2.21 (m, 2H), 1.79 (m, 2H), 1.43 (s, 9H).

The general preparation of **3.43**.

To a 10 mL round-bottom flask was added a solution of **3.42** (1eq) in DMF (5 mL), then DIEA (3eq) and HATU (1.5eq) were added and the mixture was stirred at room temperature for 15 min, then NH_4OH (3eq) was added and the mixture was stirred for 2 h. Upon completion, the mixture was added with water, extracted with DCM, the organic layers were combined, washed with brine, dried by Na_2SO_4 , condensed and purified by flash column chromatography using a gradient of 0-8% MeOH/DCM to give **3.43**.

3-amino-4-[4-[4-(4-methylpiperazine-1-carbonyl)phenyl]-1,4-diazepan-1-yl]thieno[2,3-b]pyridine-2-carboxamide (3.43a)

80 mg, 83% yield. ESI-MS m/z : 494 ($[M+H]^+$). NMR (300MHz, $CDCl_3$): 8.46 (d, $J=5.2$ Hz, 1H), 7.37 (d, $J=8.8$ Hz, 2H), 6.99 (s, 2H), 6.92 (d, $J=5.2$ Hz, 1H), 6.71 (d, $J=8.8$ Hz, 2H), 5.43 (s, 2H), 3.79(m, 2H), 3.65 (m, 6H), 3.37 (s, 2H), 3.26 (s, 2H), 2.43 (m, 4H), 2.32 (s, 3H), 2.21 (m, 2H).

tert-butyl 4-[4-[4-(3-amino-2-carbamoyl-thieno[2,3-b]pyridin-4-yl)-1,4-diazepan-1-yl]benzoyl]piperazine-1-carboxylate (3.43b)

87 mg, 75% yield. ESI-MS m/z : 580 ($[M+H]^+$). 1H -NMR (300MHz, $CDCl_3$): 8.47 (d, $J=5.6$ Hz, 1H), 7.37 (d, $J=8.9$ Hz, 2H), 6.98 (s, 2H), 6.93 (d, $J=5.6$ Hz, 1H), 6.72 (d, $J=8.9$ Hz, 2H), 5.39 (s, 2H), 3.79(m, 2H), 3.64 (m, 6H), 3.46 (m, 4H), 3.37 (s, 2H), 3.27 (s, 2H), 2.21 (m, 2H), 1.47 (s, 9H).

4-[4-[4-(4-acetylpiperazine-1-carbonyl)phenyl]-1,4-diazepan-1-yl]-3-amino-thieno[2,3-b]pyridine-2-carboxamide (3.43c)

38 mg, 39% yield. ESI-MS m/z : 522 ($[M+H]^+$). 1H -NMR (300MHz, $DMSO-d_6$): 8.40 (d, $J=5.2$ Hz, 1H), 7.31 (d, $J=8.8$ Hz, 2H), 7.11 (s, 2H), 7.09 (d, $J=5.2$ Hz, 1H), 6.98 (s, 2H), 6.80 (d, $J=8.8$ Hz, 2H), 3.82 (m, 2H), 3.59 (t, $J=5.7$ Hz, 2H), 3.54 (m, 2H), 3.47 (m, 6H), 3.30 (m, 2H), 3.21 (m, 2H), 2.16 (m, 2H), 2.02 (s, 3H).

3-amino-4-[4-[4-(4-cyclopropylpiperazine-1-carbonyl)phenyl]-1,4-diazepan-1-yl]thieno[2,3-b]pyridine-2-carboxamide (3.43d)

96 mg, 49% yield. ESI-MS m/z : 520 ($[M+H]^+$). 1H -NMR (300MHz, $DMSO-d_6$): 8.40 (d, $J=5.4$ Hz, 1H), 7.27 (d, $J=8.9$ Hz, 2H), 7.10 (s, 2H), 7.07 (d, $J=5.4$ Hz, 1H), 7.00 (s, 2H), 6.79 (d, $J=8.9$ Hz, 2H), 3.82 (m, 2H), 3.58 (t, $J=5.7$ Hz, 2H), 3.46 (m, 4H), 3.30 (m, 2H), 3.20 (m, 2H), 2.53 (m, 4H), 2.16 (m, 2H), 1.64 (m, 1H), 0.43 (m, 2H), 0.33 (m, 2H).

3-amino-4-[4-[4-(4-cyclopentylpiperazine-1-carbonyl)phenyl]-1,4-diazepan-1-yl]thieno[2,3-b]pyridine-2-carboxamide (3.43e)

240 mg, 66% yield. ESI-MS m/z : 548 ($[M+H]^+$). 1H -NMR (300MHz, DMSO- d_6): 8.39 (d, $J=5.4$ Hz, 1H), 7.27 (d, $J=8.7$ Hz, 2H), 7.10 (s, 2H), 7.07 (d, $J=5.4$ Hz, 1H), 6.99 (s, 2H), 6.78 (d, $J=8.7$ Hz, 2H), 3.82 (m, 2H), 3.58 (t, $J=5.9$ Hz, 2H), 3.50 (m, 4H), 3.30 (m, 2H), 3.20 (m, 2H), 2.45 (m, 5H), 2.16 (m, 2H), 1.78 (m, 2H), 1.60 (m, 2H), 1.49 (m, 2H), 1.34 (m, 2H).

3-amino-4-[4-[4-(4-cyclohexylpiperazine-1-carbonyl)phenyl]-1,4-diazepan-1-yl]thieno[2,3-b]pyridine-2-carboxamide (3.43f)

40 mg, 48% yield. ESI-MS m/z : 562 ($[M+H]^+$). 1H -NMR (300MHz, DMSO- d_6): 8.40 (d, $J=5.3$ Hz, 1H), 7.26 (d, $J=8.3$ Hz, 2H), 7.11 (s, 2H), 7.07 (d, $J=5.3$ Hz, 1H), 6.99 (s, 2H), 6.78 (d, $J=8.3$ Hz, 2H), 3.82 (m, 2H), 3.58 (t, $J=5.6$ Hz, 2H), 3.48 (m, 4H), 3.30 (m, 2H), 3.19 (m, 2H), 2.16 (m, 2H), 1.74 (m, 4H), 1.56 (m, 1H), 1.18 (m, 10H).

3-amino-4-[4-[4-(3-hydroxypropylcarbamoyl)phenyl]-1,4-diazepan-1-yl]thieno[2,3-b]pyridine-2-carboxamide (3.43g)

50 mg, 49%. ESI-MS m/z : 469 ($[M+H]^+$). 1H -NMR (300MHz, DMSO- d_6): 8.40 (d, $J=5.3$ Hz, 1H), 8.08 (t, $J=5.6$ Hz, 1H), 7.71 (d, $J=8.8$ Hz, 2H), 7.10 (s, 2H), 7.07 (d, $J=5.3$ Hz, 1H), 7.00 (s, 2H), 6.79 (d, $J=8.8$ Hz, 2H), 4.48 (t, $J=5.7$ Hz, 1H), 3.83 (m, 2H), 3.61 (t, $J=6.5$ Hz, 2H), 3.45 (q, $J=6.0$ Hz, 2H), 3.29 (m, 4H), 3.17 (m, 2H), 2.16 (m, 2H), 1.65 (m, 2H).

3-amino-4-[4-[4-[3-hydroxypropyl(methyl)carbamoyl]phenyl]-1,4-diazepan-1-yl]thieno[2,3-b]pyridine-2-carboxamide (3.43h)

74 mg, 55%. ESI-MS m/z : 483 ($[M+H]^+$). 1H -NMR (300MHz, DMSO- d_6): 8.40 (d, $J=5.6$ Hz, 1H), 7.27 (d, $J=8.7$ Hz, 2H), 7.10 (s, 2H), 7.08 (d, $J=5.6$ Hz, 1H), 7.00 (s, 2H), 6.78 (d, $J=8.7$ Hz, 2H), 4.47 (t, $J=5.4$ Hz, 1H), 3.81 (m, 2H), 3.59 (t, $J=6.5$ Hz, 2H), 3.41 (m, 4H), 3.30 (m, 2H), 3.20 (m, 2H), 2.95 (s, 3H), 2.16 (m, 2H), 1.70 (m, 2H).

*tert-butyl N-[3-[[4-[4-(3-amino-2-carbamoyl-thieno[2,3-*b*]pyridin-4-yl)-1,4-diazepan-1-yl]benzoyl]-methyl-amino]propyl]carbamate (3.43i)*

149 mg, 61%. ESI-MS m/z : 582 ($[M+H]^+$). 1H -NMR (300MHz, $CDCl_3$): 8.47 (d, $J=5.8$ Hz, 1H), 7.36 (d, $J=8.9$ Hz, 2H), 6.97 (s, 2H), 6.94 (d, $J=5.8$ Hz, 1H), 6.71 (d, $J=8.9$ Hz, 2H), 5.39 (s, 2H), 3.80 (t, $J=5.6$ Hz, 2H), 3.65 (t, $J=6.7$ Hz, 2H), 3.55 (m, 2H), 3.37 (m, 2H), 3.28 (m, 2H), 3.14 (m, 2H), 3.05 (s, 3H), 2.20 (m, 2H), 1.79 (m, 2H), 1.43 (s, 9H).

*3-amino-4-[4-[4-(piperazine-1-carbonyl)phenyl]-1,4-diazepan-1-yl]thieno[2,3-*b*]pyridine-2-carboxamide (3.44a)*

To a 25 mL round-bottom flask was added a solution of *tert-butyl 4-[4-[4-(3-amino-2-carbamoyl-thieno[2,3-*b*]pyridin-4-yl)-1,4-diazepan-1-yl]benzoyl]piperazine-1-carboxylate* (0.11 mmol, 62 mg) in DCM (3 mL), then TFA (0.6 mL) was added. The mixture was stirred at room temperature for 4h. Upon completion, the mixture was condensed to give *3-amino-4-[4-[4-(piperazine-1-carbonyl)phenyl]-1,4-diazepan-1-yl]thieno[2,3-*b*]pyridine-2-carboxamide* (33 mg, 64%). ESI-MS m/z : 480 ($[M+H]^+$). 1H -NMR (300MHz, $CDCl_3$): 8.47 (d, $J=5.4$ Hz, 1H), 7.37 (d, $J=8.6$ Hz, 2H), 6.99 (s, 2H), 6.93 (d, $J=5.4$ Hz, 1H), 6.72 (d, $J=8.6$ Hz,

2H), 5.40 (s, 2H), 3.79 (m, 2H), 3.65 (m, 6H), 3.38 (m, 2H), 3.27 (s, 2H), 2.91 (m, 4H), 2.21 (m, 2H), 1.98 (s, 1H).

3-amino-4-[4-[4-[3-aminopropyl(methyl)carbamoyl]phenyl]-1,4-diazepan-1-yl]thieno[2,3-b]pyridine-2-carboxamide (3.44b)

To a 25 mL round-bottom flask was added a solution of tert-butyl N-[3-[[4-[4-(3-amino-2-carbamoyl-thieno[2,3-b]pyridin-4-yl)-1,4-diazepan-1-yl]benzoyl]-methyl-amino]propyl]carbamate (0.19 mmol, 113 mg) in DCM (5 mL). Then TFA (1 mL) was added and the mixture was stirred at room temperature for 4h. Upon completion, the mixture was condensed and purified by flash column chromatography using a gradient of 0-9% MeOH/DCM to give 3-amino-4-[4-[4-[3-aminopropyl(methyl)carbamoyl]phenyl]-1,4-diazepan-1-yl]thieno[2,3-b]pyridine-2-carboxamide (77 mg, 82%). ESI-MS m/z : 482 ($[M + H]^+$). 1H -NMR (300MHz, DMSO- d_6): 8.41 (d, $J=5.6$ Hz, 1H), 8.26 (s, 1H), 7.31 (d, $J=8.4$ Hz, 2H), 7.11 (s, 2H), 7.08 (d, $J=5.6$ Hz, 1H), 6.97 (s, 2H), 6.79 (d, $J=8.4$ Hz, 2H), 3.82 (m, 2H), 3.60 (m, 2H), 3.46 (m, 2H), 3.31 (m, 2H), 3.21 (m, 2H), 2.98 (s, 3H), 2.79 (m, 2H), 2.15 (m, 2H), 1.85 (m, 2H).

4-[4-(6-chloro-5-cyano-pyrimidin-4-yl)-1,4-diazepan-1-yl]-N,N-dimethyl-benzamide (3.45)

To a 100 mL round-bottom flask was added a solution of 4-(1,4-diazepan-1-yl)-N,N-dimethyl-benzamide (2.02 mmol, 500 mg) and 4,6-dichloropyrimidine-5-carbonitrile (2.02 mmol, 352 mg) in acetonitrile (7 mL), then DIPEA (6.06 mmol, 78 mg) was added and the mixture was stirred at 80°C for overnight. Upon completion, the mixture was added with water, extracted with DCM, the organic

layers were combined, dried by Na₂SO₄, condensed and purified by flash column using a gradient of 0-7% MeOH/DCM to give 4-[4-(6-chloro-5-cyano-pyrimidin-4-yl)-1,4-diazepan-1-yl]-N,N-dimethyl-benzamide (369 mg, 47%). ESI-MS m/z: 438 ([M+H]⁺). ¹H-NMR (300MHz, DMSO-d₆): 8.46 (s, 1H), 7.25 (d, J=8.9 Hz, 2H), 6.79 (d, J=8.9 Hz, 2H), 4.11 (m, 2H), 3.83 (m, 2H), 3.78 (m, 2H), 3.61 (m, 2H), 2.94 (s, 6H), 2.01 (m, 2H).

4-[4-(5-cyano-6-thioxo-1H-pyrimidin-4-yl)-1,4-diazepan-1-yl]-N,N-dimethyl-benzamide (3.46)

To a 100 mL round-bottom flask was added a solution of 4-[4-(6-chloro-5-cyano-pyrimidin-4-yl)-1,4-diazepan-1-yl]-N,N-dimethyl-benzamide (0.83 mmol, 320 mg) and thiourea (2.49 mmol, 190 mg) in EtOH (5 mL). Then 1 drop of 4N HCl in dioxane was added and the mixture was refluxed for 2h. After that, the mixture was condensed and purified by flash column using a gradient of 0-7% MeOH/DCM to give 4-[4-(5-cyano-6-thioxo-1H-pyrimidin-4-yl)-1,4-diazepan-1-yl]-N,N-dimethyl-benzamide (225 mg, 71%). ESI-MS m/z: 383 ([M+H]⁺).

4-[4-(5-amino-6-cyano-thieno[2,3-d]pyrimidin-4-yl)-1,4-diazepan-1-yl]-N,N-dimethyl-benzamide (3.47)

To a 100 mL round-bottom flask was added a solution of 4-[4-(5-cyano-6-thioxo-1H-pyrimidin-4-yl)-1,4-diazepan-1-yl]-N,N-dimethyl-benzamide (0.59 mmol, 225 mg) and 2-chloroacetonitrile (0.59 mmol, 45mg) in DMF (4 mL). Then 10% KOH aq (1.18 mmol) was added and the mixture was stirred at room temperature for overnight. After that, another portion of 10% KOH aq was added and the mixture was stirred at room temperature for 4h. After that, the mixture was diluted with

DCM, then brine was added and the mixture was extracted with DCM, the organic layers were combined and dried by Na₂SO₄, condensed and purified by flash column using a gradient of 0-7% MeOH/DCM to give 4-[4-(5-amino-6-cyano-thieno[2,3-d]pyrimidin-4-yl)-1,4-diazepan-1-yl]-N,N-dimethyl-benzamide (106 mg, 43%). ESI-MS m/z: 422 ([M+H]⁺). ¹H-NMR (300MHz, DMSO-d₆): 8.28 (s, 1H), 7.15 (d, J=8.2 Hz, 2H), 6.75 (s, 2H), 6.64 (d, J=8.2 Hz, 2H), 3.85 (m, 2H), 3.70 (m, 4H), 3.49 (m, 2H), 2.92 (s, 6H), 2.09 (m, 2H).

5-amino-4-[4-[4-(dimethylcarbamoyl)phenyl]-1,4-diazepan-1-yl]thieno[2,3-d]pyrimidine-6-carboxamide (3.48)

To a 100 mL round-bottom flask was added a solution of 4-[4-(5-amino-6-cyano-thieno[2,3-d]pyrimidin-4-yl)-1,4-diazepan-1-yl]-N,N-dimethyl-benzamide (0.22 mmol, 91 mg) in t-BuOH (3 mL). Then KOH (0.43 mmol, 24 mg) was added and the mixture was stirred at room temperature for overnight. After that, another portion of 10% KOH aq was added and the mixture was stirred at 90°C for 1.5h. After that, the mixture was cooled to room temperature, condensed, water was added, extracted with DCM, the organic layers were combined, dried by Na₂SO₄, condensed and purified by flash column using a gradient of 0-7% MeOH/DCM to give 5-amino-4-[4-[4-(dimethylcarbamoyl)phenyl]-1,4-diazepan-1-yl]thieno[2,3-d]pyrimidine-6-carboxamide (10 mg, 11%). ESI-MS m/z: 440 ([M+H]⁺). ¹H-NMR (300MHz, CD₂Cl₂): 8.48 (s, 1H), 7.30 (d, J=8.9 Hz, 2H), 6.68 (d, J=8.9 Hz, 2H), 6.40 (s, 2H), 5.40 (s, 2H), 3.85 (m, 2H), 3.76 (m, 2H), 3.66 (m, 2H), 3.55 (m, 2H), 3.01 (s, 6H), 2.14 (m, 2H).

4-[4-(5-chloro-4-cyano-3-pyridyl)-1,4-diazepan-1-yl]-N,N-dimethyl-benzamide

(3.49)

To a 100 mL round-bottom flask was added a solution of 4-(1,4-diazepan-1-yl)-N,N-dimethyl-benzamide (2.02 mmol, 500 mg) and 3,5-dichloropyridine-4-carbonitrile (3.03 mmol, 525 mg) in DMF (7 mL), then DIPEA (6.06 mmol, 784 mg) was added and the mixture was stirred at 90°C for overnight. Upon completion, the mixture was cooled to room temperature, added with water, extracted with DCM, the organic layers were combined, dried by Na₂SO₄, condensed and purified by flash column using a gradient of 0-7% MeOH/DCM to give 4-[4-(5-chloro-4-cyano-3-pyridyl)-1,4-diazepan-1-yl]-N,N-dimethyl-benzamide (450 mg, 58%). ESI-MS m/z: 384 ([M+H]⁺). ¹H-NMR (300MHz, DMSO-d₆): 8.41 (s, 1H), 8.05 (s, 1H), 7.25 (d, J=8.7 Hz, 2H), 6.78 (d, J=8.7 Hz, 2H), 3.84 (m, 4H), 3.70 (m, 2H), 3.59 (m, 2H), 2.93 (s, 6H), 2.03 (m, 2H).

methyl 3-amino-4-[4-[4-(dimethylcarbamoyl)phenyl]-1,4-diazepan-1-yl]thieno[2,3-c]pyridine-2-carboxylate (3.50)

To a 100 mL round-bottom flask was added a solution of 4-[4-(5-chloro-4-cyano-3-pyridyl)-1,4-diazepan-1-yl]-N,N-dimethyl-benzamide (1.17 mmol, 450 mg) and methyl 2-sulfanylacacetate (3.52 mmol, 373 mg) in MeOH (7 mL), then MeONa (3.52 mmol, 190 mg) was added and the mixture was stirred at 100°C for overnight. Upon completion, the mixture was cooled to room temperature, condensed and purified by flash column using a gradient of 0-8% MeOH/DCM to give methyl 3-amino-4-[4-[4-(dimethylcarbamoyl)phenyl]-1,4-diazepan-1-yl]thieno[2,3-c]pyridine-2-carboxylate (442 mg, 83%). ESI-MS m/z: 454 ([M+H]⁺).

¹H-NMR (300MHz, DMSO-d₆): 8.88 (s, 1H), 8.37 (s, 1H), 7.31 (d, J=8.9 Hz, 2H), 7.10 (s, 2H), 6.80 (d, J=8.9 Hz, 2H), 3.83 (m, 2H), 3.80 (s, 3H), 3.65 (m, 2H), 3.27 (m, 2H), 3.19 (m, 2H), 2.98 (s, 6H), 2.08 (m, 2H).

3-amino-4-[4-[4-(dimethylcarbamoyl)phenyl]-1,4-diazepan-1-yl]thieno[2,3-c]pyridine-2-carboxamide (3.51)

To a 100 mL round-bottom flask was added a solution of methyl 3-amino-4-[4-[4-(dimethylcarbamoyl)phenyl]-1,4-diazepan-1-yl]thieno[2,3-c]pyridine-2-carboxylate (1 mmol, 453 mg) and LiOH-H₂O (3 mmol, 126 mg) in THF (4 mL) and water (2 mL). Then the mixture was stirred at 60 °C for overnight. After that, the mixture was condensed and dissolved in DMF (5 mL), then HATU (1.5 mmol, 568 mg) and DIEA (3 mmol, 387 mg) were added and stirred for 15 min. Then NH₄OH (6 mmol, 210 mg) was added and stirred at room temperature for 2h. Upon completion, water was added, extracted with DCM, the organic layers were combined, dried by Na₂SO₄, condensed, and purified by flash column using a gradient of 0-7% MeOH/DCM to give 3-amino-4-[4-[4-(dimethylcarbamoyl)phenyl]-1,4-diazepan-1-yl]thieno[2,3-c]pyridine-2-carboxamide (234 mg, 53%). ESI-MS m/z: 439 ([M+H]⁺). ¹H-NMR (300MHz, DMSO-d₆): 8.85 (s, 1H), 8.32 (s, 1H), 7.31 (d, J=8.7 Hz, 2H), 7.26 (s, 2H), 7.07 (s, 2H), 6.79 (d, J=8.7 Hz, 2H), 3.81 (m, 2H), 3.64 (m, 2H), 3.27 (m, 2H), 3.18 (m, 2H), 2.98 (s, 6H), 2.08 (m, 2H).

4-[4-(5-bromo-4-formyl-3-pyridyl)-1,4-diazepan-1-yl]-N,N-dimethyl-benzamide (3.52)

To a 100 mL round-bottle flask was added a solution of 3-bromo-5-fluoropyridine-4-carbaldehyde (2.5 mmol, 500 mg) and 4-(1,4-diazepan-1-yl)-N,N-

dimethyl-benzamide (2.45 mmol, 606 mg) in DMSO (6 mL). Then DIEA (7.35 mmol, 950 mg) was added and the mixture was stirred at 80°C for overnight. Upon completion, the mixture was cooled to room temperature, water was added and the mixture was extracted with DCM. The organic layers were combined, washed with brine, dried by Na₂SO₄, condensed and purified by flash column chromatography using a gradient of 0-7% MeOH/DCM to give 4-[4-(5-bromo-4-formyl-3-pyridyl)-1,4-diazepan-1-yl]-N,N-dimethyl-benzamide (553 mg, 52% yield). ESI-MS m/z: 432 ([M+H]⁺). ¹H-NMR (300MHz, CD₂Cl₂): 10.16 (s, 1H), 8.41 (s, 1H), 8.25 (s, 1H), 7.30 (d, J=8.4 Hz, 2H), 6.68 (d, J=8.4 Hz, 2H), 3.76 (t, J=5.4 Hz, 2H), 3.64 (t, J=5.4 Hz, 2H), 3.39 (m, 4H), 3.00 (s, 6H), 2.10 (m, 2H).

methyl 4-[4-[4-(dimethylcarbamoyl)phenyl]-1,4-diazepan-1-yl]thieno[2,3-c]pyridine-2-carboxylate (3.53)

To a 10 mL round-bottle flask was added a solution of 4-[4-(5-bromo-4-formyl-3-pyridyl)-1,4-diazepan-1-yl]-N,N-dimethyl-benzamide (0.93 mmol, 400 mg) and methyl 2-sulfanylacetate (1.85 mmol, 197 mg) in THF (5 mL). Then Cs₂CO₃ (1.11 mmol, 363 mg) was added, the mixture was stirred at 60°C for overnight. After that, the mixture was cooled to room temperature, water was added, extracted with DCM, the organic layers were combined, dried by Na₂SO₄ and purified by flash column chromatography using a gradient of 0-7% MeOH/DCM to give methyl 4-[4-[4-(dimethylcarbamoyl)phenyl]-1,4-diazepan-1-yl]thieno[2,3-c]pyridine-2-carboxylate (195 mg, 48% yield). ESI-MS m/z: 439 ([M+H]⁺). ¹H-NMR (300MHz, CD₂Cl₂): 8.66 (s, 1H), 8.15 (s, 1H), 8.11 (s, 1H), 7.33

(t, J=8.9 Hz, 2H), 6.75 (t, J=8.9 Hz, 2H), 3.94 (s, 3H), 3.85 (t, J=4.6 Hz, 2H), 3.69 (m, 4H), 3.85 (t, J=5.2 Hz, 2H), 3.01 (s, 6H), 2.21 (m, 2H).

4-[4-[4-(dimethylcarbamoyl)phenyl]-1,4-diazepan-1-yl]thieno[2,3-c]pyridine-2-carboxamide (3.54)

To a 10 mL tube was added a solution of methyl 4-[4-[4-(dimethylcarbamoyl)phenyl]-1,4-diazepan-1-yl]thieno[2,3-c]pyridine-2-carboxylate (0.14 mmol, 62 mg) in 2M NH₃ in methanol (2 ml). The tube was sealed and stirred at 45°C for overnight. Upon completion, the mixture was cooled to room temperature, condensed, and purified by flash column chromatography using a gradient of 0-7% MeOH/DCM to give 4-[4-[4-(dimethylcarbamoyl)phenyl]-1,4-diazepan-1-yl]thieno[2,3-c]pyridine-2-carboxamide (49 mg, 82% yield). ESI-MS m/z: 424 ([M+H]⁺). ¹H-NMR (300MHz, DMSO-d₆): 8.69 (s, 1H), 8.49 (s, 1H), 8.15 (s, 1H), 8.06 (s, 1H), 7.78 (s, 1H), 7.27 (d, J=8.0 Hz, 2H), 6.78 (t, J=8.0 Hz, 2H), 3.82 (m, 2H), 3.64 (m, 4H), 3.49 (m, 2H), 2.94 (s, 6H), 2.11 (m, 2H).

methyl thieno[2,3-b]pyridine-2-carboxylate (3.56)

To a 25 mL round-bottom flask was added a solution of 2-chloropyridine-3-carbaldehyde (7.1 mmol, 1 g) and methyl 2-sulfanylacacetate (10.6 mmol, 1.12 g) in DMF (15 mL). Then K₂CO₃ (21.2 mmol, 2.93 g) was added and the mixture was stirred at 80°C for overnight. Upon completion, the mixture was cooled to room temperature, diluted with water and extracted with diethyl ether. The organic layers were combined, dried by Na₂SO₄, condensed, and purified by flash column chromatography with a gradient of 0-5% MeOH/DCM to give methyl thieno[2,3-b]pyridine-2-carboxylate (848 mg, 62%). ESI-MS m/z: 194 ([M+H]⁺). ¹H-NMR

(300MHz, CDCl₃): 8.67 (dd, J=4.5, 1.5 Hz, 1H), 8.15 (dd, J=8.3, 1.5 Hz, 1H), 8.00 (s, 1H), 7.35 (dd, J=8.3, 4.5 Hz, 1H), 3.96 (s, 3H).

methyl 4-chlorothieno[2,3-b]pyridine-2-carboxylate (3.57)

To a 50 mL round-bottom flask was added a solution of methyl thieno[2,3-b]pyridine-2-carboxylate (2.07 mmol, 400 mg) in CHCl₃ (10 mL) and cooled to 0°C, then mCPBA (3.73 mmol, 643 mg) was added. The mixture was stirred at room temperature for overnight. Upon completion, the mixture was condensed, dissolved in DCM and washed with sat NaHCO₃ aq, the aqueous phase was then extracted with DCM, the organic layers were combined and dried by Na₂SO₄, condensed, dissolved in CHCl₃ (10 mL) and cooled to 0°C, then POCl₃ (12.8 mmol, 1.97 g) was added, the mixture was stirred at 0°C for 3h. After that, ice water was added and sat Na₂CO₃ aq was added to make the pH=9, extracted with DCM, the organic layers were combined and dried by Na₂SO₄, condensed, and purified by flash column chromatography via a gradient of 0-5% MeOH/DCM to give methyl 4-chlorothieno[2,3-b]pyridine-2-carboxylate (338 mg, 69%). ESI-MS m/z: 228 ([M + H]⁺). ¹H-NMR (300MHz, CDCl₃): 8.56 (d, J=5.1 Hz, 1H), 8.14 (s, 1H), 7.38 (d, J=5.1 Hz, 1H), 3.98 (s, 3H).

methyl 4-[4-[4-(dimethylcarbamoyl)phenyl]-1,4-diazepan-1-yl]thieno[2,3-b]pyridine-2-carboxylate (3.58)

To a 50 mL round-bottom flask was added a solution of methyl 4-chlorothieno[2,3-b]pyridine-2-carboxylate (1.45 mmol, 329 mg) and 4-(1,4-diazepan-1-yl)-N,N-dimethyl-benzamide (2.2 mmol, 536 mg) in DMSO (5 mL). Then DIPEA (4.34 mmol, 560 mg) was added and the mixture was stirred at 110°C

for overnight. Upon completion, the mixture was cooled to room temperature, water was added, extracted with DCM, the organic layers were combined and dried by Na_2SO_4 , condensed, and purified by flash column chromatography via a gradient of 0-7% MeOH/DCM to give methyl 4-[4-[4-(dimethylcarbamoyl)phenyl]-1,4-diazepan-1-yl]thieno[2,3-b]pyridine-2-carboxylate (221 mg, 35%). ESI-MS m/z : 439 ($[\text{M} + \text{H}]^+$). $^1\text{H-NMR}$ (300MHz, CDCl_3): 8.20 (d, $J=5.9$ Hz, 1H), 8.12 (s, 1H), 7.32 (d, $J=8.6$ Hz, 2H), 6.68 (d, $J=8.6$ Hz, 2H), 6.49 (d, $J=5.9$ Hz, 1H), 3.90 (s, 3H), 3.84 (m, 4H), 3.70 (t, $J=4.9$ Hz, 2H), 3.57 (t, $J=6.8$ Hz, 2H), 3.01 (s, 6H), 2.14 (m, 2H).

4-[4-[4-(dimethylcarbamoyl)phenyl]-1,4-diazepan-1-yl]thieno[2,3-b]pyridine-2-carboxamide (3.59)

To a 25 mL round-bottom flask was added a solution of methyl 4-[4-[4-(dimethylcarbamoyl)phenyl]-1,4-diazepan-1-yl]thieno[2,3-b]pyridine-2-carboxylate (0.46 mmol, 200 mg) in THF (3 mL) and water (3 mL), then LiOH-H₂O (1.37 mmol, 57 mg) was added. The mixture was stirred at 50°C for overnight. Upon completion, the mixture was condensed and dissolved in DMF (5 mL). Then HATU (0.68 mmol, 259 mg), DIPEA (1.37 mmol, 177 mg) were added and stirred for 15 min. After that, NH₄OH (1.82 mmol, 64 mg) was added and the mixture was stirred for 2h. Upon completion, the mixture was diluted with water, extracted with DCM, the organic layers were combined, dried by Na_2SO_4 , condensed and purified by flash column chromatography using a gradient of 0-7% MeOH/DCM to give 4-[4-[4-(dimethylcarbamoyl)phenyl]-1,4-diazepan-1-yl]thieno[2,3-b]pyridine-2-carboxamide (36 mg, 19%). ESI-MS m/z : 424 ($[\text{M} + \text{H}]^+$). $^1\text{H-NMR}$ (300MHz,

DMSO-d₆): 8.28 (s, 1H), 8.15 (s, 1H), 8.09 (d, J=5.6 Hz, 1H), 7.58 (s, 1H), 7.24 (d, J=9.2 Hz, 2H), 6.76 (d, J=9.2 Hz, 1H), 6.65 (d, J=6.2 Hz, 1H), 3.89 (m, 2H), 3.83 (m, 2H), 3.75 (m, 2H), 3.56 (m, 2H), 2.92 (s, 6H), 2.02 (m, 2H).

4-[4-(3-cyano-2-thioxo-1H-pyridin-4-yl)-1,4-diazepan-1-yl]-N,N-dimethyl-benzamide (3.61)

To a 25 mL round-bottom flask was added a solution of 4-[4-(2-chloro-3-cyano-4-pyridyl)-1,4-diazepan-1-yl]-N,N-dimethyl-benzamide (1.58 mmol, 608 mg) in EtOH (10 mL). Then thiourea (4.8 mmol, 362 mg) and 1 drop 4N HCl in dioxane were added, the mixture was refluxed for 2h. Upon completion, the mixture was cooled to room temperature, condensed, 1N NaOH aq was added and extracted with diethyl ether, the aqueous phase was then acidified by 2N HCl to pH=3, extracted with DCM, the organic layers were combined, dried by Na₂SO₄, condensed and purified by flash column chromatography using a gradient of 0-7% MeOH/DCM to give 4-[4-(3-cyano-2-thioxo-1H-pyridin-4-yl)-1,4-diazepan-1-yl]-N,N-dimethyl-benzamide (548 mg, 91%). ESI-MS m/z: 382 ([M+H]⁺). ¹H-NMR (300MHz, CDCl₃): 12.14 (s, 1H), 7.37 (d, J=8.4 Hz, 2H), 7.27 (d, J=7.7 Hz, 1H), 6.69 (d, J=8.4 Hz, 2H), 6.22 (d, J=7.7 Hz, 1H), 4.13 (m, 2H), 3.84 (m, 2H), 3.72 (m, 2H), 3.62 (m, 2H), 3.07 (s, 6H), 2.11 (m, 2H).

4-[4-(3-amino-2-cyano-thieno[2,3-b]pyridin-4-yl)-1,4-diazepan-1-yl]-N,N-dimethyl-benzamide (3.62)

To a 25 mL round-bottom flask was added a solution of 4-[4-(3-cyano-2-thioxo-1H-pyridin-4-yl)-1,4-diazepan-1-yl]-N,N-dimethyl-benzamide (0.68 mmol, 260 mg) and MeONa (1.4 mmol, 74 mg) in MeOH (10 mL). Then 2-

chloroacetonitrile (0.68 mmol, 52 mg) was added, and stirred at room temperature for overnight. After that, another equivalent of MeONa (1.4 mmol, 74 mg) was added and the mixture was stirred at 90°C for overnight. Upon completion, the mixture was cooled to room temperature and condensed, then purified by flash column using a gradient of 0-7% MeOH/DCM to give 4-[4-(3-amino-2-cyano-thieno[2,3-b]pyridin-4-yl)-1,4-diazepan-1-yl]-N,N-dimethyl-benzamide (78 mg, 27%). ESI-MS m/z : 421 ($[M+H]^+$). 1H -NMR (300MHz, DMSO- d_6): 8.44 (d, $J=5.5$ Hz, 1H), 7.30 (d, $J=8.9$ Hz, 2H), 7.14 (d, $J=5.5$ Hz, 1H), 6.91 (s, 2H), 6.76 (d, $J=8.9$ Hz, 2H), 3.77 (t, $J=4.1$ Hz, 2H), 3.56 (t, $J=6.4$ Hz, 2H), 3.37 (m, 2H), 3.22 (m, 2H), 2.96 (s, 6H), 2.13 (m, 2H).

methyl 2-[[3-cyano-4-[4-[4-(dimethylcarbamoyl)phenyl]-1,4-diazepan-1-yl]-2-pyridyl]oxy]acetate (3.63)

To a 100 mL round-bottom flask was added a solution of 4-[4-(2-chloro-3-cyano-4-pyridyl)-1,4-diazepan-1-yl]-N,N-dimethyl-benzamide (1.1 mmol, 411 mg) and methyl 2-hydroxyacetate (5.4 mmol, 482 mg) in 1,2-dimethoxyethane (7 mL). Then NaH (5.4 mmol, 123 mg) was added and the mixture was protected with nitrogen, stirred at 60°C for 4h. Upon completion, the mixture was cooled to room temperature, sat NH_4Cl aq was added and extracted with DCM, the organic layers were combined, washed with brine, dried by Na_2SO_4 , condensed and purified by flash column chromatography using a gradient of 0-7% MeOH/DCM to give methyl 2-[[3-cyano-4-[4-[4-(dimethylcarbamoyl)phenyl]-1,4-diazepan-1-yl]-2-pyridyl]oxy]acetate (356 mg, 76%). ESI-MS m/z : 438 ($[M+H]^+$). 1H -NMR (300MHz, DMSO- d_6): 7.77 (d, $J=6.5$ Hz, 1H), 7.26 (d, $J=8.7$ Hz, 2H), 6.78 (d, $J=8.9$

Hz, 2H), 6.61 (d, J=6.1 Hz, 1H), 4.92 (s, 2H), 3.93 (m, 2H), 3.77 (m, 2H), 3.72 (m, 2H), 3.64 (s, 3H), 3.56 (m, 2H), 2.94 (s, 6H), 1.98 (m, 2H).

methyl 3-amino-4-[4-[4-(dimethylcarbamoyl)phenyl]-1,4-diazepan-1-yl]furo[2,3-b]pyridine-2-carboxylate (3.64)

To a 100 mL round-bottom flask was added a solution of methyl 2-[[3-cyano-4-[4-[4-(dimethylcarbamoyl)phenyl]-1,4-diazepan-1-yl]-2-pyridyl]oxy]acetate (0.67 mmol, 292 mg) in THF (6 mL) and cooled to 0°C. Then Lithium bis(trimethylsilyl)amide (2 mmol, 335 mg) was added and the mixture was stirred at 0°C for 40 min. Then the reaction was quenched by sat NaHCO₃ aq, extracted with DCM, the organic layers were combined, dried by Na₂SO₄, condensed, and purified flash column by using a gradient of 0-5% MeOH/DCM to give methyl 3-amino-4-[4-[4-(dimethylcarbamoyl)phenyl]-1,4-diazepan-1-yl]furo[2,3-b]pyridine-2-carboxylate (136 mg, 47%). ESI-MS m/z: 438 ([M+H]⁺). ¹H-NMR (300MHz, CD₂Cl₂): 8.16 (d, J=5.4 Hz, 1H), 7.33 (d, J=8.9 Hz, 2H), 6.71 (d, J=8.9 Hz, 2H), 6.70 (d, J=5.4 Hz, 1H), 5.18 (s, 2H), 3.89 (s, 3H), 3.77 (m, 2H), 3.60 (m, 4H), 3.46 (m, 2H), 3.01 (s, 6H), 2.19 (m, 2H).

3-amino-4-[4-[4-(dimethylcarbamoyl)phenyl]-1,4-diazepan-1-yl]furo[2,3-b]pyridine-2-carboxamide (3.65)

To a 100 mL round-bottom flask was added a solution of methyl 3-amino-4-[4-[4-(dimethylcarbamoyl)phenyl]-1,4-diazepan-1-yl]thieno[2,3-c]pyridine-2-carboxylate (0.25 mmol, 109 mg) and LiOH-H₂O (0.5 mmol, 22 mg) in THF (4 mL) and water (2 mL). Then the mixture was stirred at 60 °C for overnight. After that, the mixture was condensed and dissolved in DMF (5 mL), then HATU (0.37 mmol,

142 mg) and DIEA (0.5 mmol, 64 mg) were added and stirred for 15 min. Then NH_4OH (1.49 mmol, 52 mg) was added and stirred at room temperature for 2h. Upon completion, water was added, extracted with DCM, the organic layers were combined, dried by Na_2SO_4 , condensed, and purified by flash column using a gradient of 0-7% MeOH/DCM to give 3-amino-4-[4-[4-(dimethylcarbamoyl)phenyl]-1,4-diazepan-1-yl]furo[2,3-b]pyridine-2-carboxamide (54 mg, 51%). ESI-MS m/z : 423 ($[\text{M}+\text{H}]^+$). $^1\text{H-NMR}$ (300MHz, DMSO-d_6): 8.00 (d, $J=5.5$ Hz, 1H), 7.38 (s, 2H), 7.26 (d, $J=8.5$ Hz, 2H), 6.75 (d, $J=8.5$ Hz, 2H), 6.70 (d, $J=5.5$ Hz, 1H), 5.71 (s, 2H), 3.74 (s, 4H), 3.55 (m, 4H), 2.94 (s, 6H), 2.11 (m, 2H).

methyl 4-chloro-1H-pyrrolo[2,3-b]pyridine-2-carboxylate (3.67)

To a 10 mL round-bottom flask was added a solution of methyl 1H-pyrrolo[2,3-b]pyridine-2-carboxylate (0.57 mmol, 100 mg) in diethyl ether (4 mL) and cooled to 0°C , then mCPBA (0.57 mmol, 98 mg) was added. The mixture was stirred at room temperature for overnight. Upon completion, the mixture was condensed, dissolved in DCM and washed with sat NaHCO_3 aq, the aqueous phase was then extracted with DCM, the organic layers were combined and dried by Na_2SO_4 , condensed, dissolved in DMF (3 mL), then MsCl (2.6 mmol, 298 mg) was added, the mixture was stirred at 60°C for overnight. After that, the mixture was cooled to room temperature and ice water was added, extracted with DCM, the organic layers were combined and dried by Na_2SO_4 , condensed, and purified by flash column chromatography via a gradient of 0-5% MeOH/DCM to give methyl 4-chloro-1H-pyrrolo[2,3-b]pyridine-2-carboxylate (99 mg, 90%). ESI-MS m/z : 211

($[M+H]^+$). $^1\text{H-NMR}$ (300MHz, CDCl_3): 12.33 (s, 1H), 8.53 (d, $J=5.4$ Hz, 1H), 7.29 (d, $J=2.2$ Hz, 1H), 7.22 (d, $J=5.2$ Hz, 1H), 4.02 (s, 3H).

methyl 4-[4-[4-(dimethylcarbamoyl)phenyl]-1,4-diazepan-1-yl]-1H-pyrrolo[2,3-b]pyridine-2-carboxylate (3.68)

To a 10 mL round-bottom flask was added a solution of methyl 4-chloro-1H-pyrrolo[2,3-b]pyridine-2-carboxylate (2.98 mmol, 627 mg) and 4-(1,4-diazepan-1-yl)-N,N-dimethyl-benzamide (2.98 mmol, 736 mg) in NMP (5 mL), then DIPEA (6 mmol, 770 mg) was added. The mixture was microwaved at 160°C for 1h. Upon completion, water was added, the mixture was extracted with DCM, the organic layers were combined and dried by Na_2SO_4 , condensed, and purified by flash column chromatography via a gradient of 0-8% MeOH/DCM to give methyl 4-[4-[4-(dimethylcarbamoyl)phenyl]-1,4-diazepan-1-yl]-1H-pyrrolo[2,3-b]pyridine-2-carboxylate (96 mg, 8%). ESI-MS m/z : 422 ($[M+H]^+$). $^1\text{H-NMR}$ (300MHz, CDCl_3): 8.20 (d, $J=5.9$ Hz, 1H), 7.37 (d, $J=8.8$ Hz, 2H), 7.27 (s, 1H), 6.72 (d, $J=8.8$ Hz, 2H), 6.29 (d, $J=5.9$ Hz, 1H), 3.98 (m, 2H), 3.85 (m, 2H), 3.74 (m, 2H), 3.56 (m, 2H), 3.06 (s, 6H), 2.19 (m, 2H).

4-[4-[4-(dimethylcarbamoyl)phenyl]-1,4-diazepan-1-yl]-1H-pyrrolo[2,3-b]pyridine-2-carboxamide (3.69)

To a 25 mL round-bottom flask was added a solution of methyl 4-[4-[4-(dimethylcarbamoyl)phenyl]-1,4-diazepan-1-yl]-1H-pyrrolo[2,3-b]pyridine-2-carboxylate (0.21 mmol, 88 mg) in THF (3 mL) and water (3 mL), then LiOH-H₂O (0.84 mmol, 35 mg) was added. The mixture was stirred at 50°C for overnight. Upon completion, the mixture was condensed and dissolved in DMF (5 mL). Then

HATU (0.31 mmol, 119 mg), DIPEA (0.42 mmol, 54 mg) were added and stirred for 15 min. After that, NH₄OH (0.84 mmol, 30 mg) was added and the mixture was stirred for 2h. Upon completion, the mixture was diluted with water, extracted with DCM, the organic layers were combined, dried by Na₂SO₄, condensed and purified by flash column chromatography using a gradient of 0-7% MeOH/DCM to give 4-[4-[4-(dimethylcarbamoyl)phenyl]-1,4-diazepan-1-yl]-1H-pyrrolo[2,3-b]pyridine-2-carboxamide (28 mg, 33%). ESI-MS m/z: 407 ([M + H]⁺). ¹H-NMR (300MHz, DMSO-d₆): 11.72 (s, 1H), 7.87 (d, J=6.2 Hz, 1H), 7.33 (s, 2H), 7.30 (s, 1H), 7.25 (d, J=8.9 Hz, 2H), 6.76 (d, J=8.9 Hz, 2H), 6.30 (d, J=5.8 Hz, 1H), 3.89 (m, 2H), 3.80 (m, 2H), 3.72 (m, 2H), 3.53 (m, 2H), 2.93 (s, 6H), 3.03 (m, 2H).

methyl 4-chloro-3-nitro-1H-pyrrolo[2,3-b]pyridine-2-carboxylate (3.70)

To a 100 mL round-bottom flask was added a solution of methyl 4-chloro-1H-pyrrolo[2,3-b]pyridine-2-carboxylate (0.36 mmol, 76 mg) in conc. H₂SO₄ (0.5 mL) and cooled to 0°C. Then the solution of pre-cooled HNO₃ (0.5 mL) and conc. H₂SO₄ (1 mL) was added slowly, the mixture was then stirred at 0°C for 3h. After that, ice water was added and the mixture was filtered and the residue was washed with water and then dried under vacuum to give methyl 4-chloro-3-nitro-1H-pyrrolo[2,3-b]pyridine-2-carboxylate (60 mg, 65%) and used without further purification. ESI-MS m/z: 256 ([M + H]⁺). ¹H-NMR (300MHz, DMSO-d₆): 14.07 (s, 1H), 8.53 (d, J=5.3 Hz, 1H), 7.55 (d, J=5.3 Hz, 1H), 3.93 (s, 3H).

methyl 4-[4-[4-(dimethylcarbamoyl)phenyl]-1,4-diazepan-1-yl]-3-nitro-1H-pyrrolo[2,3-b]pyridine-2-carboxylate (3.71)

To a 100 mL round-bottom flask was added a solution of methyl 4-chloro-3-nitro-1H-pyrrolo[2,3-b]pyridine-2-carboxylate (3.58 mmol, 914 mg) and 4-(1,4-diazepan-1-yl)-N,N-dimethyl-benzamide (3.58 mmol, 884 mg) in t-BuOH (5 mL). Then DIPEA (7.15 mmol, 924 mg) was added and the mixture was stirred at 90°C for overnight. Upon completion, the mixture was diluted with DCM, water was added, extracted with DCM, the organic layers were combined, dried by Na₂SO₄, condensed and purified by flash column chromatography using a gradient of 0-7% MeOH/DCM to give methyl 4-[4-[4-(dimethylcarbamoyl)phenyl]-1,4-diazepan-1-yl]-3-nitro-1H-pyrrolo[2,3-b]pyridine-2-carboxylate (734 mg, 44%). ESI-MS m/z: 467 ([M+H]⁺). ¹H-NMR (300MHz, DMSO-d₆): 13.42 (s, 1H), 7.98 (d, J=6.4 Hz, 1H), 7.19 (d, J=8.6 Hz, 2H), 6.68 (d, J=8.6 Hz, 2H), 6.66 (d, J=6.4 Hz, 1H), 3.85 (s, 3H), 3.67 (m, 2H) 3.64 (m, 2H), 6.51 (m, 4H), 2.91 (s, 6H), 2.01 (m, 2H).

4-[4-[4-(dimethylcarbamoyl)phenyl]-1,4-diazepan-1-yl]-3-nitro-1H-pyrrolo[2,3-b]pyridine-2-carboxylic acid (3.72)

To a 10 mL round-bottom flask was added a solution of methyl 4-[4-[4-(dimethylcarbamoyl)phenyl]-1,4-diazepan-1-yl]-3-nitro-1H-pyrrolo[2,3-b]pyridine-2-carboxylate (0.64 mmol, 300 mg) and LiOH-H₂O (1.3 mmol, 54 mg) in MeOH (4 mL) and water (1 mL). Then the mixture was stirred at 70°C for 5h. Upon completion, the mixture was condensed and purified by flash column to give 4-[4-[4-(dimethylcarbamoyl)phenyl]-1,4-diazepan-1-yl]-3-nitro-1H-pyrrolo[2,3-b]pyridine-2-carboxylic acid (214 mg, 74%). ESI-MS m/z: 453 ([M+H]⁺). ¹H-NMR (300MHz, DMSO-d₆): 8.05 (d, J=6.1 Hz, 1H), 7.22 (d, J=8.9 Hz, 2H), 6.70 (d, J=8.9

Hz, 2H), 6.68 (d, J=6.1 Hz, 1H), 3.68 (m, 2H), 3.51 (m, 4H), 3.42 (m, 2H), 2.92 (s, 6H), 2.01 (m, 2H).

4-[4-[4-(dimethylcarbamoyl)phenyl]-1,4-diazepan-1-yl]-1H-pyrrolo[2,3-b]pyridine-2-carboxamide (3.73)

To a 25 mL round-bottom flask was added a solution of 4-[4-[4-(dimethylcarbamoyl)phenyl]-1,4-diazepan-1-yl]-3-nitro-1H-pyrrolo[2,3-b]pyridine-2-carboxylic acid (0.4 mmol, 181 mg) in DMF (5 mL). Then HATU (0.6 mmol, 228 mg), DIPEA (1.2 mmol, 155 mg) were added and stirred for 15 min. After that, NH₄OH (2.4 mmol, 84 mg) was added and the mixture was stirred for 2h. Upon completion, the mixture was diluted with water, extracted with DCM, the organic layers were combined, dried by Na₂SO₄, condensed and purified by flash column chromatography using a gradient of 0-7% MeOH/DCM to give 4-[4-[4-(dimethylcarbamoyl)phenyl]-1,4-diazepan-1-yl]-3-nitro-1H-pyrrolo[2,3-b]pyridine-2-carboxamide (53 mg, 30%). ESI-MS m/z: 452 ([M+H]⁺).

3-amino-4-[4-[4-(dimethylcarbamoyl)phenyl]-1,4-diazepan-1-yl]-1H-pyrrolo[2,3-b]pyridine-2-carboxamide (3.74)

To a 10 mL round-bottom flask was added a solution of 4-[4-[4-(dimethylcarbamoyl)phenyl]-1,4-diazepan-1-yl]-3-nitro-1H-pyrrolo[2,3-b]pyridine-2-carboxamide (0.12 mmol, 53 mg) in EtOH (2 mL) and THF (2 mL). Then Pd/C (0.01 mmol, 10 mg) was added and the mixture was saturated with hydrogen and stirred at room temperature for overnight. Upon completion, the mixture was filtered, washed with DCM, the filtration was condensed and purified by flash column to give 3-amino-4-[4-[4-(dimethylcarbamoyl)phenyl]-1,4-diazepan-1-yl]-

1H-pyrrolo[2,3-b]pyridine-2-carboxamide (16 mg, 32%). ESI-MS m/z: 422 ($[M+H]^+$). $^1\text{H-NMR}$ (300MHz, DMSO- d_6): 10.70 (s, 1H), 7.99 (d, $J=5.6$ Hz, 1H), 7.28 (d, $J=8.6$ Hz, 2H), 7.08 (s, 2H), 6.76 (d, $J=8.6$ Hz, 2H), 6.45 (d, $J=5.6$ Hz, 1H), 5.50 (s, 2H), 3.76 (m, 2H), 3.55 (m, 4H), 3.37 (m, 2H), 2.95 (s, 6H), 2.14 (m, 2H).

2-thioxo-1H-pyridine-3-carbonitrile (3.76)

To a 100 mL round-bottom flask was added a solution of 2-chloropyridine-3-carbonitrile (14.4 mmol, 2 g) and thiourea (18.8 mmol, 1.43 g) in EtOH (20 mL). Then the mixture was refluxed for 4h. After that, the mixture was cooled to room temperature, basified by 1N NaOH to pH=10, extracted with ethyl acetate, the aqueous phase was then acidified by 4N HCl to pH=3, the precipitation was collected and washed with water, dried to give 2-thioxo-1H-pyridine-3-carbonitrile (1.65 g, 84% yield). ESI-MS m/z: 137 ($[M+H]^+$). $^1\text{H-NMR}$ (300MHz, DMSO- d_6): 14.22 (s, 1H), 8.11 (dd, $J=7.5, 1.8$ Hz, 1H), 7.94 (dd, $J=6.3, 1.7$ Hz, 1H), 6.86 (t, $J=6.4$ Hz, 1H).

3-aminothieno[2,3-b]pyridine-2-carbonitrile (3.77)

To a 100 mL round-bottom flask was added a solution of 2-thioxo-1H-pyridine-3-carbonitrile (5.87 mmol, 800 mg) and 2-chloroacetonitrile (5.87 mmol, 444 mg) in acetone (15 mL). Then K_2CO_3 (11.7 mmol, 1.62 g) was added and the mixture was stirred at room temperature for 4h. After that, the mixture was filtered and washed with acetone, the organic layers were combined, condensed, dissolved in MeOH (15 mL). MeONa (11.7 mmol, 635 mg) was added and the mixture was stirred at 80°C for 3h. Upon completion, the mixture was cooled to room temperature, water was added, extracted with DCM, the organic layers were

combined and dried by Na_2SO_4 , condensed, and purified by flash column chromatography using a gradient of 0-5% MeOH/DCM to give 3-aminothieno[2,3-b]pyridine-2-carbonitrile (642 mg, 62% yield). ESI-MS m/z : 176 ($[\text{M} + \text{H}]^+$). $^1\text{H-NMR}$ (300MHz, DMSO-d_6): 8.71 (dd, $J=4.6, 1.2$ Hz, 1H), 8.50 (dd, $J=8.2, 1.4$ Hz, 1H), 7.52 (dd, $J=8.2, 4.6$ Hz, 1H), 7.33 (s, 2H).

3-bromo-7-oxido-thieno[2,3-b]pyridin-7-ium-2-carbonitrile (3.78)

To a 100 mL round-bottom flask was added a solution of CuBr_2 (4.16 mmol, 928 mg) and $t\text{-BuONO}$ (5.3 mmol, 546 mg) in acetonitrile (5 mL). The reaction was protected with nitrogen and stirred at room temperature for 10 min. Then 3-aminothieno[2,3-b]pyridine-2-carbonitrile (3.78 mmol, 663 mg) was added and the mixture was stirred at 60°C for 1.5h with nitrogen protection. After that, the mixture was cooled to room temperature, diluted with water, extracted with ethyl acetate. The organic layers were combined, dried by Na_2SO_4 , condensed, and dissolved in DCM (5 mL) and cooled to 0°C , then $m\text{CPBA}$ (4.38 mmol, 756 mg) was added and stirred at room temperature for overnight. After that, the mixture was condensed, and sat NaHCO_3 aq was added, extracted with DCM, the organic layers were combined and dried by Na_2SO_4 , condensed, and purified by flash column chromatography using a gradient of 0-5% MeOH/DCM to give 3-bromo-7-oxido-thieno[2,3-b]pyridin-7-ium-2-carbonitrile (290 mg, 65% yield). ESI-MS m/z : 256 ($[\text{M} + \text{H}]^+$). $^1\text{H-NMR}$ (300MHz, CD_2Cl_2): 8.50 (d, $J=6.2$ Hz, 1H), 7.82 (d, $J=8.2$ Hz, 1H), 7.57 (dd, $J=8.2, 6.2$ Hz, 1H).

3-bromo-4-chloro-thieno[2,3-b]pyridine-2-carbonitrile (3.79)

To a 100 mL round-bottom flask was added a solution of 3-bromo-7-oxido-thieno[2,3-b]pyridin-7-ium-2-carbonitrile (1.87 mmol, 477 mg) in DMF (6 mL) and cooled to 0°C, then POCl₃ (22.4 mmol, 3.44 g) was added and the reaction was stirred at 70 °C for 2h. Then the mixture was cooled to room temperature, ice water was added, adjust the pH to 10 using sat Na₂CO₃ aq, extracted with DCM, the organic layers were combined, dried by Na₂SO₄, condensed, and purified by flash column chromatography using a gradient of 0-5% MeOH/DCM to give 3-bromo-4-chloro-thieno[2,3-b]pyridine-2-carbonitrile (140 mg, 27% yield). ESI-MS m/z: 274 ([M+H]⁺). ¹H-NMR (300MHz, CD₂Cl₂): 8.62 (d, J=5.2 Hz, 1H), 7.52 (d, J=5.2 Hz, 1H).

4-[4-(3-bromo-2-cyano-thieno[2,3-b]pyridin-4-yl)-1,4-diazepan-1-yl]-N,N-dimethylbenzamide (3.80)

To a 100 mL round-bottom flask was added a solution of 3-bromo-4-chloro-thieno[2,3-b]pyridine-2-carbonitrile (0.49 mmol, 135 mg), 4-(1,4-diazepan-1-yl)-N,N-dimethylbenzamide (0.74 mmol, 183 mg), and DIEA (1.48 mmol, 191 mg) in DMSO (4 mL). Then the reaction was stirred at 110°C for overnight. Upon completion, the mixture was cooled to room temperature, diluted with DCM, water was added, extracted with DCM, the organic layers were combined, dried by Na₂SO₄, condensed, and purified by flash column chromatography using a gradient of 0-7% MeOH/DCM to give 4-[4-(3-bromo-2-cyano-thieno[2,3-b]pyridin-4-yl)-1,4-diazepan-1-yl]-N,N-dimethylbenzamide (151 mg, 63% yield). ESI-MS m/z: 485 ([M+H]⁺). ¹H-NMR (300MHz, CD₂Cl₂): 8.45 (d, J=5.5 Hz, 1H), 7.35 (d, J= 9.0 Hz, 2H), 6.96 (d, J=5.5 Hz, 1H), 6.72 (d, J=9.0 Hz, 1H), 3.83 (t, J=4.5 Hz,

2H), 3.61 (t, J=6.9 Hz, 2H), 3.52 (t, J=5.9 Hz, 2H), 3.42 (t, J=5.1 Hz, 2H), 3.03 (s, 6H), 2.28 (m, 2H).

4-[4-(5-amino-7-thia-3,4,9-triazatricyclo[6.4.0.0²,6]dodeca-1(12),2(6),4,8,10-pentaen-12-yl)-1,4-diazepan-1-yl]-N,N-dimethyl-benzamide (3.81)

To a 10 mL microwave flask was added a solution of 4-[4-(3-bromo-2-cyano-thieno[2,3-b]pyridin-4-yl)-1,4-diazepan-1-yl]-N,N-dimethyl-benzamide (0.31 mmol, 151 mg) in DMSO (3 mL). Then NH₂NH₂·H₂O (0.94 mmol, 47 mg) was added and the mixture was sealed and microwaved for 10 min at 150°C. Upon completion, the mixture was cooled to room temperature, diluted with DCM, water was added, extracted with DCM, the organic layers were combined, dried by Na₂SO₄, condensed, and purified by flash column chromatography using a gradient of 0-7% MeOH/DCM to give 4-[4-(5-amino-7-thia-3,4,9-triazatricyclo[6.4.0.0²,6]dodeca-1(12),2(6),4,8,10-pentaen-12-yl)-1,4-diazepan-1-yl]-N,N-dimethyl-benzamide (58 mg, 43% yield). ESI-MS m/z: 436 ([M+H]⁺). ¹H-NMR (300MHz, DMSO-d₆): 12.14 (s, 1H), 8.00 (d, J=5.8 Hz, 1H), 7.25 (d, J=8.7 Hz, 2H), 6.72 (d, J=8.7 Hz, 3H), 5.49 (s, 2H), 4.26 (m, 2H), 3.86 (m, 2H), 3.62 (m, 2H), 3.52 (m, 2H), 2.94 (s, 6H), 1.98 (m, 2H).

4-[4-(6-amino-8-thia-3,5,10-triazatricyclo[7.4.0.0²,7]trideca-1(13),2(7),3,5,9,11-hexaen-13-yl)-1,4-diazepan-1-yl]-N,N-dimethyl-benzamide (3.82)

To a 100 mL round-bottom flask was added a solution of 4-[4-(3-amino-2-cyano-thieno[2,3-b]pyridin-4-yl)-1,4-diazepan-1-yl]-N,N-dimethyl-benzamide (0.5 mmol, 208 mg) and formamidine acetate (0.5 mmol, 52 mg) in formamide (4 mL). The mixture was then stirred at 150°C for 6h. Upon completion, the mixture was

cooled to room temperature, ice water was added, filtered, the residue was washed with water, dried under vacuum, then purified by flash column chromatography using a gradient of 0-9% MeOH/DCM to give 4-[4-(6-amino-8-thia-3,5,10-triazatricyclo[7.4.0.0^{2,7}]trideca-1(13),2(7),3,5,9,11-hexaen-13-yl)-1,4-diazepan-1-yl]-N,N-dimethyl-benzamide (143 mg, 65%). ESI-MS *m/z*: 448 ($[M+H]^+$). ¹H-NMR (300MHz, DMSO-*d*₆): 8.53 (s, 1H), 8.26 (d, *J*=5.9 Hz, 1H), 7.40 (s, 2H), 7.24 (d, *J*=8.9 Hz, 2H), 6.94 (d, *J*=5.9 Hz, 1H), 6.72 (d, *J*=8.9 Hz, 2H), 4.02 (m, 2H), 3.77 (m, 2H), 3.71 (m, 2H), 3.56 (m, 2H), 2.94 (s, 6H), 2.09 (m, 2H).

3.4.2 Docking studies

Molecular docking was performed on a previously reported CDK8 crystal structure (PDB ID: 4F7S) using the Induced Fit module within the Maestro Interface. The 2020 version of the Small Molecule Drug Discovery Suite containing these components was used (Schrodinger, Inc.).

3.4.3 Pharmacology

293-NFκB-luc cell-based assay. The detailed procedure for this NFκB-dependent cell-based CDK8/19i activity assay was previously described.¹⁸⁰ Briefly, 293-WT-NFκB-LUC#8 (293-WT) and 293-dKO-NFκB-LUC#2 (293-KO) cells were seeded in 96-well plates, cultured for 24 hours and then treated with tested compounds at different concentrations with 10 ng/mL TNF-α added for 3 hours. 4 μL potassium luciferin solution (15 mg/mL, GoldBio) was then added to each well to determine the luciferase reporter activity, represented by the luminescence intensities measured by the SpectraMax iD5 Microplate Reader. Reporter activities of inhibitor-treated cells were normalized by the reporter

activities of cells without the inhibitor and further processed with GraphPad Prism 7.0 for curve-fitting and IC_{50} calculation.

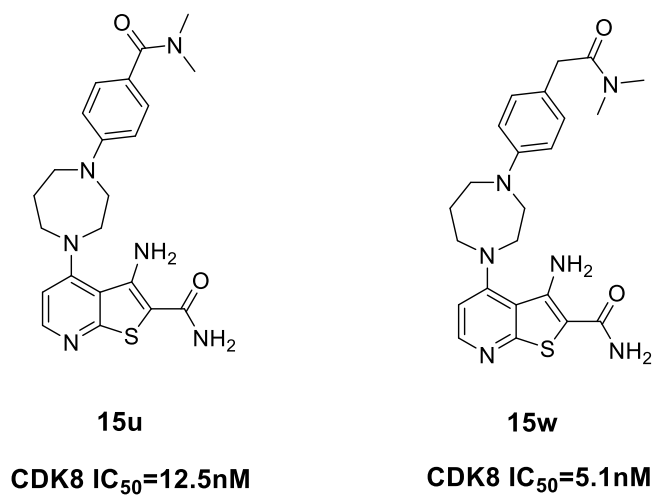


Figure 3.1 The chemical structures of 15u (**3.1**) and 15w (**3.2**).

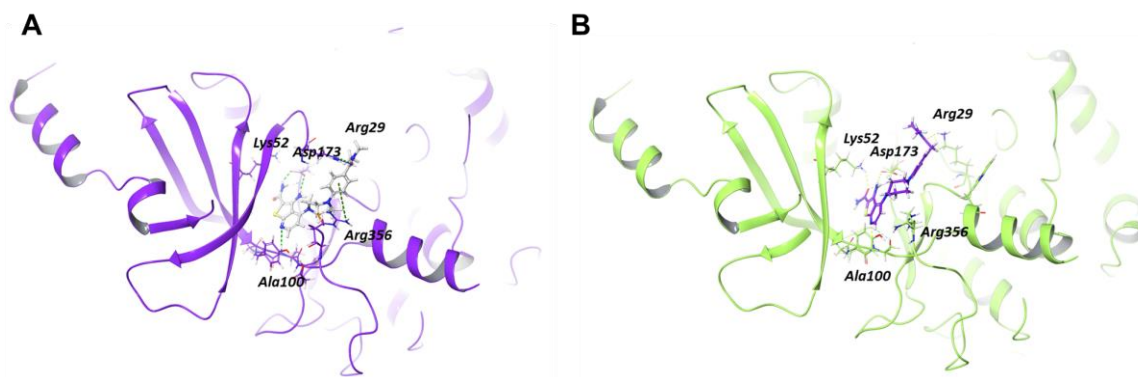


Figure 3.2 The predicted binding model of 15u (**A**) and 15w (**B**) that docked to CDK8 protein (PDB code: 4F7S).

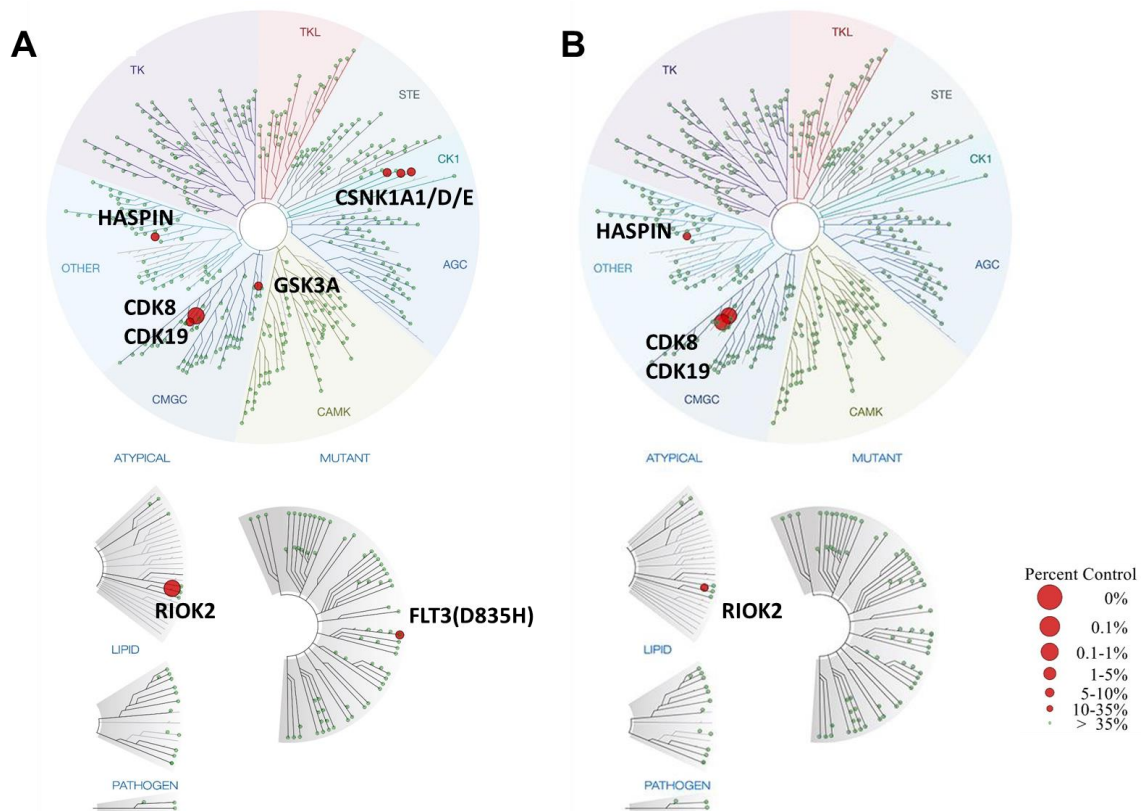


Figure 3.3 The kinome profiling of 15u (**A**) at 2 μ M and 15w (**B**) at 500nM.

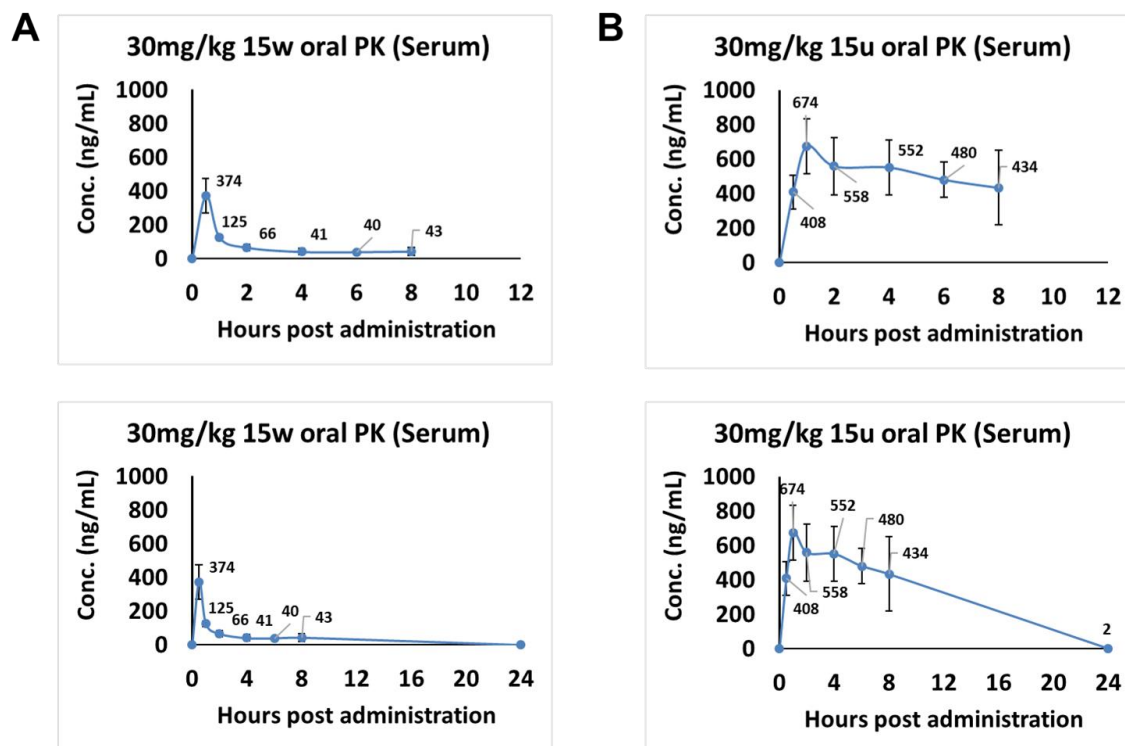
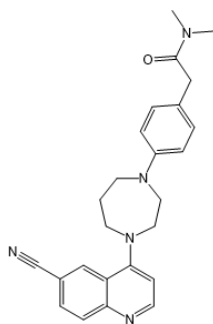
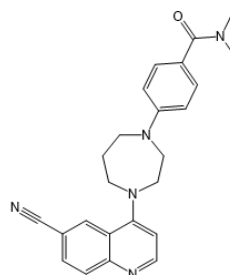
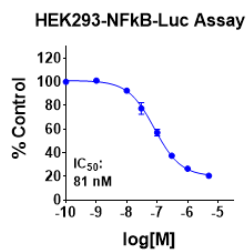


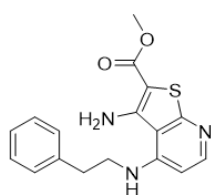
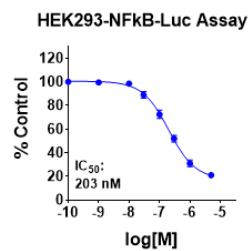
Figure 3.4 15w and 15u oral PK in female CD-1 mice (30mg/kg).



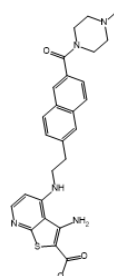
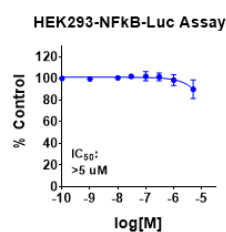
3.6a



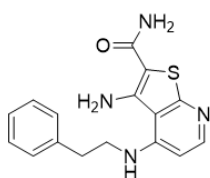
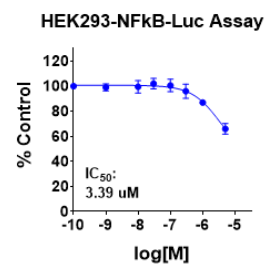
3.6b



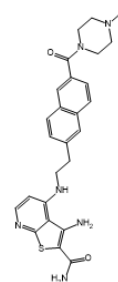
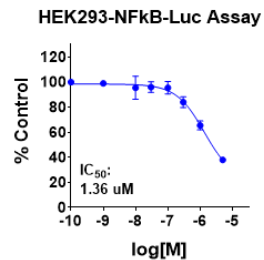
3.9a



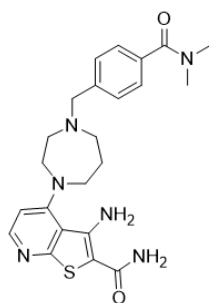
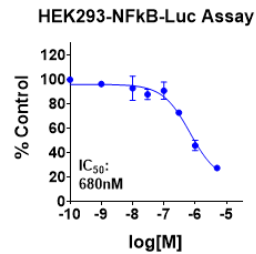
3.9b



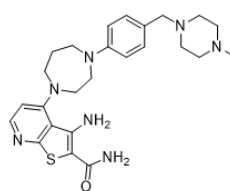
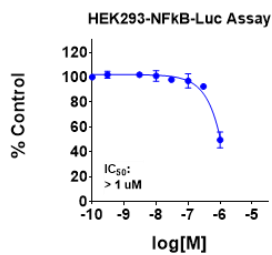
3.11a



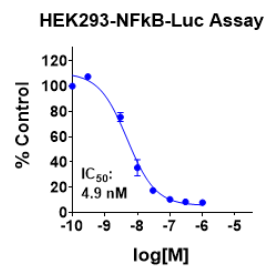
3.11b

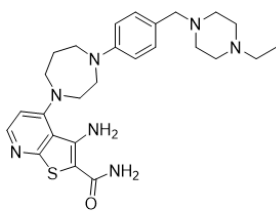


3.19

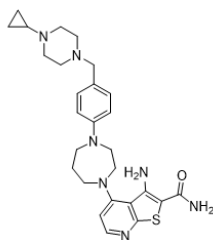
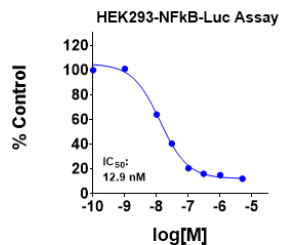


3.26a

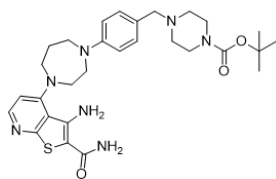
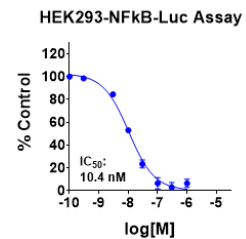




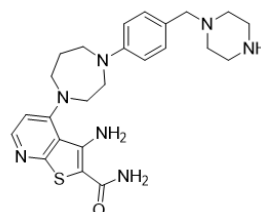
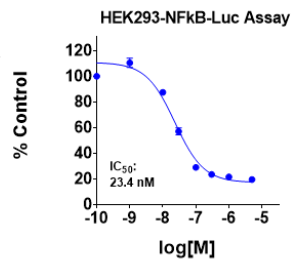
3.26b



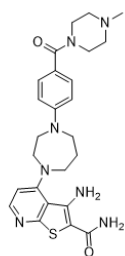
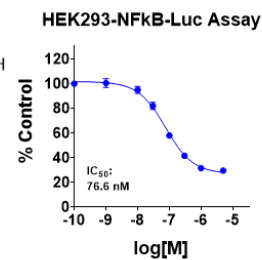
3.26c



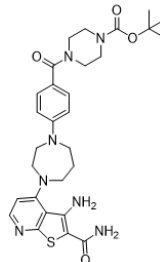
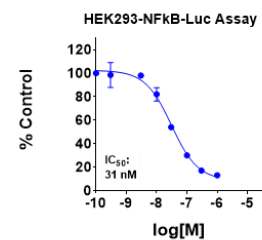
3.32



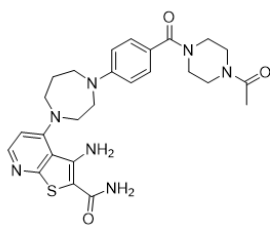
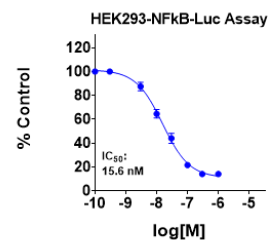
3.33



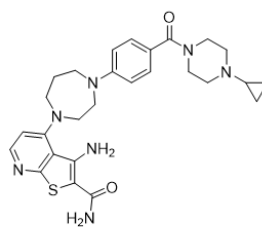
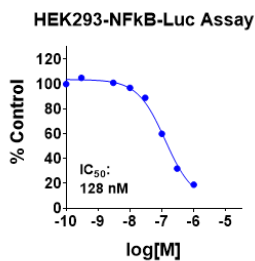
3.43a



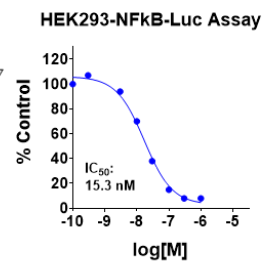
3.43b

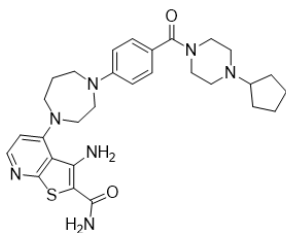


3.43c

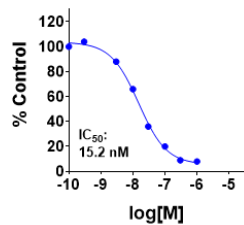


3.43d

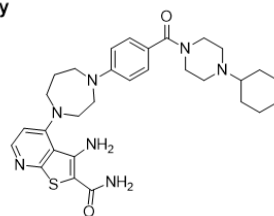




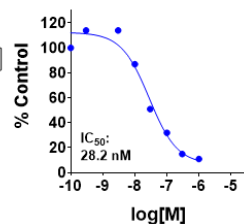
HEK293-NFkB-Luc Assay



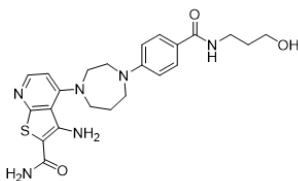
3.43e



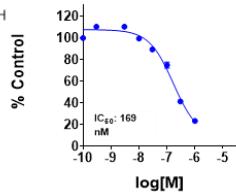
HEK293-NFkB-Luc Assay



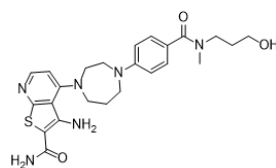
3.43f



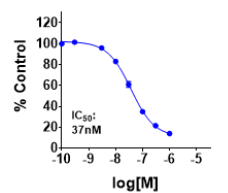
HEK293-NFkB-Luc Assay



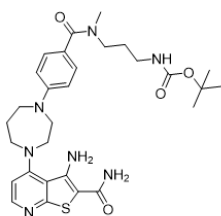
3.43g



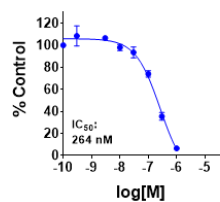
HEK293-NFkB-Luc Assay



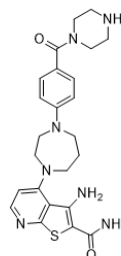
3.43h



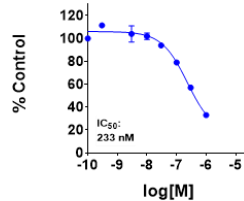
HEK293-NFkB-Luc Assay



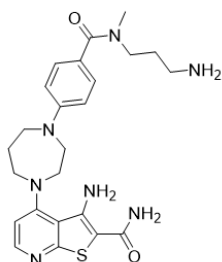
3.43i



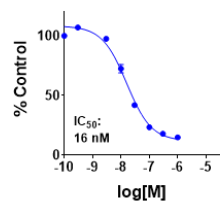
HEK293-NFkB-Luc Assay



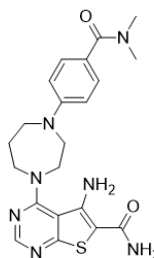
3.44a



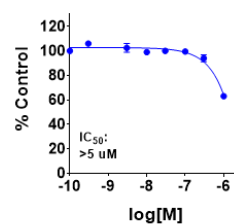
HEK293-NFkB-Luc Assay



3.44b



HEK293-NFkB-Luc Assay



3.48

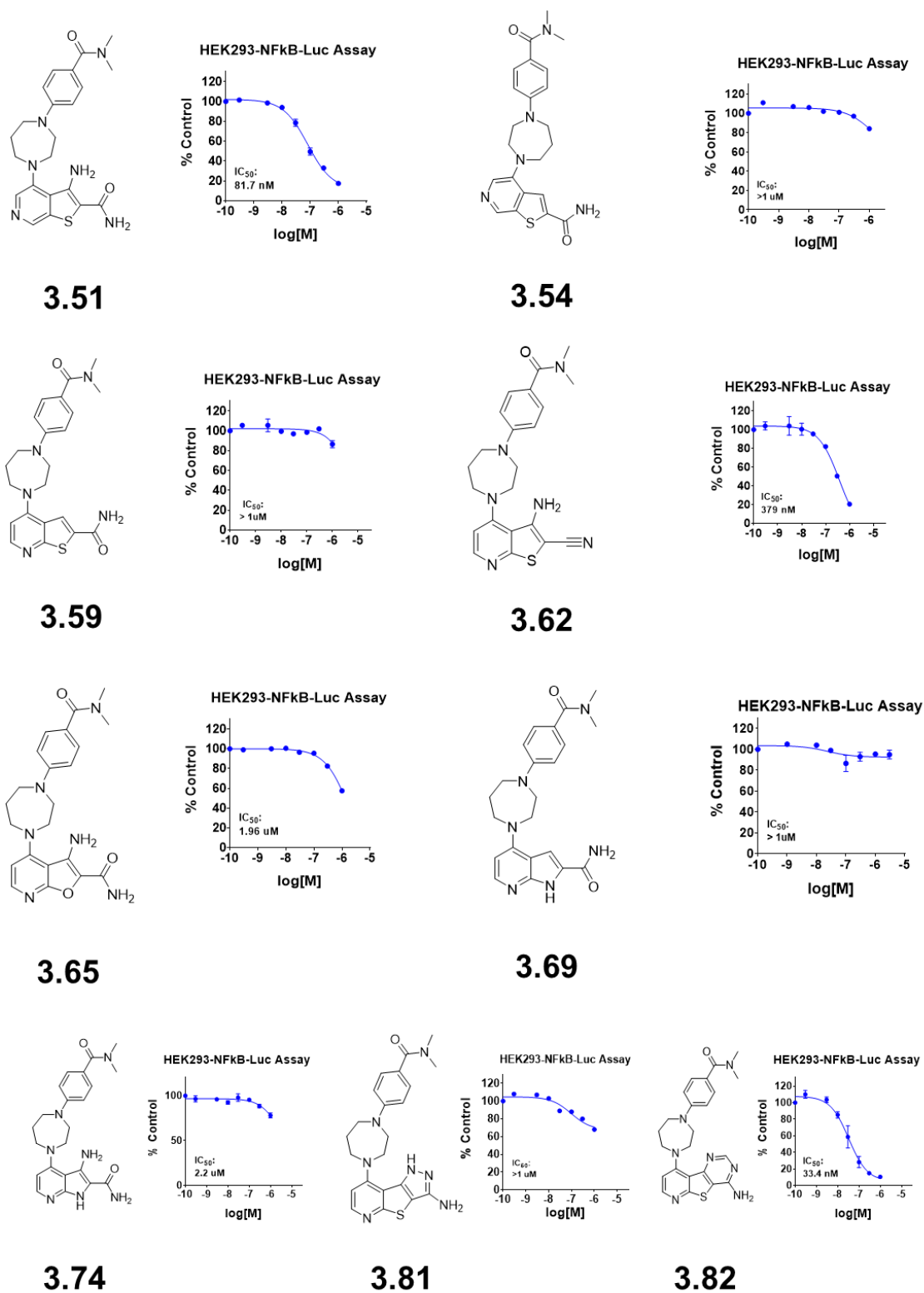


Figure 3.5 The HEK293-NFκB-Luc IC₅₀ curves of tested compounds.

Table 3.1 Structure-activity relationship of hybrid analogues

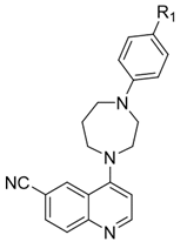
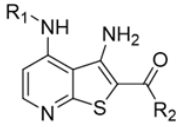
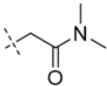
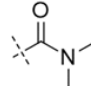
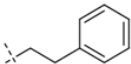
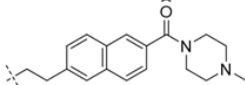
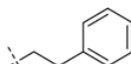
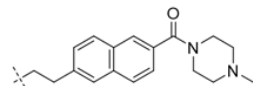
<div style="display: flex; justify-content: space-around; align-items: center;"> <div style="text-align: center;">  <p>3.6</p> </div> <div style="text-align: center;">  <p>3.9, 3.11</p> </div> </div>			
Compound	R1	R2	HEK293-Luc IC ₅₀ (nM)
3.6a		-	81
3.6b		-	203
3.9a		OCH ₃	>5000
3.9b		NH ₂	3390
3.11a		OCH ₃	1360
3.11b		NH ₂	680

Table 3.2 Structure-activity relationship of 15w analogues

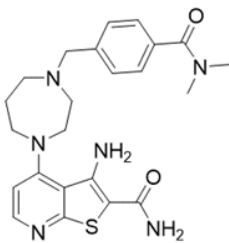
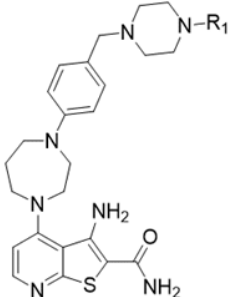
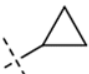
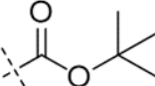
<hr/>		
	3.19	
	3.26, 3.32, 3.33	
<hr/>		
Compound	R1	HEK293-Luc IC ₅₀ (nM)
3.19	-	>1000
3.26a	CH ₃	4.9
3.26b	CH ₂ CH ₃	12.9
3.26c		10.4
3.32		23.4
3.33	H	76.6
<hr/>		

Table 3.3 Structure-activity relationship of 15u analogues

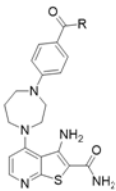
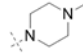
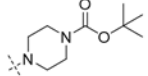
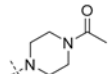
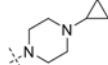
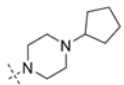
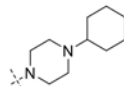
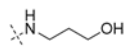
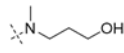
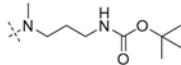
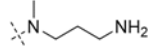
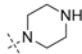
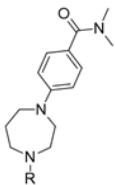
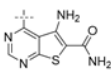
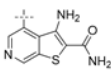
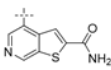
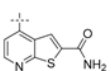
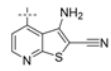
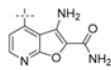
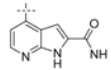
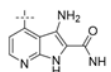
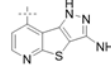
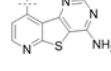
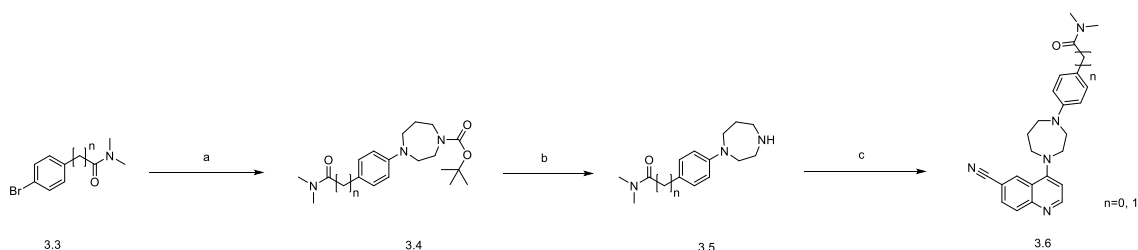
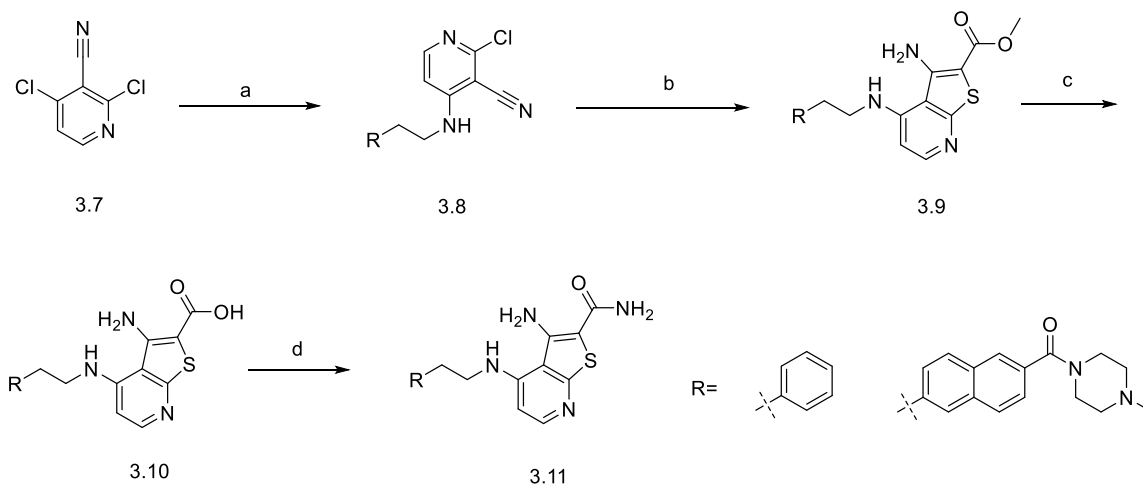
		
Compound	R	HEK293-Luc IC ₅₀ (nM)
3.43a		31
3.43b		15.6
3.43c		128
3.43d		15.3
3.43e		15.2
3.43f		28.2
3.43g		169
3.43h		37
3.43i		264
3.44a		233
3.44b		16

Table 3.4 Structure-activity relationship of 15u analogues

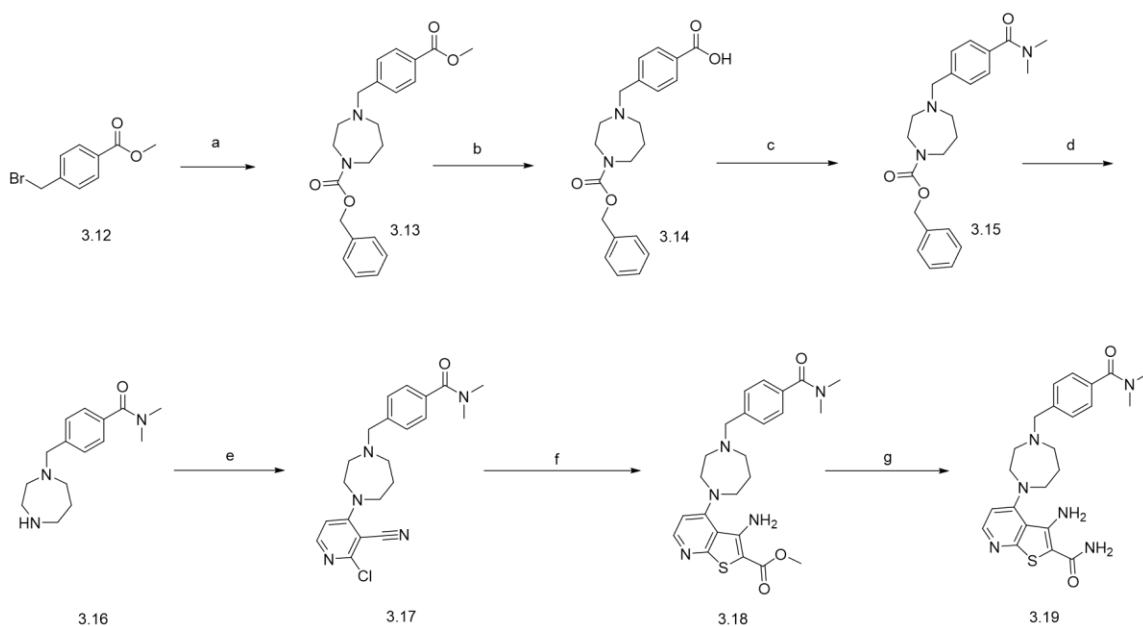
		
Compound	R	HEK293-Luc IC ₅₀ (nM)
3.48		>1000
3.51		81.7
3.54		>1000
3.59		>1000
3.62		379
3.65		>1000
3.69		>1000
3.74		>1000
3.81		>1000
3.82		33.4



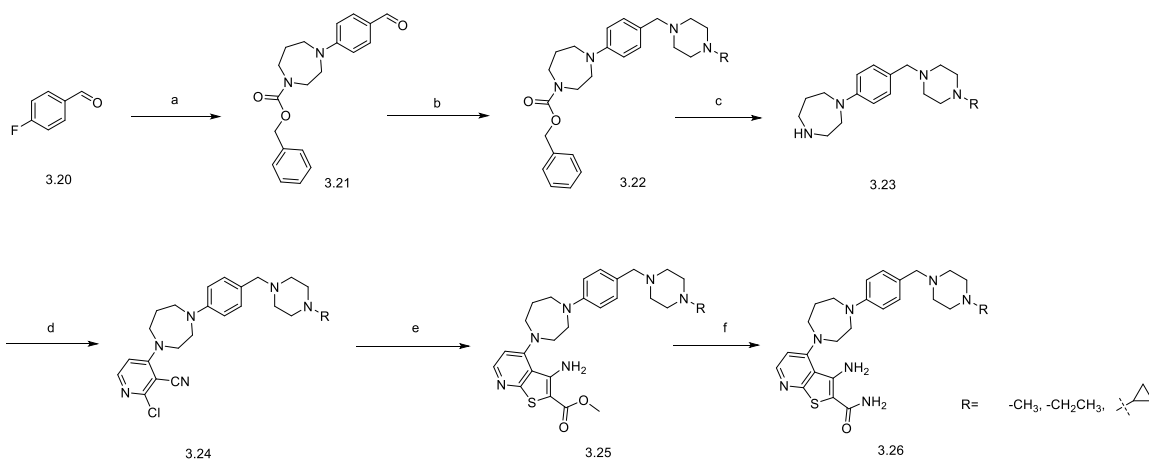
Scheme 3.1 The synthesis of 3.6. Reagents and conditions: (a) tert-butyl 1,4-diazepane-1-carboxylate, 2-dicyclohexylphosphino-2'-(N,N-dimethylamino)biphenyl, $\text{Pd}_2(\text{dba})_3$, t-BuONa, t-BuOH, dioxane, reflux; (b) TFA, DCM, r.t.; (c) 4-chloro-6-(trifluoromethyl)quinoline, TEA, DMSO, 110°C.



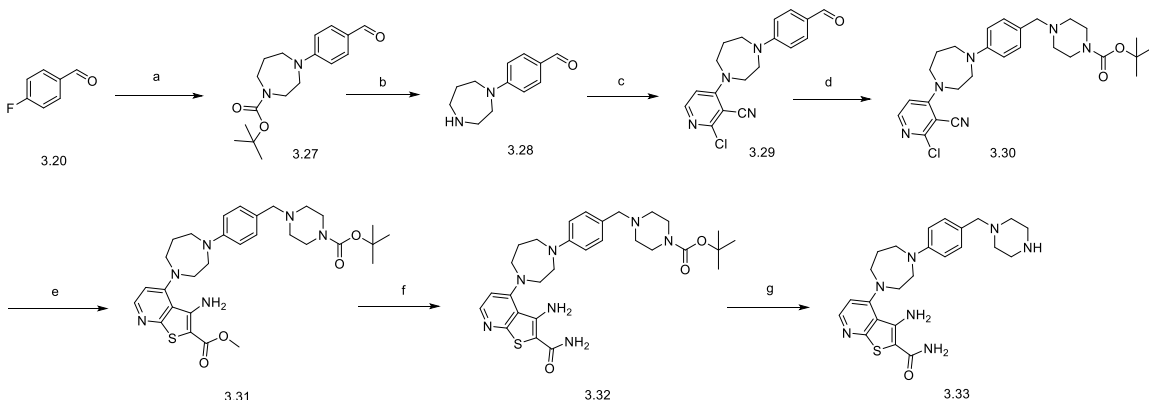
Scheme 3.2 The synthesis of 3.11. Reagents and conditions: (a) 2-phenylethanamine, acetonitrile, TEA, r.t. or 60°C; (b) Na_2CO_3 , methyl 2-sulfanylacetate, DMF, 60°C; (c) LiOH-H₂O, methanol, water, 70°C; (d) HATU, TEA, NH_4OH , DMF, r.t..



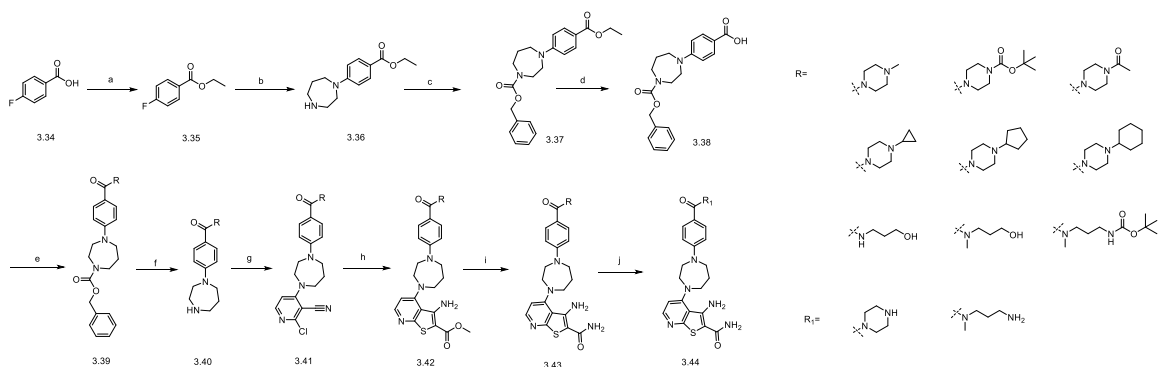
Scheme 3.3 The synthesis of 3.19. Reagents and conditions: (a) benzyl 1,4-diazepane-1-carboxylate, DIEA, THF, reflux; (b) NaOH, EtOH, water, reflux; (c) HATU, TEA, dimethylamine, DMF, r.t.; (d) Pd/C, EtOH, ethyl acetate, H₂, r.t.; (e) 2,4-dichloropyridine-3-carbonitrile, DIPEA, 80°C; (f) methyl 2-sulfanylacetate, MeONa, MeOH, 100°C; (g) LiOH-H₂O, THF, water, 50°C; HATU, DIEA, NH₄OH, DMF, r.t..



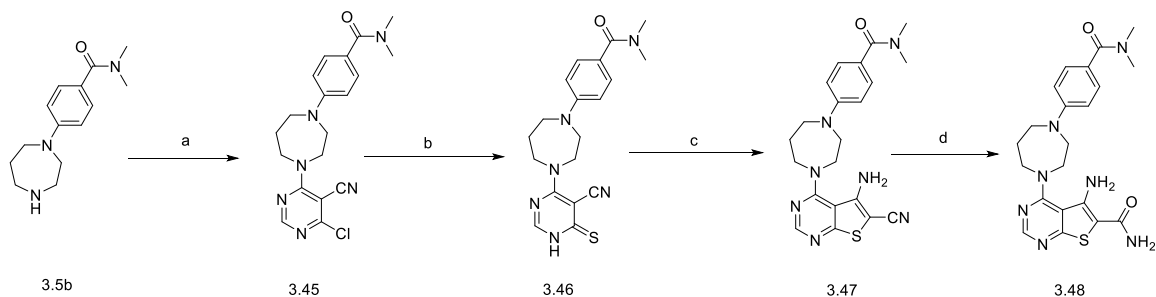
Scheme 3.4 The synthesis of 3.26. Reagents and conditions: (a) benzyl 1,4-diazepane-1-carboxylate, K_2CO_3 , DMF, 90°C ; (b) 1-substituted-piperazine, acetic acid, NaBH_3CN , DCM, r.t.; (c) conc. HCl, r.t.; (d) 2,4-dichloropyridine-3-carbonitrile, DIPEA, 80°C ; (e) methyl 2-sulfanylacetate, MeONa, MeOH, 100°C ; (f) LiOH-H₂O, THF, water, 50°C ; HATU, DIEA, NH_4OH , DMF, r.t..



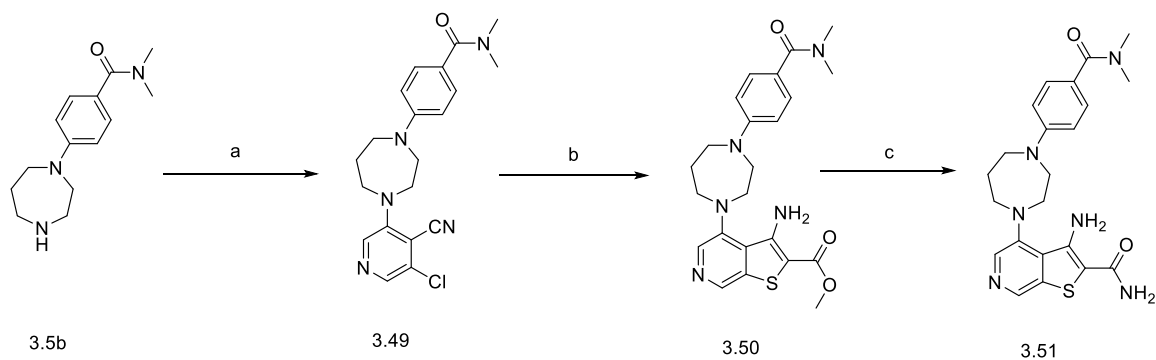
Scheme 3.5 The synthesis of 3.33. Reagents and conditions: (a) tert-butyl 1,4-diazepane-1-carboxylate, K_2CO_3 , DMSO, 110°C ; (b) TFA, DCM, r.t.; (c) 2,4-dichloropyridine-3-carbonitrile, DIPEA, 80°C ; (d) 1-Boc-piperazine, acetic acid, NaBH_3CN , DCM, r.t.; (e) methyl 2-sulfanylacetate, MeONa, MeOH, 100°C ; (f) LiOH-H₂O, THF, water, 50°C ; HATU, DIEA, NH_4OH , DMF, r.t.; (g) TFA, DCM, r.t..



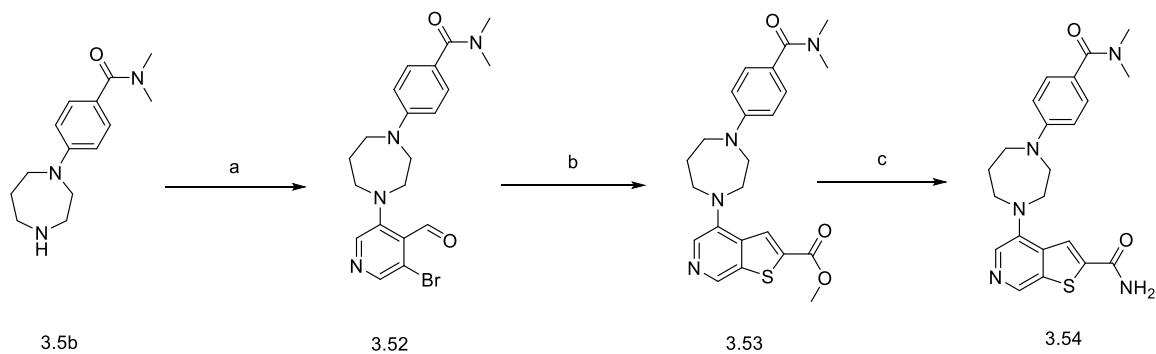
Scheme 3.6 The synthesis of 3.44. Reagents and conditions: (a) ethanol, conc. H_2SO_4 , reflux; (b) 1,4-diazepane, DMSO, $120^\circ C$; (c) benzyl carbonochloridate, DIEA, DCM, r.t.; (d) NaOH, MeOH, water, reflux; (e) amine, HATU, DIEA, DCM, r.t.; (f) Pd/C, H_2 , EtOH, ethyl acetate, r.t.; (g) 2,4-dichloropyridine-3-carbonitrile, DIPEA, $80^\circ C$; (h) methyl 2-sulfanylacacetate, MeONa, MeOH, $100^\circ C$; (i) LiOH- H_2O , THF, water, $50^\circ C$; HATU, DIEA, NH_4OH , DMF, r.t.; (j) TFA, DCM, r.t..



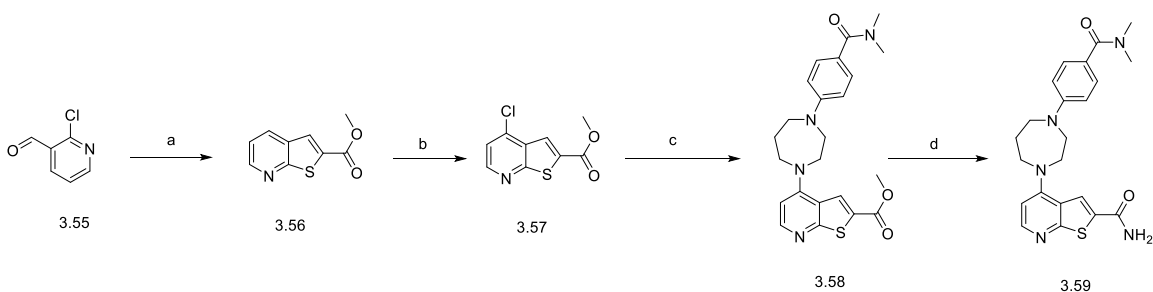
Scheme 3.7 The synthesis of 3.48. Reagents and conditions: (a) 4,6-dichloropyrimidine-5-carbonitrile, DIEA, acetonitrile, $80^\circ C$; (b) thiourea, EtOH, 4N HCl in dioxane, reflux; (c) 2-chloroacetonitrile, KOH, DMF, water, r.t.; (d) KOH, t-BuOH, r.t..



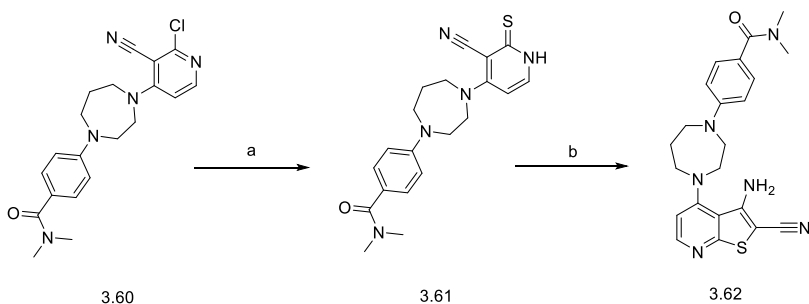
Scheme 3.8 The synthesis of 3.51. Reagents and conditions: (a) 3,5-dichloropyridine-4-carbonitrile, DIEA, DMF, 90°C; (b) methyl 2-sulfanylacetate, MeONa, MeOH, 100°C; (c) LiOH-H₂O, THF, water, 50°C; HATU, DIEA, NH₄OH, DMF, r.t.; (g) TFA, DCM, r.t..



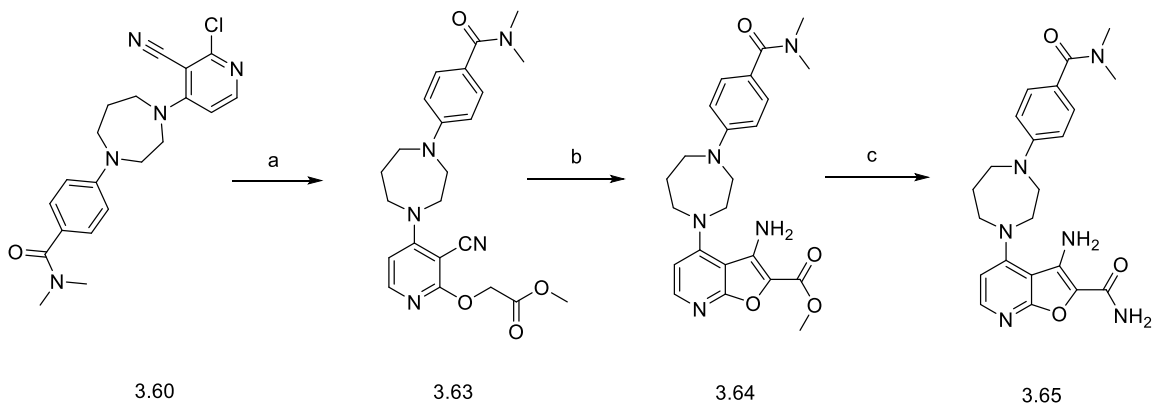
Scheme 3.9 The synthesis of 3.54. Reagents and conditions: (a) 3-bromo-5-fluoro-pyridine-4-carbaldehyde, DIEA, DMSO, 80°C; (b) methyl 2-sulfanylacetate, Cs₂CO₃, THF, 60°C; (c) 2M NH₃ in methanol, sealed, 45°C.



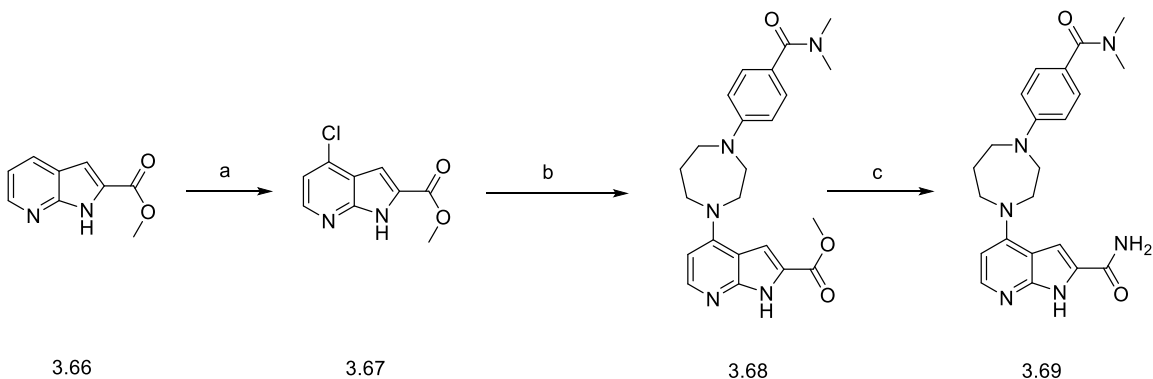
Scheme 3.10 The synthesis of 3.59. Reagents and conditions: (a) methyl 2-sulfanylacrylate, K_2CO_3 , DMF, $80^\circ C$; (b) mCPBA, $CHCl_3$, r.t.; $POCl_3$, $CHCl_3$, $0^\circ C$ to r.t.; (c) 4-(1,4-diazepan-1-yl)-N,N-dimethylbenzamide, DIEA, DMSO, $110^\circ C$; (d) $LiOH \cdot H_2O$, THF, water, $50^\circ C$; HATU, DIEA, NH_4OH , DMF, r.t..



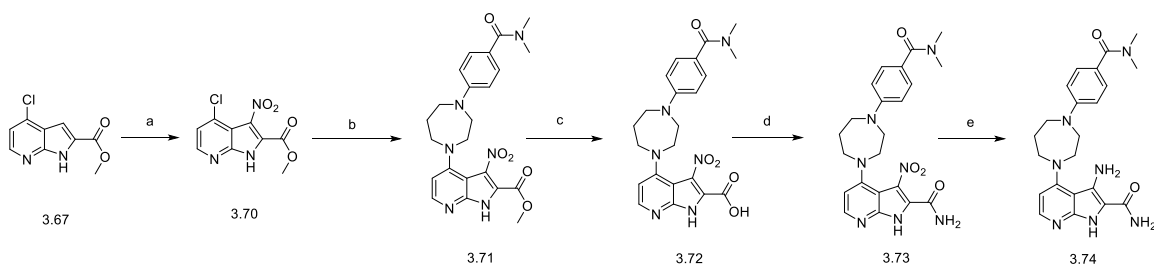
Scheme 3.11 The synthesis of 3.62. Reagents and conditions: (a) thiourea, EtOH, 4N HCl in dioxane, reflux; (b) 2-chloroacetonitrile, KOH, DMF, water, r.t..



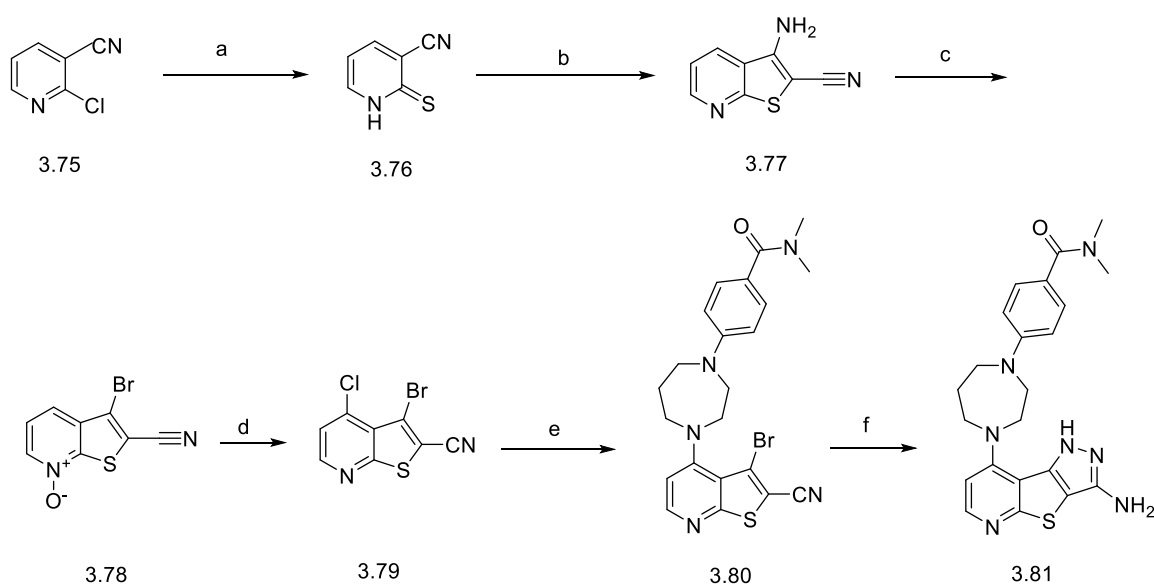
Scheme 3.12 The synthesis of 3.65. Reagents and conditions: (a) methyl 2-hydroxyacetate, NaH, 1,2-dimethoxyethane, nitrogen protected, 60°C; (b) lithium bis(trimethylsilyl)amide, THF, 0°C; (c) LiOH-H₂O, THF, water, 50°C; HATU, DIEA, NH₄OH, DMF, r.t..



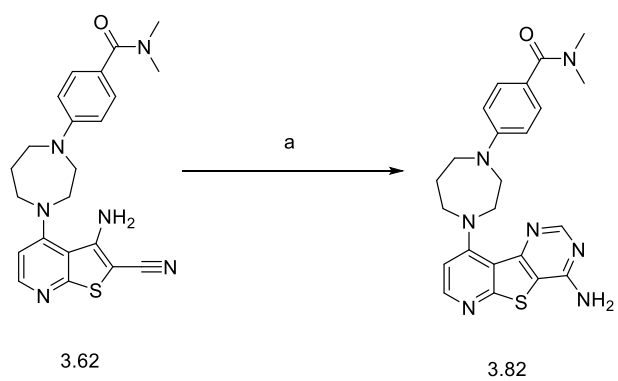
Scheme 3.13 The synthesis of 3.69. Reagents and conditions: (a) mCPBA, diethyl ether, 0°C to r.t.; MsCl, DMF, 60°C; (b) 4-(1,4-diazepan-1-yl)-N,N-dimethyl-benzamide, DIEA, NMP, microwaved at 160°C; (c) LiOH-H₂O, THF, water, 50°C; HATU, DIEA, NH₄OH, DMF, r.t..



Scheme 3.14 The synthesis of 3.74. Reagents and conditions: (a) conc. H₂SO₄, HNO₃, 0°C; (b) 4-(1,4-diazepan-1-yl)-N,N-dimethyl-benzamide, DIEA, t-BuOH, 90°C; (c) LiOH, MeOH, water, 70°C; (d) HATU, DIEA, NH₄OH, DMF, r.t.; (e) Pd/C, EtOH, THF, H₂, r.t..



Scheme 3.15 The synthesis of 3.81. Reagents and conditions: (a) thiourea, EtOH, reflux; (b) 2-chloroacetonitrile, K₂CO₃, acetone, r.t.; (c) CuBr₂, t-BuONO, acetonitrile, 60°C; mCPBA, DCM, 0°C to r.t.; (d) POCl₃, DMF, 0°C to 70 °C; (e) 4-(1,4-diazepan-1-yl)-N,N-dimethyl-benzamide, DIEA, DMSO, 110°C; (f) NH₂NH₂·H₂O, DMSO, sealed and microwaved at 150°C.



Scheme 3.16 Reagents and conditions: (a) formamidine acetate, formamide, 150°C.

CHAPTER 4

DEVELOPMENT OF CDK8/19 DEGRADERS AS POTENTIAL ANTI-CANCER AGENTS

4.1 Introduction

Small molecule drugs are the most frequently used drug modality to regulate the activity of kinases due to their unique advantages, favorable aqueous solubility, good cellular permeability, superb tissue distribution, low manufacture cost, and ease of storage. Despite that, the development of small molecule inhibitors still faces several challenges. First of all, inhibitors are effective in an occupancy-driven pharmacology manner that requires over 90% target occupancy to achieve clinical benefits.⁹ In order to achieve this, high inhibitor concentration is required at the action sites, however, this often leads to adverse effects and toxicity. The long-term use of inhibitors often causes drug resistance due to multiple factors including target protein overexpression, accumulation, mutations, and compensatory pathways.¹⁰⁻¹³ In addition, owing to the high conservation of ATP binding sites among kinases, many kinase inhibitors lack selectivity and result in off-target effects, which reduces the potency of the inhibitors and limits their clinical application.^{183,184} The development of highly selective inhibitors, on the contrary, is difficult and time-consuming. Moreover, kinases often possess both

enzymatic and non-enzymatic functions, such as scaffolding and allosteric regulation.^{1,185} However, the inhibitors can only block the catalytic activity and thus can result in limited therapeutic outcomes. Moreover, drug targets without appropriate binding sites for high affinity can be beyond the scope of small molecule inhibitors and thus classified as undruggable.¹⁸⁶ In order to overcome these challenges and achieve better therapeutic benefits, drug modalities with alternative mechanisms are needed.

The PRoteolysis TArgeting Chimera (PROTAC) strategy, a novel validated modality for target protein degradation, despite its invention and first application two decades ago, has only recently entered the mainstream and become widely applied to a variety of targets, especially kinases. The concept of a PROTAC is derived from UPS-mediated protein degradation.¹⁸⁷ The UPS-mediated degradation can be divided into two steps, protein ubiquitination and proteasome degradation. Protein ubiquitination is carried out by the cooperation of three enzymes, E1 activating enzyme, E2 conjugating enzyme, and E3 ligating enzyme as shown in **Figure 4.1**.¹⁸⁸ Briefly, the C-terminal carboxyl group of ubiquitin molecule forms a thioester bond with the cysteine residue of E1 activating enzyme.¹⁸⁹ Then E1 activating enzyme recruits an E2 conjugating enzyme and passes the ubiquitin molecule onto the cysteine residue of this enzyme through trans(thio)esterification reaction.¹⁹⁰ Finally, an E3 ligating enzyme recruits both target protein and the E2. The ubiquitin on the E2 is transferred directly or indirectly to the substrate protein and forms an iso-peptide bond between the C-terminal glycine of the ubiquitin molecule and the lysine of target protein.¹⁹¹ There are 2

E1s (UBA1 and UBA6), 40 E2s and more than 600 E3s that have been identified as responsible for the ubiquitination of diverse substrate proteins.¹⁹²⁻¹⁹⁴

The ubiquitination process usually forms a polyubiquitin chain on the substrate protein. Since ubiquitin has eight ubiquitin ligation sites (seven lysine residues (Lys6, Lys11, Lys27, Lys29, Lys33, Lys48 and Lys63) and one N-terminal methionine amino group), the final polyubiquitin chain can be homogeneous, mixed or branched, resulting in distinct biological events.¹⁸⁸ For example, lysine 11, 29 and 48 linked polyubiquitin chains cause the degradation of substrate proteins.¹⁹⁵⁻¹⁹⁹ On the contrary, lysine 63 linked polyubiquitin chains exhibit a scaffolding function for substrate recruitment.^{196,200} Once the target proteins are polyubiquitinated at either lysine 11, 29, or 48 with over 4 ubiquitin units, they can be recognized by 26S proteasome in human and undergo degradation.^{198,201} The 26S proteasome consists of one 20S core particle and two 19S regulatory particles.²⁰² The 20S core particle presents a four-stacked heptameric ring structure, the outer two rings (β subunits) bind to 19S regulatory particles, the inner two rings (α subunits) are used for protein degradation. The 19S particle has 19 individual proteins and forms two subunits, the inner 9 protein-subunit ligates to the 20S particle's outer ring, the remaining 10 protein-subunit forms the proteasome lid. The 19S particles can recognize the polyubiquitin chain on target protein, unfold and transfer the protein to 20S core particle for proteolysis in an ATP-dependent manner.^{203,204} Despite that, the polyubiquitinated proteins do not always undergo degradation due to the presence of deubiquitinases (DUBs). The DUBs cause insufficient ubiquitination of target proteins that can either escape

from or not be recognized by proteasome. There are over 100 DUBs that have been identified in humans.^{205,206} By taking advantage of the UPS system, PROTAC technology has been developed and optimized. A PROTAC is a bifunctional molecule that generally contains three components, an E3 ligase binder, a protein of interest (POI) ligand, and linker that connects the two functional molecules. It can therefore recruit both E3 ligase and POI and can then lead to POI being polyubiquitinated by the E3 ligase and recognized by proteasome for degradation (**Figure 4.2**).

Unlike small molecule inhibitors, PROTACs induce POI degradation in an event-driven pharmacology manner. After protein ubiquitination, the PROTAC molecule can be released and becomes involved in another round of the ubiquitination cycle in a catalytic manner. This approach only therefore needs lower concentrations of PROTAC at the action site and potentially reducing side effects and toxicity. Through protein degradation, PROTACs are thus able to eliminate both the enzymatic and non-enzymatic functions of proteins which is particularly important in kinase targeting. For drug targets that lack catalytic binding sites and are undruggable by small molecules, PROTACs can be used since the POI ligands used do not require biological activity and are less dependent on good binding affinity. Even ligands that bind with less affinity to the shallow pockets of target protein may still be adequate for PROTAC development. The mechanism of PROTAC activity makes it less susceptible to drug resistance that develops with small molecule inhibitors. Firstly, POI ligands used in PROTACs are less susceptible to point mutations that diminish biological activity of inhibitors.

Meanwhile, POI degradation by a PROTAC avoids protein accumulation and counteracts compensatory protein overexpression.²⁰⁷⁻²⁰⁹ PROTAC-mediated degradation achieves more extended therapeutic effects than small molecule inhibitors due to its non-stoichiometric property and targeting of protein re-synthesis. Early PROTACs used peptides as the E3 binding motif thus resulting in high molecular weight, poor cellular permeability and lower potency.²¹⁰ The discovery of small molecule E3 ligase ligands significantly reduced the molecular weight of PROTACs. Effective current PROTACs are in the range of 700-1000 Daltons and are more like small molecules that can achieve favorable cell penetration and tissue distribution.²⁰⁹ Compared with kinase inhibitors, PROTACs achieve an additional layer of selectivity due to their bivalent nature and through the E3 engagement thus potentially reducing off-target effects.^{211,212} The advantages of PROTACs described above make them promising agents in both chemical biology studies and drug discovery.

Till now, PROTAC technology has been applied to over 40 drug targets and two PROTACs, ARV-110 and ARV-471 targeting AR and ER respectively are currently under clinical trials for metastatic castration-resistant prostate cancer and advanced/metastatic ER+/Her2- breast cancer.²¹³ Available phase I data has shown that both PROTACs are well tolerated in patients with overall favorable safety and pharmacokinetic profiles, thus representing an exciting milestone in the field of targeted protein degradation. Among PROTACs currently published, kinases are the most frequently studied targets. This is because there are many existing kinase inhibitors with available crystal structures and structure-activity

relationships. In addition, current kinase inhibitors are often associated with the development of drug resistance, which may be overcome by PROTAC-mediated protein degradation. The first PROTACs targeting kinases were peptide-based, however, they were characterized by unfavorable cell permeability, stability and limited potency.^{214,215} The appearance of small molecule E3 ligase binders changed this field and resulted in numerous small molecule-based PROTACs with significantly improved potency and PK profiles.^{216,217} One advantage of a PROTAC is its sub-stoichiometric pharmacology based on using a reversible POI binder. Despite that, some PROTACs targeting kinases have taken advantage of covalent kinase inhibitors.^{218,219} The covalent inhibitor based PROTAC molecule despite losing sub-stoichiometric activities,²¹⁸ achieve increased residence time at the target protein. Therefore, in some cases where reversible PROTACs exhibit minimal degradation effects, covalent based molecules induce significant degradation.¹⁸⁷ Meanwhile, in other cases, the covalent PROTACs ended up with decreased potency.¹⁸⁷ Early development of PROTACs did not progress beyond the *in vitro* level, on the other hand, recent PROTACs advanced to *in vivo* studies mainly due to the improvements in potency and physicochemical properties. In addition, the testing animals are not limited to rodents; large animals such as pigs and monkeys have also been used thus promoting the clinical use of PROTAC molecules.^{220,221}

Current PROTAC development is still largely empirical and laborious without general rules, however, several key features have been identified by further studies.^{20,222-224} The formation of the ternary complex is necessary for

induced degradation, however, it is not sufficient. The ternary complex is formed via PROTAC-mediated protein-protein interactions between E3 ligase and POI. Meanwhile, the PROTAC linker offers additional interactions with recruited proteins due to its flexibility and contributes to the specificity of PROTAC molecule.^{225,226} The formation of the ternary complex is necessary for PROTAC-induced degradation.^{226,227} Despite that, only forming ternary complex is not enough to induce degradation since protein conformation and orientation are critical contributing factors. The protein degradation specificity is dependent on the combination of E3 ligase and the POI. In addition, binding affinity, and selectivity of PROTACs generally are not correlated to their degradation potency and specificity, and a successful PROTAC depends on harmonization of all three components: POI ligand, E3 binder, and linker.

Despite its rapid development and achievements in both preclinical and clinical studies, PROTAC technology still faces several challenges. Although the average molecular weight of effective PROTACs is around 700-1000 Daltons, it is associated with a larger polar surface area, beyond the rule of five for orally available drugs and therefore often encounters cellular permeability and tissue distribution issues. Careful design and refinement of PROTAC molecules may solve these issues and achieve reasonable *in vivo* profile.^{221,228,229} Over 600 E3 ligases exist, however, only fewer than 10 E3 ligases have been used for PROTAC development: CRBN, VHL, Inhibitors of apoptosis proteins (IAPs), Mouse double minute 2 homolog (MDM2), DDB1 and CUL4 associated factor 15 (DCAF15), DCAF16, and Ring finder protein 114 (RNF114).²³⁰⁻²³⁴ Choosing the right

combination of the E3 ligase and POI thus plays an important role in the potency and specificity of PROTAC-mediated degradation.²³⁵ In order to keep pace with the rapid PROTAC development, there is an urgent need for E3 ligase binder discovery. Meanwhile, although PROTAC technology is able to deal with undruggable targets, the majority of current PROTACs are directed at druggable targets with existing ligands. Discovery of ligands for undruggable targets is needed to expand the application of PROTAC technology. The final therapeutic outcome of PROTAC-induced degradation is not merely dependent on the potency of the PROTAC. Other factors including target protein re-synthesis rate and PROTAC 'hook effect'²³⁶ are also significant factors. Compared to small molecule inhibitors, PROTACs are less susceptible to drug resistance due to their mechanism of action. Despite that, studies have shown that long-term use of PROTACs could also cause drug resistance.²³⁷ The resistance does not result from POI binding site mutations but rather from genomic alterations of core components in E3 ligase complexes.²³⁷ In addition, PROTACs are more susceptible to efflux pumps possibly due to their higher molecular weight and flexibility.²³⁸ These unfavorable factors can reduce PROTAC's therapeutic potency and should be taken into consideration at the early stage of PROTAC development.

CDK8 as well as its paralog CDK19 not only exhibit catalytic activity, but also possess non-enzymatic functions which are beyond the scope of conventional CDK8/19 inhibitors.^{90,91,239,240} In such situation, PROTACs targeting CDK8 and CDK19 offer a solution. Currently, there are two published PROTACs that

specifically target CDK8, JH-XI-10-02 and YKL-06-101. JH-XI-10-02 resulted from conjugation between CDK8 inhibitor JH-VIII-49 and CRBN binder pomalidomide via a PEG linker. It induced significant CDK8 degradation at 1 μ M in Jurkat cells without affecting the level of CDK19. In addition, it reduced the phosphorylation of STAT1, a substrate of CDK8.²⁴¹ YKL-06-101, obtained via conjugating the CDK8 inhibitor THZ4-55 with CRBN binder thalidomide through a PEG linker, not only selectively degrades CDK8, but also inhibits mTOR as well. YKL-06-101 induced cell death in human leukemic cells via the combination of CDK8 degradation and mTOR inhibition, which could not be achieved through kinase inhibition alone, suggesting the kinase-independent role of CDK8 in BCR-ABL positive leukemia.⁹⁰

In this chapter, three series of PROTAC molecules are designed and synthesized based on three different CDK8/19 inhibitors: 15u, Senexin C, and BI-1347. The degradation efficacy of resulting PROTACs was determined and the therapeutic potency of candidate PROTACs was evaluated. The candidate PROTAC molecules can be powerful tools in understanding the biological role of CDK8 and CDK19 as well as potential anti-cancer agents.

4.2 Results and Discussion

4.2.1 Synthesis and Structure-Activity Relationship (SAR)

Analysis of PROTACs Targeting CDK8 and CDK19

Three series of PROTAC molecules targeting CDK8/19 were designed and synthesized based on three chemically distinct CDK8/19 kinase inhibitors, 15u, Senexin C, and BI-1347 ²⁴². The three inhibitors were connected with different ubiquitin E3 ligase ligands (CRBN E3 ligase ligand pomalidomide, von Hippel-

Lindau (VHL) VHL ligand VH032 or DCAF16 E3 ligase ligand KB02) via different polyethylene glycol or long-chain alkane linkers. The synthesis schemes of all the compounds are described in detail in Experimental Section. **Table 4.1** presents the structures of 32 obtained PROTAC molecules along with their CDK8 degradation efficacy (at 1 μ M concentration) 293 cells. The most potent PROTACs in each series and corresponding CDK8/19 kinase inhibitors, as well as the previously reported PROTAC JH-XI-10-02 ²⁴¹ are shown in **Figure 4.3**.

According to the results in **Table 4.1**, pomalidomide is effective as the E3 ligase moiety whereas VHL or DCAF16 E3 ligase ligands are not. The degradation efficacy of three series is BI-1347 based PROTACs (**4.45**, **4.48**) > Senexin C based PROTACs (**4.3e**, **4.27d**) > 15u based PROTAC (**4.52**). JH-XI-10-02 (52% CDK8 remaining after 1 μ M treatment) is less potent than the newly developed lead PROTACs. Both polyethylene glycol or long-chain alkane linkers yielded efficient PROTACs, however, the ones with long-chain alkane linkers are more potent, like **4.27d** vs **4.3e** and **4.48** vs **4.45**. Remarkably, the addition of piperazine group between the CDK8-targeting moiety and the linker drastically increased the CDK8 degradation efficiency in different series, as can be seen by the differences between Senexin C-based PROTACs (**4.3a** vs **4.3e**), BI1347-based PROTACs (**4.45** vs **4.51**) and 15u-based PROTACs (**4.52** vs **4.4c**). This is very likely due to the fact that piperazine ring gives an appropriate orientation for the PROTAC molecule at the front pocket of CDK8 that contributes to the ternary complex formation. In addition, the CDK8 inhibitory activity of JH-XI-10-02, Senexin C-based PROTACs (**4.3a** and **4.3e**), and BI1347-based PROTACs (**4.45** and **4.51**)

were determined via HEK293 NF κ B cell based assay. JH-XI-10-02 and **4.3e** exhibit negligible inhibitory activity with IC₅₀ values over 5 μ M. **4.3a** shows a IC₅₀ value of 2.5 μ M. Meanwhile, the CDK8 inhibitory IC₅₀ values of **4.45** and **4.51** are 80nM and 41nM, suggesting that BI1347-based PROTACs **4.45** and **4.51** act as both CDK8 inhibitors and degraders.

The CDK8 and CDK19 degradation of lead PROTACs as well as reported PROTAC JH-XI-10-02 in **Figure 4.3** were evaluated in HEK293 cells via western blots as shown in **Figure 4.4**. **4.48** is the most potent CDK8 degrader in this set and JH-XI-10-02 is the least potent. In addition, both Senexin C-based and BI1347-based PROTACs induce significant degradation of CDK19 (**Figure 4.4B, D, E**), whereas JH-XI-10-02 has no effect on CDK19. Therefore, the lead PROTACs are not only more efficient than JH-XI-10-02 but also induce the degradation of both CDK8 and CDK19. Moreover, the level of CCNC, the binding partner of CDK8 and CDK19, is also decreased by the lead PROTACs, which is known to be protected from proteolytic degradation by its interaction with CDK8.²⁴³ The DC₅₀ (half maximal degradation concentration) values of most potent Senexin C- and BI1347-based PROTACs on CDK8 and CDK19 degradation in 293 cells were calculated as shown in **Figure 4.4F, G**. The corresponding CDK8 DC₅₀ values are 46 nM for **4.27d**, 6.6 nM for **4.45** and 2.8 nM for **4.48**, and CDK19 DC₅₀ values are 1 μ M for **4.27d**, 25 nM for **4.45** and 10 nM for **4.48**.

The UPS-dependent degradation of CDK8/19 by the newly developed PROTACs was confirmed as shown in **Figure 4.5**. The effects of Senexin C-based PROTAC **4.3e** (200 nM and 1 μ M) on CDK8 degradation in HEK293 cells in the

presence or absence of a proteasome inhibitor MG132 (5 μ M), CRBN E3 ligase ligand pomalidomide (5 μ M) and CDK8/19 inhibitor Senexin C (5 μ M). Only **4.3e** but not pomalidomide or Senexin C induced CDK8 degradation, and the effect of HP8580 was reversed by proteasome inhibition with MG132 as well as by competition with pomalidomide or Senexin C.

4.2.2 Novel PROTACs Induce the Degradation of CDK8 and CDK19 in Different Cell Lines and Species

Since the PROTAC JH-XI-10-02 was reported to exert its strongest CDK8 degradation effect in Jurkat leukemia (T-ALL) cells ²⁴¹, the lead Senexin C-based PROTACs (**4.3e** and **4.27d**) and BI-1347-based PROTACs (**4.45** and **4.48**) along with JH-XI-10-02 were tested in Jurkat leukemia cell line as well (**Figure 4.6**). CDK8 degradation by JH-XI-10-02 was at a similar extent in Jurkat and HEK293 and the effects of both Senexin C-based and BI-1347-based PROTACs were much stronger than those of JH-XI-10-02. Furthermore, these PROTACs induced CDK19 and CCNC degradation, whereas JH-XI-10-02 had no apparent effect on these proteins.

The CDK8/19 degradation effects of lead PROTACs **4.3e**, **4.27d** and **4.48** were also evaluated in other human cell lines as shown in **Figure 4.7**, including 22Rv1 prostate cancer (expressing more CDK19 than CDK8), MV4-11 (AML) and HAP-1 (CML) leukemia cell lines, HTB-185 medulloblastoma, and SAOS2 and SJSA-1 osteosarcoma (SJSA-1 naturally only express CDK19 but not CDK8). Although the extent of CDK8 and CDK19 degradation varied between different cell

lines, both **4.48** and **4.27d** significantly degraded CDK8 and CDK19 in all the tested cell lines.

4.48 was also tested for the ability to degrade CDK8 and CDK19 in cell lines from other mammalian species, including murine CT26 colon carcinoma (**Figure 4.8A**) and canine Abrams osteosarcoma (**Figure 4.8B**) cells, and was found to induce CDK8 degradation in both cell lines and induce CDK19 degradation in Abrams cells (CT26 does not express CDK19). **Figure 4.9** shows the time course of CDK8 degradation by 100 nM **4.48** in human HEK293 and murine CT26 cells. Both the extent and the kinetics of CDK8 degradation were similar between two cell lines, with maximum degradation after 8 hours PROTAC treatment.

Hence the novel PROTACs degrade CDK8 and CDK19 in a broad spectrum of cell types and mammals.

4.2.3 Cellular Effects of CDK8/19 Degrading PROTACs.

CDK8 and CDK19 are known to phosphorylate transcription factor STAT1 at S727 (although STAT1 S727 phosphorylation can also be exerted by other kinases)¹⁷⁸. The effects of **4.3e**, **4.27d**, **4.45** and **4.48** on CDK8 degradation and STAT1 S727 phosphorylation in HEK293, 22Rv1 and Jurkat cells were evaluated as shown in **Figure 4.10**. As expected, CDK8 degradation by all PROTACs was associated with decreased STAT1 S727 phosphorylation.

CDK8/19 act as transcriptional regulators, and therefore the effects of 3-day treatment with 200 nM PROTAC **4.48** along with 200 nM CDK8/19 kinase inhibitor BI-1347 on a series of CDK8/19-regulated genes were evaluated via qPCR. As shown in **Figure 4.11**, both **4.48** and **BI-1347** exhibit similar effects on

the expression of tested genes in wild-type HEK293 cells; meanwhile, in HEK293 dKO cells, **4.48** and **BI-1347** had no effects in dKO cells as well, confirming their target selectivity. Thus, CDK8/19 PROTACs are able to reproduce the transcriptional effects of CDK8/19 kinase inhibitors and CDK8/19 knockout.

The stability of transcriptional changes induced either by PROTAC or by a kinase inhibitor were evaluated as shown in **Figure 12A**. HEK293 cells were treated with 200 nM of BI-1347 or **4.48** for 3 days, and then the inhibitor and PROTAC were washed off and the restoration of transcriptional changes was monitored 24 hrs and 48 hrs after wash-off. The effects of BI-1347 were largely maintained 24 hrs after wash-off but mostly disappeared 48 hrs after wash-off. In contrast, the transcriptional effects of the PROTAC **4.48** were maintained even 48 hrs after wash-off, indicating that CDK8/19 PROTACs have a more sustained transcriptional effect than CDK8/19 kinase inhibitors. In concordance with this observation, the WB result (**Figure 12B**) shows that the effects of **4.48** on CDK8/CDK19/CCNC protein degradation and STAT1 S727 phosphorylation remained nearly unchanged in HEK293 cells within 24 hours after wash-off.

4.2.4 Effects of CDK8/19 PROTACs on Leukemia Cell Growth

The anti-proliferative effects of the most potent PROTAC **4.48** and its parental kinase inhibitor **BI-1347** were compared in leukemia cell lines. In the long-term treatment experiment as shown in **Figure 13A**. Jurkat cells (0.1 million cells) were continuously treated with vehicle control (0.1% DMSO), 200 nM BI-1347 or 200 nM **4.48** for 32 days (each condition in biological triplicates; every 7-8 days, cells were counted and 0.1 million cells were passaged to a new T25 flask to

propagate under the same treatment conditions). The kinase inhibitor **BI-1347** had a stronger growth inhibition effect than the PROTAC **4.48** at the first passage. However, in later passages, the growth rates of **BI-1347** treated cells were increasing, indicating the development of resistance, while the growth rates of **4.48** treated cells were decreasing, demonstrating that PROTAC can provide a more sustained growth inhibition of CDK8/19-dependent leukemia cells. This sustained inhibition property of PROTAC was also observed in MV4-11, a leukemia cell line highly sensitive to CDK8/19 kinase inhibitors. As shown in **Figure 13B**, BI-1347 strongly inhibited MV4-11 cells at the beginning, however, resistance developed in ~5-6 weeks. On the other hand, growth inhibition by **4.48** was much more stable than by BI-1347.

The stability of short-term growth inhibition induced by PROTAC **4.48** and inhibitor BI-1347 was evaluated via a wash-off study in Jurkat cells as shown in **Figure 13C**. Jurkat cells were pre-treated with 200 nM **BI-1347** or **4.48** for 8 days before removal of drug-containing media and further cultured in either drug-containing (200 nM) or drug-free media for 8 days before counting the cell numbers. Removal of **BI-1347** led to 7.1 fold increase of the cell number while removal of **4.48** increased the cell number only 1.8 fold, indicating that PROTACs can provide more benefits than CDK8/19 kinase inhibitors in treating leukemia.

4.2.5 *In vivo* activity of CDK8/19-degrading PROTACs

To determine if CDK8/19 targeting PROTACs can degrade CDK8 and affect CDK8-regulated gene expression *in vivo*, the PROTACs **4.45** and **4.48** were tested in a CT26 murine colon carcinoma mice model, where the PROTACs were able to

degrade CDK8 in CT26 cells. CT26 cells were injected subcutaneously into syngeneic Balb/c female mice and allowed to grow to 150~200 mm³. Tumor-bearing mice then received PROTACs **4.45** or **4.48** by oral gavage at 20 mg/kg in 30% propylene glycol / 70% PEG-400 vehicle. Tumors were collected 2, 8 or 24 hrs after dosing and used to measure protein levels of CDK8, pSTAT1 at Ser727, and total STAT1 (by western blotting) and mRNA expression of CCL12, a gene that is inhibited by different CDK8/19 inhibitors in CT26 tumors *in vivo* (by qPCR). As shown in **Figure 14A**, CDK8 levels were decreased in most of the tumor extracts collected 2 hrs or 8 hrs after dosing with **4.45** and in some of the tumors 2 hrs or 8 hrs after dosing with **4.48**. In addition, the levels of pSTAT1 at Ser727 and total STAT1 were decreased as well in most of the tumors collected 2 hrs or 8 hrs after dosing with **4.45** or **4.48**. The levels of CCL12 were also decreased in tumors treated with **4.45** or **4.48** 2 hrs or 8 hrs (but not 24 hrs) after dosing (**Figure 14B**). Hence, PROTACs **4.45** and **4.48** can induce CDK8 degradation and inhibit CDK8 activity *in vivo*.

4.2.6 Senexin C-based PROTACs distinguish between Cyclin C-bound and unbound CDK8

The CDK8 degradation effect of Senexin C-based PROTAC **4.27d** were tested in different cell lines. However, in the Loucy cells (T-cell leukemia), **4.27d** induced only very weak degradation of CDK8 and CDK19 (**Figure 15A**). This cell line is naturally lacking Cyclin C (CCNC), the binding partner of CDK8/19. To test if the absence of CDK8-bound CCNC was responsible for the degradation activity loss of **4.27d**, PROTAC **4.27d** was tested on a HEK293 derivative cell line

(CRISPR-mediated knockout of CCNC). While **4.27d** efficiently degraded CDK8 and CDK19 in the wild-type 293 cells, it was ineffective in the CCNC-defective HEK293 cells (**Figure 15B**), demonstrating that CCNC-unbound conformation of CDK8/19 is resistant to degradation by Senexin C-based PROTACs. In contrast, BI-1347-based PROTACs **4.45** and **4.48** efficiently degraded CDK8 and CDK19 in CCNC-defective HEK293 cells (**Figure 15C**) as well as in Loucy cells (**Figure 15D**). These results indicate that the Senexin C- and BI-1347- based PROTACs can be used as chemical probes to identify the fractions of CDK8 or CDK19 that are bound or unbound to CCNC.

4.3 Conclusions

Three series of novel PROTAC molecules targeting CDK8 and CDK19 have been designed and synthesized. The lead PROTACs are much more potent than the reported PROTAC JH-XI-10-02, and significantly degrade both CDK8 and CDK19 along with their binding partner CCNC in a broad spectrum of human and other mammalian cell lines. PROTAC inhibits STAT1-s727 phosphorylation and reproduces the transcriptional effects of its parental CDK8/19 inhibitor, however, in a more sustained manner. In addition, PROTAC exhibits stronger long-term inhibition of leukemia cell growth compared to the parental CDK8/19 inhibitor. Moreover, the Senexin C-based PROTACs degrade CDK8/19 only in the presence of Cyclin C, while the BI-1347-based PROTACs are Cyclin C-independent. These novel CDK8/19 PROTACs not only can be used as chemical probes to study the biological roles of CDK8/19 but also as potential anti-cancer agents. Furthermore,

the achieved SAR can be used for the further PROTAC development and optimization.

4.4 Experimental Section

4.4.1 Chemistry

All chemical reagents and solvents were purchased from commercial sources and used without further purification. The reactions were monitored by thin-layer chromatography (TLC), visualized by UV light (254 or 365 nm). The microwave oven reactions were conducted via Biotage microwave reactor. The purification of the products was finished by Biotage flash chromatography using silica gel columns. All NMR spectra were recorded with a Bruker spectrometer at 300 or 400 MHz in deuterated solvents. High-performance liquid chromatography (HPLC) and Mass spectra (MS) were used to confirm the purity and molecular weight of each compound. All compounds are >95% pure by HPLC analysis (data included in the Supporting Information).

The general preparation of **4.1**.

To a 10 mL microwave tube was added a solution of 2-(2,6-dioxo-3-piperidyl)-4-fluoro-isoindoline-1,3-dione (1eq) in DMF. Then amine analogs (1eq) and DIEA (3eq) were added and the mixture was microwaved at 150°C for 2h. Upon completion, the mixture was condensed and purified by flash column chromatography using a gradient of 0-10% MeOH/DCM to give target compounds **4.1**.

tert-butyl 3-[2-[2-[[2-(2,6-dioxo-3-piperidyl)-1,3-dioxo-isoindolin-4-yl]amino]ethoxy]ethoxy]propanoate (**4.1a** (n=2))

A yellow solid (216 mg, 49% yield). ESI-MS m/z : 490 ($[M+H]^+$). 1H -NMR (300MHz, CD_2Cl_2): 8.35 (s, 1H), 7.51 (t, $J=7.8$ Hz, 1H), 7.07 (d, $J=7.4$ Hz, 1H), 6.96 (d, $J=7.4$ Hz, 1H), 6.48 (m, 1H), 4.91 (m, 1H), 3.69 (m, 4H), 3.61 (m, 4H), 3.46 (q, $J=5.3$ Hz, 2H), 2.81 (m, 2H), 2.73 (m, 1H), 2.45 (t, $J=6.6$ Hz, 2H), 2.12 (m, 1H), 1.42 (s, 9H).

tert-butyl 3-[2-[2-[2-[[2-(2,6-dioxo-3-piperidyl)-1,3-dioxo-isoindolin-4-yl]amino]ethoxy]ethoxy]ethoxy]propanoate (**4.1b** ($n=3$))

A yellow solid (199 mg, 47% yield). ESI-MS m/z : 534 ($[M+H]^+$). 1H -NMR (300MHz, DMSO- d_6): 11.07 (s, 1H), 7.58 (t, $J=8.5$ Hz, 1H), 7.15 (d, $J=8.4$ Hz, 1H), 7.04 (d, $J=8.5$ Hz, 1H), 6.60 (m, 1H), 5.06 (m, 1H), 3.61-3.47 (m, 14H), 2.88 (m, 1H), 2.57 (m, 2H), 2.39 (t, $J=6.4$ Hz, 2H), 2.02 (m, 1H), 1.38 (s, 9H).

tert-butyl 3-[2-[2-[2-[2-[[2-(2,6-dioxo-3-piperidyl)-1,3-dioxo-isoindolin-4-yl]amino]ethoxy]ethoxy]ethoxy]ethoxy]propanoate (**4.1c** ($n=4$))

A yellow solid (209 mg, 50% yield). ESI-MS m/z : 578 ($[M+H]^+$). 1H -NMR (300MHz, DMSO- d_6): 11.07 (s, 1H), 7.58 (t, $J=8.5$ Hz, 1H), 7.15 (d, $J=8.4$ Hz, 1H), 7.04 (d, $J=8.5$ Hz, 1H), 6.60 (m, 1H), 5.06 (m, 1H), 3.62-3.44 (m, 18H), 2.89 (m, 1H), 2.55 (m, 2H), 2.40 (t, $J=6.4$ Hz, 2H), 2.02 (m, 1H), 1.38 (s, 9H).

tert-butyl 3-[2-[2-[2-[2-[2-[[2-(2,6-dioxo-3-piperidyl)-1,3-dioxo-isoindolin-4-yl]amino]ethoxy]ethoxy]ethoxy]ethoxy]ethoxy]propanoate (**4.1d** ($n=5$))

A yellow solid (254 mg, 51% yield). ESI-MS m/z : 622 ($[M+H]^+$). 1H -NMR (300MHz, CD_2Cl_2): 8.59 (s, 1H), 7.51 (t, $J=8.1$ Hz, 1H), 7.07 (d, $J=6.9$ Hz, 1H), 6.96 (d, $J=6.9$ Hz, 1H), 6.52 (m, 1H), 4.91 (m, 1H), 3.69-3.45 (m, 22H), 2.77 (m, 3H), 2.45 (t, $J=6.4$ Hz, 2H), 2.10 (m, 1H), 1.43 (s, 9H).

tert-butyl 3-[2-[2-[2-[2-[2-[2-[(2,6-dioxo-3-piperidyl)-1,3-dioxo-isoindolin-4-yl]amino]ethoxy]ethoxy]ethoxy]ethoxy]ethoxy]ethoxy]propanoate (**4.1e (n=6)**)

A yellow solid (177 mg, 33% yield). ESI-MS m/z : 666 ($[M+H]^+$). 1H -NMR (300MHz, CD_2Cl_2): 8.36 (s, 1H), 7.51 (t, $J=8.1$ Hz, 1H), 7.07 (d, $J=6.9$ Hz, 1H), 6.96 (d, $J=6.9$ Hz, 1H), 6.49 (m, 1H), 4.90 (m, 1H), 3.71-3.52 (m, 24H), 3.47 (m, 2H), 2.79 (m, 3H), 2.46 (t, $J=6.4$ Hz, 2H), 2.11 (m, 1H), 1.42 (s, 9H).

The general preparation of **4.2**.

To a 10 mL round was added a solution of **4.1** (1eq) in formic acid. Then the mixture was stirred at room temperature for overnight. Upon completion, the mixture was condensed and purified by flash column chromatography using a gradient of 0-10% MeOH/DCM to give target compounds **4.2**.

3-[2-[2-[[2-(2,6-dioxo-3-piperidyl)-1,3-dioxo-isoindolin-4-yl]amino]ethoxy]ethoxy]propanoic acid (**4.2a (n=2)**)

A yellow solid (186 mg, 97% yield). ESI-MS m/z : 434 ($[M+H]^+$). 1H -NMR (300MHz, CD_2Cl_2): 8.76 (s, 1H), 7.51 (t, $J=8.0$ Hz, 1H), 7.07 (d, $J=7.4$ Hz, 1H), 6.95 (d, $J=7.4$ Hz, 1H), 6.50 (m, 1H), 4.93 (m, 1H), 3.71 (m, 4H), 3.64 (s, 4H), 3.46 (m, 2H), 2.78 (m, 3H), 2.60 (t, $J=6.4$ Hz, 2H), 2.11 (m, 1H).

3-[2-[2-[2-[[2-(2,6-dioxo-3-piperidyl)-1,3-dioxo-isoindolin-4-yl]amino]ethoxy]ethoxy]ethoxy]propanoic acid (**4.2b (n=3)**)

A yellow solid (143 mg, 80% yield). ESI-MS m/z : 478 ($[M+H]^+$). 1H -NMR (300MHz, CD_2Cl_2): 8.91 (s, 1H), 7.51 (t, $J=8.0$ Hz, 1H), 7.07 (d, $J=7.4$ Hz, 1H), 6.95 (d, $J=7.4$ Hz, 1H), 6.50 (m, 1H), 4.93 (m, 1H), 3.71 (m, 2H), 3.63 (s, 4H), 3.60 (s, 4H), 3.46 (m, 2H), 2.78 (m, 3H), 2.58 (t, $J=6.4$ Hz, 2H), 2.11 (m, 1H).

3-[2-[2-[2-[2-[[2-(2,6-dioxo-3-piperidyl)-1,3-dioxo-isoindolin-4-

yl]amino]ethoxy]ethoxy]ethoxy]ethoxy]propanoic acid (4.2c (n=4))

A yellow solid (177 mg, 98% yield). ESI-MS m/z : 522 ($[M+H]^+$). 1H -NMR (300MHz, DMSO- d_6): 11.09 (s, 1H), 8.15 (s, 1H), 7.58 (t, $J=8.3$ Hz, 1H), 7.15 (d, $J=8.9$ Hz, 1H), 7.04 (d, $J=7.2$ Hz, 1H), 6.60 (m, 1H), 5.05 (m, 1H), 3.62-3.44 (m, 18H), 2.88 (m, 1H), 2.55 (m, 2H), 2.43 (t, $J=6.4$ Hz, 2H), 2.02 (m, 1H).

3-[2-[2-[2-[2-[2-[[2-(2,6-dioxo-3-piperidyl)-1,3-dioxo-isoindolin-4-

yl]amino]ethoxy]ethoxy]ethoxy]ethoxy]ethoxy]propanoic acid (4.2d (n=5))

A yellow solid (200 mg, 92% yield) and used without further purification. ESI-MS m/z : 566 ($[M+H]^+$).

3-[2-[2-[2-[2-[2-[2-[[2-(2,6-dioxo-3-piperidyl)-1,3-dioxo-isoindolin-4-

yl]amino]ethoxy]ethoxy]ethoxy]ethoxy]ethoxy]ethoxy]propanoic acid (4.2e (n=6))

A yellow solid (143 mg, 94% yield) and used without further purification. ESI-MS m/z : 610 ($[M+H]^+$).

The general preparation of **4.3**.

To a 10 mL round-bottle flask was added a solution of **4.2** (1eq) and **2.20** (1eq) in DMF. Then EDC-HCl (2eq), HOAt (2eq), and N-methylmorpholine (5eq) were added and the mixture was stirred at room temperature for overnight. Upon completion, the mixture was diluted with DCM, added with water, extracted with DCM, the organic layers were combined, dried by Na_2SO_4 , condensed and purified by flash column chromatography using a gradient of 0-10% MeOH/DCM to give target compounds **4.3**.

6-[2-[(6-cyano-4-quinolyl)amino]ethyl]-N-[3-[3-[2-[2-[2-[2-[2-(2,6-dioxo-3-piperidyl)-1,3-dioxo-isoindolin-4-yl]amino]ethoxy]ethoxy]ethoxy]ethoxy]propanoylamino]propyl]-N-methyl-naphthalene-2-carboxamide (**4.3a** (**n=4**, **R₁=3**))

A yellow solid (41 mg, 28% yield). ESI-MS *m/z*: 940 ($[M+H]^+$). ¹H-NMR (300MHz, CD₂Cl₂): 8.51 (m, 1H), 8.28 (m, 1H), 7.94 (d, *J*=8.1 Hz, 1H), 7.77 (m, 4H), 7.63 (s, 1H), 7.44 (t, *J*=8.1 Hz, 2H), 7.37 (d, *J*=8.1 Hz, 1H), 7.05 (m, 1H), 7.00 (d, *J*=7.5 Hz, 1H), 6.87 (d, *J*=8.1 Hz, 1H), 6.55 (m, 1H), 6.43 (m, 1H), 6.23 (m, 1H), 4.90 (m, 1H), 3.66-3.57 (m, 17H), 3.39 (m, 4H), 3.30 (m, 2H), 3.08 (m, 4H), 2.96 (m, 2H), 2.74 (m, 3H), 2.44 (m, 2H), 2.07 (m, 2H), 1.83 (m, 1H).

3-amino-4-[4-[4-[3-[3-[2-[2-[2-(2,6-dioxo-3-piperidyl)-1,3-dioxo-isoindolin-4-yl]amino]ethoxy]ethoxy]propanoylamino]propyl-methyl-carbamoyl]phenyl]-1,4-diazepan-1-yl]thieno[2,3-*b*]pyridine-2-carboxamide (**4.3b** (**n=4**, **R₁=2**))

A yellow solid (58 mg, 56% yield). ESI-MS *m/z*: 898 ($[M+H]^+$). ¹H-NMR (300MHz, CD₃CN): 9.32 (s, 1H), 8.47 (d, *J*=5.5 Hz, 1H), 8.39 (s, 1H), 7.91-7.77 (m, 6H), 7.50-7.43 (m, 3H), 7.00 (d, *J*=6.9 Hz, 1H), 6.98 (d, *J*=2.2 Hz, 1H), 6.96 (d, *J*=4.3 Hz, 1H), 6.65 (d, *J*=6.0 Hz, 1H), 6.47 (m, 1H), 6.44 (t, *J*=5.6 Hz, 1H), 4.91 (m, 1H), 3.70 (m, 2H), 3.66 (t, *J*=5.6 Hz, 2H), 3.62 (t, *J*=5.6 Hz, 2H), 3.57 (m, 2H), 3.54 (m, 2H), 3.50 (s, 10H), 3.42 (q, *J*=5.6 Hz, 2H), 3.18 (m, 4H), 2.69 (m, 3H), 2.50 (m, 10H), 2.35 (t, *J*=5.6 Hz, 2H), 2.07 (m, 1H), 1.63 (m, 2H).

4-[2-[6-[4-[3-[2-[2-[2-(2,6-dioxo-3-piperidyl)-1,3-dioxo-isoindolin-4-yl]amino]ethoxy]ethoxy]propanoyl]piperazine-1-carbonyl]-2-naphthyl]ethylamino]quinoline-6-carbonitrile (**4.3c** (**n=2**, **R₁=1**))

A yellow solid (42 mg, 21% yield). ESI-MS m/z : 852 ($[M+H]^+$). 1H -NMR (300MHz, DMSO- d_6): 11.1 (s, 1H), 8.87 (s, 1H), 8.52 (d, $J=5.4$ Hz, 1H), 7.91 (m, 6H), 7.76 (m, 1H), 7.56 (t, $J=9.2$ Hz, 2H), 7.49 (d, $J=8.5$ Hz, 1H), 7.11 (m, 1H), 7.02 (d, $J=7.7$ Hz, 1H), 6.73 (d, $J=5.4$ Hz, 1H), 6.58 (s, 1H), 5.05 (m, 1H), 3.70-3.45 (m, 20H), 3.17 (t, $J=7.2$ Hz, 2H), 2.87 (m, 1H), 2.56 (m, 4H), 2.01 (m, 1H).

4-[2-[6-[4-[3-[2-[2-[2-[[2-(2,6-dioxo-3-piperidyl)-1,3-dioxo-isoindolin-4-yl]amino]ethoxy]ethoxy]ethoxy]propanoyl]piperazine-1-carbonyl]-2-naphthyl]ethylamino]quinoline-6-carbonitrile (4.3d (n=3, R₁=1))

A yellow solid (36 mg, 27% yield). ESI-MS m/z : 896 ($[M+H]^+$). 1H -NMR (300MHz, DMSO- d_6): 11.1 (s, 1H), 8.87 (s, 1H), 8.52 (d, $J=5.4$ Hz, 1H), 7.93 (m, 6H), 7.76 (m, 1H), 7.56 (t, $J=9.2$ Hz, 2H), 7.49 (d, $J=8.5$ Hz, 1H), 7.11 (d, $J=9.2$ Hz, 1H), 7.02 (d, $J=7.7$ Hz, 1H), 6.72 (d, $J=5.4$ Hz, 1H), 6.58 (s, 1H), 5.05 (m, 1H), 3.75-3.56 (m, 24H), 3.18 (t, $J=7.2$ Hz, 2H), 2.87 (m, 1H), 2.56 (m, 4H), 2.00 (m, 1H).

4-[2-[6-[4-[3-[2-[2-[2-[2-[[2-(2,6-dioxo-3-piperidyl)-1,3-dioxo-isoindolin-4-yl]amino]ethoxy]ethoxy]ethoxy]ethoxy]propanoyl]piperazine-1-carbonyl]-2-naphthyl]ethylamino]quinoline-6-carbonitrile (4.3e (n=4, R₁=1)):

A yellow solid (63 mg, 35% yield). ESI-MS m/z : 940 ($[M+H]^+$). 1H -NMR (300MHz, CD₂Cl₂): 8.57 (d, $J=5.4$ Hz, 1H), 8.21 (d, $J=6.9$ Hz, 1H), 7.98 (d, $J=8.9$ Hz, 1H), 7.82 (m, 3H), 7.71 (d, $J=8.9$ Hz, 1H), 7.68 (s, 1H), 7.45 (m, 3H), 7.02 (d, $J=6.9$ Hz, 1H), 6.91 (d, $J=8.7$ Hz, 1H), 6.57 (d, $J=5.4$ Hz, 1H), 6.45 (t, $J=5.4$ Hz, 1H), 5.87 (m, 1H), 4.91 (m, 1H), 3.75-3.56 (m, 26H), 3.43 (m, 2H), 3.19 (m, 2H), 2.76 (m, 3H), 2.62 (m, 2H), 2.10 (m, 1H).

4-[2-[6-[4-[3-[2-[2-[2-[2-[2-[2-[2-[(2,6-dioxo-3-piperidyl)-1,3-dioxo-isoindolin-4-yl]amino]ethoxy]ethoxy]ethoxy]ethoxy]ethoxy]ethoxy]propanoyl]piperazine-1-carbonyl]-2-naphthyl]ethylamino]quinoline-6-carbonitrile (4.3f (n=5, R₁=1))

A yellow solid (15 mg, 17% yield). ESI-MS *m/z*: 954 ([M+H]⁺). ¹H-NMR (300MHz, CD₂Cl₂): 8.94 (m, 1H), 8.60 (d, J=5.1 Hz, 1H), 8.21 (s, 1H), 8.02 (d, J=8.9 Hz, 1H), 7.88 (s, 1H), 7.85 (d, J=8.3 Hz, 1H), 7.81 (d, J=8.3 Hz, 1H), 7.72 (d, J=8.6 Hz, 1H), 7.69 (s, 1H), 7.48 (d, J=8.0 Hz, 2H), 7.43 (d, J=8.9 Hz, 1H), 7.03 (d, J=7.2 Hz, 1H), 6.91 (d, J=8.0 Hz, 1H), 6.58 (d, J=5.6 Hz, 1H), 6.46 (t, J=6.4 Hz, 1H), 5.91 (m, 1H), 4.90 (m, 1H), 3.75-3.56 (m, 30H), 3.44 (m, 2H), 3.20 (t, J=7.6 Hz, 2H), 2.77 (m, 3H), 2.63 (m, 2H), 2.10 (m, 1H).

4-[2-[6-[4-[3-[2-[2-[2-[2-[2-[2-[2-[(2,6-dioxo-3-piperidyl)-1,3-dioxo-isoindolin-4-yl]amino]ethoxy]ethoxy]ethoxy]ethoxy]ethoxy]ethoxy]ethoxy]propanoyl]piperazine-1-carbonyl]-2-naphthyl]ethylamino]quinoline-6-carbonitrile (4.3g (n=6, R₁=1))

A yellow solid (30 mg, 36% yield). ESI-MS *m/z*: 1028 ([M+H]⁺). ¹H-NMR (300MHz, CD₂Cl₂): 8.94 (m, 1H), 8.60 (d, J=5.1 Hz, 1H), 8.17 (s, 1H), 8.00 (d, J=8.9 Hz, 1H), 7.88 (s, 1H), 7.86 (d, J=8.3 Hz, 1H), 7.83 (d, J=8.3 Hz, 1H), 7.72 (d, J=8.6 Hz, 1H), 7.71 (s, 1H), 7.49 (d, J=8.0 Hz, 2H), 7.44 (d, J=8.9 Hz, 1H), 7.04 (d, J=7.2 Hz, 1H), 6.92 (d, J=8.0 Hz, 1H), 6.59 (d, J=5.6 Hz, 1H), 6.47 (t, J=6.4 Hz, 1H), 5.91 (m, 1H), 4.90 (m, 1H), 3.75-3.56 (m, 34H), 3.44 (m, 2H), 3.21 (t, J=7.6 Hz, 2H), 2.77 (m, 3H), 2.63 (m, 2H), 2.11 (m, 1H).

The general preparation of **4.4**: To a 10 mL round-bottle flask was added a solution of **4.2** (1eq) and **3.44b** (1eq) in DMF. Then EDC-HCl (2eq), HOAt (2eq), and N-methylmorpholine (5eq) were added and the mixture was stirred at room temperature for overnight. Upon completion, the mixture was diluted with DCM, added with water, extracted with DCM, the organic layers were combined, dried by Na₂SO₄, condensed and purified by flash column chromatography using a gradient of 0-10% MeOH/DCM to give target compounds **4.4**.

3-amino-4-[4-[4-[3-[3-[2-[2-[[2-(2,6-dioxo-3-piperidyl)-1,3-dioxo-isoindolin-4-yl]amino]ethoxy]ethoxy]propanoylamino]propyl-methyl-carbamoyl]phenyl]-1,4-diazepan-1-yl]thieno[2,3-b]pyridine-2-carboxamide (4.4a (n=2))

A yellow solid (58 mg, 56% yield). ESI-MS m/z: 898 ([M+H]⁺). ¹H-NMR (300MHz, DMSO-d₆): 9.50 (s, 1H), 8.44 (d, J=5.4 Hz, 1H), 8.07 (s, 1H), 7.49 (t, J=8.1 Hz, 1H), 7.35 (d, J=8.7 Hz, 2H), 7.06 (d, J=7.5 Hz, 1H), 6.96 (d, J=5.4 Hz, 1H), 6.93 (d, J=8.7 Hz, 2H), 6.91 (d, J=7.5 Hz, 1H), 6.73 (d, J=8.7 Hz, 2H), 6.51 (m, 1H), 5.58 (m, 2H), 4.91 (m, 1H), 3.79 (m, 2H), 3.70 (m, 4H), 3.62 (m, 6H), 3.51 (m, 2H), 3.44 (m, 1H), 3.36 (m, 2H), 3.27 (m, 2H), 3.19 (m, 2H), 3.00 (s, 3H), 2.76 (m, 3H), 2.40 (m, 2H), 2.17 (m, 2H), 2.10 (m, 1H), 1.76 (m, 2H).

3-amino-4-[4-[4-[3-[3-[2-[2-[2-[[2-(2,6-dioxo-3-piperidyl)-1,3-dioxo-isoindolin-4-yl]amino]ethoxy]ethoxy]ethoxy]propanoylamino]propyl-methyl-carbamoyl]phenyl]-1,4-diazepan-1-yl]thieno[2,3-b]pyridine-2-carboxamide (4.4b (n=3))

A yellow solid (60 mg, 61% yield). ESI-MS m/z: 942 ([M+H]⁺). ¹H-NMR (300MHz, DMSO-d₆): 9.40 (s, 1H), 8.44 (d, J=5.4 Hz, 1H), 8.07 (s, 1H), 7.47 (t, J=8.1 Hz, 1H), 7.34 (d, J=8.7 Hz, 2H), 7.04 (d, J=7.5 Hz, 1H), 6.96 (d, J=5.4 Hz,

3.71-3.58 (m, 28H), 3.50-3.36 (m, 6H), 3.28 (m, 2H), 3.20 (m, 2H), 3.02 (s, 3H), 2.77 (m, 3H), 2.40 (m, 2H), 2.17 (m, 2H), 2.10 (m, 1H).

(2S,4R)-1-((S)-2-(tert-butyl)-19-(4-(6-(2-((6-cyanoquinolin-4-yl)amino)ethyl)-2-naphthoyl)piperazin-1-yl)-4,19-dioxo-7,10,13,16-tetraoxa-3-azanonadecanoyl)-4-hydroxy-N-(4-(4-methylthiazol-5-yl)benzyl)pyrrolidine-2-carboxamide (4.5)

To a 10 mL round-bottle flask was added a solution of 3-[2-[2-[2-[3-oxo-3-[[rac-(1S)-2,2-dimethyl-1-[rac-(2S,4R)-4-hydroxy-2-[[4-(4-methylthiazol-5-yl)phenyl]methylcarbonyl]pyrrolidine-1-carbonyl]propyl]amino]propoxy]ethoxy]ethoxy]ethoxy]propanoic acid (0.071 mmol, 50 mg) and 4-[2-[6-(piperazine-1-carbonyl)-2-naphthyl]ethylamino]quinoline-6-carbonitrile (0.071 mmol, 31 mg) in DMF (2 mL). Then EDC-HCl (0.14 mmol, 27 mg), HOAt (0.14 mmol, 19 mg), and N-methylmorpholine (0.35 mmol, 36 mg) were added and the mixture was stirred at room temperature for overnight. Upon completion, the mixture was diluted with DCM, added with water, extracted with DCM, the organic layers were combined, dried by Na₂SO₄, condensed and purified by flash column chromatography using a gradient of 0-10% MeOH/DCM to give *(2S,4R)-1-((S)-2-(tert-butyl)-19-(4-(6-(2-((6-cyanoquinolin-4-yl)amino)ethyl)-2-naphthoyl)piperazin-1-yl)-4,19-dioxo-7,10,13,16-tetraoxa-3-azanonadecanoyl)-4-hydroxy-N-(4-(4-methylthiazol-5-yl)benzyl)pyrrolidine-2-carboxamide* (21 mg, 26% yield). ESI-MS *m/z*: 1125 ([M+H]⁺). ¹H-NMR (300MHz, CD₂Cl₂): 8.63 (s, 1H), 8.56 (d, J=5.1 Hz, 1H), 8.31 (s, 1H), 7.97 (d, J=8.6 Hz, 1H), 7.86 (s, 1H), 7.83 (d, J=8.6 Hz, 1H), 7.80 (d, J=8.6 Hz, 1H), 7.72 (dd, J=8.6, 1.5 Hz, 1H), 7.68 (s, 1H), 7.44 (m, 3H), 7.34 (m, 4H), 7.03 (d, J=8.6 Hz, 1H), 6.59 (d, J=5.5 Hz, 1H), 6.26 (m, 1H),

4.63 (t, J=8.1 Hz, 2H), 4.49 (m 3H), 4.28 (m, 1H), 3.99 (m, 1H), 3.75-3.55 (m, 28H), 3.20 (t, J=7.2 Hz, 2H), 2.62 (m, 2H), 2.45 (m, 2H), 2.44 (s, 3H), 2.34 (m, 1H), 2.09 (m, 1H), 0.93 (s, 9H).

N-[3-[4-[6-[2-[(6-cyano-4-quinolyl)amino]ethyl]naphthalene-2-carbonyl]piperazin-1-yl]-3-oxo-propyl]-3-[2-[2-[2-[[2-(2,6-dioxo-3-piperidyl)-1,3-dioxo-isoindolin-4-yl]amino]ethoxy]ethoxy]ethoxy]propanamide (**4.6a** (**n=3**))

To a 10 mL round-bottle flask was added a solution of 3-[2-[2-[2-[[2-(2,6-dioxo-3-piperidyl)-1,3-dioxo-isoindolin-4-yl]amino]ethoxy]ethoxy]ethoxy]propanoic acid (0.10 mmol, 50 mg) and 4-[2-[6-[4-(3-aminopropanoyl)piperazine-1-carbonyl]-2-naphthyl]ethylamino]quinoline-6-carbonitrile (0.10 mmol, 53 mg) in DMF (2 mL). Then EDC-HCl (0.21 mmol, 40 mg), HOAt (0.21 mmol, 29 mg), and N-methylmorpholine (0.52 mmol, 53 mg) were added and the mixture was stirred at room temperature for overnight. Upon completion, the mixture was diluted with DCM, added with water, extracted with DCM, the organic layers were combined, dried by Na₂SO₄, condensed and purified by flash column chromatography using a gradient of 0-10% MeOH/DCM to give *N*-[3-[4-[6-[2-[(6-cyano-4-quinolyl)amino]ethyl]naphthalene-2-carbonyl]piperazin-1-yl]-3-oxo-propyl]-3-[2-[2-[2-[[2-(2,6-dioxo-3-piperidyl)-1,3-dioxo-isoindolin-4-yl]amino]ethoxy]ethoxy]ethoxy]propanamide (15 mg, 15% yield). ESI-MS *m/z*: 967 ([*M*+*H*]⁺). ¹H-NMR (300MHz, CD₂Cl₂): 9.59 (m, 1H), 8.59 (d, J=5.1 Hz, 1H), 8.22 (s, 1H), 7.97 (d, J=9.2 Hz, 1H), 7.86 (s, 1H), 7.82 (t, J=8.8 Hz, 2H), 7.70 (d, J=10.6 Hz, 2H), 7.72 (d, J=8.6 Hz, 1H), 7.71 (s, 1H), 7.46 (m, 3H), 7.03 (d, J=7.4 Hz, 1H), 6.91 (d, J=8.3 Hz, 2H), 6.57 (d, J=5.5 Hz, 1H), 6.48 (d, J=5.4 Hz, 1H), 5.89 (m,

1H), 4.91 (m, 1H), 3.71-3.42 (m, 24H), 3.19 (t, J=7.5 Hz, 2H), 2.75 (m, 3H), 2.53 (m, 2H), 2.36 (t, J=6.6 Hz, 2H), 2.09 (m, 2H), 2.01 (m, 1H).

N-[3-[4-[6-[2-[(6-cyano-4-quinolyl)amino]ethyl]naphthalene-2-carbonyl]piperazin-1-yl]-3-oxo-propyl]-3-[2-[2-[2-[2-[[2-(2,6-dioxo-3-piperidyl)-1,3-dioxo-isoindolin-4-yl]amino]ethoxy]ethoxy]ethoxy]ethoxy]propanamide (**4.6b** (n=4))

The method is the same as 28a. A yellow solid (15 mg, 16% yield). ESI-MS m/z : 1011 ($[M+H]^+$). 1H -NMR (300MHz, CD_2Cl_2): 9.20 (m, 1H), 8.61 (d, J=5.1 Hz, 1H), 8.15 (s, 1H), 7.99 (d, J=9.2 Hz, 1H), 7.88 (s, 1H), 7.83 (t, J=8.8 Hz, 2H), 7.73 (d, J=10.6 Hz, 2H), 7.72 (d, J=8.6 Hz, 1H), 7.71 (s, 1H), 7.47 (m, 3H), 7.04 (d, J=7.4 Hz, 1H), 6.92 (d, J=8.3 Hz, 1H), 6.88 (m, 1H), 6.60 (d, J=5.5 Hz, 1H), 6.48 (t, J=5.4 Hz, 1H), 5.61 (m, 1H), 4.91 (m, 1H), 3.71-3.43 (m, 28H), 3.22 (t, J=7.5 Hz, 2H), 2.76 (m, 3H), 2.53 (m, 2H), 2.37 (t, J=6.6 Hz, 2H), 2.12 (m, 2H), 2.05 (m, 1H).

4-fluoro-2-(1-methyl-2,6-dioxo-3-piperidyl)isoindoline-1,3-dione (**4.7**)

To a 10 mL round-bottle flask was added a solution of 2-(2,6-dioxo-3-piperidyl)-4-fluoro-isoindoline-1,3-dione (1.81 mmol, 500 mg), iodomethane (1.99 mmol, 283 mg), and K_2CO_3 (1.99 mmol, 275 mg) in DMF (5 mL). The mixture was stirred at room temperature for 7h. Upon completion, the mixture was quenched by water, extracted with DCM, the organic layers were combined, dried by Na_2SO_4 , condensed and purified by flash column chromatography using a gradient of 0-5% MeOH/DCM to give 4-fluoro-2-(1-methyl-2,6-dioxo-3-piperidyl)isoindoline-1,3-dione (500 mg, 95% yield). ESI-MS m/z : 291 ($[M+H]^+$). 1H -NMR (300MHz,

CD₂Cl₂): 7.81 (m, 1H), 7.73 (d, J=7.3 Hz, 1H), 7.47 (t, J=8.7 Hz, 1H), 5.01 (m, 1H), 3.19 (s, 3H), 2.96 (m, 1H), 2.80 (m, 2H), 2.15 (m, 1H).

tert-butyl 3-[2-[2-[2-[2-[[2-(1-methyl-2,6-dioxo-3-piperidyl)-1,3-dioxo-isoindolin-4-yl]amino]ethoxy]ethoxy]ethoxy]ethoxy]propanoate (4.8)

To a 10 mL microwave tube was added a solution of 4-fluoro-2-(1-methyl-2,6-dioxo-3-piperidyl)isoindoline-1,3-dione (1.03 mmol, 300 mg), *tert-butyl 3-[2-[2-[2-(2-aminoethoxy)ethoxy]ethoxy]ethoxy]propanoate* (1.03 mmol, 332 mg), and DIEA (3.1 mmol, 401 mg) in DMF (5 mL). The mixture was microwaved at 110°C for 2h. Upon completion, the mixture was condensed and purified by flash column chromatography using a gradient of 0-9% MeOH/DCM to give *tert-butyl 3-[2-[2-[2-[2-[[2-(1-methyl-2,6-dioxo-3-piperidyl)-1,3-dioxo-isoindolin-4-yl]amino]ethoxy]ethoxy]ethoxy]ethoxy]propanoate* (500 mg, 82% yield). ESI-MS *m/z*: 291 ([M+H]⁺). ¹H-NMR (300MHz, CD₂Cl₂): 7.52 (t, J=7.8 Hz, 1H), 7.07 (d, J=7.0 Hz, 1H), 6.97 (d, J=7.0 Hz, 1H), 6.48 (m, 1H), 4.91 (m, 1H), 3.60 (m, 18H), 3.15 (s, 3H), 2.92 (m, 1H), 2.75 (m, 2H), 2.57 (t, J=6.3 Hz, 2H), 2.08 (m, 2H).

3-[2-[2-[2-[2-[[2-(1-methyl-2,6-dioxo-3-piperidyl)-1,3-dioxo-isoindolin-4-yl]amino]ethoxy]ethoxy]ethoxy]ethoxy]propanoic acid (4.9)

To a 10 mL round-bottom flask was added a solution of *tert-butyl 3-[2-[2-[2-[2-[[2-(1-methyl-2,6-dioxo-3-piperidyl)-1,3-dioxo-isoindolin-4-yl]amino]ethoxy]ethoxy]ethoxy]ethoxy]propanoate* (0.85 mmol, 500 mg) in formic acid (3 mL). The mixture was stirred at room temperature for overnight. Upon completion, the mixture was condensed to give *3-[2-[2-[2-[2-[[2-(1-methyl-2,6-dioxo-3-piperidyl)-1,3-dioxo-isoindolin-4-*

yl]amino]ethoxy]ethoxy]ethoxy]ethoxy]propanoic acid (332 mg, 73% yield) and used without further purification. ESI-MS m/z : 536 ($[M+H]^+$).

4-[2-[6-[4-[3-[2-[2-[2-[2-[[2-(1-methyl-2,6-dioxo-3-piperidyl)-1,3-dioxo-isoindolin-4-yl]amino]ethoxy]ethoxy]ethoxy]ethoxy]propanoyl]piperazine-1-carbonyl]-2-naphthyl]ethylamino]quinoline-6-carbonitrile (4.10)

To a 10 mL round-bottle flask was added a solution of 3-[2-[2-[2-[2-[[2-(1-methyl-2,6-dioxo-3-piperidyl)-1,3-dioxo-isoindolin-4-yl]amino]ethoxy]ethoxy]ethoxy]ethoxy]propanoic acid (0.32 mmol, 170 mg) and 4-[2-[6-(piperazine-1-carbonyl)-2-naphthyl]ethylamino]quinoline-6-carbonitrile (0.32 mmol, 138 mg) in DMF (3 mL). Then EDC-HCl (0.64 mmol, 122 mg), HOAt (0.64 mmol, 86 mg), and N-methylmorpholine (1.6 mmol, 161 mg) were added and the mixture was stirred at room temperature for overnight. Upon completion, the mixture was diluted with DCM, added with water, extracted with DCM, the organic layers were combined, dried by Na_2SO_4 , condensed and purified by flash column chromatography using a gradient of 0-10% MeOH/DCM to give 4-[2-[6-[4-[3-[2-[2-[2-[2-[[2-(1-methyl-2,6-dioxo-3-piperidyl)-1,3-dioxo-isoindolin-4-yl]amino]ethoxy]ethoxy]ethoxy]ethoxy]propanoyl]piperazine-1-carbonyl]-2-naphthyl]ethylamino]quinoline-6-carbonitrile (54 mg, 18% yield). ESI-MS m/z : 954 ($[M+H]^+$). 1H -NMR (300MHz, CD_2Cl_2): 8.55 (d, $J=5.1$ Hz, 1H), 8.23 (s, 1H), 7.95 (d, $J=8.5$ Hz, 1H), 7.84 (m, 3H), 7.74 (d, $J=9.1$ Hz, 1H), 7.69 (s, 1H), 7.45 (m, 3H), 7.02 (d, $J=7.4$ Hz, 1H), 6.91 (d, $J=8.5$ Hz, 1H), 6.61 (d, $J=6.7$ Hz, 1H), 6.43 (m, 1H), 5.95 (m, 1H), 4.90 (m, 1H), 3.75-3.53 (m, 26H), 3.45 (m, 2H), 3.20 (m, 2H), 3.13 (s, 3H), 2.90 (m, 1H), 2.72 (m, 2H), 2.62 (m, 2H), 2.07 (m, 1H).

The general preparation of **4.11**: To a 10 mL round-bottle flask was added a solution of 2-(2,6-dioxo-3-piperidyl)-4-fluoro-isoindoline-1,3-dione (1eq) and amine analogs (1eq) in DMF. Then DIEA (3eq) was added and the mixture was microwaved at 100°C for 2h. Upon completion, the mixture was condensed and purified by flash column chromatography using a gradient of 0-2% MeOH/DCM to give target compounds **4.11**.

tert-butyl 3-[[2-(2,6-dioxo-3-piperidyl)-1,3-dioxo-isoindolin-4-yl]amino]propanoate
(4.11a (n=2))

A yellow solid (70 mg, 24% yield). ESI-MS m/z : 402 ($[M+H]^+$).

tert-butyl 4-[[2-(2,6-dioxo-3-piperidyl)-1,3-dioxo-isoindolin-4-yl]amino]butanoate
(4.11b (n=3))

To a 10 mL round-bottle flask was added a solution of 2-(2,6-dioxo-3-piperidyl)-4-fluoro-isoindoline-1,3-dione (0.72 mmol, 200 mg) and *tert-butyl 4-aminobutanoate* (0.72 mmol, 115 mg) in DMF (2 mL). Then DIEA (2.2 mmol, 372 μ L) was added and the mixture was microwaved at 100°C for 2h. Upon completion, the mixture was condensed and purified by flash column chromatography using a gradient of 0-2% MeOH/DCM to give *tert-butyl 4-[[2-(2,6-dioxo-3-piperidyl)-1,3-dioxo-isoindolin-4-yl]amino]butanoate* (70 mg, 23% yield). ESI-MS m/z : 416 ($[M+H]^+$).

tert-butyl 5-[[2-(2,6-dioxo-3-piperidyl)-1,3-dioxo-isoindolin-4-yl]amino]pentanoate
(4.11c (n=4))

To a 10 mL microwave flask was added a solution of 2-(2,6-dioxo-3-piperidyl)-4-fluoro-isoindoline-1,3-dione (0.72 mmol, 200 mg) and *tert-butyl 5-*

aminopentanoate (0.72 mmol, 125 mg) in DMF (2 mL). Then DIEA (2.2 mmol, 372 μ L) was added and the mixture was microwaved at 100°C for 2h. Upon completion, the mixture was condensed and purified by flash column chromatography using a gradient of 0-5% MeOH/DCM to give tert-butyl 5-[[2-(2,6-dioxo-3-piperidyl)-1,3-dioxo-isoindolin-4-yl]amino]pentanoate (143 mg, 46% yield). ESI-MS m/z: 430 ($[M+H]^+$).

tert-butyl 6-[[2-(2,6-dioxo-3-piperidyl)-1,3-dioxo-isoindolin-4-yl]amino]hexanoate
(4.11d (n=5))

To a 10 mL microwave flask was added a solution of 2-(2,6-dioxo-3-piperidyl)-4-fluoro-isoindoline-1,3-dione (0.72 mmol, 200 mg) and tert-butyl 6-aminohexanoate (0.72 mmol, 136 mg) in DMF (2 mL). Then DIEA (2.2 mmol, 372 μ L) was added and the mixture was microwaved at 100°C for 2 h. Upon completion, the mixture was condensed and purified by flash column chromatography using a gradient of 0-5% MeOH/DCM to give tert-butyl 6-[[2-(2,6-dioxo-3-piperidyl)-1,3-dioxo-isoindolin-4-yl]amino]hexanoate (145 mg, 45% yield). ESI-MS m/z: 444 ($[M+H]^+$).

The general preparation of **4.12**: To a 10 mL round-bottle flask was added a solution of **4.11** (1eq) in formic acid. Then the mixture was stirred at room temperature for overnight. Upon completion, the mixture was condensed and purified by flash column chromatography using a gradient of 0-4% MeOH/DCM to give target compounds **4.12**.

3-[[2-(2,6-dioxo-3-piperidyl)-1,3-dioxo-isoindolin-4-yl]amino]propanoic acid (**4.12a**
(n=2))

A yellow solid (43 mg, 71% yield). ESI-MS m/z : 346 ($[M+H]^+$). 1H -NMR (300MHz, DMSO- d_6): 11.1 (s, 1H), 7.59 (t, $J=7.7$ Hz, 1H), 7.15 (d, $J=8.4$ Hz, 1H), 7.04 (d, $J=7.7$ Hz, 1H), 6.66 (t, $J=6.1$ Hz, 1H), 5.04 (m, 1H), 3.52 (t, $J=6.9$ Hz, 2H), 2.87 (m, 1H), 2.57 (m, 2H), 2.56 (t, $J=6.9$ Hz, 2H), 2.02 (m, 1H).

4-[[2-(2,6-dioxo-3-piperidyl)-1,3-dioxo-isoindolin-4-yl]amino]butanoic acid (4.12b (n=3))

A yellow solid (40 mg, 66% yield). ESI-MS m/z : 360 ($[M+H]^+$). 1H -NMR (300MHz, CD_2Cl_2): 8.45 (s, 1H), 7.53 (t, $J=8.0$ Hz, 1H), 7.08 (d, $J=7.4$ Hz, 1H), 6.96 (d, $J=7.4$ Hz, 1H), 4.92 (m, 1H), 3.37 (q, $J=6.6$ Hz, 2H), 2.82 (m, 1H), 2.76 (m, 2H), 2.49 (t, $J=7.2$ Hz, 2H), 2.12 (m, 1H), 1.99 (m, 2H).

5-[[2-(2,6-dioxo-3-piperidyl)-1,3-dioxo-isoindolin-4-yl]amino]pentanoic acid (4.12c (n=4))

A yellow solid (56 mg, 45% yield). ESI-MS m/z : 374 ($[M+H]^+$). 1H -NMR (300MHz, CD_2Cl_2): 8.77 (s, 1H), 7.51 (t, $J=8.1$ Hz, 1H), 7.06 (d, $J=7.3$ Hz, 1H), 6.92 (d, $J=7.4$ Hz, 1H), 6.27 (m, 1H), 4.92 (m, 1H), 3.31 (q, $J=6.6$ Hz, 2H), 2.82 (m, 1H), 2.76 (m, 2H), 2.41 (t, $J=7.2$ Hz, 2H), 2.12 (m, 1H), 1.73 (m, 4H).

tert-butyl N-[5-[[2-(2,6-dioxo-3-piperidyl)-1,3-dioxo-isoindolin-4-yl]amino]pentyl]carbamate (4.13)

To a 10 mL round-bottle flask was added a solution of 2-(2,6-dioxo-3-piperidyl)-4-fluoro-isoindoline-1,3-dione (0.72 mmol, 200 mg) and *tert*-butyl *N*-(5-aminopentyl)carbamate (0.72 mmol, 146 mg) in DMF (2 mL). Then DIEA (2.2 mmol, 372 μ L) was added and the mixture was microwaved at 100°C for 2 h. Upon completion, the mixture was condensed and purified by flash column

chromatography using a gradient of 0-2% MeOH/DCM to give tert-butyl N-[5-[[2-(2,6-dioxo-3-piperidyl)-1,3-dioxo-isoindolin-4-yl]amino]pentyl]carbamate (120 mg, 36% yield). ESI-MS m/z: 459 ($[M+H]^+$).

4-(5-aminopentylamino)-2-(2,6-dioxo-3-piperidyl)isoindoline-1,3-dione (4.14)

To a 10 mL round-bottle flask was added a solution of tert-butyl N-[5-[[2-(2,6-dioxo-3-piperidyl)-1,3-dioxo-isoindolin-4-yl]amino]pentyl]carbamate (0.26 mmol, 120 mg) in formic acid (2 mL). Then the mixture was stirred at room temperature for overnight. Upon completion, the mixture was condensed and purified by flash column chromatography using a gradient of 0-4% MeOH/DCM to give 4-(5-aminopentylamino)-2-(2,6-dioxo-3-piperidyl)isoindoline-1,3-dione (85 mg, 91% yield). ESI-MS m/z: 359 ($[M+H]^+$). $^1\text{H-NMR}$ (300MHz, DMSO- d_6): 11.1 (s, 1H), 7.58 (t, $J=7.3$ Hz, 1H), 7.09 (d, $J=8.7$ Hz, 1H), 7.03 (d, $J=8.7$ Hz, 1H), 6.54 (m, 1H), 5.05 (m, 1H), 3.29 (m, 2H), 2.85 (m, 1H), 2.79 (m, 2H), 2.55 (m, 2H), 2.03 (m, 1H), 1.58 (m, 4H), 1.39 (m, 2H).

tert-butyl 10-[4-[6-[2-[(6-cyano-4-quinolyl)amino]ethyl]naphthalene-2-carbonyl]piperazin-1-yl]-10-oxo-decanoate (4.15)

To a 10 mL round-bottle flask was added a solution of 10-tert-butoxy-10-oxo-decanoic acid (0.47 mmol, 121 mg) in DCM (5 mL). Then HATU (0.70 mmol, 266 mg), DIEA (1.40 mmol, 240 μL) were added and the mixture was stirred at room temperature for 15 min, then 4-[2-[6-(piperazine-1-carbonyl)-2-naphthyl]ethylamino]quinoline-6-carbonitrile (0.47 mmol, 203 mg) was added and the mixture was stirred for 2h. Upon completion, water was added, the mixture was extracted with DCM, the organic layers were combined, washed with sat NaHCO_3

aq, dried by Na₂SO₄, condensed and purified by flash column chromatography using a gradient of 0-5% MeOH/DCM to give tert-butyl 10-[4-[6-[2-[(6-cyano-4-quinolyl)amino]ethyl]naphthalene-2-carbonyl]piperazin-1-yl]-10-oxo-decanoate (73 mg, 23% yield). ESI-MS m/z: 676 ([M+H]⁺). ¹H-NMR (300MHz, CD₂Cl₂): 8.54 (d, J=5.7 Hz, 1H), 8.27 (s, 1H), 7.95 (d, J=9.0 Hz, 1H), 7.88 (s, 1H), 7.83 (t, J=7.9 Hz, 2H), 7.75 (dd, J=8.8, 1.7 Hz, 1H), 7.67 (s, 1H), 7.48 (dd, J=8.8, 1.7 Hz, 1H), 7.42 (dd, J=8.8, 1.7 Hz, 1H), 6.61 (d, J=5.7 Hz, 1H), 6.11 (m, 1H), 4.60 (m, 1H), 3.68 (m, 2H), 3.57 (m, 8H), 3.20 (t, J=7.6 Hz, 2H), 2.33 (m, 2H), 2.17 (t, J=8.4 Hz, 2H), 1.58 (m, 4H), 1.42 (s, 9H), 1.30 (m, 8H).

10-[4-[6-[2-[(6-cyano-4-quinolyl)amino]ethyl]naphthalene-2-carbonyl]piperazin-1-yl]-10-oxo-decanoic acid (4.16)

To a 10 mL round-bottle flask was added a solution of tert-butyl 10-[4-[6-[2-[(6-cyano-4-quinolyl)amino]ethyl]naphthalene-2-carbonyl]piperazin-1-yl]-10-oxo-decanoate (0.11 mmol, 73 mg) in formic acid (2 mL). Then the mixture was stirred at room temperature for overnight. Upon completion, the mixture was condensed to give 10-[4-[6-[2-[(6-cyano-4-quinolyl)amino]ethyl]naphthalene-2-carbonyl]piperazin-1-yl]-10-oxo-decanoic acid (66 mg, 98% yield) and used without further purification. ESI-MS m/z: 620 ([M+H]⁺).

The general preparation **4.17**.

To a 10 mL round-bottle flask was added a solution of acid analogs (1eq) in DCM. Then HATU (1.5eq), DIEA (3eq) were added and the mixture was stirred at room temperature for 15 min, then **2.20c** (1eq) was added and the mixture was stirred for 4h. Upon completion, water was added, the mixture was extracted with

DCM, the organic layers were combined, washed with sat NaHCO₃ aq, dried by Na₂SO₄, condensed and purified by flash column chromatography using a gradient of 0-5% MeOH/DCM to give target compounds **4.17**.

tert-butyl *N*-[9-[4-[6-[2-[(6-cyano-4-quinolyl)amino]ethyl]naphthalene-2-carbonyl]piperazin-1-yl]-9-oxo-nonyl]carbamate (**4.17a** (**m=8**))

A light yellow solid (48 mg, 15% yield). ESI-MS *m/z*: 691 ([*M*+*H*]⁺). ¹H-NMR (300MHz, CD₂Cl₂): 8.60 (d, *J*=5.7 Hz, 1H), 8.17 (s, 1H), 7.97 (d, *J*=9.3 Hz, 1H), 7.89 (s, 2H), 7.83 (t, *J*=9.3 Hz, 1H), 7.73 (dd, *J*=8.8, 1.7 Hz, 1H), 7.71 (s, 1H), 7.49 (dd, *J*=8.8, 1.7 Hz, 1H), 7.45 (dd, *J*=8.8, 1.7 Hz, 1H), 6.60 (d, *J*=5.7 Hz, 1H), 5.63 (m, 1H), 4.60 (m, 1H), 3.70 (q, *J*=6.6 Hz, 2H), 3.57 (m, 8H), 3.22 (t, *J*=7.4 Hz, 2H), 3.05 (q, *J*=6.6 Hz, 2H), 2.32 (m, 2H), 1.59 (m, 2H), 1.41 (s, 9H), 1.30 (m, 10H).

tert-butyl *N*-[10-[4-[6-[2-[(6-cyano-4-quinolyl)amino]ethyl]naphthalene-2-carbonyl]piperazin-1-yl]-10-oxo-decyl]carbamate (**4.17b** (**m=9**))

A light yellow solid (89 mg, 37% yield). ESI-MS *m/z*: 705 ([*M*+*H*]⁺). ¹H-NMR (300MHz, CD₂Cl₂): 8.56 (d, *J*=5.6 Hz, 1H), 8.26 (s, 1H), 7.95 (d, *J*=8.6 Hz, 1H), 7.88 (s, 1H), 7.83 (d, *J*=7.7 Hz, 2H), 7.73 (dd, *J*=8.8, 1.7 Hz, 1H), 7.68 (s, 1H), 7.48 (dd, *J*=8.8, 1.7 Hz, 1H), 7.42 (dd, *J*=8.8, 1.7 Hz, 1H), 6.60 (d, *J*=5.6 Hz, 1H), 6.02 (m, 1H), 4.62 (m, 1H), 3.67 (q, *J*=7.3 Hz, 2H), 3.56 (m, 8H), 3.19 (t, *J*=7.6 Hz, 2H), 3.05 (q, *J*=6.8 Hz, 2H), 2.32 (m, 2H), 1.59 (m, 2H), 1.41 (s, 12H), 1.27 (m, 9H).

tert-butyl *N*-[12-[4-[6-[2-[(6-cyano-4-quinolyl)amino]ethyl]naphthalene-2-carbonyl]piperazin-1-yl]-12-oxo-dodecyl]carbamate (**4.17c** (**m=10**))

A light yellow solid (44 mg, 13% yield). ESI-MS *m/z*: 733 ([*M*+*H*]⁺). ¹H-NMR (300MHz, CD₂Cl₂): 8.60 (d, *J*=5.6 Hz, 1H), 8.16 (s, 1H), 7.97 (d, *J*=8.6 Hz, 1H),

7.89 (s, 2H), 7.84 (d, J=8.6 Hz, 1H), 7.73 (dd, J=8.8, 1.7 Hz, 1H), 7.71 (s, 1H), 7.49 (dd, J=8.8, 1.7 Hz, 1H), 7.45 (dd, J=8.8, 1.7 Hz, 1H), 6.60 (d, J=5.6 Hz, 1H), 5.63 (m, 1H), 4.60 (m, 1H), 3.71 (q, J=7.3 Hz, 2H), 3.57 (m, 8H), 3.22 (t, J=7.6 Hz, 2H), 3.05 (q, J=6.8 Hz, 2H), 2.32 (m, 2H), 2.00 (m, 2H), 1.59 (m, 2H), 1.41 (s, 9H), 1.27 (m, 12H).

tert-butyl N-[12-[4-[6-[2-[(6-cyano-4-quinolyl)amino]ethyl]naphthalene-2-carbonyl]piperazin-1-yl]-12-oxo-dodecyl]carbamate (4.17d (m=11))

A light yellow solid (36 mg, 11% yield). ESI-MS m/z: 733 ($[M+H]^+$). $^1\text{H-NMR}$ (300MHz, CD_2Cl_2): 8.60 (d, J=5.6 Hz, 1H), 8.17 (s, 1H), 7.97 (d, J=8.6 Hz, 1H), 7.88 (s, 2H), 7.83 (d, J=8.6 Hz, 1H), 7.73 (dd, J=8.8, 1.7 Hz, 1H), 7.72 (s, 1H), 7.49 (dd, J=8.8, 1.7 Hz, 1H), 7.45 (dd, J=8.8, 1.7 Hz, 1H), 6.60 (d, J=5.6 Hz, 1H), 5.65 (m, 1H), 4.59 (m, 1H), 3.71 (q, J=7.3 Hz, 2H), 3.58 (m, 8H), 3.22 (t, J=7.6 Hz, 2H), 3.05 (q, J=6.8 Hz, 2H), 2.32 (m, 2H), 1.86 (m, 4H), 1.59 (m, 2H), 1.41 (s, 9H), 1.27 (m, 12H).

The general preparation of **4.18**.

To a 10 mL round-bottle flask was added a solution of **4.17** (1eq) in formic acid. The mixture was stirred at room temperature for overnight. Upon completion, the mixture was condensed to give target compounds **4.18** and used without further purification.

4-[2-[6-[4-(9-aminononanoyl)piperazine-1-carbonyl]-2-naphthyl]ethylamino]quinoline-6-carbonitrile (4.18a (m=8))

A white solid (40 mg, 98% yield) and used without further purification. ESI-MS m/z: 591 ($[M+H]^+$).

4-[2-[6-[4-(10-aminodecanoyl)piperazine-1-carbonyl]-2-naphthyl]ethylamino]quinoline-6-carbonitrile (4.18b (m=9))

A white solid (67 mg, 98% yield) and used without further purification. ESI-MS m/z : 605 ($[M+H]^+$).

4-[2-[6-[4-(12-aminododecanoyl)piperazine-1-carbonyl]-2-naphthyl]ethylamino]quinoline-6-carbonitrile (4.18c (m=10))

A white solid (38 mg, 98% yield) and used without further purification. ESI-MS m/z : 633 ($[M+H]^+$).

4-[2-[6-[4-(12-aminododecanoyl)piperazine-1-carbonyl]-2-naphthyl]ethylamino]quinoline-6-carbonitrile (4.18d (m=11))

A white solid (31 mg, 98% yield) and used without further purification. ESI-MS m/z : 633 ($[M+H]^+$).

tert-butyl N-[2-[2-[2-[3-[4-[6-[2-[(6-cyano-4-quinolyl)amino]ethyl]naphthalene-2-carbonyl]piperazin-1-yl]-3-oxo-propoxy]ethoxy]ethoxy]ethyl]carbamate (4.19)

To a 10 mL round-bottle flask was added a solution of 3-[2-[2-(tert-butoxycarbonylamino)ethoxy]ethoxy]ethoxy]propanoic acid (0.47 mmol, 150 mg) in DCM (5 mL). Then HATU (0.61 mmol, 230 mg), DIEA (1.40 mmol, 240 μ L) were added and the mixture was stirred at room temperature for 15 min, then 4-[2-[6-(piperazine-1-carbonyl)-2-naphthyl]ethylamino]quinoline-6-carbonitrile (0.47 mmol, 203 mg) was added and the mixture was stirred for 2h. Upon completion, water was added, the mixture was extracted with DCM, the organic layers were combined, washed with sat NaHCO_3 aq, dried by Na_2SO_4 , condensed and purified by flash column chromatography using a gradient of 0-5% MeOH/DCM to give tert-

butyl *N*-[2-[2-[2-[3-[4-[6-[2-[(6-cyano-4-quinolyl)amino]ethyl]naphthalene-2-carbonyl]piperazin-1-yl]-3-oxo-propoxy]ethoxy]ethoxy]ethyl]carbamate (82 mg, 24% yield). ESI-MS *m/z*: 739 ($[M+H]^+$). ¹H-NMR (300MHz, CD₂Cl₂): 8.61 (d, *J*=5.7 Hz, 1H), 8.17 (s, 1H), 7.99 (d, *J*=9.3 Hz, 1H), 7.89 (s, 2H), 7.83 (d, *J*=9.3 Hz, 1H), 7.77 (d, *J*=7.5 Hz, 2H), 7.74 (dd, *J*=8.8, 1.7 Hz, 1H), 7.71 (s, 1H), 7.49 (dd, *J*=8.8, 1.7 Hz, 1H), 7.45 (dd, *J*=8.8, 1.7 Hz, 1H), 6.61 (d, *J*=5.7 Hz, 1H), 5.69 (m, 1H), 5.11 (m, 1H), 3.73 (m, 8H), 3.57 (m, 12H), 3.47 (m, 2H), 3.22 (m, 4H), 2.63 (m, 2H), 1.40 (s, 9H).

tert-butyl N-[2-[2-[2-[3-[4-[6-[2-[(6-cyano-4-quinolyl)amino]ethyl]naphthalene-2-carbonyl]piperazin-1-yl]-3-oxo-propoxy]ethoxy]ethoxy]ethyl]carbamate (**4.20**)

To a 10 mL round-bottle flask was added a solution of *tert-butyl N*-[2-[2-[2-[3-[4-[6-[2-[(6-cyano-4-quinolyl)amino]ethyl]naphthalene-2-carbonyl]piperazin-1-yl]-3-oxo-propoxy]ethoxy]ethoxy]ethyl]carbamate (0.11 mmol, 82 mg) in DCM (5 mL). Then TFA (1 mL) was added and the mixture was stirred at room temperature for 4h. Upon completion, the mixture was condensed to give 4-[2-[6-[4-[3-[2-[2-(2-aminoethoxy)ethoxy]ethoxy]propanoyl]piperazine-1-carbonyl]-2-naphthyl]ethylamino]quinoline-6-carbonitrile (70 mg, 99% yield) and used without further purification. ESI-MS *m/z*: 639 ($[M+H]^+$).

N-[2-[2-[2-[3-[4-[6-[2-[(6-cyano-4-quinolyl)amino]ethyl]naphthalene-2-carbonyl]piperazin-1-yl]-3-oxo-propoxy]ethoxy]ethoxy]ethyl]-3-[[2-(2,6-dioxo-3-piperidyl)-1,3-dioxo-isoindolin-4-yl]amino]propanamide (**4.21**)

To a 10 mL round-bottle flask was added a solution of 4-[2-[6-[4-[3-[2-[2-(2-aminoethoxy)ethoxy]ethoxy]propanoyl]piperazine-1-carbonyl]-2-

naphthyl]ethylamino]quinoline-6-carbonitrile (0.11 mmol, 70 mg) and 3-[[2-(2,6-dioxo-3-piperidyl)-1,3-dioxo-isoindolin-4-yl]amino]propanoic acid (0.11 mmol, 38 mg) in DMF (2 mL). Then EDC-HCl (0.22 mmol, 42 mg), HOAt (0.22 mmol, 30 mg), and N-methylmorpholine (0.55 mmol, 55 mg) were added and the mixture was stirred at room temperature for overnight. Upon completion, the mixture was diluted with DCM, added with water, extracted with DCM, the organic layers were combined, dried by Na₂SO₄, condensed and purified by flash column chromatography using a gradient of 0-10% MeOH/DCM to give N-[2-[2-[2-[3-[4-[6-[2-[(6-cyano-4-quinolyl)amino]ethyl]naphthalene-2-carbonyl]piperazin-1-yl]-3-oxo-propoxy]ethoxy]ethoxy]ethyl]-3-[[2-(2,6-dioxo-3-piperidyl)-1,3-dioxo-isoindolin-4-yl]amino]propanamide (62 mg, 59% yield). ESI-MS m/z: 967 ([M+H]⁺). ¹H-NMR (300MHz, CD₂Cl₂): 9.00 (m, 1H), 8.60 (d, J=5.7 Hz, 1H), 8.17 (s, 1H), 7.98 (d, J=8.9 Hz, 1H), 7.88 (s, 1H), 7.83 (t, J=8.3 Hz, 2H), 7.71 (d, J=8.9 Hz, 1H), 7.69 (s, 1H), 7.47 (d, J=8.4 Hz, 2H), 7.42 (t, J=8.3 Hz, 2H), 6.98 (d, J=7.2 Hz, 1H), 6.90 (d, J=7.2 Hz, 1H), 6.71 (m, 1H), 6.58 (d, J=5.6 Hz, 1H), 6.52 (t, J=6.1 Hz, 1H), 5.75 (m, 1H), 4.89 (m, 1H), 3.75 (t, J=6.7 Hz, 2H), 3.68 (t, J=5.9 Hz, 2H), 3.55 (m, 18H), 3.37 (m, 2H), 3.20 (t, J=7.5 Hz, 2H), 2.80 (m, 1H), 2.73 (m, 2H), 2.60 (m, 2H), 2.48 (t, J=6.4 Hz, 2H), 2.08 (m, 1H), 1.94 (m, 2H).

tert-butyl 3-[2-[[2-(2,6-dioxo-3-piperidyl)-1,3-dioxo-isoindolin-4-yl]amino]ethoxy]propanoate (**4.22**)

To a 10 mL round-bottle flask was added a solution of 2-(2,6-dioxo-3-piperidyl)-4-fluoro-isoindoline-1,3-dione (0.72 mmol, 200 mg) and *tert-butyl* 3-(2-aminoethoxy)propanoate (0.72 mmol, 137 mg) in DMF (2 mL). Then DIEA (1.1

mmol, 186 uL) was added and the mixture was microwaved at 100°C for 2h. Upon completion, the mixture was condensed and purified by flash column chromatography using a gradient of 0-2% MeOH/DCM to give tert-butyl 3-[2-[[2-(2,6-dioxo-3-piperidyl)-1,3-dioxo-isoindolin-4-yl]amino]ethoxy]propanoate (200 mg, 62% yield). ESI-MS m/z : 446 ($[M+H]^+$).

3-[2-[[2-(2,6-dioxo-3-piperidyl)-1,3-dioxo-isoindolin-4-yl]amino]ethoxy]propanoic acid (4.23)

To a 10 mL round-bottle flask was added a solution of tert-butyl 3-[2-[[2-(2,6-dioxo-3-piperidyl)-1,3-dioxo-isoindolin-4-yl]amino]ethoxy]propanoate (0.45 mmol, 200 mg) in formic acid (2 mL). Then the mixture was stirred at room temperature for overnight. Upon completion, the mixture was condensed and purified by flash column chromatography using a gradient of 0-4% MeOH/DCM to give 3-[2-[[2-(2,6-dioxo-3-piperidyl)-1,3-dioxo-isoindolin-4-yl]amino]ethoxy]propanoic acid (127 mg, 73% yield). ESI-MS m/z : 390 ($[M+H]^+$).

$^1\text{H-NMR}$ (300MHz, CD_2Cl_2): 8.72 (m, 1H), 7.50 (t, $J=8.1$ Hz, 1H), 7.07 (d, $J=7.3$ Hz, 1H), 6.95 (d, $J=8.1$ Hz, 1H), 6.46 (m, 1H), 4.94 (m, 1H), 3.74 (t, $J=6.1$ Hz, 2H), 3.69 (t, $J=5.6$ Hz, 2H), 3.46 (m, 2H), 2.78 (m, 1H), 2.76 (t, $J=10.7$ Hz, 2H), 2.59 (t, $J=6.1$ Hz, 2H), 2.11 (m, 1H).

N-[9-[4-[6-[2-[(6-cyano-4-quinolyl)amino]ethyl]naphthalene-2-carbonyl]piperazin-1-yl]-9-oxo-nonyl]-3-[2-[[2-(2,6-dioxo-3-piperidyl)-1,3-dioxo-isoindolin-4-yl]amino]ethoxy]propanamide (4.24)

To a 10 mL round-bottle flask was added a solution of 4-[2-[6-[4-(9-aminononanoyl)piperazine-1-carbonyl]-2-naphthyl]ethylamino]quinoline-6-

carbonitrile (0.07 mmol, 40 mg) and 3-[2-[[2-(2,6-dioxo-3-piperidyl)-1,3-dioxo-isoindolin-4-yl]amino]ethoxy]propanoic acid (0.07 mmol, 26 mg) in DMF (2 mL). Then EDC-HCl (0.14 mmol, 26 mg), HOAt (0.14 mmol, 18 mg), and N-methylmorpholine (0.33 mmol, 34 mg) were added and the mixture was stirred at room temperature for overnight. Upon completion, the mixture was diluted with DCM, added with water, extracted with DCM, the organic layers were combined, dried by Na₂SO₄, condensed and purified by flash column chromatography using a gradient of 0-10% MeOH/DCM to give N-[9-[4-[6-[2-[(6-cyano-4-quinolyl)amino]ethyl]naphthalene-2-carbonyl]piperazin-1-yl]-9-oxo-nonyl]-3-[2-[[2-(2,6-dioxo-3-piperidyl)-1,3-dioxo-isoindolin-4-yl]amino]ethoxy]propanamide (52 mg, 80% yield). ESI-MS m/z: 963 ([M+H]⁺). ¹H-NMR (300MHz, CD₂Cl₂): 9.22 (m, 1H), 8.59 (d, J=5.1 Hz, 1H), 8.24 (s, 1H), 7.99 (d, J=9.2 Hz, 1H), 7.87 (s, 1H), 7.84 (d, J=8.3 Hz, 1H), 7.81 (d, J=8.3 Hz, 1H), 7.70 (d, J=9.1 Hz, 1H), 7.69 (s, 1H), 7.49 (t, J=8.3 Hz, 2H), 7.42 (d, J=8.3 Hz, 1H), 7.05 (d, J=6.8 Hz, 1H), 6.92 (d, J=6.8 Hz, 1H), 6.57 (d, J=5.4 Hz, 1H), 6.47 (m, 1H), 6.15 (m, 1H), 6.00 (m, 1H), 4.91 (m, 1H), 3.72 (t, J=6.0 Hz, 2H), 3.67 (t, J=5.2 Hz, 2H), 3.56 (m, 6H), 3.44 (q, J=5.2 Hz, 2H), 3.19 (t, J=7.5 Hz, 2H), 3.12 (q, J=6.7 Hz, 2H), 2.77 (m, 3H), 2.40 (t, J=6.6 Hz, 2H), 2.30 (m, 2H), 2.24 (m, 2H), 2.10 (m, 1H), 1.55 (m, 2H), 1.38 (m, 2H), 1.22 (m, 10H).

10-[4-[6-[2-[(6-cyano-4-quinolyl)amino]ethyl]naphthalene-2-carbonyl]piperazin-1-yl]-N-[5-[[2-(2,6-dioxo-3-piperidyl)-1,3-dioxo-isoindolin-4-yl]amino]pentyl]-10-oxo-decanamide (4.25)

To a 10 mL round-bottom flask was added a solution of 10-[4-[6-[2-[(6-cyano-4-quinolyl)amino]ethyl]naphthalene-2-carbonyl]piperazin-1-yl]-10-oxo-decanoic acid (0.11 mmol, 66 mg) and 6-[[2-(2,6-dioxo-3-piperidyl)-1,3-dioxo-isindolin-4-yl]amino]hexanoic acid (0.11 mmol, 42 mg) in DMF (2 mL). Then EDC-HCl (0.21 mmol, 41 mg), HOAt (0.21 mmol, 29 mg), and N-methylmorpholine (0.53 mmol, 54 mg) were added and the mixture was stirred at room temperature for overnight. Upon completion, the mixture was diluted with DCM, added with water, extracted with DCM, the organic layers were combined, dried by Na₂SO₄, condensed and purified by flash column chromatography using a gradient of 0-10% MeOH/DCM to give 10-[4-[6-[2-[(6-cyano-4-quinolyl)amino]ethyl]naphthalene-2-carbonyl]piperazin-1-yl]-N-[5-[[2-(2,6-dioxo-3-piperidyl)-1,3-dioxo-isindolin-4-yl]amino]pentyl]-10-oxo-decanamide (35 mg, 34% yield). ESI-MS m/z: 961 ([M + H]⁺). ¹H-NMR (300MHz, CD₂Cl₂): 8.99 (m, 1H), 8.60 (d, J=5.7 Hz, 1H), 8.21 (s, 1H), 7.98 (d, J=8.9 Hz, 1H), 7.88 (s, 1H), 7.83 (t, J=8.3 Hz, 2H), 7.71 (d, J=8.9 Hz, 1H), 7.69 (s, 1H), 7.48 (d, J=8.4 Hz, 2H), 7.45 (t, J=8.3 Hz, 2H), 7.02 (d, J=7.2 Hz, 1H), 6.88 (d, J=8.2 Hz, 1H), 6.57 (d, J=5.5 Hz, 1H), 6.22 (t, J=5.5 Hz, 1H), 5.86 (t, J=5.0 Hz, 1H), 5.72 (t, J=5.5 Hz, 1H), 4.89 (m, 1H), 3.59 (m, 8H), 3.21 (m, 6H), 2.80 (m, 1H), 2.74 (m, 2H), 2.31 (m, 2H), 2.11 (m, 1H), 2.10 (t, J=7.4 Hz, 2H), 1.88 (m, 2H), 1.55 (m, 8H), 1.27 (s, 10H).

rac-(2*S*,4*R*)-4-hydroxy-*N*-[[4-(4-methylthiazol-5-yl)phenyl]methyl]-1-[*rac*-(2*S*)-2-[[10-[4-[6-[2-[(6-cyano-4-quinolyl)amino]ethyl]naphthalene-2-carbonyl]piperazin-1-yl]-10-oxo-decanoyl]amino]-3,3-dimethyl-butanoyl]pyrrolidine-2-carboxamide (4.26)

To a 10 mL round-bottle flask was added a solution of 10-[4-[6-[2-[(6-cyano-4-quinolyl)amino]ethyl]naphthalene-2-carbonyl]piperazin-1-yl]-10-oxo-decanoic acid (0.13 mmol, 80 mg) and 5-[[2-(2,6-dioxo-3-piperidyl)-1,3-dioxo-isoindolin-4-yl]amino]pentanoic acid (0.13 mmol, 49 mg) in DMF (2 mL). Then EDC-HCl (0.27 mmol, 51 mg), HOAt (0.27 mmol, 36 mg), and N-methylmorpholine (0.27 mmol, 67 mg) were added and the mixture was stirred at room temperature for overnight. Upon completion, the mixture was diluted with DCM, added with water, extracted with DCM, the organic layers were combined, dried by Na₂SO₄, condensed and purified by flash column chromatography using a gradient of 0-10% MeOH/DCM to give N-[10-[4-[6-[2-[(6-cyano-4-quinolyl)amino]ethyl]naphthalene-2-carbonyl]piperazin-1-yl]-10-oxo-decyl]-5-[[2-(2,6-dioxo-3-piperidyl)-1,3-dioxo-isoindolin-4-yl]amino]pentanamide (73 mg, 61% yield). ESI-MS m/z: 1033 ([M+H]⁺). ¹H-NMR (300MHz, CD₂Cl₂): 8.63 (s, 1H), 8.57 (d, J=5.5 Hz, 1H), 8.30 (s, 1H), 7.96 (d, J=9.3 Hz, 1H), 7.86 (s, 1H), 7.81 (t, J=8.8 Hz, 2H), 7.71 (dd, J=8.8, 1.5 Hz, 1H), 7.67 (s, 1H), 7.43 (m, 3H), 7.34 (m, 5H), 6.59 (d, J=6.0 Hz, 1H), 6.32 (d, J=9.3 Hz, 1H), 6.28 (m, 1H), 4.64 (m, 1H), 4.51 (m, 2H), 4.28 (m, 1H), 3.97 (m, 1H), 3.70-3.53 (m, 12H), 3.19 (t, J=6.8 Hz, 2H), 2.44 (m, 2H), 2.32 (m, 2H), 2.15 (m, 2H), 2.12 (s, 3H), 1.56 (m, 4H), 1.25 (m, 8H), 0.94 (s, 9H).

The general preparation of **4.27**

To a 10 mL round-bottle flask was added a solution of **4.18** (1eq) and **4.12** (1eq) in DMF. Then EDC-HCl (2eq), HOAt (2eq), and N-methylmorpholine (5eq) were added and the mixture was stirred at room temperature for overnight. Upon completion, the mixture was diluted with DCM, added with water, extracted with

DCM, the organic layers were combined, dried by Na₂SO₄, condensed and purified by flash column chromatography using a gradient of 0-10% MeOH/DCM to give target compounds **4.27**.

N-[9-[4-[6-[2-[(6-cyano-4-quinolyl)amino]ethyl]naphthalene-2-carbonyl]piperazin-1-yl]-9-oxo-nonyl]-5-[[2-(2,6-dioxo-3-piperidyl)-1,3-dioxo-isoindolin-4-yl]amino]pentanamide (**4.27a** (**m=8**, **n=4**))

A yellow solid (33 mg, 25% yield). ESI-MS *m/z*: 947 ([*M*+*H*)⁺). ¹H-NMR (300MHz, DMSO-*d*₆): 11.10 (s, 1H), 8.86 (s, 1H), 8.52 (d, *J*=5.3 Hz, 1H), 7.97 (s, 1H), 7.93 (d, *J*=5.3 Hz, 1H), 7.89 (d, *J*=5.3 Hz, 1H), 7.88 (s, 3H), 7.76 (t, *J*=5.7 Hz, 1H), 7.70 (t, *J*=5.7 Hz, 1H), 7.54 (m, 3H), 7.07 (d, *J*=8.7 Hz, 1H), 7.01 (d, *J*=7.0 Hz, 1H), 6.71 (d, *J*=5.7 Hz, 1H), 6.56 (t, *J*=5.4 Hz, 1H), 5.05 (m, 1H), 3.65 (q, *J*=7.3 Hz, 2H), 3.50 (m, 6H), 3.28 (m, 2H), 3.18 (t, *J*=7.3 Hz, 2H), 3.00 (q, *J*=6.4 Hz, 2H), 2.88 (m, 1H), 2.57 (m, 2H), 2.29 (m, 2H), 2.08 (m, 2H), 2.00 (m, 1H), 1.54 (m, 4H), 1.46 (m, 2H), 1.35 (m, 2H), 1.22 (s, 10H).

N-[10-[4-[6-[2-[(6-cyano-4-quinolyl)amino]ethyl]naphthalene-2-carbonyl]piperazin-1-yl]-10-oxo-decyl]-6-[[2-(2,6-dioxo-3-piperidyl)-1,3-dioxo-isoindolin-4-yl]amino]hexanamide (**4.27b** (**m=9**, **n=5**))

A yellow solid (80 mg, 74% yield). ESI-MS *m/z*: 975 ([*M*+*H*)⁺). ¹H-NMR (300MHz, DMSO-*d*₆): 11.11 (s, 1H), 8.86 (s, 1H), 8.52 (d, *J*=5.3 Hz, 1H), 7.97 (s, 1H), 7.93 (d, *J*=5.3 Hz, 1H), 7.89 (d, *J*=5.3 Hz, 1H), 7.88 (s, 3H), 7.71 (m, 2H), 7.54 (m, 3H), 7.06 (d, *J*=8.7 Hz, 1H), 7.00 (d, *J*=7.0 Hz, 1H), 6.71 (d, *J*=5.7 Hz, 1H), 6.51 (t, *J*=5.4 Hz, 1H), 5.05 (m, 1H), 3.65 (q, *J*=6.4 Hz, 2H), 3.51 (m, 6H), 3.27 (q, *J*=6.4 Hz, 2H), 3.18 (t, *J*=7.3 Hz, 2H), 2.99 (q, *J*=6.4 Hz, 2H), 2.88 (m, 1H), 2.57

(m, 2H), 2.29 (m, 2H), 2.04 (m, 2H), 2.00 (m, 1H), 1.51 (m, 6H), 1.32 (m, 4H), 1.22 (s, 12H).

N-[9-[4-[6-[2-[(6-cyano-4-quinolyl)amino]ethyl]naphthalene-2-carbonyl]piperazin-1-yl]-9-oxo-nonyl]-6-[[2-(2,6-dioxo-3-piperidyl)-1,3-dioxo-isoindolin-4-yl]amino]hexanamide (**4.27c** (**m=8**, **n=5**))

A yellow solid (51 mg, 31% yield). ESI-MS *m/z*: 961 ($[M+H]^+$). $^1\text{H-NMR}$ (300MHz, DMSO- d_6): 11.11 (s, 1H), 8.86 (s, 1H), 8.52 (d, *J*=5.7 Hz, 1H), 7.97 (s, 1H), 7.93 (d, *J*=5.3 Hz, 1H), 7.89 (d, *J*=5.3 Hz, 1H), 7.88 (s, 3H), 7.71 (m, 2H), 7.54 (m, 3H), 7.06 (d, *J*=8.7 Hz, 1H), 7.00 (d, *J*=7.0 Hz, 1H), 6.71 (d, *J*=5.7 Hz, 1H), 6.51 (t, *J*=5.4 Hz, 1H), 5.05 (m, 1H), 3.65 (q, *J*=6.4 Hz, 2H), 3.51 (m, 6H), 3.26 (q, *J*=6.4 Hz, 2H), 3.18 (t, *J*=7.3 Hz, 2H), 2.99 (q, *J*=6.4 Hz, 2H), 2.86 (m, 1H), 2.57 (m, 2H), 2.29 (m, 2H), 2.05 (m, 2H), 1.51 (m, 6H), 1.32 (m, 4H), 1.22 (s, 10H).

N-[12-[4-[6-[2-[(6-cyano-4-quinolyl)amino]ethyl]naphthalene-2-carbonyl]piperazin-1-yl]-12-oxo-dodecyl]-3-[[2-(2,6-dioxo-3-piperidyl)-1,3-dioxo-isoindolin-4-yl]amino]propanamide (**4.27d** (**m=10**, **n=3**))

A yellow solid (44 mg, 75% yield). ESI-MS *m/z*: 961 ($[M+H]^+$). $^1\text{H-NMR}$ (300MHz, DMSO- d_6): 11.10 (s, 1H), 8.93 (s, 1H), 8.53 (d, *J*=5.9 Hz, 1H), 8.10 (m, 1H), 7.97 (s, 2H), 7.94 (s, 1H), 7.92 (s, 1H), 7.89 (s, 2H), 7.81 (t, *J*=5.4 Hz, 1H), 7.58 (d, *J*=7.5 Hz, 2H), 7.52 (t, *J*=7.0 Hz, 1H), 7.10 (d, *J*=8.6 Hz, 1H), 7.01 (d, *J*=7.0 Hz, 1H), 6.79 (d, *J*=5.9 Hz, 1H), 6.62 (t, *J*=5.9 Hz, 1H), 5.05 (m, 1H), 3.71 (q, *J*=7.3 Hz, 2H), 3.51 (m, 6H), 3.34 (m, 2H), 3.29 (m, 2H), 3.19 (t, *J*=7.3 Hz, 2H), 3.02 (q, *J*=6.0 Hz, 2H), 2.87 (m, 1H), 2.56 (m, 2H), 2.30 (m, 2H), 2.14 (t, *J*=7.4 Hz, 2H), 2.02 (m, 1H), 1.77 (m, 2H), 1.47 (m, 2H), 1.36 (m, 2H), 1.22 (s, 12H).

N-[12-[4-[6-[2-[(6-cyano-4-quinolyl)amino]ethyl]naphthalene-2-carbonyl]piperazin-1-yl]-12-oxo-dodecyl]-3-[[2-(2,6-dioxo-3-piperidyl)-1,3-dioxo-isoindolin-4-yl]amino]propanamide (**4.27e** (**m=11**, **n=2**))

A yellow solid (34 mg, 72% yield). ESI-MS *m/z*: 961 ($[M+H]^+$). $^1\text{H-NMR}$ (300MHz, DMSO- d_6): 11.10 (s, 1H), 8.87 (s, 1H), 8.52 (d, *J*=5.9 Hz, 1H), 8.10 (m, 1H), 7.97 (s, 1H), 7.94 (d, *J*=4.2 Hz, 2H), 7.89 (d, *J*=4.2 Hz, 2H), 7.88 (s, 2H), 7.73 (t, *J*=5.4 Hz, 1H), 7.59 (d, *J*=7.5 Hz, 2H), 7.52 (t, *J*=7.0 Hz, 1H), 7.12 (d, *J*=8.6 Hz, 1H), 7.02 (d, *J*=7.0 Hz, 1H), 6.72 (d, *J*=5.9 Hz, 1H), 6.69 (t, *J*=5.9 Hz, 1H), 5.04 (m, 1H), 3.66 (q, *J*=7.3 Hz, 2H), 3.50 (m, 10H), 3.18 (t, *J*=7.3 Hz, 2H), 3.02 (q, *J*=6.0 Hz, 2H), 2.88 (m, 1H), 2.55 (m, 2H), 2.39 (t, *J*=6.2 Hz, 2H), 2.31 (m, 2H), 2.00 (m, 1H), 1.47 (m, 2H), 1.34 (m, 2H), 1.19 (s, 14H).

N-[10-[4-[6-[2-[(6-cyano-4-quinolyl)amino]ethyl]naphthalene-2-carbonyl]piperazin-1-yl]-10-oxo-decyl]-5-[[2-(2,6-dioxo-3-piperidyl)-1,3-dioxo-isoindolin-4-yl]amino]pentanamide (**4.27f** (**m=9**, **n=4**))

A yellow solid (28 mg, 22% yield). ESI-MS *m/z*: 961 ($[M+H]^+$). $^1\text{H-NMR}$ (300MHz, CD_2Cl_2): 8.95 (m, 1H), 8.59 (d, *J*=5.7 Hz, 1H), 8.21 (s, 1H), 8.00 (d, *J*=8.9 Hz, 1H), 7.88 (s, 1H), 7.83 (t, *J*=8.3 Hz, 2H), 7.71 (d, *J*=8.9 Hz, 1H), 7.69 (s, 1H), 7.48 (d, *J*=8.4 Hz, 2H), 7.45 (t, *J*=8.3 Hz, 2H), 7.02 (d, *J*=7.2 Hz, 1H), 6.87 (d, *J*=8.2 Hz, 1H), 6.57 (d, *J*=5.7 Hz, 1H), 6.24 (t, *J*=5.5 Hz, 1H), 5.93 (m, 1H), 5.74 (t, *J*=5.5 Hz, 1H), 4.90 (m, 1H), 3.68 (q, *J*=5.5 Hz, 2H), 3.54 (m, 6H), 3.21 (m, 6H), 2.78 (m, 2H), 2.71 (m, 1H), 2.31 (m, 2H), 2.17 (t, *J*=6.5 Hz, 2H), 2.10 (m, 1H), 1.69 (m, 4H), 1.58 (m, 2H), 1.44 (m, 2H), 1.26 (s, 12H).

2-(2,6-dioxo-3-piperidyl)-5-fluoro-isoindoline-1,3-dione (**4.28**)

To a 100 mL round-bottle flask was added a solution of 5-fluoroisobenzofuran-1,3-dione (6.02 mmol, 1 g) and 3-aminopiperidine-2,6-dione (6.02 mmol, 771 mg) in acetic acid (10 mL). Then sodium acetate (12 mmol, 988 mg) was added and the mixture was stirred at 130°C for overnight. Upon completion, the mixture was cooled to room temperature, condensed. The residue was added with ice water, the precipitation was filtered and washed with water and EtOH, dried to give 2-(2,6-dioxo-3-piperidyl)-5-fluoro-isoindoline-1,3-dione (1.35 g, 81% yield) and used for the next step without further purification. ESI-MS m/z : 277 ($[M+H]^+$).

tert-butyl 4-((2-(2,6-dioxopiperidin-3-yl)-1,3-dioxoisoindolin-5-yl)amino)butanoate
(4.29)

To a 20 mL microwave flask was added a solution of 2-(2,6-dioxo-3-piperidyl)-5-fluoro-isoindoline-1,3-dione (1.67 mmol, 266 mg), *tert*-butyl 4-aminobutanoate (1.67 mmol, 266 mg), and DIEA (4.55 mmol, 588 mg) in NMP (5 mL). Then the mixture was microwaved at 130°C for 1h. Upon completion, the mixture was poured in EtOAc, and washed with water and brine. The organic phase was dried by Na₂SO₄, condensed to give *tert*-butyl 4-((2-(2,6-dioxopiperidin-3-yl)-1,3-dioxoisoindolin-5-yl)amino)butanoate and used for the next step without further purification. ESI-MS m/z : 416 ($[M+H]^+$).

4-[[2-(2,6-dioxo-3-piperidyl)-1,3-dioxo-isoindolin-5-yl]amino]butanoic acid (4.30)

To a 10 mL round bottle flask was added a solution of *tert*-butyl 4-((2-(2,6-dioxopiperidin-3-yl)-1,3-dioxoisoindolin-5-yl)amino)butanoate in formic acid. The mixture was then stirred at room temperature for overnight. Upon completion, the

mixture was condensed to give 4-[[2-(2,6-dioxo-3-piperidyl)-1,3-dioxo-isoindolin-5-yl]amino]butanoic acid (170 mg, 31% yield) and used for the next step without further purification. ESI-MS m/z : 360 ($[M+H]^+$).

N-[11-[4-[6-[2-[(6-cyano-4-quinolyl)amino]ethyl]naphthalene-2-carbonyl]piperazin-1-yl]-11-oxo-undecyl]-4-[[2-(2,6-dioxo-3-piperidyl)-1,3-dioxo-isoindolin-5-yl]amino]butanamide (**4.31**)

To a 10 mL round-bottle flask was added a solution of 4-[2-[6-[4-(11-aminoundecanoyl)piperazine-1-carbonyl]-2-naphthyl]ethylamino]quinoline-6-carbonitrile (0.08 mmol, 50 mg) and 4-[[2-(2,6-dioxo-3-piperidyl)-1,3-dioxo-isoindolin-5-yl]amino]butanoic acid (0.08 mmol, 29 mg) in DMF (2 mL). Then EDC-HCl (0.16 mmol, 31 mg), HOAt (0.16 mmol, 22 mg), and *N*-methylmorpholine (0.40 mmol, 41 mg) were added and the mixture was stirred at room temperature for overnight. Upon completion, the mixture was diluted with DCM, added with water, extracted with DCM, the organic layers were combined, dried by Na_2SO_4 , condensed and purified by flash column chromatography using a gradient of 0-10% MeOH/DCM to give *N*-[11-[4-[6-[2-[(6-cyano-4-quinolyl)amino]ethyl]naphthalene-2-carbonyl]piperazin-1-yl]-11-oxo-undecyl]-4-[[2-(2,6-dioxo-3-piperidyl)-1,3-dioxo-isoindolin-5-yl]amino]butanamide (46 mg, 59% yield). ESI-MS m/z : 961 ($[M+H]^+$). $^1\text{H-NMR}$ (300MHz, DMSO-d_6): 11.10 (s, 1H), 8.93 (s, 1H), 8.53 (d, $J=5.9$ Hz, 1H), 8.10 (m, 1H), 7.97 (s, 2H), 7.94 (s, 1H), 7.92 (s, 1H), 7.89 (s, 2H), 7.81 (t, $J=5.4$ Hz, 1H), 7.58 (d, $J=7.5$ Hz, 2H), 7.52 (t, $J=7.0$ Hz, 1H), 7.10 (d, $J=8.6$ Hz, 1H), 7.01 (d, $J=7.0$ Hz, 1H), 6.79 (d, $J=5.9$ Hz, 1H), 6.62 (t, $J=5.9$ Hz, 1H), 5.05 (m, 1H), 3.71 (q, $J=7.3$ Hz, 2H), 3.51 (m, 6H),

3.34 (m, 2H), 3.29 (m, 2H), 3.19 (t, J=7.3 Hz, 2H), 3.02 (q, J=6.0 Hz, 2H), 2.87 (m, 1H), 2.56 (m, 2H), 2.30 (m, 2H), 2.14 (t, J=7.4 Hz, 2H), 2.02 (m, 1H), 1.77 (m, 2H), 1.47 (m, 2H), 1.36 (m, 2H), 1.22 (s, 12H).

tert-butyl 4-[[2-(2,6-dioxo-3-piperidyl)-1-oxo-isoindolin-4-yl]amino]butanoate (4.32)

To a 100 mL round-bottom flask was added a solution of 3-(4-amino-1-oxo-isoindolin-2-yl)piperidine-2,6-dione (3.86 mmol, 1 g), *tert*-butyl 4-bromobutanoate (4.24 mmol, 947 mg), and DIEA (11.6 mmol, 1.5 g) in NMP (5 mL). Then the mixture was stirred at 130°C for overnight. Upon completion, the mixture was cooled to room temperature and poured into EtOAc, washed with water and brine. The organic phase was dried by Na₂SO₄, condensed and purified by flash column chromatography using a gradient of 0-5% MeOH/DCM to give *tert*-butyl 4-[[2-(2,6-dioxo-3-piperidyl)-1-oxo-isoindolin-4-yl]amino]butanoate (538 mg, 35% yield). ESI-MS *m/z*: 360 ([M+H]⁺). ¹H-NMR (300MHz, DMSO-d₆): 11.02 (s, 1H), 7.28 (t, J=7.7 Hz, 1H), 6.93 (d, J=7.5Hz, 1H), 6.75 (d, J=7.7 Hz, 1H), 5.65 (t, J=5.7 Hz, 1H), 5.12 (dd, J=13.8, 5.2 Hz, 1H), 4.17 (q, J=17.2 Hz, 2H), 3.13 (q, J=7.3 Hz, 2H), 2.93 (m, 1H), 2.62 (m, 1H), 2.33 (t, J=7.9 Hz, 2H), 2.28 (m, 1H), 2.03 (m, 1H), 1.79 (m, 2H), 1.39 (s, 9H).

tert-butyl 4-[[2-(2,6-dioxo-3-piperidyl)-1-oxo-isoindolin-4-yl]amino]butanoate (4.33)

To a 10 mL round-bottom flask was added a solution of *tert*-butyl 4-[[2-(2,6-dioxo-3-piperidyl)-1-oxo-isoindolin-4-yl]amino]butanoate (0.4 mmol, 160 mg) in formic acid (3 mL). Then the mixture was stirred at room temperature for overnight. Upon completion, the mixture was condensed and purified by flash column chromatography using a gradient of 0-7% MeOH/DCM to give 4-[[2-(2,6-dioxo-3-

piperidyl)-1-oxo-isoindolin-4-yl]amino]butanoic acid (126 mg, 92% yield). ESI-MS m/z : 346 ($[M+H]^+$). 1H -NMR (300MHz, DMSO- d_6): 12.23 (s, 1H), 11.02 (s, 1H), 7.28 (t, $J=7.7$ Hz, 1H), 6.93 (d, $J=7.5$ Hz, 1H), 6.76 (d, $J=7.7$ Hz, 1H), 5.65 (m, 1H), 5.12 (dd, $J=12.8, 5.2$ Hz, 1H), 4.18 (q, $J=17.2$ Hz, 2H), 3.14 (m, 2H), 2.93 (m, 1H), 2.62 (m, 1H), 2.34 (t, $J=7.9$ Hz, 2H), 2.24 (m, 1H), 2.04 (m, 1H), 1.80 (m, 2H).

N-[11-[4-[6-[2-[(6-cyano-4-quinolyl)amino]ethyl]naphthalene-2-carbonyl]piperazin-1-yl]-11-oxo-undecyl]-4-[[2-(2,6-dioxo-3-piperidyl)-1-oxo-isoindolin-4-yl]amino]butanamide (**4.34**)

To a 10 mL round-bottle flask was added a solution of 4-[2-[6-[4-(11-aminoundecanoyl)piperazine-1-carbonyl]-2-naphthyl]ethylamino]quinoline-6-carbonitrile (0.08 mmol, 50 mg) and 4-[[2-(2,6-dioxo-3-piperidyl)-1-oxo-isoindolin-4-yl]amino]butanoic acid (0.08 mmol, 28 mg) in DMF (2 mL). Then EDC-HCl (0.16 mmol, 31 mg), HOAt (0.16 mmol, 22 mg), and *N*-methylmorpholine (0.40 mmol, 41 mg) were added and the mixture was stirred at room temperature for overnight. Upon completion, the mixture was diluted with DCM, added with water, extracted with DCM, the organic layers were combined, dried by Na_2SO_4 , condensed and purified by flash column chromatography using a gradient of 0-10% MeOH/DCM to give *N*-[11-[4-[6-[2-[(6-cyano-4-quinolyl)amino]ethyl]naphthalene-2-carbonyl]piperazin-1-yl]-11-oxo-undecyl]-4-[[2-(2,6-dioxo-3-piperidyl)-1-oxo-isoindolin-4-yl]amino]butanamide (36 mg, 47% yield). ESI-MS m/z : 947 ($[M+H]^+$). 1H -NMR (300MHz, DMSO- d_6): 11.02 (s, 1H), 8.86 (s, 1H), 8.52 (d, $J=5.9$ Hz, 1H), 7.97 (s, 1H), 7.93 (d, $J=4.9$ Hz, 1H), 7.89 (s, 1H), 7.88 (s, 3H), 7.78 (t, $J=5.4$ Hz, 1H), 7.71 (t, $J=5.4$ Hz, 1H), 7.58 (d, $J=7.8$ Hz, 1H), 7.50 (d, $J=7.8$ Hz, 1H), 7.27 (t,

J=7.8 Hz, 1H), 6.92 (d, J=7.4 Hz, 1H), 6.73 (d, J=7.8 Hz, 1H), 6.71 (d, J=5.4 Hz, 1H), 5.64 (m, 1H), 5.11 (m, 1H), 4.16 (q, J=17.0 Hz, 2H), 3.65 (q, J=6.9 Hz, 2H), 3.51 (m, 6H), 3.19 (t, J=7.6 Hz, 2H), 3.00 (m, 4H), 2.61 (m, 1H), 2.30 (m, 3H), 2.17 (t, J=7.6 Hz, 1H), 2.03 (m, 2H), 1.79 (m, 1H), 1.47 (m, 2H), 1.34 (m, 2H), 1.22 (s, 12H).

2-chloro-1-(6-hydroxy-3,4-dihydro-2H-quinolin-1-yl)ethanone (4.35)

To a 100 mL round-bottle flask was added a solution of 1,2,3,4-tetrahydroquinolin-6-ol (6.70 mmol, 1 g) and NaOH (8.0 mmol, 320 mg) in water/dioxane (1:1, 20 mL) at 0°C. Then chloroacetyl chloride (7.40 mmol, 0.59 mL) was added dropwise over 5 minutes and then the reaction was stirred at room temperature for 4h. Upon completion, the reaction mixture was acidified with 1N HCl to pH 4, extracted with ethyl acetate. The organic layers were combined and washed with brine, dried over anhydrous Na₂SO₄, condensed and purified by flash column chromatography using a gradient of 0-4% MeOH/DCM to give 2-chloro-1-(6-hydroxy-3,4-dihydro-2H-quinolin-1-yl)ethanone (1.4g, 93% yield). ESI-MS m/z: 226 ([M+H]⁺). ¹H-NMR (300MHz, DMSO-d₆): 9.43 (s, 1H), 7.33 (m, 1H), 6.59 (s, 2H), 4.38 (s, 2H), 3.64 (t, J=5.9 Hz, 2H), 2.61 (m, 2H), 1.84 (m, 2H).

tert-butyl 2-[[1-(2-chloroacetyl)-3,4-dihydro-2H-quinolin-6-yl]oxy]acetate (4.36)

To a 100 mL round-bottle flask was added a solution of 2-chloro-1-(6-hydroxy-3,4-dihydro-2H-quinolin-1-yl)ethanone (2.22 mmol, 500 mg) in DMF (5 mL). Then Cs₂CO₃ (3.32 mmol, 1.08 g) and tert-butyl 2-bromoacetate (2.77 mmol, 540 mg) were added and the reaction was stirred at room temperature for 3h. Upon completion, the reaction mixture was diluted with ethyl acetate, acidified with 1N

HCl to pH 4, extracted with ethyl acetate. The organic layers were combined and washed with brine, dried over anhydrous Na₂SO₄, condensed and to give tert-butyl 2-[[1-(2-chloroacetyl)-3,4-dihydro-2H-quinolin-6-yl]oxy]acetate (550 mg, 73% yield) and used without further purification. ESI-MS m/z: 340 ([M+H]⁺). ¹H-NMR (300MHz, DMSO-d₆): 7.47 (m, 1H), 6.74 (m, 2H), 4.62 (s, 2H), 4.47 (s, 2H), 3.66 (t, J=5.9 Hz, 2H), 2.67 (m, 2H), 1.87 (m, 2H), 1.43 (s, 9H).

4-[[1-(2-chloroacetyl)-3,4-dihydro-2H-quinolin-6-yl]oxy]butanoic acid (4.37)

To a 10 mL round-bottle flask was added a solution of tert-butyl 2-[[1-(2-chloroacetyl)-3,4-dihydro-2H-quinolin-6-yl]oxy]acetate (0.88 mmol, 300 mg) in DCM (5 mL). Then TFA (1 mL) was added and the reaction was stirred at room temperature for 4h. Upon completion, the reaction mixture was condensed and to give 2-[[1-(2-chloroacetyl)-3,4-dihydro-2H-quinolin-6-yl]oxy]acetic acid (220 mg, 88% yield) and used without further purification. ESI-MS m/z: 284 ([M+H]⁺). ¹H-NMR (300MHz, DMSO-d₆): 12.99 (s, 1H), 7.47 (m, 1H), 6.75 (m, 2H), 4.65 (s, 2H), 4.47 (m, 2H), 3.66 (t, J=5.9 Hz, 2H), 3.40 (m, 2H), 2.68 (m, 2H), 1.87 (m, 2H).

2-[[1-(2-chloroacetyl)-3,4-dihydro-2H-quinolin-6-yl]oxy]-N-[10-[4-[6-[2-[(6-cyano-4-quinolyl)amino]ethyl]naphthalene-2-carbonyl]piperazin-1-yl]-10-oxo-decyl]acetamide (4.38)

To a 10 mL round-bottle flask was added a solution of 4-[2-[6-[4-(10-aminodecanoyl)piperazine-1-carbonyl]-2-naphthyl]ethylamino]quinoline-6-carbonitrile (0.057 mmol, 34 mg) and 2-[[1-(2-chloroacetyl)-3,4-dihydro-2H-quinolin-6-yl]oxy]acetic acid (0.057 mmol, 16 mg) in DMF (2 mL). Then EDC-HCl (0.11 mmol, 22 mg), HOAt (0.11 mmol, 15 mg), and N-methylmorpholine (0.28

mmol, 29 mg) were added and the mixture was stirred at room temperature for overnight. Upon completion, the mixture was diluted with DCM, added with water, extracted with DCM, the organic layers were combined, dried by Na₂SO₄, condensed and purified by flash column chromatography using a gradient of 0-10% MeOH/DCM to give 2-[[1-(2-chloroacetyl)-3,4-dihydro-2H-quinolin-6-yl]oxy]-N-[10-[4-[6-[2-[(6-cyano-4-quinolyl)amino]ethyl]naphthalene-2-carbonyl]piperazin-1-yl]-10-oxo-decyl]acetamide (15 mg, 31% yield). ESI-MS m/z: 871 ([M+H]⁺). ¹H-NMR (300MHz, CD₂Cl₂): 8.58 (d, J=4.9 Hz, 1H), 8.27 (s, 1H), 7.96 (d, J=8.2 Hz, 1H), 7.88 (s, 1H), 7.83 (d, J=8.9 Hz, 2H), 7.72 (d, J=9.7 Hz, 1H), 7.69 (s, 1H), 7.48 (d, J=8.2 Hz, 1H), 7.43 (d, J=8.2 Hz, 1H), 7.11 (m, 1H), 6.77 (m, 2H), 6.59 (d, J=5.8 Hz, 2H), 5.97 (m, 1H), 4.43 (s, 2H), 4.20 (m, 2H), 3.74 (m, 2H), 3.69 (q, J=5.6 Hz, 2H), 3.58 (m, 6H), 3.29 (q, J=6.6 Hz, 2H), 3.20 (t, J=6.6 Hz, 2H), 2.70 (m, 2H), 2.31 (m, 2H), 1.95 (m, 2H), 1.58 (m, 2H), 1.51 (m, 2H), 1.28 (s, 12H).

tert-butyl 2-[4-(4-bromophenyl)pyrazol-1-yl]acetate (4.39)

To a 100 mL round-bottle flask was added a solution of 4-(4-bromophenyl)-1H-pyrazole (5.38 mmol, 1.00 g) and tert-butyl 2-bromoacetate (5.38 mmol, 1.05 g) in acetonitrile (10 mL). Then K₂CO₃ (4.30 mmol, 1.45 g) was added and the mixture was stirred at room temperature for overnight. Upon completion, the mixture was condensed, and sat NH₄Cl aq was added, the mixture was extracted with DCM, the organic layers were combined, dried by Na₂SO₄, condensed and purified by flash column chromatography using a gradient of 0-2% MeOH/DCM to give tert-butyl 2-[4-(4-bromophenyl)pyrazol-1-yl]acetate (1.45 g, 96% yield). ESI-

MS m/z: 338 ($[M+H]^+$). $^1\text{H-NMR}$ (300MHz, DMSO- d_6): 8.20 (s, 1H), 7.95 (s, 1H), 7.54 (s, 4H), 4.96 (s, 2H), 1.43 (s, 9H).

tert-butyl 2-[4-[4-(4,4,5,5-tetramethyl-1,3,2-dioxaborolan-2-yl)phenyl]pyrazol-1-yl]acetate (4.40)

To a 100 mL round-bottle flask was added a solution of *tert-butyl 2-[4-(4-bromophenyl)pyrazol-1-yl]acetate* (1.48 mmol, 500 mg) and 4,4,5,5-tetramethyl-2-(4,4,5,5-tetramethyl-1,3,2-dioxaborolan-2-yl)-1,3,2-dioxaborolane (2.22 mmol, 565 mg) in dioxane (10 mL). Then CH_3COOK (4.45 mmol, 437 mg) and Pd(dppf)Cl_2 (0.148 mmol, 108 mg) were added and the mixture was degassed and stirred at 95°C for overnight. Upon completion, the mixture was cooled to room temperature, then sat NaHCO_3 aq was added, the mixture was extracted with DCM, the organic layers were combined, dried by Na_2SO_4 , condensed and purified by flash column chromatography using a gradient of 0-2% MeOH/DCM to give *tert-butyl 2-[4-[4-(4,4,5,5-tetramethyl-1,3,2-dioxaborolan-2-yl)phenyl]pyrazol-1-yl]acetate* (550 mg, 97% yield). ESI-MS m/z: 385 ($[M+H]^+$). $^1\text{H-NMR}$ (300MHz, DMSO- d_6): 8.21 (s, 1H), 7.96 (s, 1H), 7.63 (q, $J=8.1$ Hz, 4H), 4.96 (s, 2H), 1.43 (s, 9H), 1.29 (s, 12H).

tert-butyl 2-(4-(4-(isoquinolin-4-yl)phenyl)-1H-pyrazol-1-yl)acetate (4.41)

To a 100 mL round-bottle flask was added a solution of *tert-butyl 2-[4-[4-(4,4,5,5-tetramethyl-1,3,2-dioxaborolan-2-yl)phenyl]pyrazol-1-yl]acetate* (1.41 mmol, 540 mg) and 4-bromoisoquinoline (1.41 mmol, 292 mg) in dioxane (10 mL). Then K_2CO_3 (4.22 mmol, 583 mg) and Tetrakis(triphenylphosphine)palladium(0) (0.14 mmol, 162 mg) were added and the mixture was degassed and stirred at

100°C for overnight. Upon completion, the mixture was cooled to room temperature, then sat NaHCO₃ aq was added, the mixture was extracted with DCM, the organic layers were combined, dried by Na₂SO₄, condensed to give tert-butyl 2-(4-(4-(isoquinolin-4-yl)phenyl)-1H-pyrazol-1-yl)acetate (500 mg, 92%) and used for the next step without further purification. ESI-MS m/z: 386 ([M+H]⁺).

2-(4-(4-(isoquinolin-4-yl)phenyl)-1H-pyrazol-1-yl)acetic acid (4.42)

To a 10 mL round-bottle flash was added a solution of tert-butyl 2-(4-(4-(isoquinolin-4-yl)phenyl)-1H-pyrazol-1-yl)acetate (500 mg) dissolved in DCM (5 mL). Then TFA (2 mL) was added and the mixture was stirred at room temperature for 4h. Upon completion, the mixture was condensed to give 2-(4-(4-(isoquinolin-4-yl)phenyl)-1H-pyrazol-1-yl)acetic acid (400 mg, 94%) and used for the next step without further purification. ESI-MS m/z: 330 ([M+H]⁺).

tert-butyl 2-[4-[4-(4,4,5,5-tetramethyl-1,3,2-dioxaborolan-2-yl)phenyl]pyrazol-1-yl]acetate (4.43)

To a 10 mL round-bottle flash was added a solution of 2-(4-(4-(isoquinolin-4-yl)phenyl)-1H-pyrazol-1-yl)acetic acid (400 mg, 1.21 mmol) HATU (1.82 mmol, 691 mg) and DIEA (3.64 mmol, 624 uL) were added and the mixture was stirred at room temperature for 15 min, then tert-butyl piperazine-1-carboxylate (1.21 mmol, 226 mg) was added and the mixture was stirred at room temperature for 4h. Upon completion, sat NaHCO₃ aq was added and the mixture was extracted with DCM, the organic layers were combined and dried over Na₂SO₄, condensed and purified by flash column chromatography using a gradient of 0-5% MeOH/DCM to give tert-butyl 4-[2-[4-[4-(4-isoquinolyl)phenyl]pyrazol-1-yl]acetyl]piperazine-1-carboxylate

(247 mg, 35% yield). ESI-MS m/z : 498 ($[M+H]^+$). 1H -NMR (300MHz, DMSO- d_6): 9.24 (s, 1H), 8.48 (s, 1H), 8.06 (d, $J=7.9$ Hz, 1H), 7.97 (d, $J=7.9$ Hz, 1H), 7.88 (s, 2H), 7.68 (m, 4H), 7.54 (d, $J=7.9$ Hz, 2H), 5.06 (s, 2H), 3.59 (m, 2H), 3.52 (m, 2H), 3.44 (m, 4H), 1.45 (s, 9H).

2-[4-[4-(4-isoquinolyl)phenyl]pyrazol-1-yl]-1-piperazin-1-yl-ethanone (4.44)

To a 10 mL round-bottle flask was added a solution of tert-butyl 4-[2-[4-[4-(4-isoquinolyl)phenyl]pyrazol-1-yl]acetyl]piperazine-1-carboxylate (0.47 mmol, 233 mg) in DCM (5 mL). Then TFA (1 mL) was added and the reaction was stirred at room temperature for 4h. Upon completion, the reaction mixture was condensed and to give 2-[4-[4-(4-isoquinolyl)phenyl]pyrazol-1-yl]-1-piperazin-1-yl-ethanone (186 mg, 99% yield) and used without further purification. ESI-MS m/z : 398 ($[M+H]^+$).

2-(2,6-dioxo-3-piperidyl)-4-[2-[2-[2-[3-[4-[2-[4-[4-(4-isoquinolyl)phenyl]pyrazol-1-yl]acetyl]piperazin-1-yl]-3-oxo-propoxy]ethoxy]ethoxy]ethylamino]isoindoline-1,3-dione (4.45)

To a 10 mL round-bottle flask was added a solution of 2-[4-[4-(4-isoquinolyl)phenyl]pyrazol-1-yl]-1-piperazin-1-yl-ethanone (0.091 mmol, 36 mg) and 3-[2-[2-[2-[2-[2-(2,6-dioxo-3-piperidyl)-1,3-dioxo-isoindolin-4-yl]amino]ethoxy]ethoxy]ethoxy]ethoxy]propanoic acid (0.091 mmol, 47 mg) in DMF (2 mL). Then EDC-HCl (0.18 mmol, 35 mg), HOAt (0.18 mmol, 25 mg), and N-methylmorpholine (0.45 mmol, 46 mg) were added and the mixture was stirred at room temperature for overnight. Upon completion, the mixture was diluted with DCM, added with water, extracted with DCM, the organic layers were combined,

dried by Na₂SO₄, condensed and purified by flash column chromatography using a gradient of 0-10% MeOH/DCM to give 2-(2,6-dioxo-3-piperidyl)-4-[2-[2-[2-[3-[4-[2-[4-[4-(4-isoquinolyl)phenyl]pyrazol-1-yl]acetyl]piperazin-1-yl]-3-oxo-propoxy]ethoxy]ethoxy]ethoxy]ethylamino]isoindoline-1,3-dione (15 mg, 18% yield). ESI-MS m/z: 901 ([M+H]⁺). ¹H-NMR (300MHz, CD₂Cl₂): 9.24 (s, 1H), 8.48 (s, 1H), 8.06 (d, J=7.9 Hz, 1H), 7.97 (d, J=7.9 Hz, 1H), 7.89 (s, 2H), 7.67 (m, 5H), 7.51 (m, 3H), 7.06 (d, J=7.5 Hz, 1H), 6.95 (d, J=8.2 Hz, 1H), 6.50 (t, J=5.3 Hz, 1H), 5.09 (s, 2H), 4.91 (m, 1H), 3.77-3.46 (m, 26H), 2.77 (m, 3H), 2.62 (m, 2H), 2.10 (m, 1H).

tert-butyl N-[11-[4-[2-[4-[4-(4-isoquinolyl)phenyl]pyrazol-1-yl]acetyl]piperazin-1-yl]-11-oxo-undecyl]carbamate (4.46)

To a 10 mL round-bottle flask was added a solution of 2-[4-[4-(4-isoquinolyl)phenyl]pyrazol-1-yl]-1-piperazin-1-yl-ethanone (0.81 mmol, 322 mg) in DCM (5 mL), HATU (1.22 mmol, 461 mg) and DIEA (2.43 mmol, 416 µL) were added and the mixture was stirred at room temperature for 15 min, then 11-(tert-butoxycarbonylamino)undecanoic acid (0.81 mmol, 244 mg) was added and the mixture was stirred at room temperature for 4 h. Upon completion, sat NaHCO₃ aq was added and the mixture was extracted with DCM, the organic layers were combined and dried over Na₂SO₄, condensed and purified by flash column chromatography using a gradient of 0-5% MeOH/DCM to give *tert-butyl N-[11-[4-[2-[4-[4-(4-isoquinolyl)phenyl]pyrazol-1-yl]acetyl]piperazin-1-yl]-11-oxo-undecyl]carbamate* (280 mg, 51% yield). ESI-MS m/z: 681 ([M+H]⁺). ¹H-NMR (300MHz, CD₂Cl₂): 9.24 (s, 1H), 8.47 (s, 1H), 8.08 (d, J=7.3 Hz, 1H), 7.98 (d, J=7.3

Hz, 1H), 7.88 (s, 2H), 7.70 (s, 2H), 7.69 (m, 4H), 7.54 (d, J=8.3 Hz, 2H), 5.09 (s, 2H), 4.62 (m, 1H), 3.69-3.49 (m, 8H), 3.06 (q, J=6.4 Hz, 2H), 2.32 (t, J=7.7 Hz, m, 2H), 1.60 (m, 2H), 1.41 (m, 11H), 1.29 (s, 12H).

11-amino-1-[4-[2-[4-[4-(4-isoquinolyl)phenyl]pyrazol-1-yl]acetyl]piperazin-1-yl]undecan-1-one (4.47)

To a 10 mL round-bottle flask was added a solution of tert-butyl tert-butyl N-[11-[4-[2-[4-[4-(4-isoquinolyl)phenyl]pyrazol-1-yl]acetyl]piperazin-1-yl]-11-oxo-undecyl]carbamate (0.41 mmol, 280 mg) in DCM (5 mL). Then TFA (1 mL) was added and the reaction was stirred at room temperature for 4h. Upon completion, the reaction mixture was condensed and to give 11-amino-1-[4-[2-[4-[4-(4-isoquinolyl)phenyl]pyrazol-1-yl]acetyl]piperazin-1-yl]undecan-1-one (220 mg, 92% yield) and used without further purification. ESI-MS m/z: 581 ([M+H]⁺).

4-[[2-(2,6-dioxo-3-piperidyl)-1,3-dioxo-isoindolin-4-yl]amino]-N-[11-[4-[2-[4-[4-(4-isoquinolyl)phenyl]pyrazol-1-yl]acetyl]piperazin-1-yl]-11-oxo-undecyl]butanamide (4.48)

To a 10 mL round-bottle flask was added a solution of 11-amino-1-[4-[2-[4-[4-(4-isoquinolyl)phenyl]pyrazol-1-yl]acetyl]piperazin-1-yl]undecan-1-one (0.11 mmol, 65 mg) and 4-[[2-(2,6-dioxo-3-piperidyl)-1,3-dioxo-isoindolin-4-yl]amino]butanoic acid (0.11 mmol, 40 mg) in DMF (2 mL). Then EDC-HCl (0.18 mmol, 35 mg), HOAt (0.22 mmol, 31 mg), and N-methylmorpholine (0.47 mmol, 103 mg) were added and the mixture was stirred at room temperature for overnight. Upon completion, the mixture was diluted with DCM, added with water, extracted with DCM, the organic layers were combined, dried by Na₂SO₄,

condensed and purified by flash column chromatography using a gradient of 0-10% MeOH/DCM to give 4-[[2-(2,6-dioxo-3-piperidyl)-1,3-dioxo-isoindolin-4-yl]amino]-N-[11-[4-[2-[4-[4-(4-isoquinolyl)phenyl]pyrazol-1-yl]acetyl]piperazin-1-yl]-11-oxo-undecyl]butanamide (43 mg, 42% yield). ESI-MS m/z : 901 ($[M+H]^+$). 1H -NMR (300MHz, CD_2Cl_2): 9.24 (s, 1H), 8.97 (m, 1H), 8.47 (s, 1H), 8.07 (d, $J=7.9$ Hz, 1H), 7.97 (d, $J=7.9$ Hz, 1H), 7.90 (s, 2H), 7.68 (m, 4H), 7.51 (m, 3H), 7.05 (d, $J=7.3$ Hz, 1H), 6.95 (d, $J=8.7$ Hz, 1H), 6.32 (t, $J=6.0$ Hz, 1H), 5.80 (m, 1H), 5.10 (s, 2H), 4.91 (m, 1H), 3.67-3.46 (m, 8H), 3.33 (q, $J=7.2$ Hz, 2H), 3.19 (q, $J=6.5$ Hz, 2H), 2.77 (m, 3H), 2.30 (m, 2H), 2.25 (t, $J=7.9$ Hz, 2H), 2.10 (m, 1H), 1.95 (m, 2H), 1.58 (m, 2H), 1.45 (m, 2H), 1.27 (s, 12H).

tert-butyl N-[2-[2-[2-[2-[2-[[2-(2,6-dioxo-3-piperidyl)-1,3-dioxo-isoindolin-4-yl]amino]ethoxy]ethoxy]ethoxy]ethoxy]ethyl]carbamate (4.49)

To a 10 mL round-bottle flask was added a solution of 2-(2,6-dioxo-3-piperidyl)-4-fluoro-isoindoline-1,3-dione (0.72 mmol, 200 mg) and *tert-butyl N-[2-[2-[2-[2-(2-aminoethoxy)ethoxy]ethoxy]ethoxy]ethyl]carbamate* (0.87 mmol, 292 mg) in DMF (2 mL). Then DIEA (2.2 mmol, 372 μ L) was added and the mixture was microwaved at 100°C for 2h. Upon completion, the mixture was condensed and purified by flash column chromatography using a gradient of 0-2% MeOH/DCM to give *tert-butyl 4-[[2-(2,6-dioxo-3-piperidyl)-1,3-dioxo-isoindolin-4-yl]amino]butanoate* (209 mg, 49% yield). ESI-MS m/z : 593 ($[M+H]^+$). 1H -NMR (300MHz, CD_2Cl_2): 8.47 (s, 1H), 7.51 (t, $J=8.1$ Hz, 1H), 7.07 (d, $J=7.3$ Hz, 1H), 6.96 (d, $J=7.4$ Hz, 1H), 6.49 (m, 1H), 5.11 (m, 1H), 4.91 (m, 1H), 3.71 (t, $J=5.5$ Hz,

2H), 3.58 (m, 14H), 3.48 (m, 2H), 3.25 (q, J=5.0 Hz, 2H), 2.78 (m, 3H), 2.12 (m, 1H), 1.41 (s, 9H).

4-[2-[2-[2-[2-(2-aminoethoxy)ethoxy]ethoxy]ethoxy]ethylamino]-2-(2,6-dioxo-3-piperidyl)isoindoline-1,3-dione (4.50)

To a 10 mL round-bottle flask was added a solution of tert-butyl N-[2-[2-[2-[2-[2-[2-[(2,6-dioxo-3-piperidyl)-1,3-dioxo-isoindolin-4-yl]amino]ethoxy]ethoxy]ethoxy]ethoxy]ethyl]carbamate (0.35 mmol, 209 mg) in formic acid (2 mL). Then the mixture was stirred at room temperature for overnight. Upon completion, the mixture was condensed and purified by flash column chromatography using a gradient of 0-4% MeOH/DCM to give 4-[2-[2-[2-[2-(2-aminoethoxy)ethoxy]ethoxy]ethoxy]ethylamino]-2-(2,6-dioxo-3-piperidyl)isoindoline-1,3-dione (160 mg, 92% yield). ESI-MS m/z: 493 ([M+H]⁺).

N-[2-[2-[2-[2-[2-[2-[(2,6-dioxo-3-piperidyl)-1,3-dioxo-isoindolin-4-yl]amino]ethoxy]ethoxy]ethoxy]ethoxy]ethyl]-2-[4-[4-(4-isoquinolyl)phenyl]pyrazol-1-yl]acetamide (4.51)

To a 10 mL round-bottle flask was added a solution of 2-[4-[4-(4-isoquinolyl)phenyl]pyrazol-1-yl]acetic acid (0.12 mmol, 40 mg) and 4-[2-[2-[2-[2-(2-aminoethoxy)ethoxy]ethoxy]ethoxy]ethylamino]-2-(2,6-dioxo-3-piperidyl)isoindoline-1,3-dione (0.12 mmol, 60 mg) in DMF (2 mL). Then EDC-HCl (0.24 mmol, 47 mg), HOAt (0.24 mmol, 33 mg), and N-methylmorpholine (0.61 mmol, 62 mg) were added and the mixture was stirred at room temperature for overnight. Upon completion, the mixture was diluted with DCM, added with water, extracted with DCM, the organic layers were combined, dried by Na₂SO₄,

condensed and purified by flash column chromatography using a gradient of 0-10% MeOH/DCM to give N-[2-[2-[2-[2-[2-[[2-(2,6-dioxo-3-piperidyl)-1,3-dioxo-isoindolin-4-yl]amino]ethoxy]ethoxy]ethoxy]ethoxy]ethyl]-2-[4-[4-(4-isoquinolyl)phenyl]pyrazol-1-yl]acetamide (26 mg, 27% yield). ESI-MS m/z : 804 ($[M+H]^+$). 1H -NMR (300MHz, CD_2Cl_2): 9.25 (s, 1H), 9.12 (s, 1H), 8.48 (s, 1H), 8.07 (d, $J=8.0$ Hz, 1H), 7.97 (q, $J=8.5$ Hz, 1H), 7.95 (s, 1H), 7.88 (s, 1H), 7.69 (m, 2H), 7.66 (d, $J=8.0$ Hz, 2H), 7.53 (d, $J=8.0$ Hz, 2H), 7.48 (t, $J=8.0$ Hz, 1H), 7.05 (d, $J=7.0$ Hz, 1H), 6.91 (d, $J=7.0$ Hz, 1H), 6.86 (m, 1H), 6.49 (m, 1H), 4.91 (m, 1H), 4.86 (s, 2H), 3.69 (t, $J=5.0$ Hz, 2H), 3.63-3.53 (m, 14H), 3.43 (q, $J=4.8$ Hz, 4H), 2.77 (m, 3H), 2.10 (m, 1H).

3-amino-4-[4-[4-[4-[3-[2-[2-[2-[2-[[2-(2,6-dioxo-3-piperidyl)-1,3-dioxo-isoindolin-4-yl]amino]ethoxy]ethoxy]ethoxy]ethoxy]propanoyl]piperazine-1-carbonyl]phenyl]-1,4-diazepan-1-yl]thieno[2,3-b]pyridine-2-carboxamide (4.52)

To a 10 mL round-bottle flask was added a solution of 3-amino-4-[4-[4-(piperazine-1-carbonyl)phenyl]-1,4-diazepan-1-yl]thieno[2,3-b]pyridine-2-carboxamide (0.083 mmol, 40 mg) and 3-[2-[2-[2-[2-[[2-(2,6-dioxo-3-piperidyl)-1,3-dioxo-isoindolin-4-yl]amino]ethoxy]ethoxy]ethoxy]ethoxy]propanoic acid (0.083 mmol, 44 mg) in DMF (2 mL). Then EDC-HCl (0.17 mmol, 32 mg), HOAt (0.17 mmol, 23 mg), and N-methylmorpholine (0.42 mmol, 42 mg) were added and the mixture was stirred at room temperature for overnight. Upon completion, the mixture was diluted with DCM, added with water, extracted with DCM, the organic layers were combined, dried by Na_2SO_4 , condensed and purified by flash column chromatography using a gradient of 0-10% MeOH/DCM to give 3-amino-4-[4-[4-

[4-[3-[2-[2-[2-[2-[[2-(2,6-dioxo-3-piperidyl)-1,3-dioxo-isoindolin-4-yl]amino]ethoxy]ethoxy]ethoxy]ethoxy]propanoyl]piperazine-1-carbonyl]phenyl]-1,4-diazepan-1-yl]thieno[2,3-b]pyridine-2-carboxamide (18 mg, 22% yield). ESI-MS m/z : 984 ($[M+H]^+$). 1H -NMR (300MHz, CD_2Cl_2): 9.11 (s, 1H), 8.45 (d, $J=5.1$ Hz, 1H), 7.49 (t, $J=7.4$ Hz, 1H), 7.35 (m, 3H), 7.06 (d, $J=7.4$ Hz, 1H), 6.96 (m, 2H), 6.87 (s, 1H), 6.75 (d, $J=9.6$ Hz, 2H), 6.49 (m, 1H), 5.65 (s, 2H), 4.91 (m, 1H), 3.80 (m, 2H), 3.76 (t, $J=6.5$ Hz, 2H), 3.70 (t, $J=6.5$ Hz, 2H), 3.64-3.54 (m, 18H), 3.46 (q, $J=5.4$ Hz, 2H), 3.38 (m, 2H), 3.29 (m, 2H), 3.05 (m, 2H), 2.96 (m, 2H), 2.79 (m, 3H), 2.67 (t, $J=7.2$ Hz, 2H), 2.15 (m, 1H), 1.86 (m, 2H).

4.4.2 Pharmacology

4.4.2.1 293-NF κ B-luc cell-based assay

The detailed procedure for this NF κ B-dependent cell-based CDK8/19i activity assay was previously described.¹⁸⁰ Briefly, 293-WT-NFKB-LUC#8 (293-WT) and 293-dKO-NFKB-LUC#2 (293-KO) cells were seeded in 96-well plates, cultured for 24 hours and then treated with tested compounds at different concentrations with 10 ng/mL TNF- α added for 3 hours. 4 μ L potassium luciferin solution (15 mg/mL, GoldBio) was then added to each well to determine the luciferase reporter activity, represented by the luminescence intensities measured by the SpectraMax iD5 Microplate Reader. Reporter activities of inhibitor-treated cells were normalized by the reporter activities of cells without the inhibitor and further processed with GraphPad Prism 7.0 for curve-fitting and IC₅₀ calculation. The IC₅₀ curves of tested compounds are shown in **Figure 4.16**.

4.4.2.2 Western Blot.

Materials. RIPA-Basic Buffer (4°C): 50 mM Tris-HCl (pH 8.0); 150 mM NaCl; 5 mM EDTA; 0.5 mM EGTA; 1% Igepal CA-630; 0.1% SDS; 0.5% Na deoxycholate. RIPA-complete lysis Buffer (-20°C): 50ml RIPA-Basic Buffer; 500 µl 1 M NaF; 500µl 20 mM Na₃VO₄; 500 µl Protease Inhibitor Cocktail (100x). IP-Basic Buffer (4°C): 20mM Tris-HCl (pH 7.4); 100 mM NaCl; 1% Igepal CA-630; 1 mM EDTA; 1 mM EGTA. IP-complete lysis Buffer (-20°C): 50ml IP-Basic Buffer; 500 µl 1 M NaF; 500 µl 20 mM Na₃VO₄; 500 µl Protease Inhibitor Cocktail (100x). 10x Transfer Buffer: 144.4 g Glycine, 30.3 g Tris-base, final Vol. 1 L (in ddH₂O). 1x Transfer Buffer: 100 mL 10x Transfer buffer; 200 mL Methanol; 700 mL H₂O. 1x Running Buffer: 700 mL H₂O with stir-bar; Tris-MOPS-SDS Running Buffer Powder with funnel; fill to 1 L. 10x TBS-T (4°C): 80.06 g NaCl in 500mL H₂O; 200 mL 1 M Tris (7.5); 10 mL Tween-20 (slowly); fill to 1 L. The primary antibodies used: CDK8 (sc-1521, SantaCruz, USA), CDK19 (HPA007053, Sigma-Aldrich), Phospho-STAT1 (ser727) (8826s, Cell Signaling Technology, Danvers, MA, USA), STAT1 (9172s, Cell Signaling Technology, Danvers, MA, USA), CCNC (A301-989A, Bethyl Laboratories, MA, USA), GAPDH (#5174, Cell Signaling Technology, Danvers, MA, USA). The secondary antibodies used: Anti-Mouse-IgG-HRP (GE NXA931), Anti-Rabbit-IgG-HRP (GE NA934V), donkey anti-goat IgG-HRP (Santa Cruz sc-2020).

Lysate preparation. Seed cells in dishes (60 mm or 100 mm) or flasks (T25 or T75) and treated with different drugs. At the end-point, there should be 5-10x10⁶ cells to be lysed. Thaw enough RIPA or IP complete lysis buffer (stored

at -20°C in 5 mL aliquots) and leave on ice. Take refrigerated 1xPBS (in 50 mL tube) out and leave on ice. Take cells out of incubator. For adherent cells, remove media, wash cells with 3~5 mL ice-cold 1xPBS twice, remove all the residual PBS and add RIPA or IP complete lysis buffer (50 µL per million cells). Rock the dish to make sure all the area is covered with lysis buffer. Leave the dish on ice for 10 min. Scrape down all the cells in the lysis buffer and transfer to 1.5 mL tube and leave on ice for 10 minutes. For suspension cells, spin down the cells, remove media, suspend the cells in 1 mL ice-cold 1xPBS and transfer to 1.5 mL tube, spin down, remove PBS and wash the cells with 1 mL ice-cold 1xPBS again, remove PBS and add RIPA or IP complete lysis buffer (50 µL per million cells), leave on ice for 10 minutes. Sonicate the lysates for 3~5 seconds (at Amplitude of 8~10) on ice. One minute later, sonicate once more. Centrifuge at 15,000 x g for 10 min. Determine protein concentration by DC protein assay (5 µL, quadruplicate). Adjust protein concentration to 3 mg/mL. Use the lysate for the following step or store the lysate at -20°C.

Electrophoresis and Transfer. Take out protein lysates, MW ladder and RIPA buffer, vortex, short-spin, and put on ice. Prepare 4x Sample Buffer (360 µL 4x Laemmli Sample Buffer BioRAD 161-0737 + 40 µL 2-mercaptoethanol). Prepare 1x Running Buffer from MOPS-SDS-Powder (GenScript). In PCR-strip tubes (13 tubes for 15-well gel; 10 tubes for 12-well gel), add 15 µL 4x Sample Buffer. Then add 45 µL lysate sample (or blank RIPA buffer) to each tube. Pipette 7-10 times to mix well samples. Short-spin. Incubate at 98°C for 10 min and cool to room temperature (on BioRAD thermocycler). Short-spin, mix by finger-tapping,

short-spin again and the samples are ready to be loaded. During sample-denaturing step, setup the pre-cast gels (GenScript), pour in 1xMOPS Running buffer. Load 3 μ L MWM ladder to both left and right lane. Load prepared sample to the indicated well (20 μ L each well). Run gels at 100 V for 90 minutes. The fractionated proteins are subsequently transferred onto Immun-Blot® PVDF Membrane (BioRad, USA). Briefly, the PVDF membrane is activated by methanol for 5 minutes. The transfer cassette is settled up by putting fiber pad, filter paper, FVDF membrane, gel, filter paper and fiber pad from positive electrode to negative electrode. Transfer in cold transferring buffer (with ice box) at 90 V for 1 hours or 60 V for 2 hours or 20 V for overnight (the current should never go above 250 mA).

Western Blotting. After transfer, take out membrane and cut off the excessive part. Put the membrane in 1xTBS-T (rocking). Block membrane in Milk Blocking solution (5% Milk in 1xTBS-T, made freshly for the day) at room temp for 60 minutes. Rinse the membrane with 1xTBS-T once and then wash membrane in 1xTBS-T for 5 minutes x 3 times. Incubate membrane with 10mL primary antibody solution (8 mL H₂O + 1 mL 10x TBS-T + 1 mL 10% BSA + 100 μ L 2% NaN₃ + 5-20 μ L Ab, stored at 4°C) at 4°C for overnight. Recycle the primary antibody solution and put back to refrigerator. Rinse the membrane with 1xTBS-T once and then wash membrane by 1xTBS-T 5 minutes x 3 times. Incubate membrane with 10mL secondary antibody solution (1:10,000 diluted in milk blocking solution) at room temp for 1 hour. Wash membrane by 1xTBS-T 5 minutes x 4 times. Prepare ECL reagent Mix (for one membrane, 2 mL of 1:1 mix). Set up BioRAD ChemiDoc image system to capture images. For second round western blotting, rinse the

membrane with ddH₂O three times. Strip the membrane in 10 mL stripping buffer at room temp for 30 minutes. Rinse the membrane with ddH₂O three times. Wash membrane by 1xTBS-T 5 minutes x 3 times. Block membrane in Milk Blocking solution (5% Milk) at room temp for 30-60 minutes. Incubate membrane with primary antibody solution and follow the same procedure as above.

4.4.2.3 RNA extraction and qPCR

Procedures for RNA-qPCR analysis of cells treated with CDK8/19i and CDK8/19 PROTACs under different culture conditions, including basal and TNF α -stimulated conditions and drug wash-off conditions, were previously described in detail.¹⁷⁸ To evaluate the effects on CDK8-dependent gene expression, 293, 293 dKO, or CT26 cells were treated with tested compounds (in 0.1% DMSO) under regular culture conditions for indicated time periods. For the wash-off study, 293 cells were pretreated with tested compounds (in 0.1% DMSO) for 3 days before removal of the drug-containing media and washed with drug-free media twice, followed by incubation with drug-free media for indicated time periods. RNA was extracted with RNeasy Mini Kit (Qiagen) and cDNAs were prepared using iScript cDNA SuperMix (QuantaBio). Gene expression was quantified with iTaq Universal SYBR Green Supermix reagent (QuantaBio) using CFX384 Real-Time System (Bio-Rad). Relative mRNA expression was calculated with the formula of $2^{-(Ct_{\text{housekeeping_gene}} - Ct_{\text{test_gene}})}$ and percentage of inhibition was calculated by normalization to the expression levels in vehicle (0.1% DMSO) control. The sequences of the primers used for qPCR are listed in **Table 4.2**.

4.4.2.4 *In vivo* studies

Animal studies were approved by the Institutional Animal Care and Use Committee (IACUC) of UofSC and performed at the Department of Laboratory Animal Research (DLAR) at UofSC. For PK/PD analysis of Senexin C, one million of murine CT26 colon carcinoma cells were injected subcutaneously in the right flank of 8-week-old female Balb/c mice and allowed to grow to 200~300 mm³. Tumor-bearing mice then received PROTACs **4.45** or **4.48** by oral gavage at 20 mg/kg in 30% propylene glycol / 70% PEG-400 vehicle. Tumors were collected 2, 8 or 24 hrs after dosing. A piece of 50~100 mg tumor sample was stabilized in RNA-later reagent (Qiagen) and several 100 mg tumor pieces were snap-frozen on dry ice and stored at -80°C for later protein and tumor PK analysis. RNA-later stabilized tumor samples were processed for RNA extraction using Direct-zol RNA Miniprep Kit (Zymo Research, Irvine, CA), followed by qPCR quantification for gene expression. Tumor samples stored at -80°C and used to measure protein levels of CDK8, pSTAT1 at Ser727, and total STAT1 by western blotting.

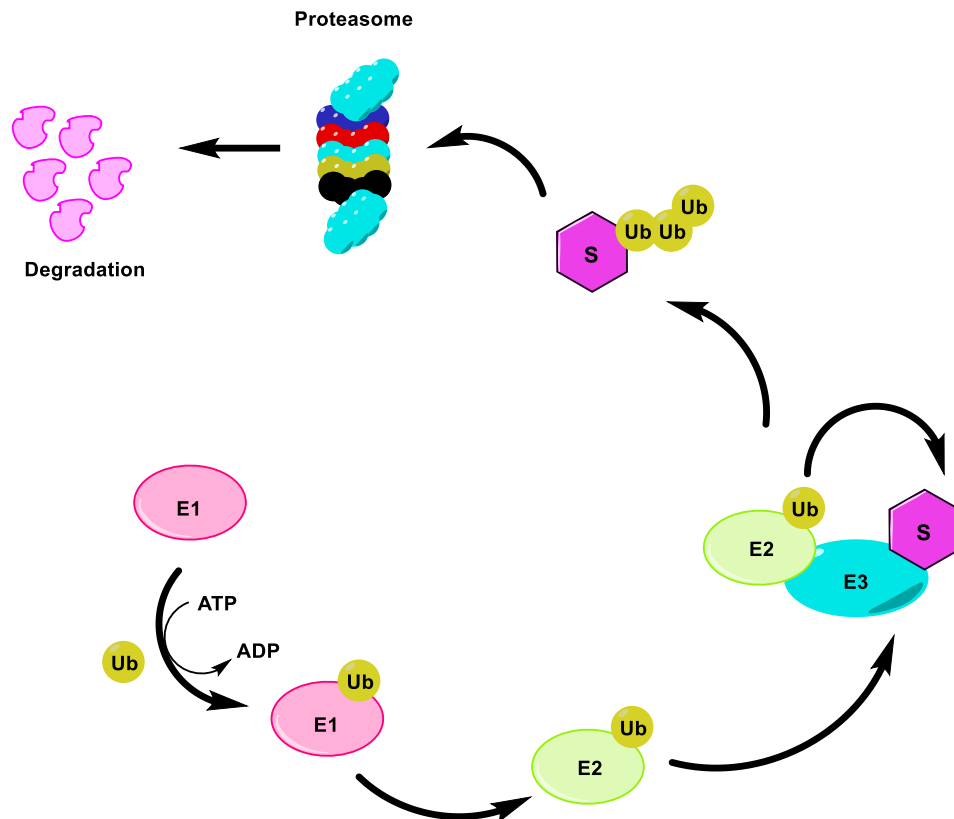


Figure 4.1 The process of protein ubiquitination via UPS.

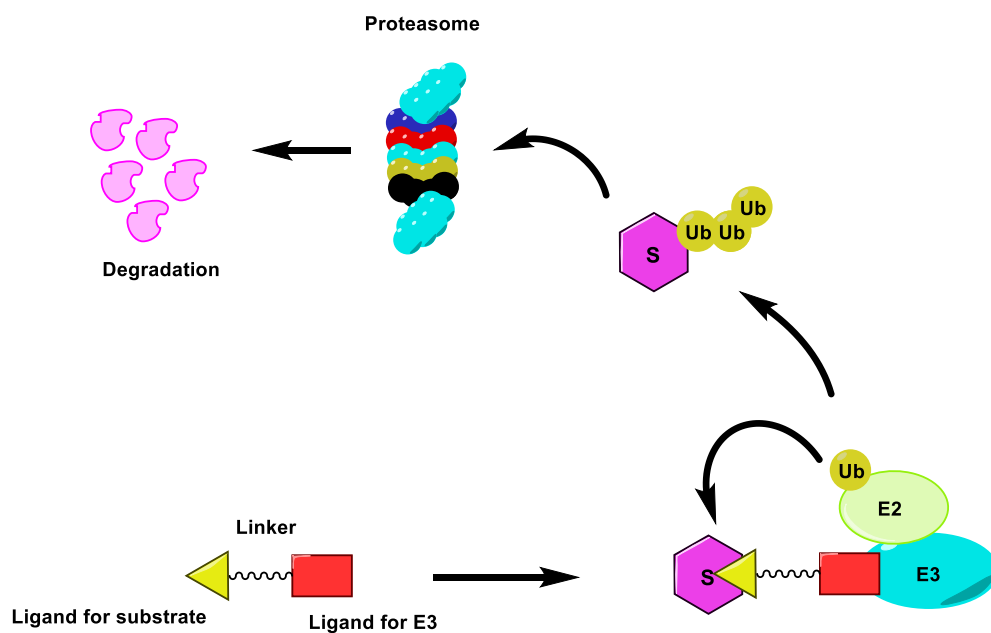


Figure 4.2 PROTAC-mediated protein degradation.

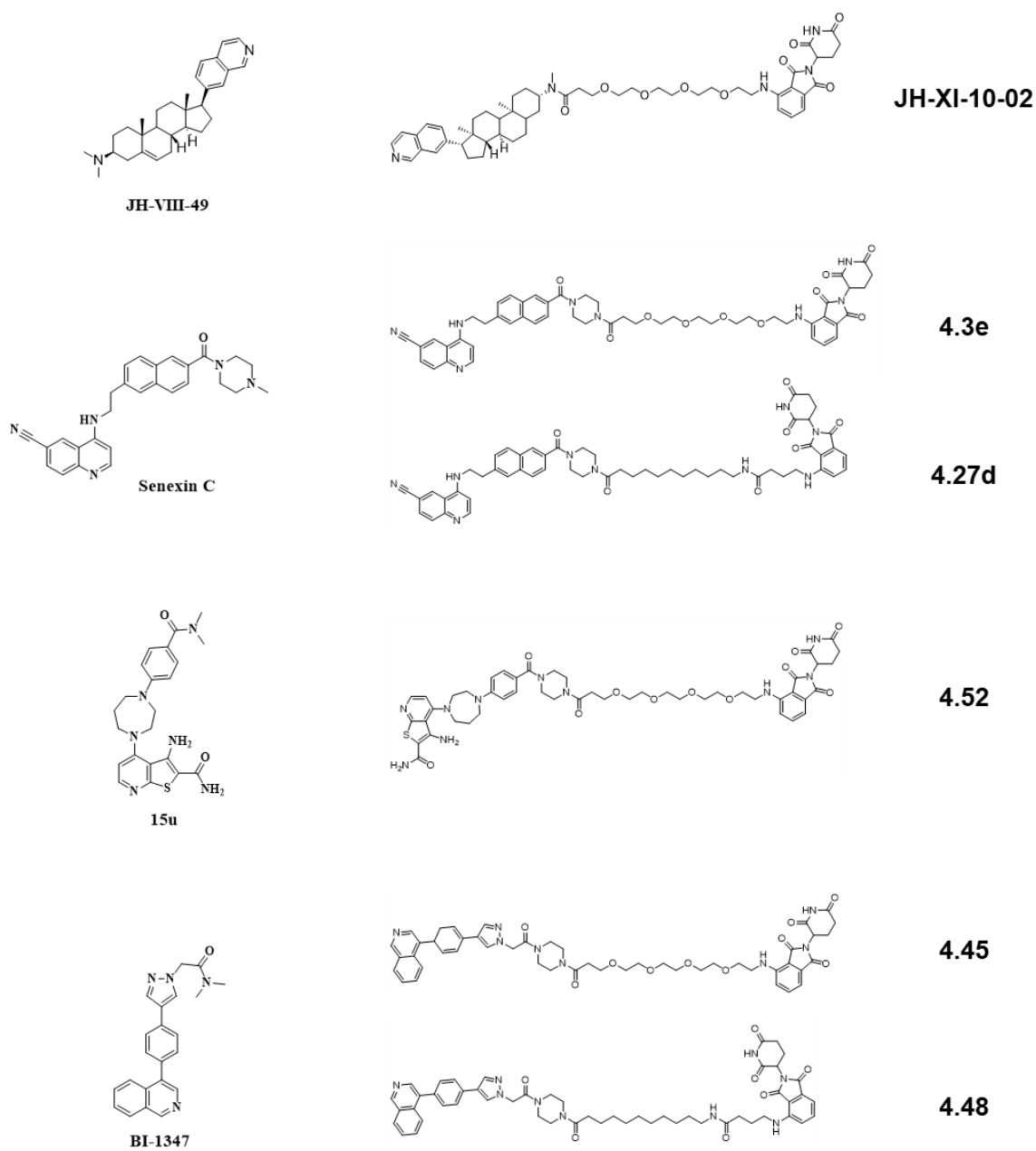


Figure 4.3 Chemical structure of selected CDK8/19i and their representative PROTAC derivatives

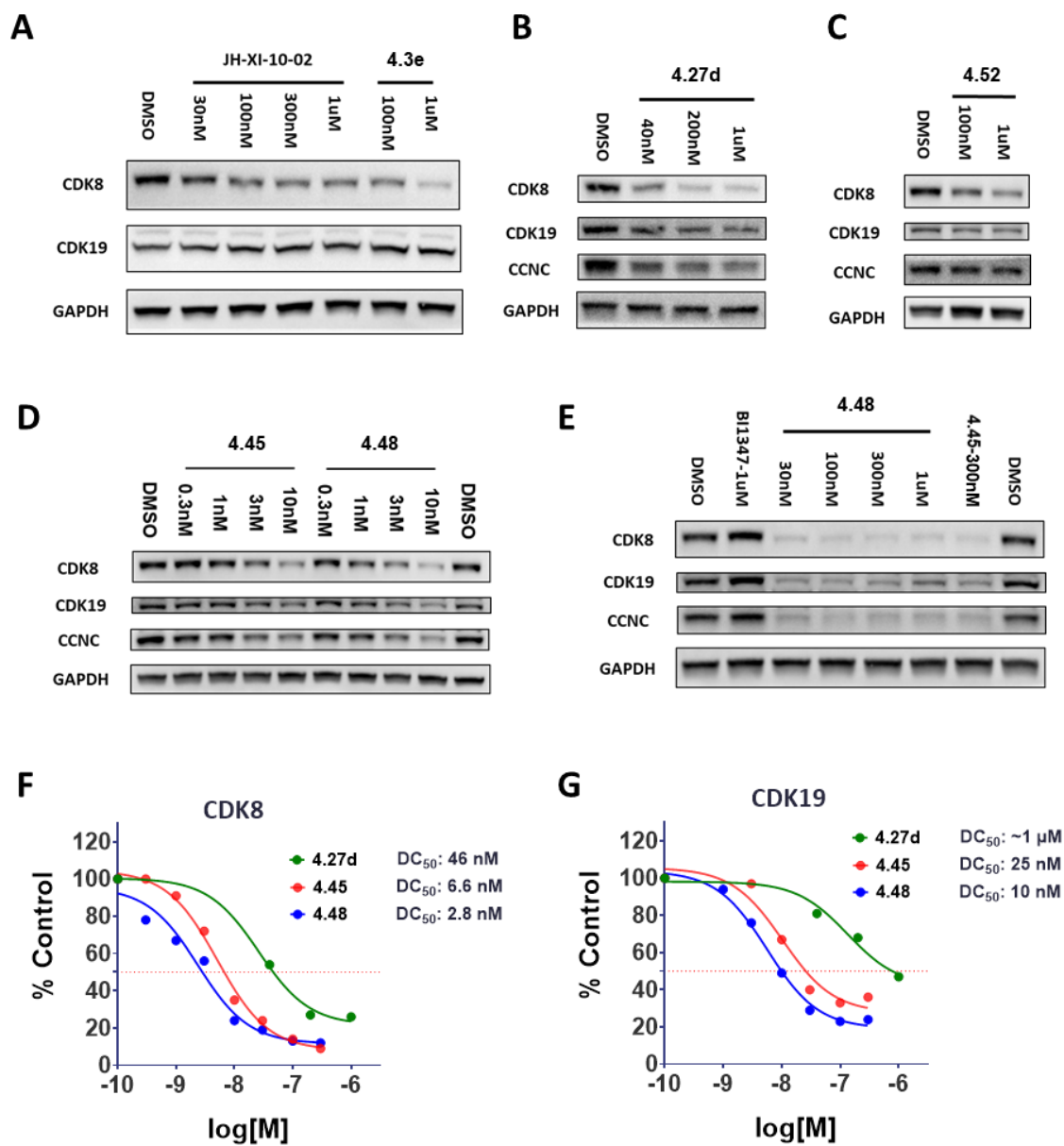


Figure 4.4 Effects of 24hr treatment with different PROTAC compounds on CDK8/CDK19/CCNC protein levels in 293 cells.

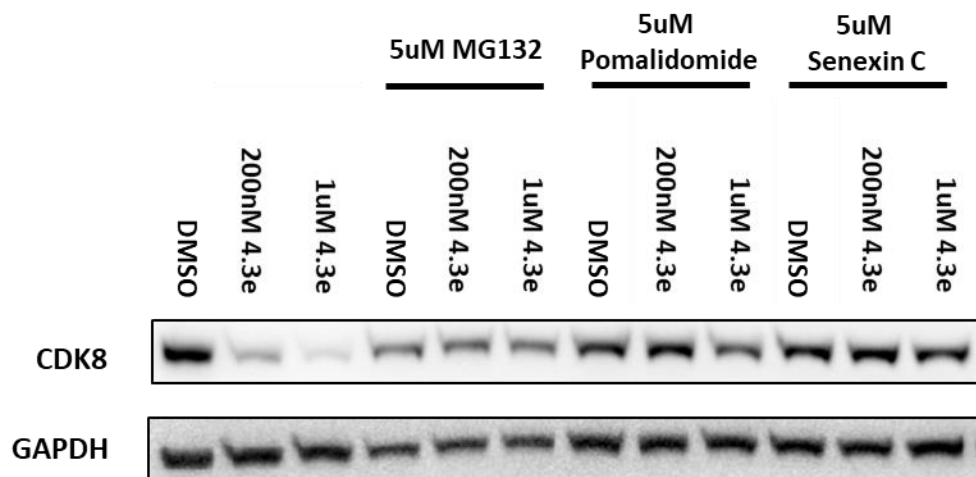


Figure 4.5 Effects of co-treatment with MG132, Pomalidomide and Senexin C on 4.3e-mediated CDK8 degradation in 293 cells.

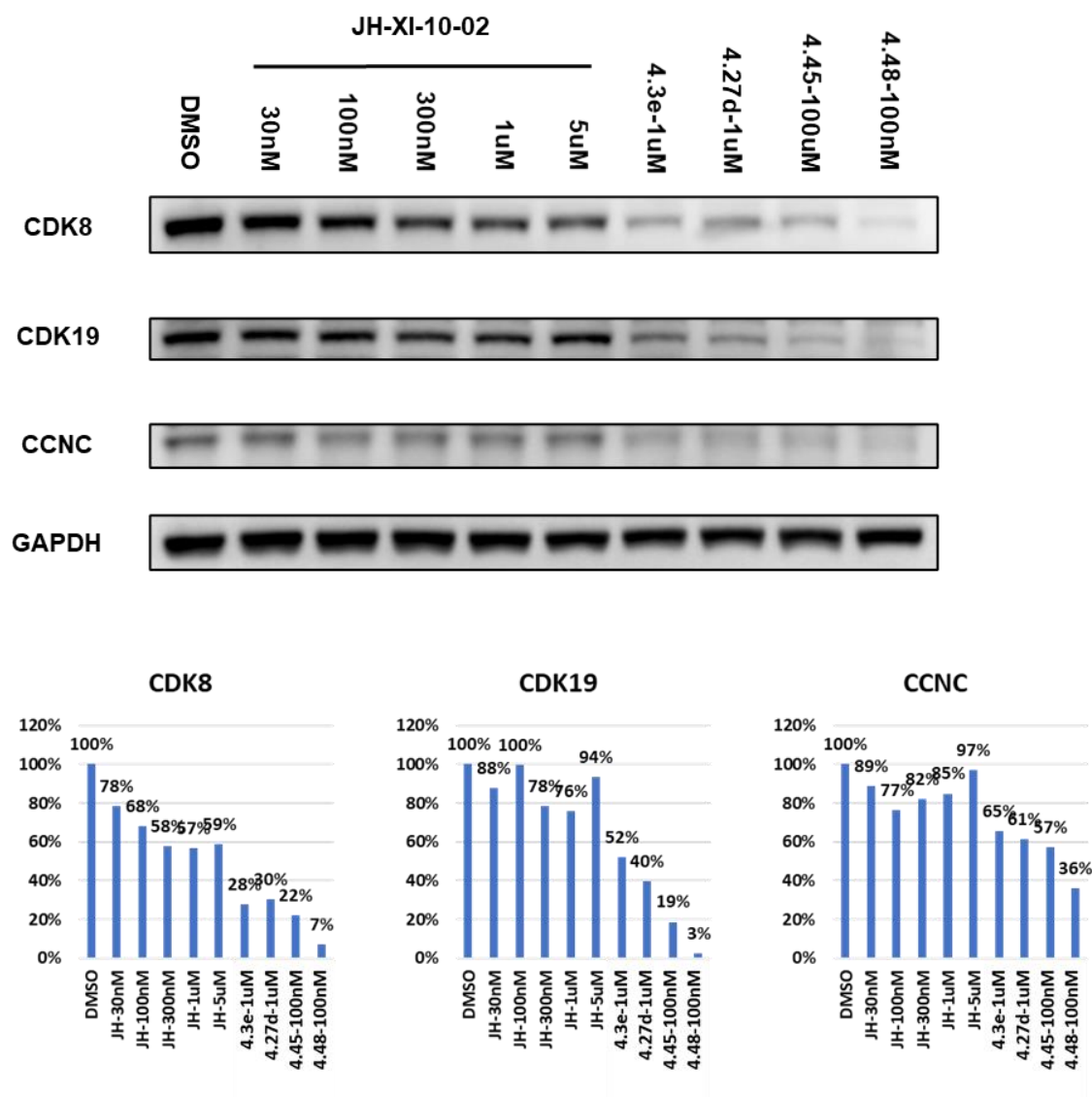


Figure 4.6 Effects of 24hr treatment with different PROTAC compounds on CDK8/CDK19/CCNC protein levels in Jurkat cells.

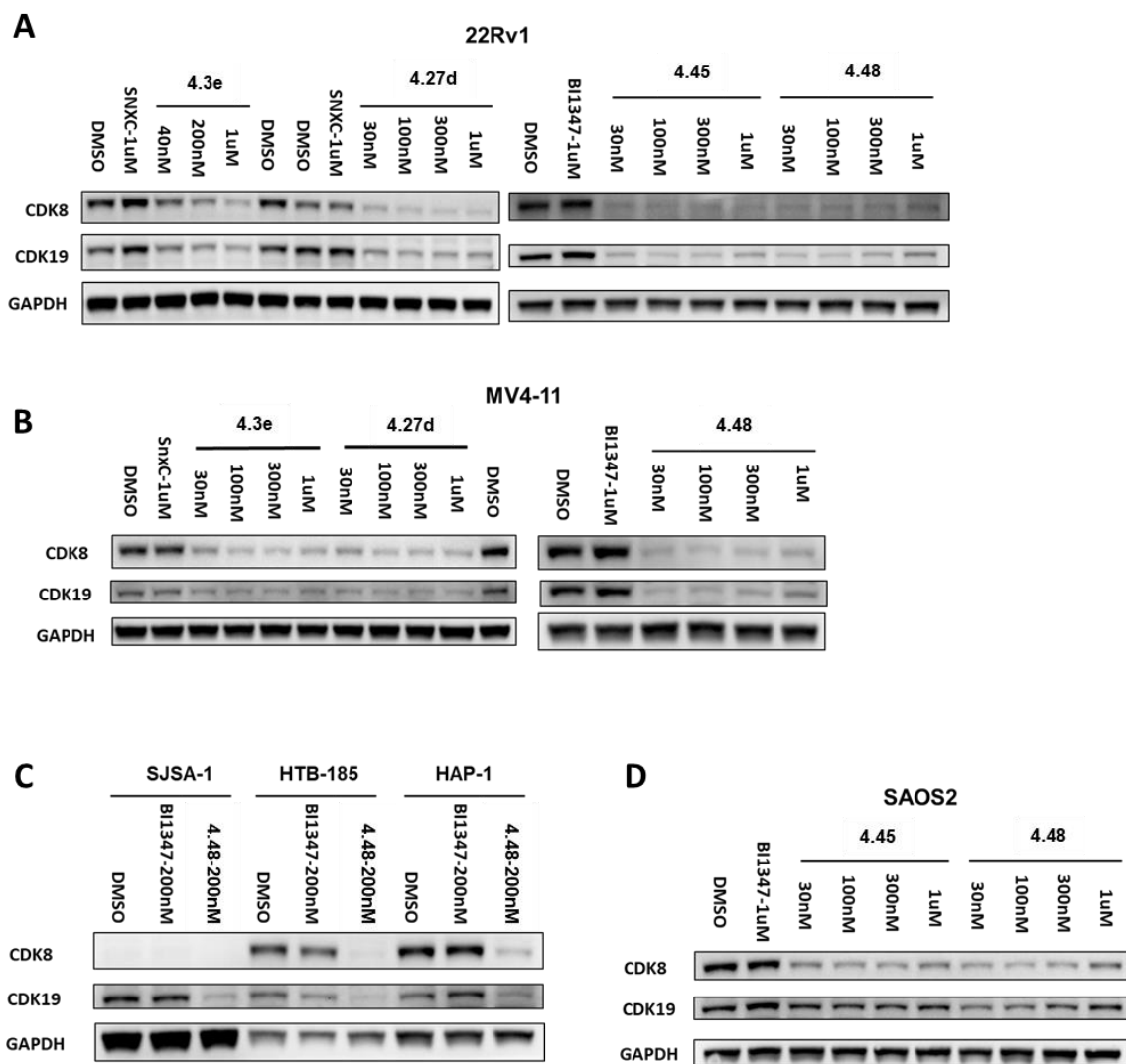


Figure 4.7 Effects of 24-hr treatment with different PROTAC compounds on CDK8/CDK19 protein levels in different human cell lines (**A**: 22Rv1; **B**: MV4-11; **C**: SJSA-1, HTB-185 and HAP-1; **D**: SAOS2).

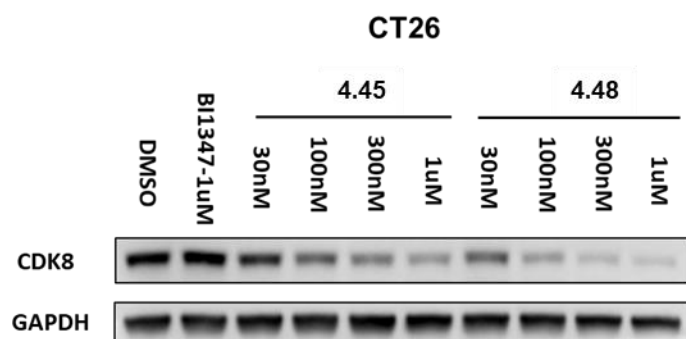
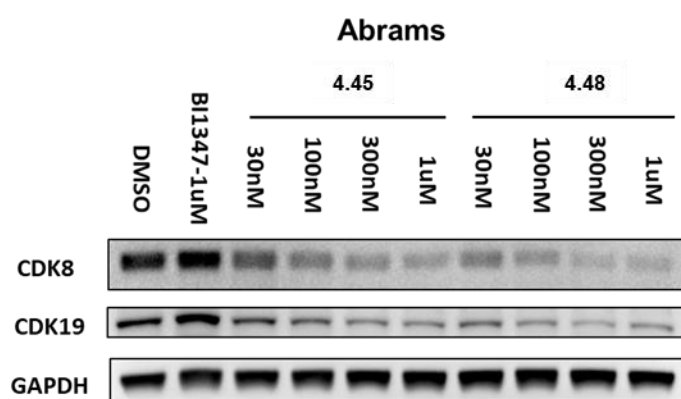
A**B**

Figure 4.8 Effects of treatment with different PROTAC compounds on CDK8/CDK19 protein levels in non-human cell lines (**A**: murine CT26; **B**: canine Abrams).

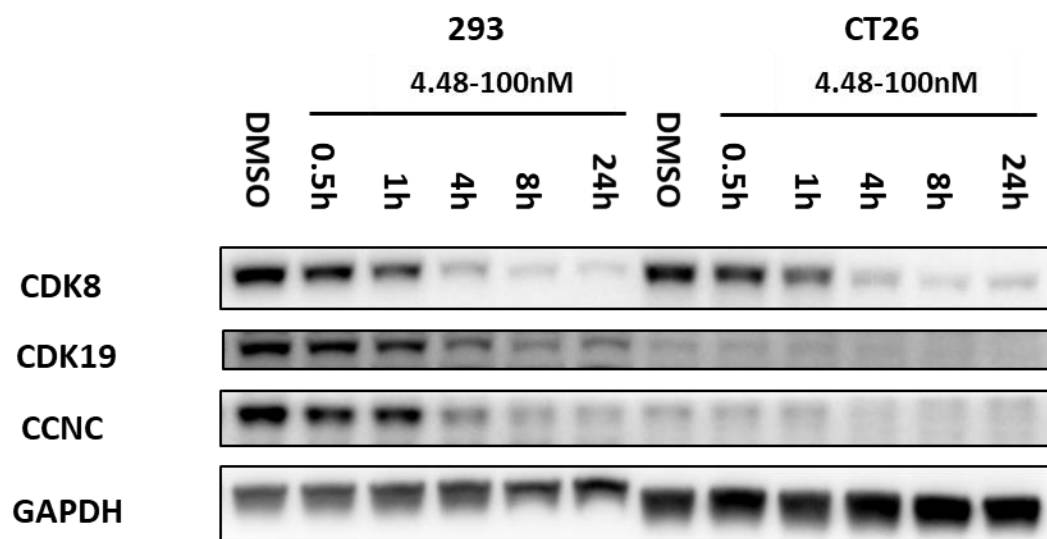


Figure 4.9 Time course of CDK8/CDK19/CCNC degradation by 4.48 in 293 and CT26 cells.

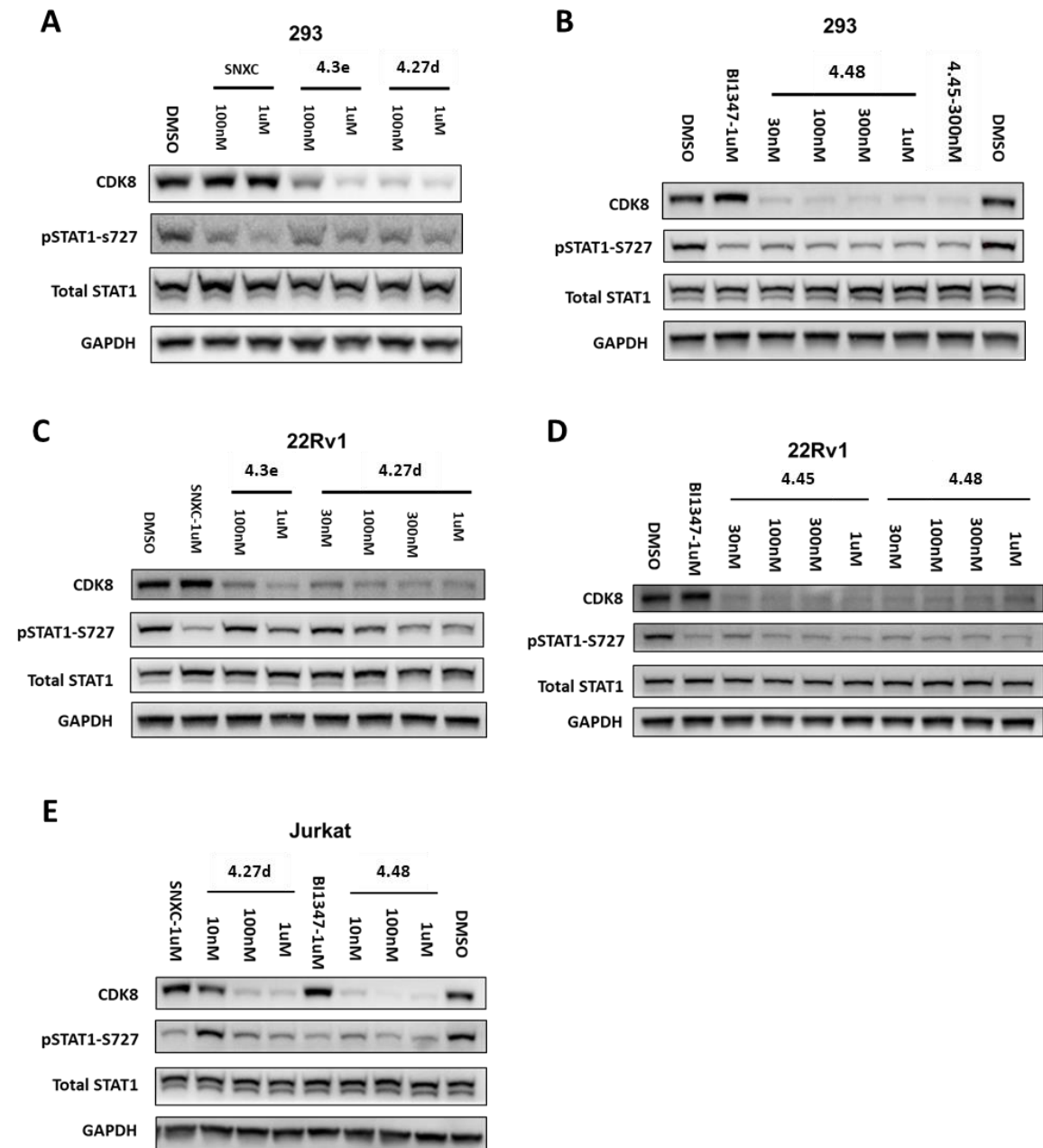


Figure 4.10 Effects of 24hr-treatment with different CDK8/19i and PROTACs on STAT1-S727 phosphorylation and CDK8 degradation.

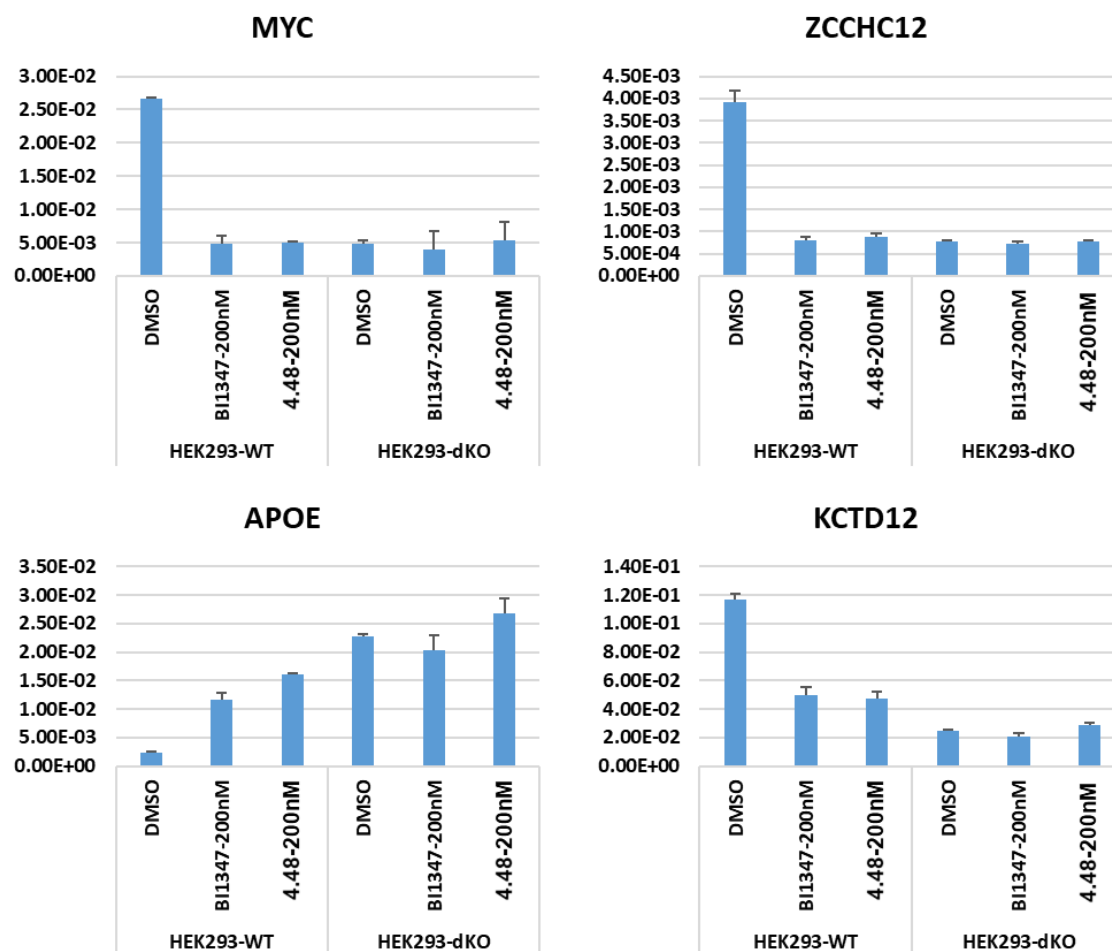


Figure 4.11 Effects of 3-day treatment with 200 nM BI-1347 and 200 nM 4.48 on CDK8/19-dependent gene expression in 293 parental (WT) and CDK8/19 double-knockout (dKO) cells.

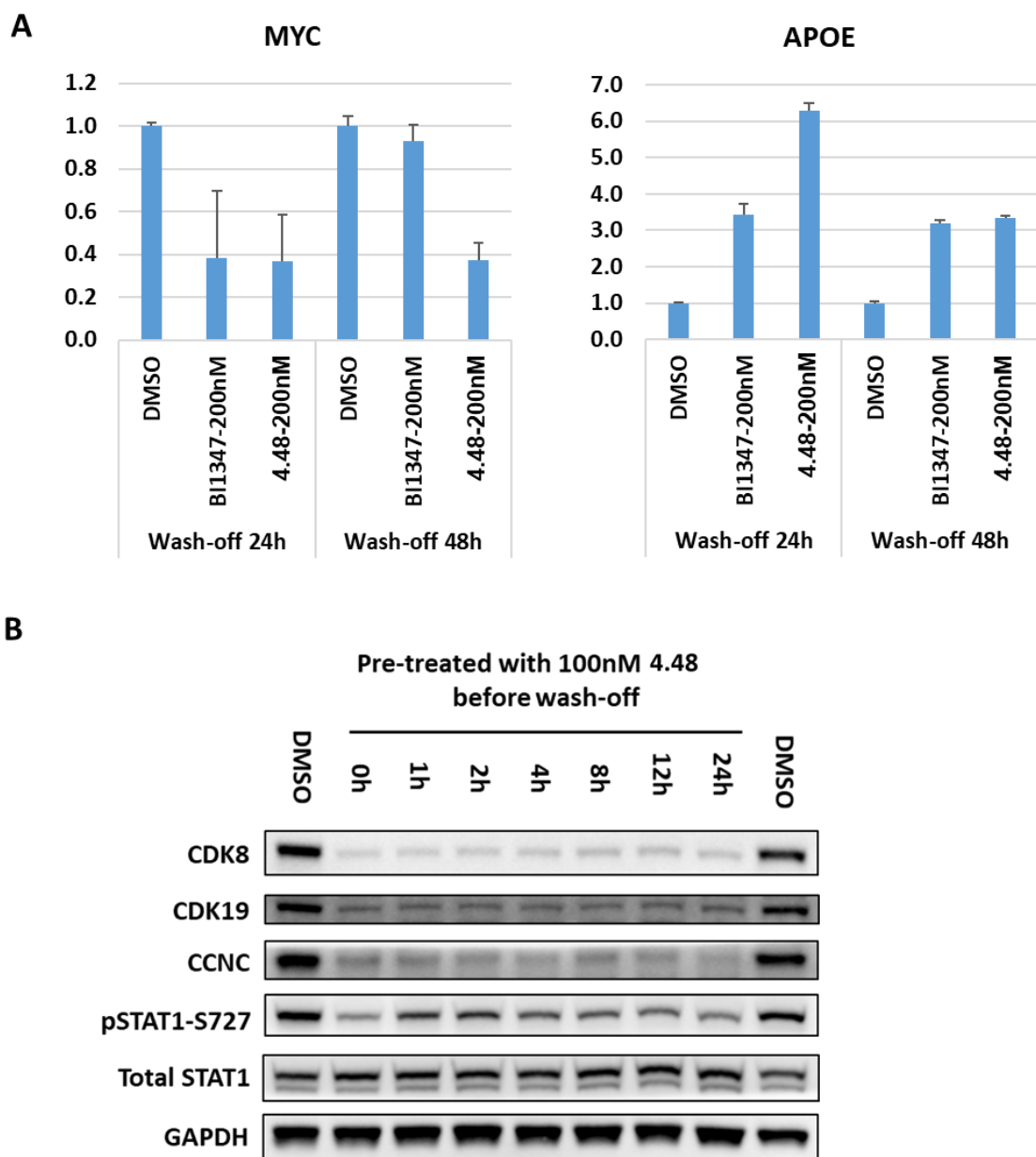


Figure 4.12 (A) Stability of transcriptional changes induced by BI1347 CDK8/19 kinase inhibitor and 4.48 PROTAC in the wash-off study in 293 cells. **(B)** Stability of pSTAT-S727 inhibition and CDK8/CDK19/CCNC degradation by 4.48 in 293 wash-off study.

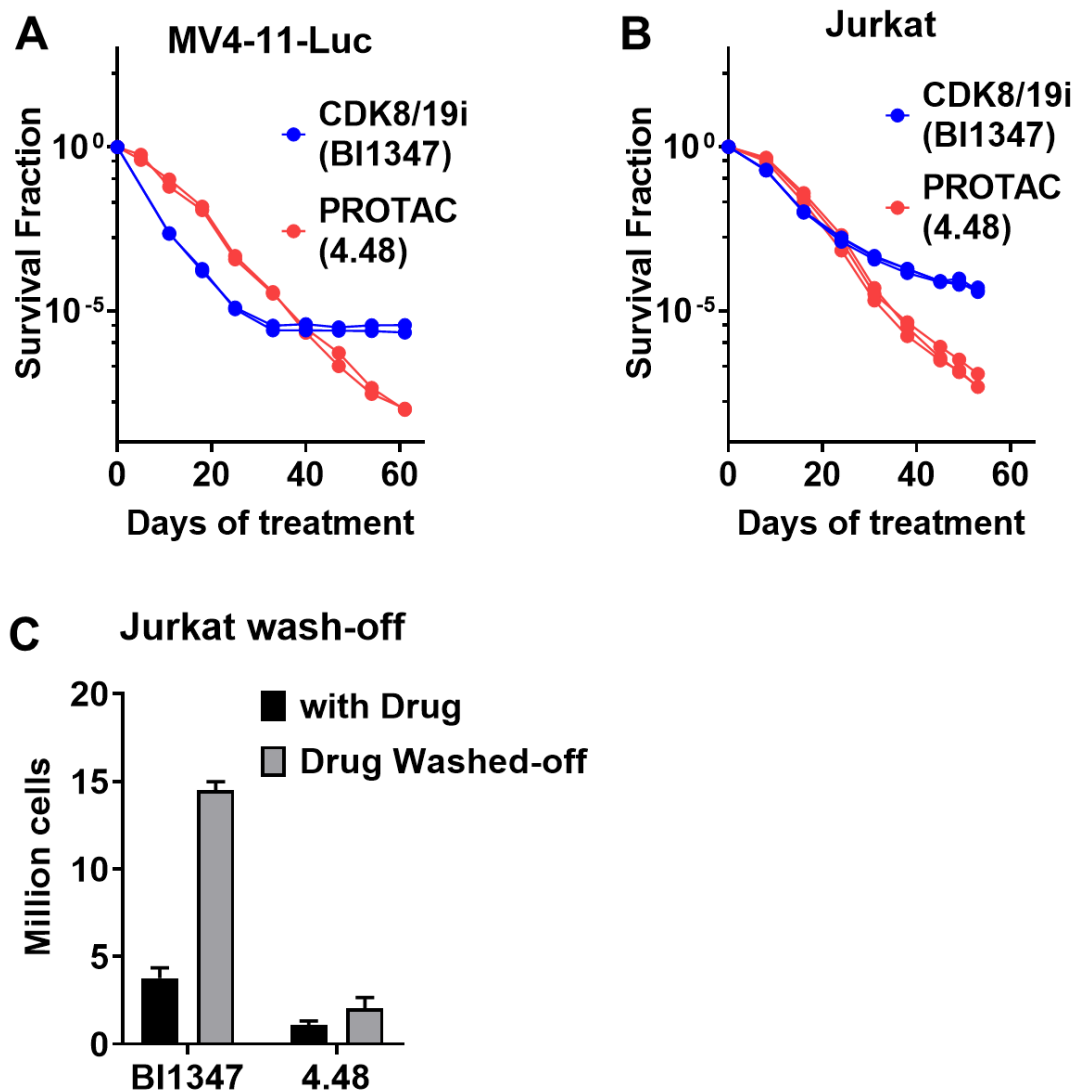


Figure 4.13 Long-term effects of CDK8/19 kinase inhibitor BI1347 and CDK8/19 PROTAC 4.48 on growth of leukemia cells. **(A)** Jurkat cells were continuously treated with 0.1% DMSO, 200 nM BI1347 or 200 nM 4.48 for 32 days. **(B)** MV4-11 cells were continuously treated with 300 nM BI1347 or 4.48 for 70 days. **(C)** Jurkat cells were pre-treated with 200 nM BI1347 or 4.48 for 8 days before removal of drug-containing media and further cultured in media containing the same compound (at 200 nM) or in drug-free media for 8 days.

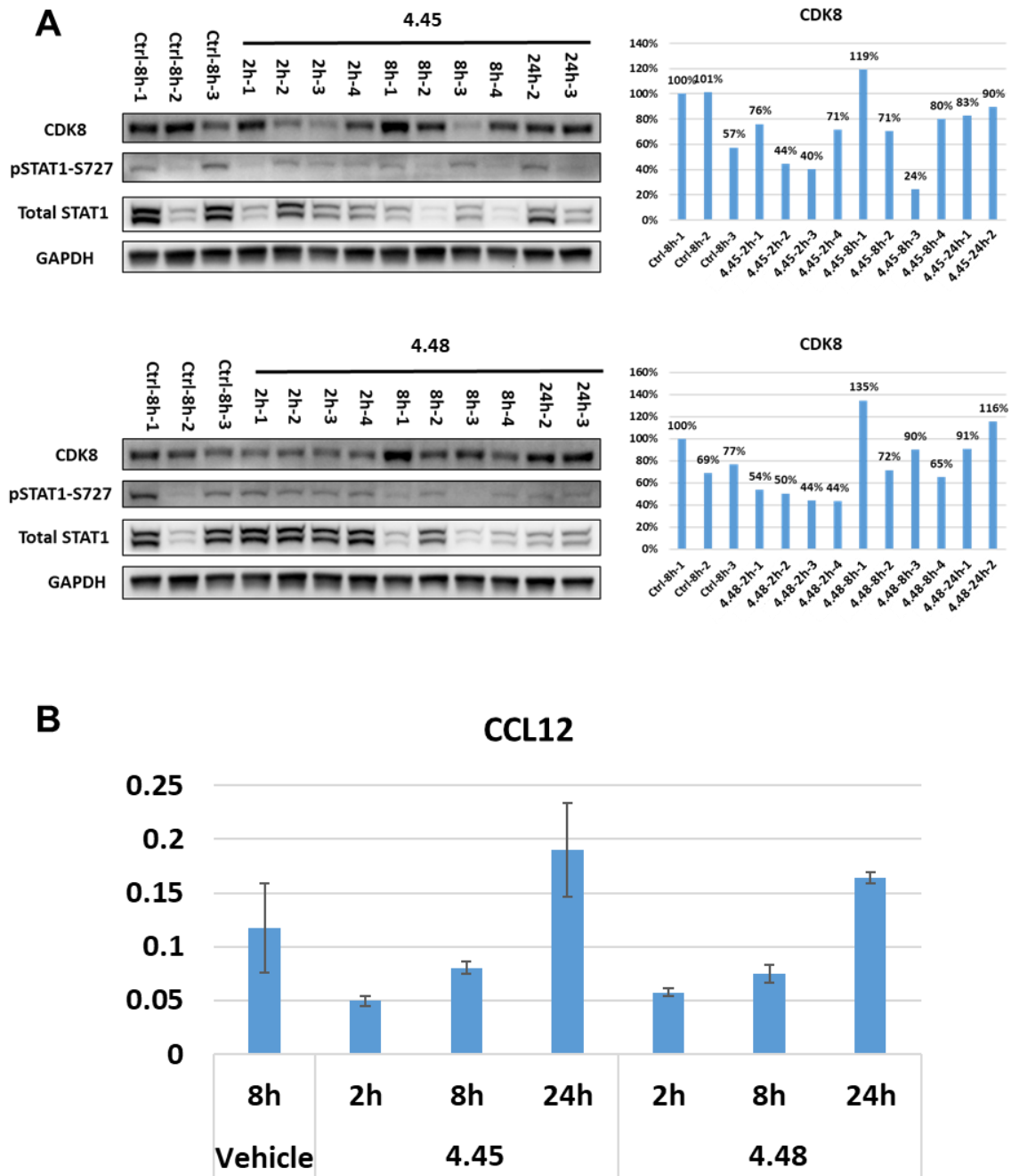
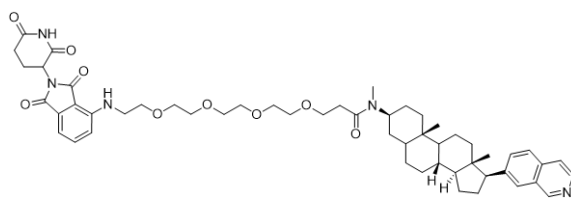
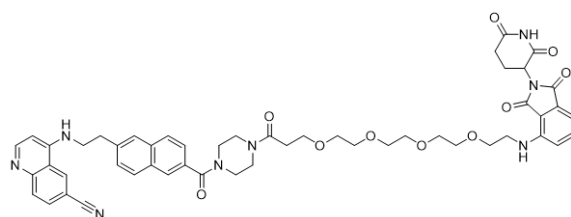
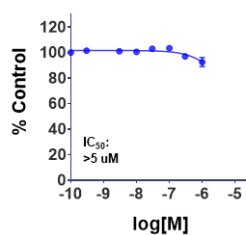


Figure 4.14 Levels of CDK8 protein and STAT1-S727 phosphorylation (**A**) and mRNA expression of the CDK8/19 dependent gene CCL12 (**B**) in CT26 tumors from mice dosed with Vehicle, 20 mg/kg 4.45 or 20 mg/kg 4.48.



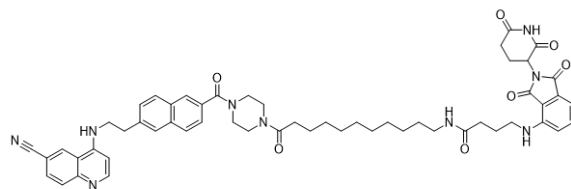
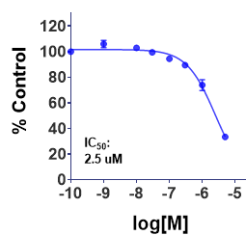
JH-XI-10-02

HEK293-Luc Assay



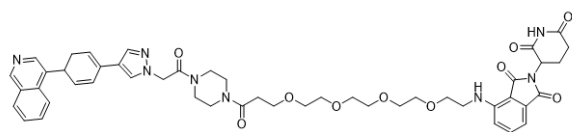
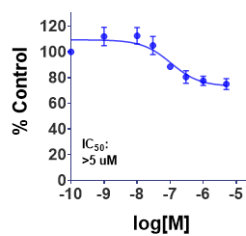
4.3a

HEK293-Luc Assay



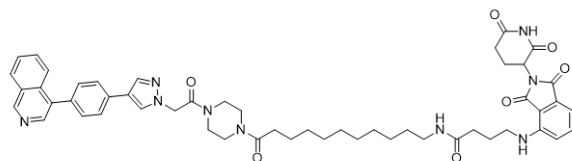
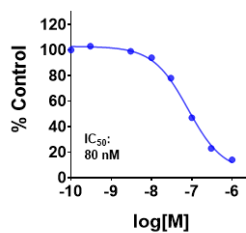
4.3e

HEK293-NFkB-Luc Assay



4.45

HEK293-NFkB Assay



4.51

HEK293-Luc Assay

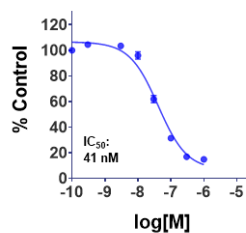
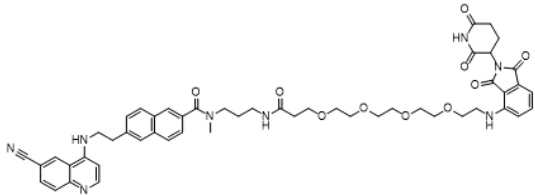
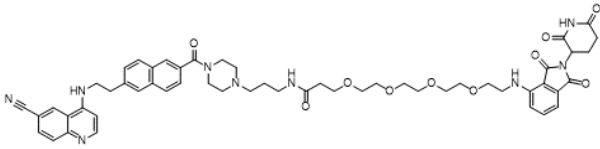
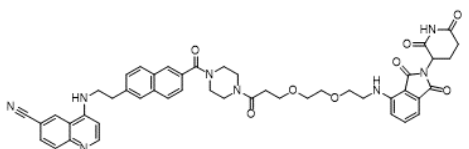
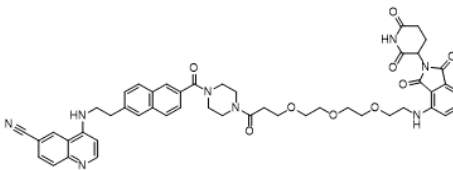
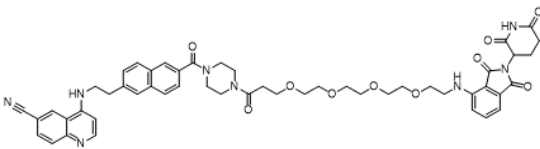
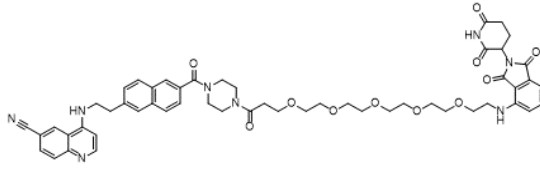
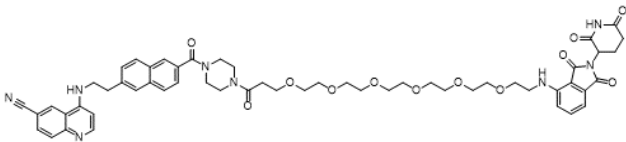
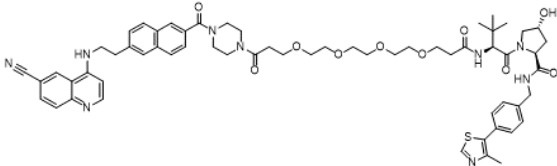
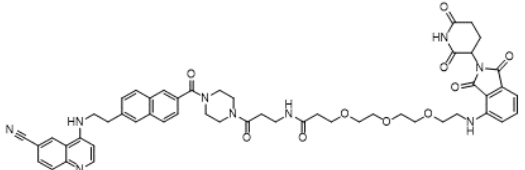
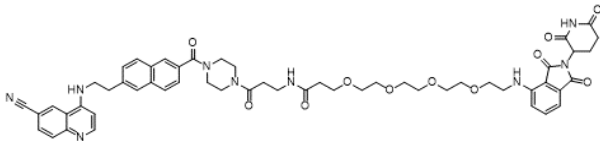
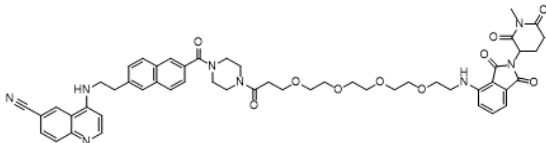
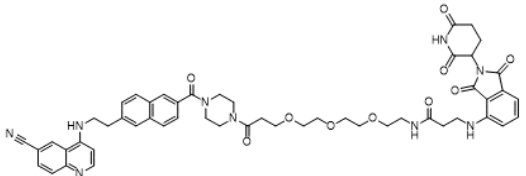
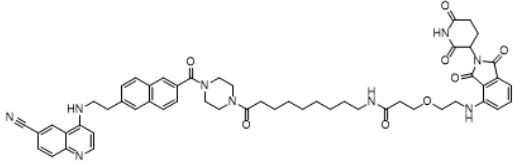
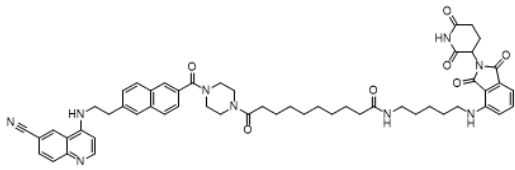
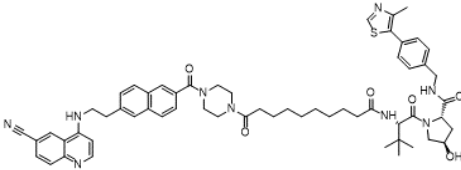
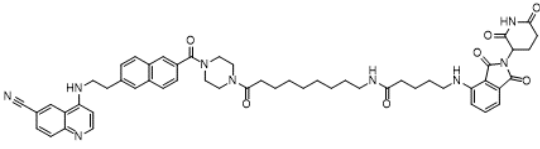
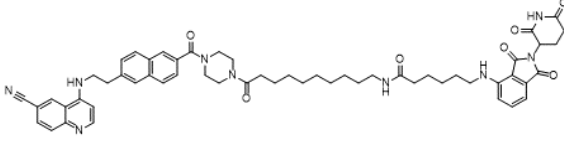
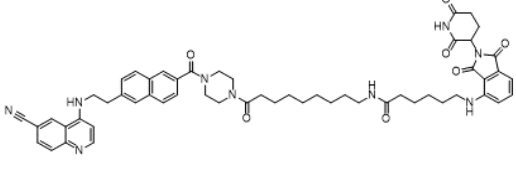
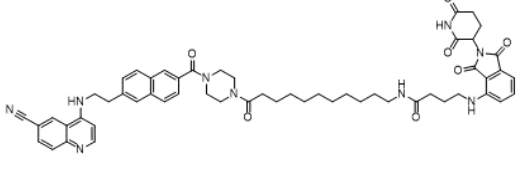
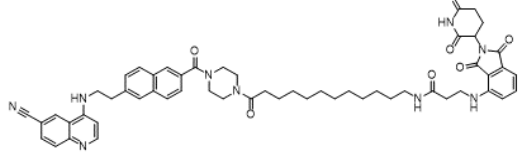


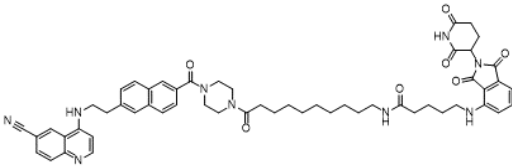
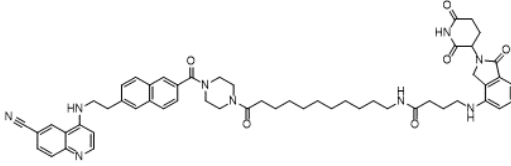
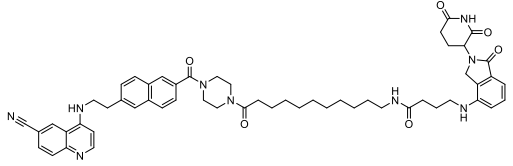
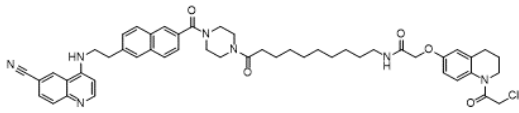
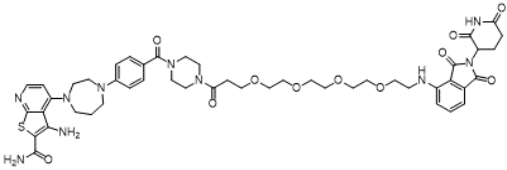
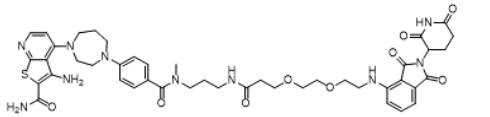
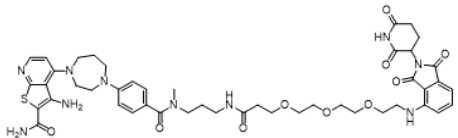
Figure 4.16 The HEK293-NFkB-Luc IC₅₀ curves of tested compounds.

Table 4.1 Structures and CDK8-degradation activities of CDK8/19 PROTACs

ID	Chemical Structure	Chemical formula	% CDK8 remaining (at 1 μ M)
4.3a		C ₅₁ H ₅₆ N ₈ O ₁₀	36%
4.3b		C ₅₄ H ₆₁ N ₉ O ₁₀	29%
4.3c		C ₄₇ H ₄₆ N ₈ O ₈	27%
4.3d		C ₄₉ H ₅₀ N ₈ O ₉	21%
4.3e		C ₅₁ H ₅₄ N ₈ O ₁₀	20%
4.3f		C ₅₃ H ₅₈ N ₈ O ₁₁	29%

4.3g		C55H62N8O12	28%
4.5		C61H73N9O10S	100%
4.6a		C52H55N9O10	66%
4.6b		C54H59N9O11	65%
4.10		C52H56N8O10	100%
4.21		C52H55N9O10	65%
4.24		C54H59N9O8	45%

4.25		C55H61N9O7	55%
4.26		C59H69N9O6S	69%
4.27a		C54H59N9O7	21%
4.27b		C56H63N9O7	81%
4.27c		C55H61N9O7	95%
4.27d		C55H61N9O7	13%
4.27e		C55H61N9O7	31%

4.27f		C55H61N9O7	19%
4.31		C55H61N9O7	39%
4.34		C55H63N9O6	43%
4.38		C50H56ClN7O5	100%
4.52		C48H58N10O11S	41%
4.4a		C44H52N10O9S	82%
4.4b		C46H56N10O10S	77%

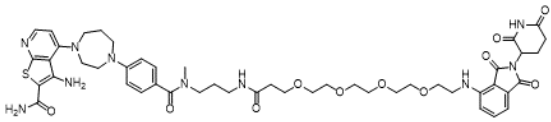
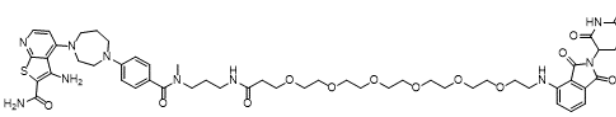
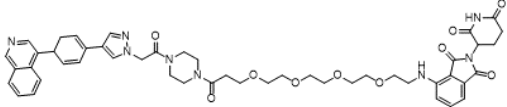
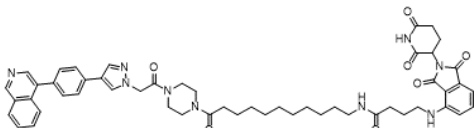
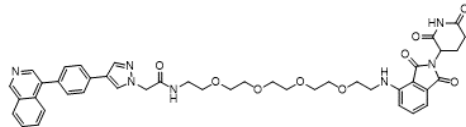
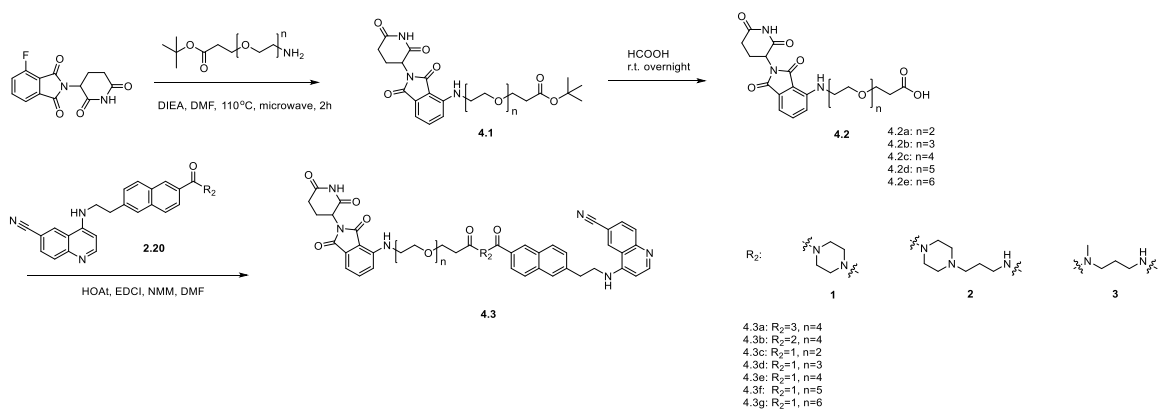
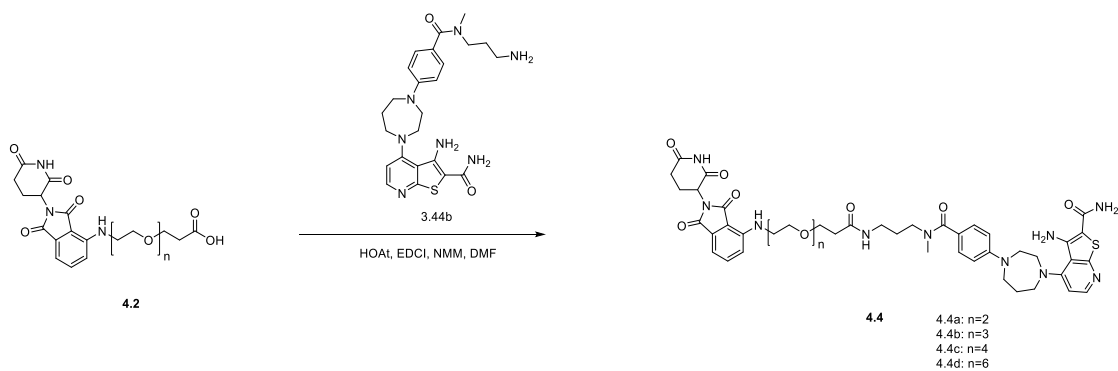
4.4c		C ₄₈ H ₆₀ N ₁₀ O ₁₁ S	74%
4.4d		C ₅₂ H ₆₈ N ₁₀ O ₁₃ S	59%
4.45		C ₄₈ H ₅₄ N ₈ O ₁₀	12%
4.48		C ₅₂ H ₅₉ N ₉ O ₇	19%
4.51		C ₄₃ H ₄₅ N ₇ O ₉	100%

Table 4.2 qPCR primer sequences

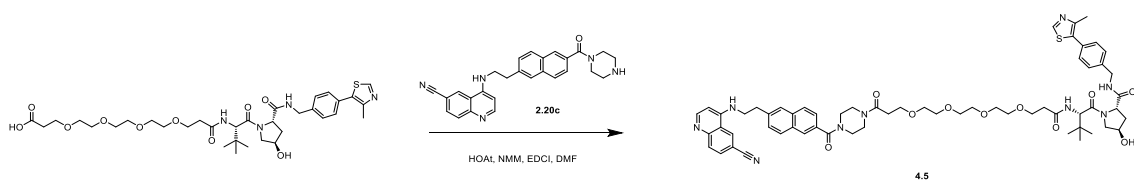
Primer Name	Species	Sequence
GAPDH-F	Human	CCATCACCATCTTCCAGGAGCG
GAPDH-R	Human	AGAGATGATGACCCTTTTGGC
MYC-F	Human	CCAACAGGAACTATGACCTCGACTAC
MYC-R	Human	CTCGAATTTCTTCCAGATATCCT
RPL13A-F	Human	GGCCCAGCAGTACCTGTTTA
RPL13A-R	Human	AGATGGCGGAGGTGCAG
KCTD12-F	Human	TTTATCACTGTGCTATCAATCAAAA
KCTD12-R	Human	TGCTGTAGAAAATATTCCTTGAAGA
APOE-F	Human	CTCCGGCTCTGTCTCCAC
APOE-R	Human	CCAATCACAGGCAGGAAGAT
ZCCHC12-F	Human	AGCTTAATCTGCAGGTGGGA
ZCCHC12-R	Human	GCAGAGGCTGGAAGTGAAAT
mRPL13A-F	Mouse	GGGCAGGTTCTGGTATTGGAT
mRPL13A-R	Mouse	GGCTCGGAAATGGTAGGGG
mGAPDH-F	Mouse	AGCCTCGTCCCGTAGACAAAAT
mGAPDH-R	Mouse	AGCCTCGTCCCGTAGACAAAAT
mCCL12-F	Mouse	CAGTCCTCAGGTATTGGCTGG
mCCL12-R	Mouse	GCTTCCGGACGTGAATCTTCT



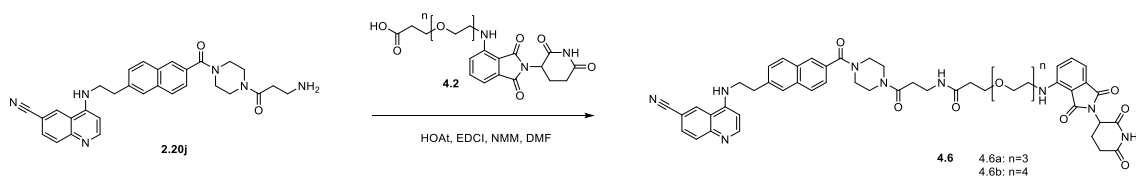
Scheme 4.1. The synthesis of PEG linker PROTACs **4.3**.



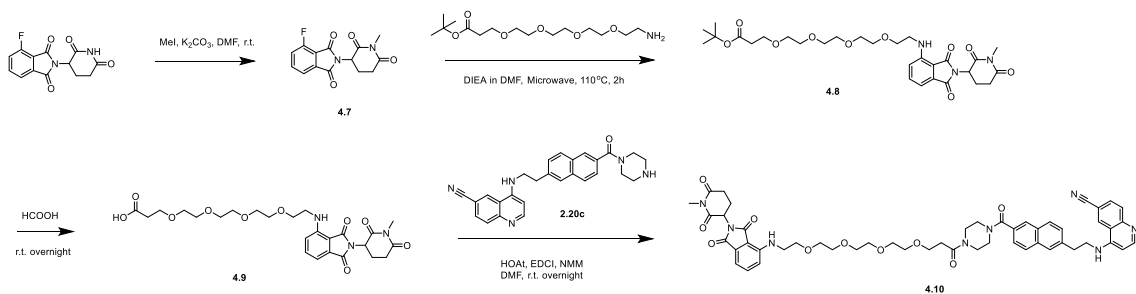
Scheme 4.2. The synthesis of PEG linker PROTACs **4.4**.



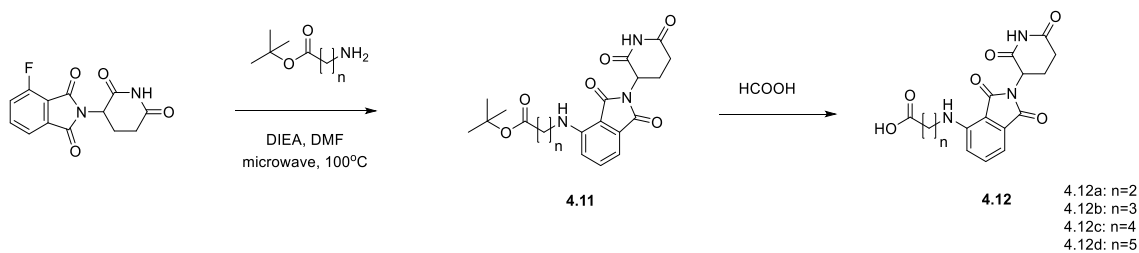
Scheme 4.3. The synthesis of VHL-based PROTAC **4.5**.



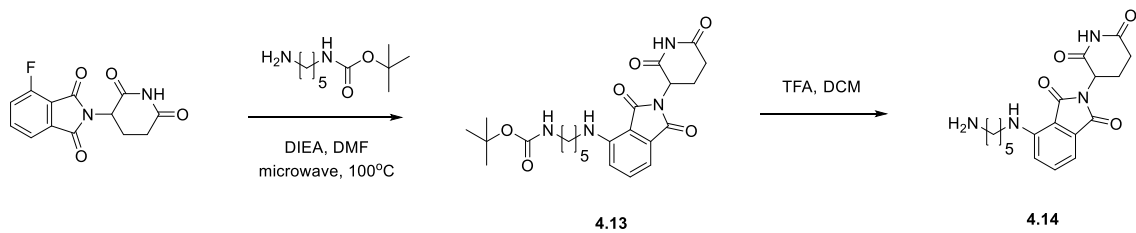
Scheme 4.4. The synthesis of PEG PROTACs **4.6**.



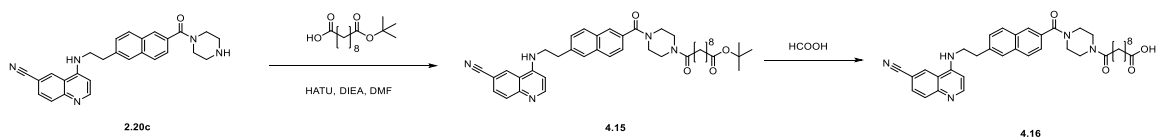
Scheme 4.5. The synthesis of inactive version of **4.3e** (**4.10**).



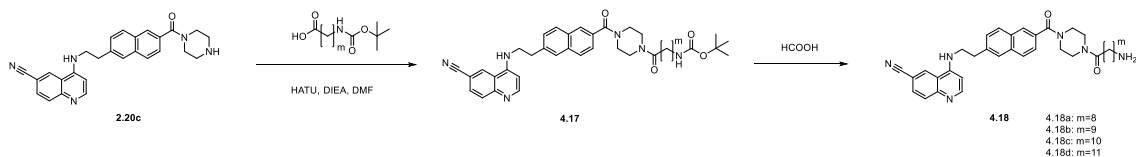
Scheme 4.6. The synthesis of pomalidomide analogs **4.12**.



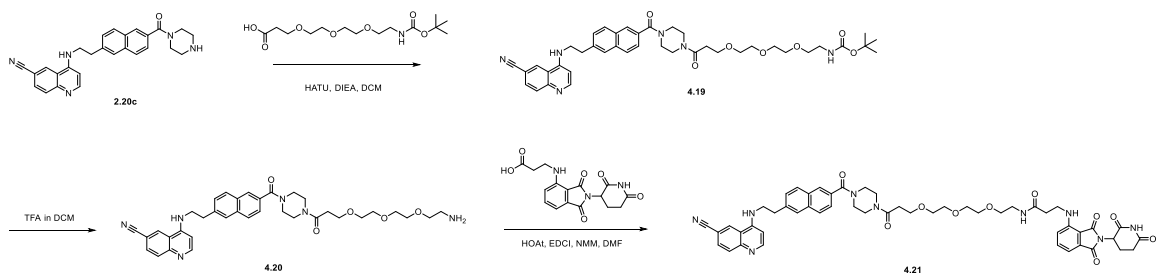
Scheme 4.7. The synthesis of pomalidomide analogs **4.14**.



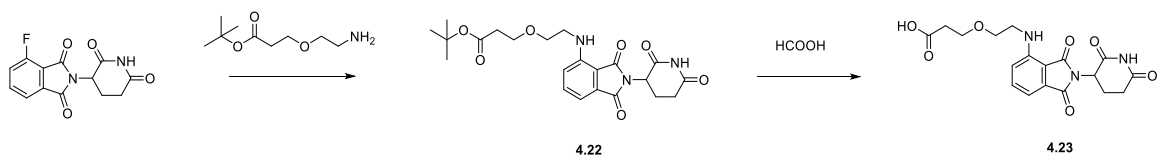
Scheme 4.8. The synthesis of **2.20c** analogs (**4.16**).



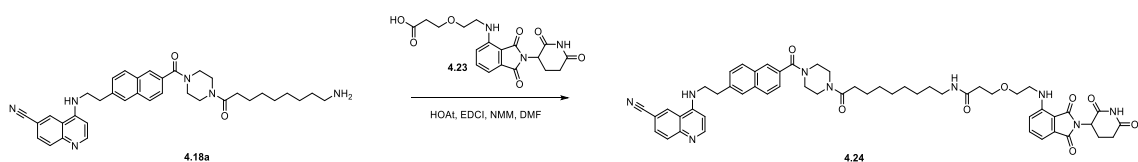
Scheme 4.9. The synthesis of **2.20c** analogs (**4.18**).



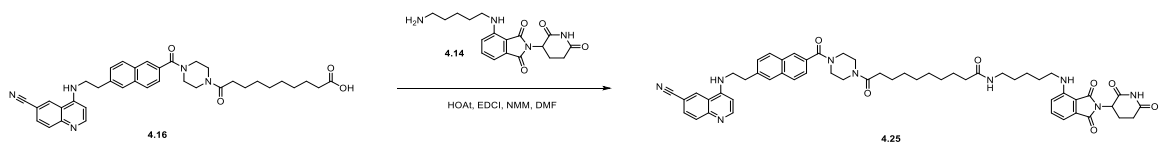
Scheme 4.10. The synthesis of PROTAC **4.21**.



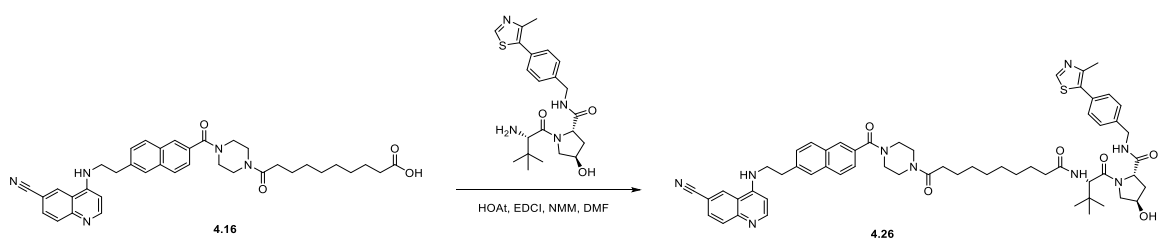
Scheme 4.11. The synthesis of pomalidomide analog **4.23**.



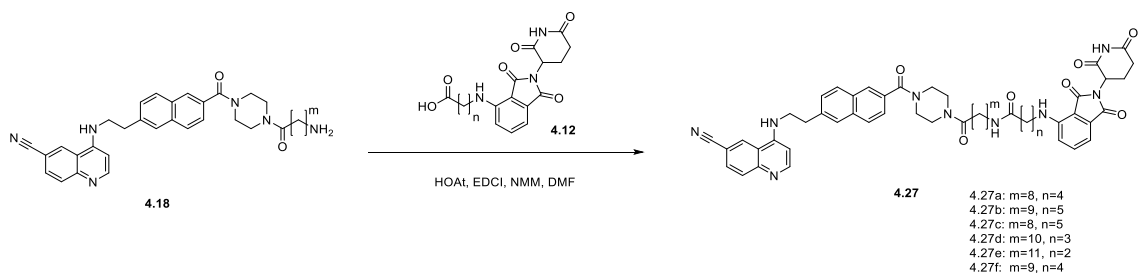
Scheme 4.12. The synthesis of PROTAC **4.24**.



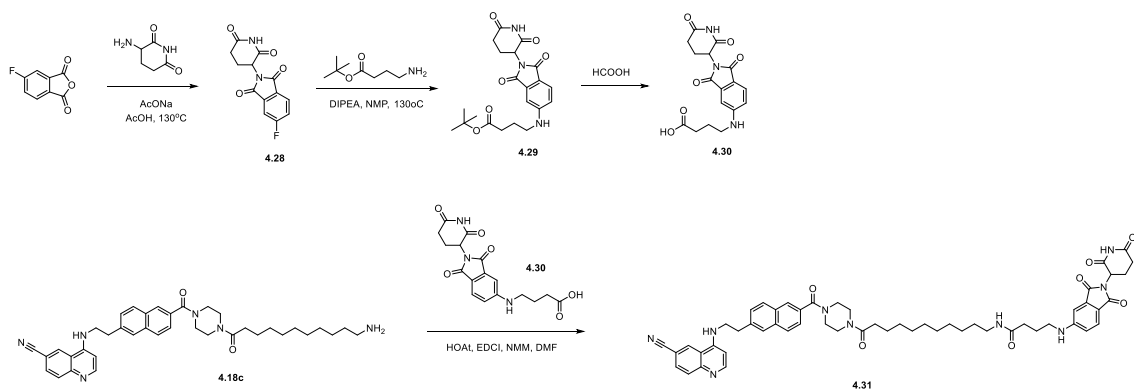
Scheme 4.13. The synthesis of PROTAC **4.25**.



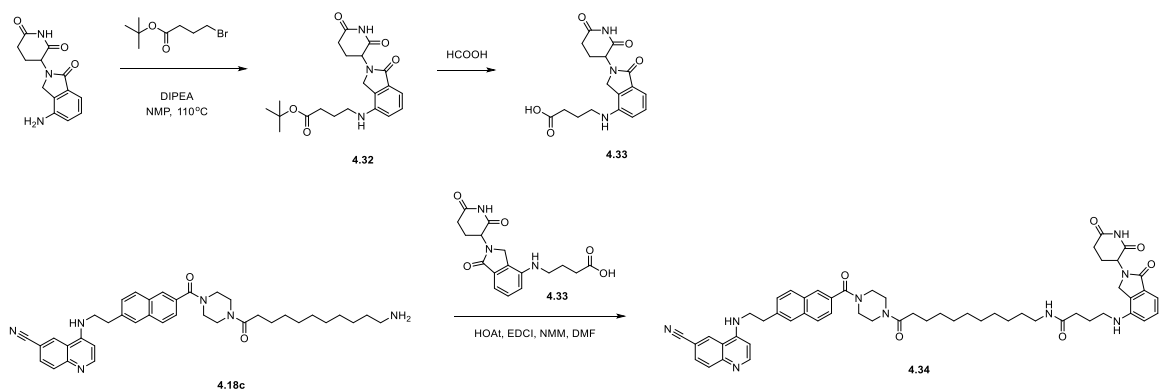
Scheme 4.14. The synthesis of PROTAC **4.26**.



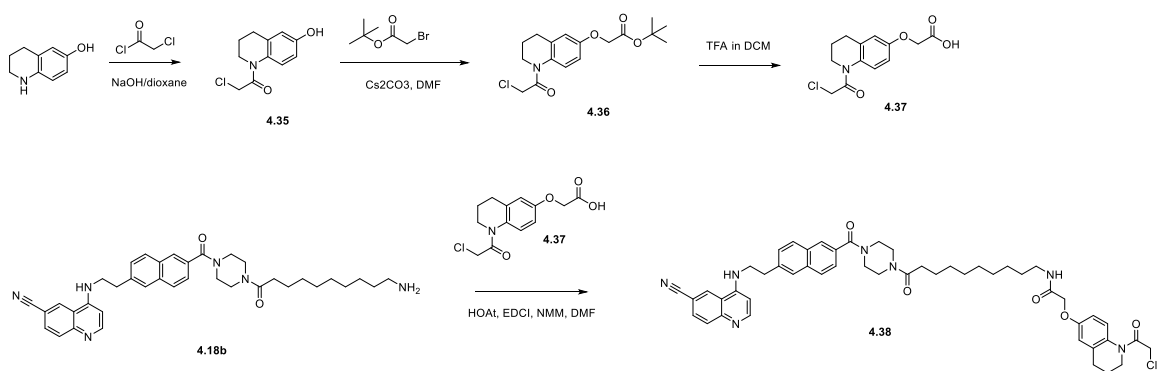
Scheme 4.15. The synthesis of PROTACs **4.27**.



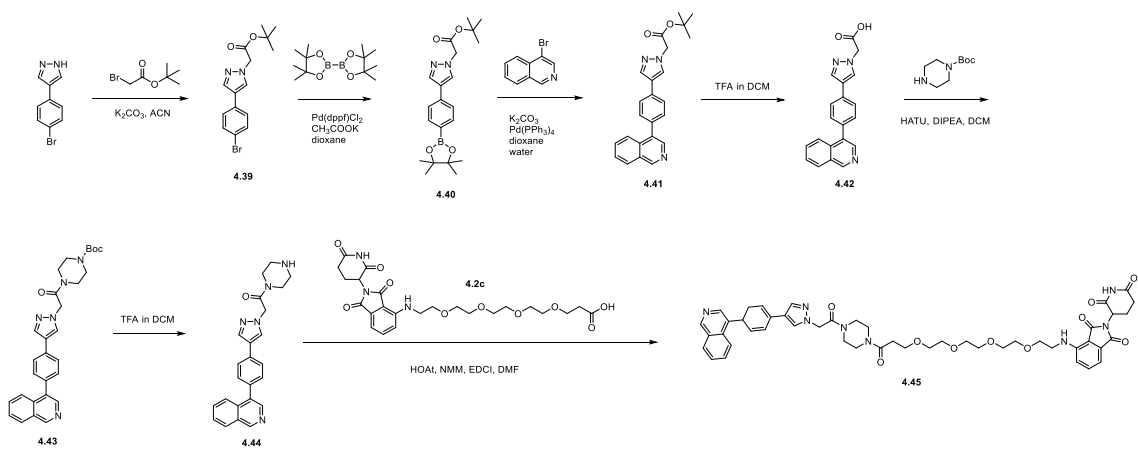
Scheme 4.16. The synthesis of PROTAC **4.31**.



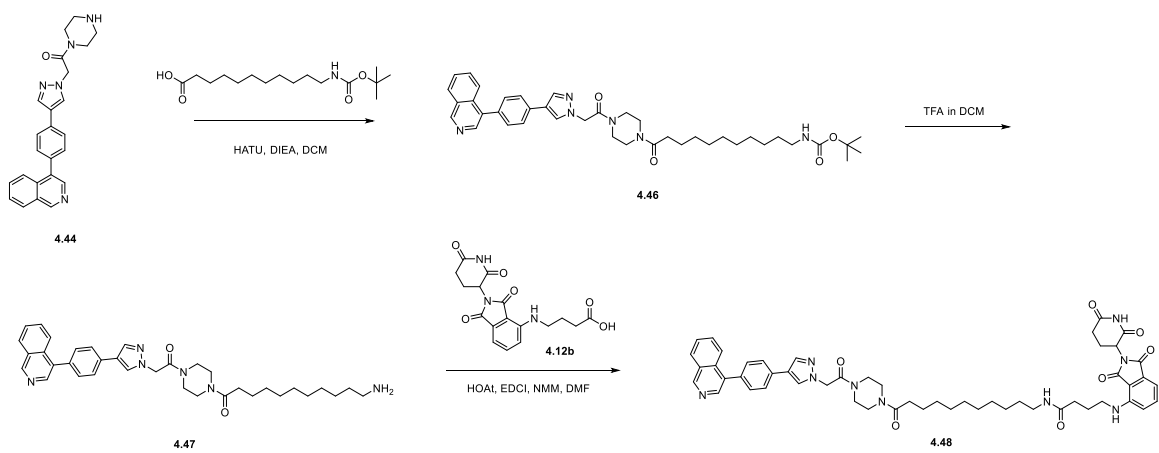
Scheme 4.17. The synthesis of PROTAC **4.34**.



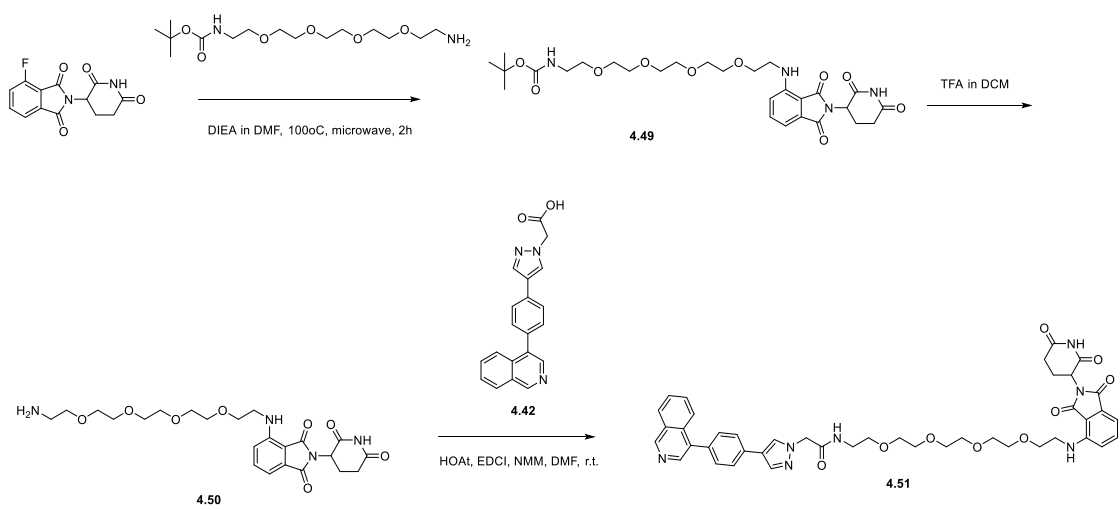
Scheme 4.18. The synthesis of PROTAC **4.38**.



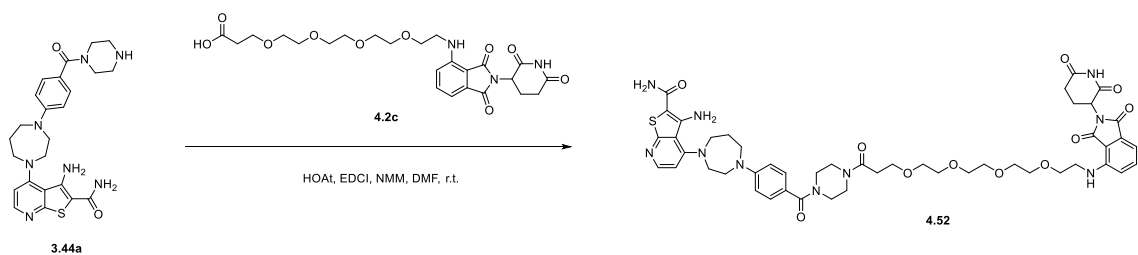
Scheme 4.19. The synthesis of PROTAC **4.45**.



Scheme 4.20. The synthesis of PROTAC **4.48**.



Scheme 4.21. The synthesis of PROTAC **4.51**.



Scheme 4.22. The synthesis of PROTAC **4.52**.

REFERENCES

- 1 Kung, J. E. & Jura, N. Structural Basis for the Non-catalytic Functions of Protein Kinases. *Structure* **24**, 7-24 (2016).
- 2 Manning, G., Whyte, D. B., Martinez, R., Hunter, T. & Sudarsanam, S. The protein kinase complement of the human genome. *Science* **298**, 1912-1934 (2002).
- 3 Matthews, D. J. & Gerritsen, M. E. *Targeting protein kinases for cancer therapy*. (John Wiley & Sons, 2011).
- 4 Lee, J. C. *et al.* A protein kinase involved in the regulation of inflammatory cytokine biosynthesis. *Nature* **372**, 739-746 (1994).
- 5 Force, T., Kuida, K., Namchuk, M., Parang, K. & Kyriakis, J. M. Inhibitors of protein kinase signaling pathways: emerging therapies for cardiovascular disease. *Circulation* **109**, 1196-1205 (2004).
- 6 Winder, W. a. & Hardie, D. AMP-activated protein kinase, a metabolic master switch: possible roles in type 2 diabetes. *American Journal of Physiology-Endocrinology* **277**, 1-10 (1999).
- 7 Cohen, P. Protein kinases—the major drug targets of the twenty-first century? *Nature reviews Drug discovery* **1**, 309-315 (2002).
- 8 Oprea, T. I. *et al.* Unexplored therapeutic opportunities in the human genome. *Nature reviews Drug discovery* **17**, 317 (2018).
- 9 Adjei, A. A. What is the right dose? The elusive optimal biologic dose in phase I clinical trials. *J Clin Oncol* **24**, 4054-4055, (2006).
- 10 Fabbro, D., Cowan-Jacob, S. W. & Moebitz, H. Ten things you should know about protein kinases: IUPHAR Review 14. *Br J Pharmacol* **172**, 2675-2700 (2015).
- 11 Graves, L. M., Duncan, J. S., Whittle, M. C. & Johnson, G. L. The dynamic nature of the kinome. *Biochem J* **450**, 1-8 (2013).
- 12 Leiser, D. *et al.* Targeting of the MET receptor tyrosine kinase by small molecule inhibitors leads to MET accumulation by impairing the receptor downregulation. *FEBS Lett* **588**, 653-658 (2014).
- 13 Spiegel, J., Cromm, P. M., Zimmermann, G., Grossmann, T. N. & Waldmann, H. Small-molecule modulation of Ras signaling. *Nat Chem Biol* **10**, 613-622 (2014).
- 14 Raina, K. & Crews, C. M. Chemical inducers of targeted protein degradation. *J Biol Chem* **285**, 11057-11060 (2010).
- 15 Tokatlian, T. & Segura, T. siRNA applications in nanomedicine. *Wiley Interdiscip Rev Nanomed Nanobiotechnol* **2**, 305-315 (2010).
- 16 Bobbin, M. L. & Rossi, J. J. RNA Interference (RNAi)-Based Therapeutics: Delivering on the Promise? *Annu Rev Pharmacol Toxicol* **56**, 103-122 (2016).

- 17 Jackson, A. L. *et al.* Expression profiling reveals off-target gene regulation by RNAi. *Nat Biotechnol* **21**, 635-637 (2003).
- 18 Fedorov, Y. *et al.* Off-target effects by siRNA can induce toxic phenotype. *RNA* **12**, 1188-1196 (2006).
- 19 Neklesa, T. K. *et al.* Small-molecule hydrophobic tagging–induced degradation of HaloTag fusion proteins. *Nature chemical biology* **7**, 538 (2011).
- 20 Pettersson, M. & Crews, C. M. Proteolysis TArgeting Chimeras (PROTACs)—past, present and future. *Drug Discovery Today: Technologies* (2019).
- 21 Nandi, D., Tahiliani, P., Kumar, A. & Chandu, D. The ubiquitin-proteasome system. *Journal of Biosciences* **31**, 137-155 (2006).
- 22 Lai, A. C. & Crews, C. M. Induced protein degradation: an emerging drug discovery paradigm. *Nature reviews Drug discovery* **16**, 101-114 (2017).
- 23 Pettersson, M. & Crews, C. M. PROTeolysis TArgeting Chimeras (PROTACs)—past, present and future. *Drug Discovery Today: Technologies* **31**, 15-27 (2019).
- 24 Burslem, G. M. & Crews, C. M. Proteolysis-targeting chimeras as therapeutics and tools for biological discovery. *Cell* **181**, 102-114 (2020).
- 25 Buss, N. A., Henderson, S. J., McFarlane, M., Shenton, J. M. & De Haan, L. Monoclonal antibody therapeutics: history and future. *Current opinion in pharmacology* **12**, 615-622 (2012).
- 26 Beck, A., Goetsch, L., Dumontet, C. & Corvaia, N. Strategies and challenges for the next generation of antibody–drug conjugates. *Nature reviews Drug discovery* **16**, 315-337 (2017).
- 27 Khongorzul, P., Ling, C. J., Khan, F. U., Ihsan, A. U. & Zhang, J. Antibody–drug conjugates: a comprehensive review. *Molecular Cancer Research* **18**, 3-19 (2020).
- 28 Gaj, T., Sirk, S. J., Shui, S.-I. & Liu, J. Genome-editing technologies: principles and applications. *Cold Spring Harbor perspectives in biology* **8** (2016).
- 29 Dhanjal, J. K., Radhakrishnan, N. & Sundar, D. Identifying synthetic lethal targets using CRISPR/Cas9 system. *Methods* **131**, 66-73 (2017).
- 30 El-Brolosy, M. A. & Stainier, D. Y. R. Genetic compensation: A phenomenon in search of mechanisms. *PLoS Genet* **13** (2017).
- 31 Doudna, J. A. & Charpentier, E. Genome editing. The new frontier of genome engineering with CRISPR-Cas9. *Science* **346**, 125809 (2014).
- 32 Hsu, P. D., Lander, E. S. & Zhang, F. Development and applications of CRISPR-Cas9 for genome engineering. *Cell* **157**, 1262-1278 (2014).
- 33 Zhou, Y., Shen, J. K., Hornicek, F. J., Kan, Q. & Duan, Z. The emerging roles and therapeutic potential of cyclin-dependent kinase 11 (CDK11) in human cancer. *Oncotarget* **7**, 40846-40859 (2016).
- 34 Fisher, R. P. Secrets of a double agent: CDK7 in cell-cycle control and transcription. *Journal of cell science* **118**, 5171-5180 (2005).

- 35 Szilagyi, Z. & Gustafsson, C. M. Emerging roles of Cdk8 in cell cycle control. *Biochimica et Biophysica Acta -Gene Regulatory Mechanisms* **1829**, 916-920 (2013).
- 36 Tassan, J. P., Jaquenoud, M., Leopold, P., Schultz, S. J. & Nigg, E. A. Identification of human cyclin-dependent kinase 8, a putative protein kinase partner for cyclin C. *Proc Natl Acad Sci U S A* **92**, 8871-8875 (1995).
- 37 Knuesel, M. T., Meyer, K. D., Donner, A. J., Espinosa, J. M. & Taatjes, D. J. The human CDK8 subcomplex is a histone kinase that requires Med12 for activity and can function independently of mediator. *Molecular cellular biology* **29**, 650-661 (2009).
- 38 Rzymiski, T., Mikula, M., Wiklik, K. & Brzózka, K. CDK8 kinase—An emerging target in targeted cancer therapy. *Biochimica et Biophysica Acta -Proteins Proteomics* **1854**, 1617-1629 (2015).
- 39 Schneider, E. *et al.* The structure of CDK8/CycC implicates specificity in the CDK/cyclin family and reveals interaction with a deep pocket binder. *Journal of molecular biology* **412**, 251-266 (2011).
- 40 Cee, V. J., Chen, D. Y. K., Lee, M. R. & Nicolaou, K. Cortistatin A is a High-Affinity Ligand of Protein Kinases ROCK, CDK8, and CDK11. *Angewandte Chemie International Edition* **48**, 8952-8957 (2009).
- 41 Tsutsui, T. *et al.* Human mediator kinase subunit CDK11 plays a negative role in viral activator VP16-dependent transcriptional regulation. *Genes to Cells* **13**, 817-826 (2008).
- 42 Westerling, T., Kuuluvainen, E. & Mäkelä, T. P. Cdk8 is essential for preimplantation mouse development. *Molecular cellular biology* **27**, 6177-6182 (2007).
- 43 Galbraith, M. D. *et al.* HIF1A employs CDK8-mediator to stimulate RNAPII elongation in response to hypoxia. *Cell* **153**, 1327-1339 (2013).
- 44 Becker, F. *et al.* Increased mediator complex subunit CDK19 expression associates with aggressive prostate cancer. *International journal of cancer* **146**, 577-588 (2020).
- 45 Tsutsui, T., Fukasawa, R., Tanaka, A., Hirose, Y. & Ohkuma, Y. Identification of target genes for the CDK subunits of the Mediator complex. *Genes to Cells* **16**, 1208-1218 (2011).
- 46 Audetat, K. A. *et al.* A kinase-independent role for cyclin-dependent kinase 19 in p53 response. *Molecular cellular biology* **37**, 00626-00616 (2017).
- 47 Tsutsui, T. *et al.* Mediator complex recruits epigenetic regulators via its two cyclin-dependent kinase subunits to repress transcription of immune response genes. *Journal of Biological Chemistry* **288**, 20955-20965 (2013).
- 48 Soutourina, J., Wydau, S., Ambroise, Y., Boschiero, C. & Werner, M. Direct interaction of RNA polymerase II and mediator required for transcription in vivo. *Science* **331**, 1451-1454 (2011).
- 49 Levine, M., Cattoglio, C. & Tjian, R. Looping back to leap forward: transcription enters a new era. *Cell* **157**, 13-25 (2014).

- 50 Kagey, M. H. *et al.* Mediator and cohesin connect gene expression and
chromatin architecture. *Nature* **467**, 430-435 (2010).
- 51 Poss, Z. C., Ebmeier, C. C. & Taatjes, D. J. The Mediator complex and
transcription regulation. *Critical reviews in biochemistry molecular biology*
48, 575-608 (2013).
- 52 Allen, B. L. & Taatjes, D. J. The Mediator complex: a central integrator of
transcription. *Nature reviews Molecular cell biology* **16**, 155-166 (2015).
- 53 Soutourina, J. Transcription regulation by the Mediator complex. *Nat Rev
Mol Cell Biol* **19**, 262-274 (2018).
- 54 Core, L. J., Waterfall, J. J. & Lis, J. T. Nascent RNA sequencing reveals
widespread pausing and divergent initiation at human promoters. *Science*
322, 1845-1848 (2008).
- 55 Seila, A. C. *et al.* Divergent transcription from active promoters. *Science*
322, 1849-1851 (2008).
- 56 Wang, G. *et al.* Mediator requirement for both recruitment and
postrecruitment steps in transcription initiation. *Molecular cell* **17**, 683-694
(2005).
- 57 Hoepfner, S., Baumli, S. & Cramer, P. Structure of the mediator subunit
cyclin C and its implications for CDK8 function. *J Mol Biol* **350**, 833-842,
doi:10.1016/j.jmb.2005.05.041 (2005).
- 58 Allen, B. L. & Taatjes, D. J. The Mediator complex: a central integrator of
transcription. *Nat Rev Mol Cell Biol* **16**, 155-166, doi:10.1038/nrm3951
(2015).
- 59 Fryer, C. J., White, J. B. & Jones, K. A. Mastermind recruits CycC: CDK8
to phosphorylate the Notch ICD and coordinate activation with turnover.
Molecular cell **16**, 509-520 (2004).
- 60 Alarcón, C. *et al.* Nuclear CDKs drive Smad transcriptional activation and
turnover in BMP and TGF- β pathways. *Cell* **139**, 757-769 (2009).
- 61 Zhao, X. *et al.* Regulation of lipogenesis by cyclin-dependent kinase 8–
mediated control of SREBP-1. *The Journal of clinical investigation* **122**,
2417-2427 (2012).
- 62 Bancerek, J. *et al.* CDK8 kinase phosphorylates transcription factor
STAT1 to selectively regulate the interferon response. *Immunity* **38**, 250-
262 (2013).
- 63 Bourbon, H.-M. Comparative genomics supports a deep evolutionary
origin for the large, four-module transcriptional mediator complex. *Nucleic
acids research* **36**, 3993-4008 (2008).
- 64 Knuesel, M. T., Meyer, K. D., Bernecky, C. & Taatjes, D. J. The human
CDK8 subcomplex is a molecular switch that controls Mediator coactivator
function. *Genes development* **23**, 439-451 (2009).
- 65 Tsai, K.-L. *et al.* A conserved Mediator–CDK8 kinase module association
regulates Mediator–RNA polymerase II interaction. *Nature structural
molecular biology* **20**, 611 (2013).
- 66 Boeing, S., Rigault, C., Heidemann, M., Eick, D. & Meisterernst, M. RNA
polymerase II C-terminal heptarepeat domain Ser-7 phosphorylation is

- established in a mediator-dependent fashion. *Journal of biological chemistry* **285**, 188-196 (2010).
- 67 Galbraith, M. D. *et al.* HIF1A employs CDK8-mediator to stimulate RNAPII elongation in response to hypoxia. *Cell* **153**, 1327-1339, doi:10.1016/j.cell.2013.04.048 (2013).
- 68 Knuesel, M. T., Meyer, K. D., Bernecky, C. & Taatjes, D. J. The human CDK8 subcomplex is a molecular switch that controls Mediator coactivator function. *Genes Dev* **23**, 439-451 (2009).
- 69 Price, D. H. P-TEFb, a cyclin-dependent kinase controlling elongation by RNA polymerase II. *Mol Cell Biol* **20**, 2629-2634 (2000).
- 70 Ebmeier, C. C. & Taatjes, D. J. Activator-Mediator binding regulates Mediator-cofactor interactions. *Proc Natl Acad Sci U S A* **107**, 11283-11288, (2010).
- 71 Donner, A. J., Ebmeier, C. C., Taatjes, D. J. & Espinosa, J. M. CDK8 is a positive regulator of transcriptional elongation within the serum response network. *Nat Struct Mol Biol* **17**, 194-201 (2010).
- 72 Daniels, D. *et al.* Mutual exclusivity of MED12/MED12L, MED13/13L, and CDK8/19 paralogs revealed within the CDK-Mediator kinase module. *J Proteomics Bioinform S* **2** (2013).
- 73 Eckelhart, E. *et al.* A novel Ncr1-Cre mouse reveals the essential role of STAT5 for NK-cell survival and development. *Blood* **117**, 1565-1573 (2011).
- 74 Witalisz-Siepracka, A. *et al.* NK cell-specific CDK8 deletion enhances antitumor responses. *Cancer immunology research* **6**, 458-466 (2018).
- 75 Shi, Y. & Massague, J. Mechanisms of TGF-beta signaling from cell membrane to the nucleus. *Cell* **113**, 685-700 (2003).
- 76 Aragón, E. *et al.* A Smad action turnover switch operated by WW domain readers of a phosphoserine code. *Genes development* **25**, 1275-1288 (2011).
- 77 Alarcón, C. *et al.* Nuclear CDKs drive Smad transcriptional activation and turnover in BMP and TGF- β pathways. *Cell* **139**, 757-769 (2009).
- 78 Dontu, G. *et al.* Role of Notch signaling in cell-fate determination of human mammary stem/progenitor cells. *Breast Cancer Res* **6**, R605-615 (2004).
- 79 Gaiano, N. & Fishell, G. The role of notch in promoting glial and neural stem cell fates. *Annu Rev Neurosci* **25**, 471-490, doi:10.1146/annurev.neuro.25.030702.130823 (2002).
- 80 Laky, K. & Fowlkes, B. J. Notch signaling in CD4 and CD8 T cell development. *Curr Opin Immunol* **20**, 197-202 (2008).
- 81 Fryer, C. J., White, J. B. & Jones, K. A. Mastermind recruits CycC:CDK8 to phosphorylate the Notch ICD and coordinate activation with turnover. *Mol Cell* **16**, 509-520 (2004).
- 82 Levy, D. E. & Darnell Jr, J. E. Stats: transcriptional control and biological impact. *Nature reviews Molecular cell biology* **3**, 651-662 (2002).
- 83 Sadzak, I. *et al.* Recruitment of Stat1 to chromatin is required for interferon-induced serine phosphorylation of Stat1 transactivation domain. *Proceedings of the National Academy of Sciences* **105**, 8944-8949 (2008).

- 84 Stark, G. R. & Darnell Jr, J. E. The JAK-STAT pathway at twenty. *Immunity* **36**, 503-514 (2012).
- 85 Agaloti, T., Chen, G. & Thanos, D. Deciphering the transcriptional histone acetylation code for a human gene. *Cell* **111**, 381-392 (2002).
- 86 Meyer, K. D. *et al.* Cooperative activity of cdk8 and GCN5L within Mediator directs tandem phosphoacetylation of histone H3. *The EMBO journal* **27**, 1447-1457 (2008).
- 87 Yokoyama, C. *et al.* SREBP-1, a basic-helix-loop-helix-leucine zipper protein that controls transcription of the low density lipoprotein receptor gene. *Cell* **75**, 187-197 (1993).
- 88 Youn, D. Y., Xiaoli, A. M., Kwon, H., Yang, F. & Pessin, J. E. The subunit assembly state of the Mediator complex is nutrient-regulated and is dysregulated in a genetic model of insulin resistance and obesity. *Journal of Biological Chemistry* **294**, 9076-9083 (2019).
- 89 Kapoor, A. *et al.* The histone variant macroH2A suppresses melanoma progression through regulation of CDK8. *Nature* **468**, 1105-1109, doi:nature09590 [pii];10.1038/nature09590 [doi] (2010).
- 90 Menzl, I. *et al.* A kinase-independent role for CDK8 in BCR-ABL1(+) leukemia. *Nat Commun* **10**, 4741, (2019).
- 91 Audetat, K. A. *et al.* A Kinase-Independent Role for Cyclin-Dependent Kinase 19 in p53 Response. *Mol Cell Biol* **37** (2017).
- 92 Steinparzer, I. *et al.* Transcriptional Responses to IFN- γ Require Mediator Kinase-Dependent Pause Release and Mechanistically Distinct CDK8 and CDK19 Functions. *Mol Cell* **76**, 485-499 (2019).
- 93 Nakayama, K. *et al.* Skp2-mediated degradation of p27 regulates progression into mitosis. *Developmental cell* **6**, 661-672 (2004).
- 94 Xu, D. *et al.* Skp2–MacroH2A1–CDK8 axis orchestrates G2/M transition and tumorigenesis. *Nature communications* **6**, 1-14 (2015).
- 95 Zhao, J., Ramos, R. & Demma, M. CDK8 regulates E2F1 transcriptional activity through S375 phosphorylation. *Oncogene* **32**, 3520-3530 (2013).
- 96 Niehrs, C. & Acebron, S. P. Mitotic and mitogenic Wnt signalling. *The EMBO journal* **31**, 2705-2713 (2012).
- 97 Akoulitchev, S., Chuikov, S. & Reinberg, D. TFIIH is negatively regulated by cdk8-containing mediator complexes. *Nature* **407**, 102-106 (2000).
- 98 Firestein, R. *et al.* CDK8 is a colorectal cancer oncogene that regulates β -catenin activity. *Nature* **455**, 547-551 (2008).
- 99 Kaur, M. *et al.* Silibinin suppresses growth of human colorectal carcinoma SW480 cells in culture and xenograft through down-regulation of β -catenin-dependent signaling. *Neoplasia* **12**, 415-424 (2010).
- 100 Cai, W.-s. *et al.* Downregulation of CDK-8 inhibits colon cancer hepatic metastasis by regulating Wnt/ β -catenin pathway. *Biomedicine Pharmacotherapy* **74**, 153-157 (2015).
- 101 Firestein, R. *et al.* CDK8 expression in 470 colorectal cancers in relation to β -catenin activation, other molecular alterations and patient survival. *International journal of cancer* **126**, 2863-2873 (2010).

- 102 Bienz, M. & Clevers, H. Linking colorectal cancer to Wnt signaling. *Cell* **103**, 311-320 (2000).
- 103 Sansom, O. J. *et al.* Myc deletion rescues Apc deficiency in the small intestine. *Nature* **446**, 676-679 (2007).
- 104 Seo, J.-O., Han, S. I. & Lim, S.-C. Role of CDK8 and β -catenin in colorectal adenocarcinoma. *Oncology reports* **24**, 285-291 (2010).
- 105 McClelland, M. L. *et al.* Cdk8 deletion in the ApcMin murine tumour model represses EZH2 activity and accelerates tumourigenesis. *The Journal of pathology* **237**, 508-519 (2015).
- 106 Warburg, O., Wind, F. & Negelein, E. The metabolism of tumors in the body. *Journal of General Physiology* **8**, 519-530 (1927).
- 107 Warburg, O., Wind, F. & Negelein, E. Killing-off of tumor cells in vitro. *J. Gen. Physiol* **8**, 519-530 (1927).
- 108 Koppenol, W., Bounds, P. & Dang, C. Otto Warburg's contributions to current concepts of cancer metabolism, 117. Cuezva JM, Chen G, Alonso AM, *et al.*, The bioenergetic signature of lung adenocarcinomas is a molecular marker of cancer diagnosis and prognosis. *Carcinogenesis* **25**, 1157-1163 (2004).
- 109 Galbraith, M. D. *et al.* CDK8 kinase activity promotes glycolysis. *Cell reports* **21**, 1495-1506 (2017).
- 110 Liang, J. *et al.* CDK8 selectively promotes the growth of colon cancer metastases in the liver by regulating gene expression of TIMP3 and matrix metalloproteinases. *Cancer research* **78**, 6594-6606 (2018).
- 111 Lin, H. *et al.* Tissue inhibitor of metalloproteinases-3 transfer suppresses malignant behaviors of colorectal cancer cells. *Cancer gene therapy* **19**, 845-851 (2012).
- 112 McDermott, M. S. *et al.* Inhibition of CDK8 mediator kinase suppresses estrogen dependent transcription and the growth of estrogen receptor positive breast cancer. *Oncotarget* **8**, 12558 (2017).
- 113 Kapoor, A. *et al.* The histone variant macroH2A suppresses melanoma progression through regulation of CDK8. *Nature* **468**, 1105-1109 (2010).
- 114 Brägelmann, J. *et al.* Pan-cancer analysis of the Mediator complex transcriptome identifies CDK19 and CDK8 as therapeutic targets in advanced prostate cancer. *Clinical Cancer Research* **23**, 1829-1840 (2017).
- 115 Xu, W. *et al.* Mutated K-ras activates CDK8 to stimulate the epithelial-to-mesenchymal transition in pancreatic cancer in part via the Wnt/ β -catenin signaling pathway. *Cancer letters* **356**, 613-627 (2015).
- 116 Wei, R. *et al.* CDK8 regulates the angiogenesis of pancreatic cancer cells in part via the CDK8- β -catenin-KLF2 signal axis. *Experimental cell research* **369**, 304-315 (2018).
- 117 Thériault, B. L., Shepherd, T. G., Mujoomdar, M. L. & Nachtigal, M. W. BMP4 induces EMT and Rho GTPase activation in human ovarian cancer cells. *Carcinogenesis* **28**, 1153-1162 (2007).
- 118 Serrao, A. *et al.* Mediator kinase CDK8/CDK19 drives YAP1-dependent BMP4-induced EMT in cancer. *Oncogene* **37**, 4792-4808 (2018).

- 119 Pelish, H. E. *et al.* Mediator kinase inhibition further activates super-enhancer-associated genes in AML. *Nature* **526**, 273-276 (2015).
- 120 Rzymiski, T. *et al.* SEL120-34A is a novel CDK8 inhibitor active in AML cells with high levels of serine phosphorylation of STAT1 and STAT5 transactivation domains. *Oncotarget* **8**, 33779 (2017).
- 121 Li, N. *et al.* Cyclin C is a haploinsufficient tumour suppressor. *Nature cell biology* **16**, 1080-1091 (2014).
- 122 Zhang, Q., Lenardo, M. J. & Baltimore, D. 30 years of NF- κ B: a blossoming of relevance to human pathobiology. *Cell* **168**, 37-57 (2017).
- 123 Chen, M. *et al.* CDK8/19 Mediator kinases potentiate induction of transcription by NF κ B. *Proceedings of the National Academy of Sciences* **114**, 10208-10213 (2017).
- 124 Xi, X., Yao, Y., Liu, N. & Li, P. MiR-297 alleviates LPS-induced A549 cell and mice lung injury via targeting cyclin dependent kinase 8. *International immunopharmacology* **80**, 106197 (2020).
- 125 Putz, E. M. *et al.* CDK8-mediated STAT1-S727 phosphorylation restrains NK cell cytotoxicity and tumor surveillance. *Cell reports* **4**, 437-444 (2013).
- 126 Jewett, A. *et al.* Natural killer cells preferentially target cancer stem cells; role of monocytes in protection against NK cell mediated lysis of cancer stem cells. *Current drug delivery* **9**, 5-16 (2012).
- 127 Rzymiski, T., Mikula, M., Wiklik, K. & Brzozka, K. CDK8 kinase-An emerging target in targeted cancer therapy. *Biochimica Et Biophysica Acta-Proteins and Proteomics* **1854**, 1617-1629 (2015).
- 128 Philip, S., Kumarasiri, M., Teo, T., Yu, M. & Wang, S. Cyclin-Dependent Kinase 8: A New Hope in Targeted Cancer. *Journal of Medicinal Chemistry*.
- 129 Xi, M. *et al.* CDK8 as a therapeutic target for cancers and recent developments in discovery of CDK8 inhibitors. *European journal of medicinal chemistry* **164**, 77-91 (2019).
- 130 Tsutsui, T. *et al.* Human mediator kinase subunit CDK11 plays a negative role in viral activator VP16-dependent transcriptional regulation. *Genes to Cells* **13**, 817-826 (2008).
- 131 Zhang, J., Yang, P. L. & Gray, N. S. Targeting cancer with small molecule kinase inhibitors. *Nature reviews cancer* **9**, 28-39 (2009).
- 132 Wu, P., Nielsen, T. E. & Clausen, M. H. FDA-approved small-molecule kinase inhibitors. *Trends in pharmacological sciences* **36**, 422-439 (2015).
- 133 Knight, Z. A. & Shokat, K. M. Features of selective kinase inhibitors. *Chemistry biology* **12**, 621-637 (2005).
- 134 Davis, M. I. *et al.* Comprehensive analysis of kinase inhibitor selectivity. *Nature biotechnology* **29**, 1046 (2011).
- 135 Scapin, G. Protein kinase inhibition: different approaches to selective inhibitor design. *Current drug targets* **7**, 1443-1454 (2006).
- 136 Krishnamurty, R. & Maly, D. J. Biochemical mechanisms of resistance to small-molecule protein kinase inhibitors. *ACS chemical biology* **5**, 121-138 (2010).

- 137 Daub, H., Specht, K. & Ullrich, A. Strategies to overcome resistance to targeted protein kinase inhibitors. *Nature reviews Drug discovery* **3**, 1001-1010 (2004).
- 138 Zhao, Z. *et al.* Exploration of type II binding mode: a privileged approach for kinase inhibitor focused drug discovery? *ACS chemical biology* **9**, 1230-1241 (2014).
- 139 Zuccotto, F., Ardini, E., Casale, E. & Angiolini, M. Through the “gatekeeper door”: exploiting the active kinase conformation. *Journal of medicinal chemistry* **53**, 2681-2694 (2010).
- 140 Schneider, E. V. *et al.* The Structure of CDK8/CycC Implicates Specificity in the CDK/Cyclin Family and Reveals Interaction with a Deep Pocket Binder. *Journal of Molecular Biology* **412**, 251-266 (2011).
- 141 Huang, W. S. *et al.* Discovery of 3-[2-(imidazo[1,2-b]pyridazin-3-yl)ethynyl]-4-methyl-N-{4-[(4-methylpiperazin-1-yl)methyl]-3-(trifluoromethyl)phenyl}benzamide (AP24534), a potent, orally active pan-inhibitor of breakpoint cluster region-abelson (BCR-ABL) kinase including the T315I gatekeeper mutant. *J Med Chem* **53**, 4701-4719, doi:10.1021/jm100395q (2010).
- 142 Albert, D. H. *et al.* Preclinical activity of ABT-869, a multitargeted receptor tyrosine kinase inhibitor. *Mol Cancer Ther* **5**, 995-1006 (2006).
- 143 Bergeron, P. *et al.* Design and development of a series of potent and selective type II inhibitors of CDK8. *ACS medicinal chemistry letters* **7**, 595-600 (2016).
- 144 Aoki, S. *et al.* Cortistatins A, B, C, and D, anti-angiogenic steroidal alkaloids, from the marine sponge *Corticium simplex*. *Journal of the American Chemical Society* **128**, 3148-3149 (2006).
- 145 Pelish, H. E. *et al.* Mediator kinase inhibition further activates super-enhancer-associated genes in AML. *Nature* **526**, 273 (2015).
- 146 Rzymiski, T. *et al.* SEL120-34A is a novel CDK8 inhibitor active in AML cells with high levels of serine phosphorylation of STAT1 and STAT5 transactivation domains. *Oncotarget* **8**, 33779-33795 (2017).
- 147 Chang, B.-D. *et al.* Effects of p21Waf1/Cip1/Sdi1 on cellular gene expression: implications for carcinogenesis, senescence, and age-related diseases. *Proceedings of the National Academy of Sciences* **97**, 4291-4296 (2000).
- 148 Porter, D. C. *et al.* Cyclin-dependent kinase 8 mediates chemotherapy-induced tumor-promoting paracrine activities. *Proceedings of the National Academy of Sciences of the United States of America* **109**, 13799-13804 (2012).
- 149 ROBINSON, I. B., PORTER, D. C. & Wentland, M. P. (Google Patents, 2013).
- 150 Broude, E. V. *et al.* Expression of CDK8 and CDK8-interacting Genes as Potential Biomarkers in Breast Cancer. *Current Cancer Drug Targets* **15**, 739-749 (2015).

- 151 Dale, T. *et al.* A selective chemical probe for exploring the role of CDK8 and CDK19 in human disease. *Nature Chemical Biology* **11**, 973-980 (2015).
- 152 Clarke, P. A. *et al.* Assessing the mechanism and therapeutic potential of modulators of the human Mediator complex-associated protein kinases. *Elife* **5** (2016).
- 153 Chen, M. *et al.* Systemic Toxicity Reported for CDK8/19 Inhibitors CCT251921 and MSC2530818 Is Not Due to Target Inhibition. *Cells* **8** (2019).
- 154 Johannessen, L. *et al.* Small-molecule studies identify CDK8 as a regulator of IL-10 in myeloid cells. *Nature Chemical Biology* **13**, 1102 (2017).
- 155 Hofmann, M. H. *et al.* Selective and potent CDK8/19 inhibitors enhance NK-Cell activity and promote tumor surveillance. *Molecular cancer therapeutics* **19**, 1018-1030 (2020).
- 156 Gupta, R. M. & Musunuru, K. Expanding the genetic editing tool kit: ZFNs, TALENs, and CRISPR-Cas9. *J Clin Invest* **124**, 4154-4161 (2014).
- 157 Dever, D. P. *et al.* CRISPR/Cas9 beta-globin gene targeting in human haematopoietic stem cells. *Nature* **539**, 384-389 (2016).
- 158 Bak, R. O., Gomez-Ospina, N. & Porteus, M. H. Gene Editing on Center Stage. *Trends Genet* **34**, 600-611 (2018).
- 159 Hatcher, J. M. *et al.* Development of highly potent and selective steroidal inhibitors and degraders of CDK8. *ACS medicinal chemistry letters* **9**, 540-545 (2018).
- 160 Menzl, I. *et al.* A kinase-independent role for CDK8 in BCR-ABL1+ leukemia. *Nature communications* **10**, 1-15 (2019).
- 161 Roninson, I., Porter, D. & Wentland, M. Cdk8/cdk19 Selective Inhibitors and Their Use in Anti-Metastatic and Chemopreventative Methods for Cancer. *WO2013116786A1* (2013).
- 162 Roninson, I. & Chen, M. Method for Treating Prostate Cancer. *WO2014071143 A1* (2014).
- 163 Porter, D. C. *et al.* (AACR, 2014).
- 164 McDermott, M. *et al.* (AACR, 2015).
- 165 Chen, M. *et al.* CDK8/19 Mediator kinases potentiate induction of transcription by NFκB. *Proceedings of the National Academy of Sciences* **114**, 10208-10213 (2017).
- 166 Middleton, D. (Portland Press Ltd., 2007).
- 167 Hosfield, D. *et al.* A fully integrated protein crystallization platform for small-molecule drug discovery. *Journal of structural biology* **142**, 207-217 (2003).
- 168 Klebe, G. Recent developments in structure-based drug design. *Journal of Molecular Medicine* **78**, 269-281 (2000).
- 169 Ferreira, L. G., Dos Santos, R. N., Oliva, G. & Andricopulo, A. D. Molecular docking and structure-based drug design strategies. *Molecules* **20**, 13384-13421 (2015).

- 170 Macalino, S. J. Y., Gosu, V., Hong, S. & Choi, S. Role of computer-aided drug design in modern drug discovery. *Archives of pharmacal research* **38**, 1686-1701 (2015).
- 171 Jorgensen, W. L. The many roles of computation in drug discovery. *Science* **303**, 1813-1818 (2004).
- 172 França, T. C. C. Homology modeling: an important tool for the drug discovery. *Journal of Biomolecular Structure Dynamics* **33**, 1780-1793 (2015).
- 173 Schwede, T., Kopp, J., Guex, N. & Peitsch, M. C. SWISS-MODEL: an automated protein homology-modeling server. *Nucleic acids research* **31**, 3381-3385 (2003).
- 174 Liu, R., Li, X. & Lam, K. S. Combinatorial chemistry in drug discovery. *Current opinion in chemical biology* **38**, 117-126 (2017).
- 175 Macarron, R. *et al.* Impact of high-throughput screening in biomedical research. *Nature reviews Drug discovery* **10**, 188-195 (2011).
- 176 Hertzberg, R. P. & Pope, A. J. High-throughput screening: new technology for the 21st century. *Current opinion in chemical biology* **4**, 445-451 (2000).
- 177 Schneider, E. V., Böttcher, J., Huber, R., Maskos, K. & Neumann, L. Structure–kinetic relationship study of CDK8/CycC specific compounds. *Proceedings of the National Academy of Sciences* **110**, 8081-8086 (2013).
- 178 Chen, M. *et al.* Systemic toxicity reported for CDK8/19 inhibitors CCT251921 and MSC2530818 is not due to target inhibition. *Cells* **8**, 1413 (2019).
- 179 Cee, V. J., Chen, D. Y. K., Lee, M. R. & Nicolaou, K. C. Cortistatin A is a High-Affinity Ligand of Protein Kinases ROCK, CDK8, and CDK11. *Angewandte Chemie International Edition* **48**, 8952-8957 (2009).
- 180 Li, J. *et al.* Characterizing CDK8/19 Inhibitors through a NFκB-Dependent Cell-Based Assay. *Cells* **8**, 1208 (2019).
- 181 Saito, K. *et al.* Discovery and structure–activity relationship of thienopyridine derivatives as bone anabolic agents. *Bioorganic medicinal chemistry* **21**, 1628-1642 (2013).
- 182 Amirhosseini, M. *et al.* Cyclin-dependent kinase 8/19 inhibition suppresses osteoclastogenesis by downregulating RANK and promotes osteoblast mineralization and cancellous bone healing. *Journal of cellular physiology* **234**, 16503-16516 (2019).
- 183 Kittler, H. & Tschandl, P. Driver mutations in the mitogen-activated protein kinase pathway: the seeds of good and evil. *Br J Dermatol* **178**, 26-27 (2018).
- 184 Noble, M. E., Endicott, J. A. & Johnson, L. N. Protein kinase inhibitors: insights into drug design from structure. *Science* **303**, 1800-1805 (2004).
- 185 Bowler, E. H., Wang, Z. H. & Ewing, R. M. How do oncoprotein mutations rewire protein-protein interaction networks? *Expert Rev Proteomic* **12**, 449-455 (2015).
- 186 Toure, M. & Crews, C. M. Small-Molecule PROTACS: New Approaches to Protein Degradation. *Angew Chem Int Ed Engl* **55**, 1966-1973 (2016).

- 187 Sakamoto, K. M. *et al.* Protacs: chimeric molecules that target proteins to the Skp1-Cullin-F box complex for ubiquitination and degradation. *Proc Natl Acad Sci U S A* **98**, 8554-8559 (2001).
- 188 Komander, D. & Rape, M. The ubiquitin code. *Annu Rev Biochem* **81**, 203-229 (2012).
- 189 Schulman, B. A. & Harper, J. W. Ubiquitin-like protein activation by E1 enzymes: the apex for downstream signalling pathways. *Nat Rev Mol Cell Biol* **10**, 319-331 (2009).
- 190 Ye, Y. & Rape, M. J. N. r. M. c. b. Building ubiquitin chains: E2 enzymes at work. **10**, 755-764 (2009).
- 191 David, Y. *et al.* E3 ligases determine ubiquitination site and conjugate type by enforcing specificity on E2 enzymes. *J Biol Chem* **286**, 44104-44115 (2011).
- 192 Jin, J., Li, X., Gygi, S. P. & Harper, J. W. J. N. Dual E1 activation systems for ubiquitin differentially regulate E2 enzyme charging. **447**, 1135 (2007).
- 193 Li, W. *et al.* Genome-wide and functional annotation of human E3 ubiquitin ligases identifies MULAN, a mitochondrial E3 that regulates the organelle's dynamics and signaling. **3**, 1487 (2008).
- 194 Deshaies, R. J. & Joazeiro, C. A. RING domain E3 ubiquitin ligases. *Annu Rev Biochem* **78**, 399-434, doi:10.1146/annurev.biochem.78.101807.093809 (2009).
- 195 Jin, L., Williamson, A., Banerjee, S., Philipp, I. & Rape, M. Mechanism of ubiquitin-chain formation by the human anaphase-promoting complex. *Cell* **133**, 653-665 (2008).
- 196 Newton, K. *et al.* Ubiquitin chain editing revealed by polyubiquitin linkage-specific antibodies. *Cell* **134**, 668-678 (2008).
- 197 Wickliffe, K. E., Williamson, A., Meyer, H.-J., Kelly, A. & Rape, M. J. T. i. c. b. K11-linked ubiquitin chains as novel regulators of cell division. **21**, 656-663 (2011).
- 198 Chau, V. *et al.* A multiubiquitin chain is confined to specific lysine in a targeted short-lived protein. *Science* **243**, 1576-1583 (1989).
- 199 Chastagner, P., Israel, A. & Brou, C. Itch/AIP4 mediates Deltex degradation through the formation of K29-linked polyubiquitin chains. *EMBO Rep* **7**, 1147-1153 (2006).
- 200 Walczak, H., Iwai, K. & Dikic, I. Generation and physiological roles of linear ubiquitin chains. *BMC Biol* **10**, 23 (2012).
- 201 Thrower, J. S., Hoffman, L., Rechsteiner, M. & Pickart, C. M. Recognition of the polyubiquitin proteolytic signal. *EMBO J* **19**, 94-102 (2000).
- 202 Dong, Y. *et al.* Cryo-EM structures and dynamics of substrate-engaged human 26S proteasome. *Nature* **565**, 49-55 (2019).
- 203 Nandi, D., Tahiliani, P., Kumar, A. & Chandu, D. The ubiquitin-proteasome system. *J Biosci* **31**, 137-155 (2006).
- 204 Liu, C. W. *et al.* ATP binding and ATP hydrolysis play distinct roles in the function of 26S proteasome. *Mol Cell* **24**, 39-50 (2006).
- 205 Nijman, S. M. *et al.* A genomic and functional inventory of deubiquitinating enzymes. *Cell* **123**, 773-786 (2005).

- 206 Komander, D., Clague, M. J. & Urbe, S. Breaking the chains: structure and
function of the deubiquitinases. *Nat Rev Mol Cell Biol* **10**, 550-563 (2009).
- 207 Rauch, J., Volinsky, N., Romano, D. & Kolch, W. The secret life of
kinases: functions beyond catalysis. *Cell Commun Signal* **9**, 23 (2011).
- 208 Vivanco, I. *et al.* A kinase-independent function of AKT promotes cancer
cell survival. *Elife* **3** (2014).
- 209 An, S. & Fu, L. Small-molecule PROTACs: An emerging and promising
approach for the development of targeted therapy drugs. *EBioMedicine*
36, 553-562 (2018).
- 210 Lai, A. C. & Crews, C. M. Induced protein degradation: an emerging drug
discovery paradigm. *Nat Rev Drug Discov* **16**, 101-114 (2017).
- 211 Zhou, F. *et al.* Development of selective mono or dual PROTAC degrader
probe of CDK isoforms. *Eur J Med Chem* **187**, 111952 (2020).
- 212 Tovell, H. *et al.* Design and Characterization of SGK3-PROTAC1, an
Isoform Specific SGK3 Kinase PROTAC Degradation. *ACS Chem Biol* **14**,
2024-2034 (2019).
- 213 Mullard, A. Arvinas's PROTACs pass first safety and PK analysis. *Nat Rev
Drug Discov* **18**, 895 (2019).
- 214 Hines, J., Gough, J. D., Corson, T. W. & Crews, C. M. Posttranslational
protein knockdown coupled to receptor tyrosine kinase activation with
phosphoPROTACs. *Proc Natl Acad Sci U S A* **110**, 8942-8947 (2013).
- 215 Henning, R. K. *et al.* Degradation of Akt using protein-catalyzed capture
agents. *J Pept Sci* **22**, 196-200 (2016).
- 216 Ito, T. *et al.* Identification of a primary target of thalidomide teratogenicity.
Science **327**, 1345-1350 (2010).
- 217 Buckley, D. L. *et al.* Targeting the von Hippel-Lindau E3 ubiquitin ligase
using small molecules to disrupt the VHL/HIF-1 α interaction. *J Am
Chem Soc* **134**, 4465-4468 (2012).
- 218 Tinworth, C. P. *et al.* PROTAC-Mediated Degradation of Bruton's Tyrosine
Kinase Is Inhibited by Covalent Binding. *ACS Chem Biol* **14**, 342-347
(2019).
- 219 Ward, C. C. *et al.* Covalent Ligand Screening Uncovers a RNF4 E3 Ligase
Recruiter for Targeted Protein Degradation Applications. *ACS Chem Biol*
14, 2430-2440 (2019).
- 220 Watt, G. F., Scott-Stevens, P. & Gaohua, L. Targeted protein degradation
in vivo with Proteolysis Targeting Chimeras: Current status and future
considerations. *Drug Discov Today Technol* **31**, 69-80 (2019).
- 221 Guo, J., Liu, J. & Wei, W. Degrading proteins in animals: "PROTAC"tion
goes in vivo. *Cell Res* **29**, 179-180 (2019).
- 222 Bondeson, D. P. *et al.* Lessons in PROTAC design from selective
degradation with a promiscuous warhead. **25**, 78-87 (2018).
- 223 Paiva, S.-L. & Crews, C. M. J. C. o. i. c. b. Targeted protein degradation:
elements of PROTAC design. **50**, 111-119 (2019).
- 224 Schapira, M., Calabrese, M. F., Bullock, A. N. & Crews, C. M. J. N. R. D.
D. Targeted protein degradation: expanding the toolbox. 1-15 (2019).

- 225 Gadd, M. S. *et al.* Structural basis of PROTAC cooperative recognition for selective protein degradation. *Nat Chem Biol* **13**, 514-521 (2017).
- 226 Nowak, R. P. *et al.* Plasticity in binding confers selectivity in ligand-induced protein degradation. *Nat Chem Biol* **14**, 706-714 (2018).
- 227 Drummond, M. L. & Williams, C. I. In Silico Modeling of PROTAC-Mediated Ternary Complexes: Validation and Application. *J Chem Inf Model* **59**, 1634-1644 (2019).
- 228 Bondeson, D. P. *et al.* Catalytic in vivo protein knockdown by small-molecule PROTACs. *Nat Chem Biol* **11**, 611-617 (2015).
- 229 Kang, C. H. *et al.* Induced protein degradation of anaplastic lymphoma kinase (ALK) by proteolysis targeting chimera (PROTAC). *Biochem Biophys Res Commun* **505**, 542-547 (2018).
- 230 Cheung, H. H., Plenchette, S., Kern, C. J., Mahoney, D. J. & Korneluk, R. G. The RING domain of cIAP1 mediates the degradation of RING-bearing inhibitor of apoptosis proteins by distinct pathways. *Mol Biol Cell* **19**, 2729-2740 (2008).
- 231 Haupt, Y., Maya, R., Kazaz, A. & Oren, M. Mdm2 promotes the rapid degradation of p53. *Nature* **387**, 296-299, doi:10.1038/387296a0 (1997).
- 232 Han, T. *et al.* Anticancer sulfonamides target splicing by inducing RBM39 degradation via recruitment to DCAF15. *Science* **356** (2017).
- 233 Zhang, X., Crowley, V. M., Wucherpfennig, T. G., Dix, M. M. & Cravatt, B. F. Electrophilic PROTACs that degrade nuclear proteins by engaging DCAF16. *Nat Chem Biol* **15**, 737-746 (2019).
- 234 Spradlin, J. N. *et al.* Harnessing the anti-cancer natural product nimbolide for targeted protein degradation. *Nat Chem Biol* **15**, 747-755 (2019).
- 235 Ishoey, M. *et al.* Translation termination factor GSPT1 is a phenotypically relevant off-target of heterobifunctional phthalimide degraders. **13**, 553-560 (2018).
- 236 Moreau, K. *et al.* PROTAC (PROteolysis TARgeting Chimeras) in drug development: a safety perspective. *Br J Pharmacol* (2020).
- 237 Zhang, L., Riley-Gillis, B., Vijay, P. & Shen, Y. Acquired Resistance to BET-PROTACs (Proteolysis-Targeting Chimeras) Caused by Genomic Alterations in Core Components of E3 Ligase Complexes. *Mol Cancer Ther* **18**, 1302-1311 (2019).
- 238 McCoull, W. *et al.* Development of a Novel B-Cell Lymphoma 6 (BCL6) PROTAC To Provide Insight into Small Molecule Targeting of BCL6. *ACS Chem Biol* **13**, 3131-3141 (2018).
- 239 Park, M. J. *et al.* Oncogenic exon 2 mutations in Mediator subunit MED12 disrupt allosteric activation of cyclin C-CDK8/19. *J Biol Chem* **293**, 4870-4882 (2018).
- 240 Steinparzer, I. *et al.* Transcriptional Responses to IFN-gamma Require Mediator Kinase-Dependent Pause Release and Mechanistically Distinct CDK8 and CDK19 Functions. *Mol Cell* **76**, 485-499 (2019).
- 241 Hatcher, J. M. *et al.* Development of Highly Potent and Selective Steroidal Inhibitors and Degraders of CDK8. *ACS Med Chem Lett* **9**, 540-545 (2018).

- 242 Hofmann, M. H. *et al.* Selective and Potent CDK8/19 Inhibitors Enhance NK-Cell Activity and Promote Tumor Surveillance. *Mol Cancer Ther* **19**, 1018-1030 (2020).
- 243 Barette, C., Jariel-Encontre, I., Piechaczyk, M. & Piette, J. Human cyclin C protein is stabilized by its associated kinase cdk8, independently of its catalytic activity. *Oncogene* **20**, 551-562 (2001).